

EXPLOITING VERTICAL FARMING
STRATEGIES FOR SUSTAINABLE
CROP PRODUCTION

DIONYSIOS (DENNIS) TOULIATOS

B.SC. BIOLOGICAL AGRICULTURE, T.E.I. OF THE IONIAN ISLANDS, GREECE

M.SC. ENVIRONMENTAL SCIENCES, UNIVERSITY OF EAST ANGLIA, UK

THIS THESIS IS SUBMITTED TO LANCASTER UNIVERSITY IN PARTIAL FULFILMENT OF
THE REQUIREMENTS FOR THE DEGREE OF DOCTOR OF PHILOSOPHY



APRIL 2017

DECLARATION

Except where reference is made to other sources, I declare that the contents in this thesis are my own work and have not been previously submitted, in part or in full, for the award of a higher degree elsewhere.

PUBLICATIONS ARISING FROM THIS WORK:

Vertical farming increases lettuce yield per unit area compared to conventional horizontal hydroponics Touliatos, D., Dodd, I.C., McAinsh, M.R. 08/2016 In: Food and Energy Security. 5, 3, p. 184-191. 8 p.

ORAL/POSTER PRESENTATIONS FROM THIS WORK:

Poster presentation at the Eucarpia 2015 Leafy Vegetables Conference, Murcia, Spain.

Speaker at the International Conference on Vertical Farming and Urban Agriculture 2014, The University Of Nottingham, UK

Poster presentation at the New Phytologist next generation scientists meeting 2014, John Innes Centre, Norwich, UK

Poster presentation at The Society of Experimental Biology (SEB) annual main meeting 2014, Manchester University, UK.

Dionysios Dennis Touliatos

Lancaster University April 2017

ACKNOWLEDGEMENTS

I am sincerely grateful to my supervisors Dr Martin McAinsh and Prof Ian Dodd, who provided me with the opportunity to do this PhD. I could not have done this without their advice and guidance, incredible support, encouragement and help with revisions and edits.

The funding of the project by the BBSRC and the vertical farming systems kindly donated by Saturn Bioionics Ltd are gratefully acknowledged.

I would like to thank all the members of the Plant Physiology group for the informative conversations and advice. In particular, I would like to thank Dr Rhydian Beynon-Davies, Dr Shane Rothwell, Dr Joe Fennell, Dr Holly Butler, Dr Doug Pickup, Dr Jaime Puertolas Simon, Dr Ros Jones, Sarah Donaldson, Laura Hodgkinson, Paul Cambre and Esti Leibar.

I am grateful to Dr Dawn Worrall, Dr Geoff Holroyd and Dr Mike Roberts for their help and guidance.

I would like to thank Novogene Bioinformatics Technology for enabling me to overcome the lost time caused by storm Desmond -through the loss of 7 months of work- by supporting the RNAseq data analysis.

The technical support of Maureen Harrison, Ian Edmondson and David Andrew is also gratefully acknowledged.

Special thanks must go to my family in Greece for being patient, understanding and supportive.

I must also mention the folk at Claver Hill community farm for being a welcomed distraction and for reminding me that plants still grow in soil.

Finally, I couldn't have done any of this without Anna.

ABSTRACT

Vertical farming systems (VFS) aim to increase productivity per unit area by extending crop production into the vertical dimension, especially in urban settings where space is limited. This thesis provides the first unequivocal demonstration that a prototype column-type VFS can produce more crop per unit area compared to horizontal hydroponics. However in lettuce, tipburn was identified as a key limitation to crop quality within the VFS. Symptoms were only observed in the top layers of the VFS, which were exposed to luxuriant growth conditions (high Photosynthetic Photon Flux Density (PPFD) and temperature). Tipburn of lettuce is an irreversible physiological disorder, and although the underlying mechanisms are not fully understood a localized calcium deficiency has been implicated. To further elucidate the events leading to tipburn symptoms, a model hydroponic system was established eliminating the multiple environmental gradients present in the VFS. Factorial PPFD and temperature treatments (stress and control) were applied to simulate the conditions within the top and bottom layers of the VFS. Two lettuce cultivars (*Lactuca sativa* L. cv. 'Frank' and cv. 'Sunstar') with contrasting susceptibility to tipburn were employed. The stress treatment (high PPFD and temperature) induced significant photoinhibition and oxidative stress in both cultivars before the visual appearance of tipburn, compared to the control. Plants responded to the treatments with marked changes in the antioxidant enzyme machinery. Tissue calcium concentration did not appear to be linked to presymptomatic tipburn induction. The findings suggested links between the induction of tipburn of lettuce and oxidative stress under luxuriant growth conditions. Furthermore, genes involved in flavonoid biosynthesis were downregulated in both cultivars under stress compared to the control, suggesting a putative presymptomatic link to lettuce tipburn, with decreased flavonoid content associated with increased lipid peroxidation. This research has contributed new mechanistic insights into the development of tipburn of lettuce and provided important perspectives on the potential and limitations of VFS, contributing to the emerging fields of vertical farming and urban agriculture.

TABLE OF CONTENTS

Chapter 1 General discussion

1.1 Context.....	2
1.2 Urbanization and the emergence of urban agriculture.....	2
1.3 Vertical farming as a tool for urban agriculture.....	4
1.4 Cultivation methods in vertical farming systems.....	7
1.5 Lettuce cultivation in vertical farming systems.....	9
1.6 Tipburn of lettuce.....	10
1.7 Environmental factors inducing tipburn of lettuce.....	22
1.8 Control and prevention of tipburn of lettuce.....	30
1.9 Thesis aims.....	34

Chapter 2 Characterising a vertical farming system

2.1 Introduction.....	37
2.2 Materials and methods.....	39
2.3 Results.....	51
2.4 Discussion.....	75
2.5 Conclusions.....	80

Chapter 3 Disentangling the contribution of light intensity and temperature to lettuce tipburn

3.1 Introduction.....	83
3.2 Materials and methods.....	85
3.3 Results.....	96
3.4 Discussion.....	113

3.5 Conclusions.....	118
Chapter 4 Do oxidative stress and calcium deficiency precede the development of lettuce tipburn?	
4.1 Introduction.....	120
4.2 Materials and methods.	122
4.3 Results.....	131
4.4 Discussion.	147
4.5 Conclusions.....	155
Chapter 5 Elucidating the molecular basis of lettuce tipburn	
5.1 Introduction.....	157
5.2 Materials and methods.	158
5.3 Results.....	162
5.4 Discussion.	172
5.5 Conclusions.....	178
Chapter 6 General discussion	
6.1 Overview of thesis.	181
6.2. Ameliorating tipburn by reducing oxidative stress.	184
6.3 Conclusions.....	188
References.....	189

List of figures	Page
 CHAPTER 1	
Figure 1.1. Vertical Farming Systems (VFS) currently used in the food production industry: (A) column-type VFS (www.towergarden.com/) in which plants are grown in upright vertical columns or pipes, (B) Pyramid like A-frame designs (www.skygreens.com/about-skygreens/) which grow plants across the sides of the pyramid, (C) Conveyor driven stacked growth systems (www.verticrop.com/) that rotate crop growing platforms to increase uniformity of light distribution within the VFS, (D) Plant factory approaches (farmedhere.com/) which entail enclosed and fully controlled systems which grow crops in stacked shelves under artificial lighting, with a dedicated lighting system for each crop producing shelf.	5
Figure 1.2. Vertical Farming Systems (VFS) within different urban environments: (A) Stacked growing shelves of a plant factory VFS within a previously abandoned factory (www.greenspiritfarms.com) (B) Vertical columns and plant factory set-up within a cafe space (farmlondon.weebly.com/index.html) (C) Protected (growup.org.uk) and (D) unprotected vertical columns on urban rooftops (bbandcnyc.com).	7
Figure 1.3. Tipburn of lettuce significantly affects crop quality and marketability. The disorder is characterised by dark black-brown necrotic leaf lesions starting at the margins of developing leaves, as indicated by the white arrows. Scale bar is 5.	11
Figure 1.4. Schematic representation of antioxidant metabolic pathways in plants.	17
Figure 1.5. Flow chart summarizing mechanisms of common tipburn inducing factors in VFS and hydroponics.	22

CHAPTER 2

Figure 2.1. The Saturn Grower VFS. The growing container formed from a single unit of moulded opaque plastic (dark green) incorporating a central core/airspace. The spacing collar formed from transparent plastic with four anti-diametrical planting apertures. When constructing the vertical column, the spacing collar was placed on the rim of the pot, allowing the installation of an additional growing	40
--	----

container on top. Each VFS was sealed at both the top and bottom to create a vertical airspace within the core of each growing column. Scale bar is 5 cm.

Figure 2.2. The Saturn Grower VFS's modular growth unit. Seedlings were 41
planted within the VFS by gently placing the dark coloured peat block on top of,
rather than planting into, the granular white perlite. Scale bar is 2 cm.

Figure 2.3. The closed-loop irrigation system of the Saturn Grower VFS. The 43
white arrows indicate the route of the nutrient solution within the VFS. Nutrient
solution was pumped to the top of the column, sprayed within the top layer by
micro-sprinklers, dripped through the vertical layers and returned to the water tank
to be re-circulated around the growing system. Scale bar is 10 cm.

Figure 2.4. The different treatments representing four different planting densities: 44
blank column (A), columns with two planted layers (2L) (B), columns with four
planted layers (4L) (C) and columns with six planted layers (6L) (D). The
photograph was taken 3 weeks after the plants were transferred to the VFS. Scale
bars are 10 cm.

Figure 2.5. The open-loop irrigation system of the VFS, demonstrated on the SL 45
VFS. The water tank at the bottom of picture (A) contained the submersible pump
and provided fresh nutrient solution to the VFS. The water tank at the top of the
picture (B) collected the effluent nutrient solution. The same approach was applied
to all VFS of the study. Scale bar is 7.5cm.

Figure 2.6. Schematic shows planting densities within the HHS and VFS. 46
Overhead view of HHS (A). Side-view of VFS (B). Overhead view of VFS (C).
The HHS occupied 0.4 m² of growing floor area, whereas the VFS occupied 0.02
m² per column of floor area. The grey rectangles show the exact position of the
400 W metal halide lamps above the growth systems. The grey circles within the
VFS show the exact measurement positions of the Macam Q203 Quantum
radiometer quantum sensor. Light measurements in the HHS were obtained
directly above the plants, at 20 cm distance from the PVC pipes. Scale bar is 20
cm.

Figure 2.7. Color photographs taken at 06:00 hrs, 09:00 hrs, 12:00 hrs, 15:00 hrs, 48
18:00 hrs on the 5th of December 2012 (Week 4) show diurnal changes in light in
the greenhouse (See Figure 2.11 for position of supplementary lighting from top of
column.) That day was sunny, according to a weather report

(www.metoffice.gov.uk).

Figure 2.8. Floor plan of the controlled environment facility (CE room) at Lancaster Environment Centre. The yellow rectangles represent the exact position of the 400 W metal halide lamps. The black circles and parallel five white rectangles represent the exact positions of the VFS and HHS respectively. The black rectangles represent the exact positions of the water tank. Measured lines (in metres) show the exact position of the Ektron II C sensor in relation to the metal halide lamps and sink and the CE room's exact dimensions. VFS and HHS are superimposed above the lamps for clarity. 51

Figure 2.9. Shoot fresh weight versus vertical layer in the VFS (solid line; closed symbols) and HHS (open symbols) respectively. The regression equation, adjusted R^2 values and significance of the regression (p-value) are reported at the top of the panel. 53

Figure 2.10. PPFD within the Vertical Farming System (VFS; closed symbols) and the Horizontal Hydroponic System (HHS; open symbols) plotted against layers in the growth systems. Values indicated with different letters indicate statistically significant differences (one-way ANOVA test; $F(4, 35) = 16.68$, $p < 0.01$ for the VFS and $F(4, 35) = 2.25$, $p = 0.06$ for the HHS, followed by Tukey post-hoc analysis), whereas those marked with the same letters show statistically similar values. Error bars represent SE ($n=8$). 54

Figure 2.11. Shoot fresh weight versus PPFD in the Vertical Farming System (VFS; solid line; closed symbols) and Horizontal Hydroponic System (HHS; open symbols) respectively. The regression equation, adjusted R^2 values, and significance of the regression (p-value) are reported at the top of the panel. 55

Figure 2.12. Floor plan of the experimental set up at Lancaster Environment Centre's glasshouse facility. The black, white, dark grey and light grey circles represent the exact position of the columns with two planted layers (2L), four planted layers (4L) and six planted layers (6L) within the glasshouse, respectively. The yellow rectangles represent the exact position of the 600 W HPS lamps. The Ektron II C sensor was positioned approximately in the middle of the glasshouse. Compass indicator shows the position of the glasshouse in relation to the North. Measured lines (in metres) show the exact position of the sensor in relation to the glasshouse's walls, distance between vertical columns and the glasshouse's exact dimensions. VFS are superimposed above the lamps for clarity. 56

Figure 2.13. Linear regression analysis of shoot fresh weight versus layer in the 2L VFS (grey symbols), 4L VFS (open symbols) and 6L VFS (closed symbols). The regression equation, adjusted R^2 values and significance of the regression (p-value) are reported. 58

Figure 2.14. Diurnal distributions of light intensity within all layers of the VFS in the glasshouse. The horizontal line within the box represents the median. The boundaries of each box represent the lower 25th and upper 75th percentiles. The spacing of components within the box indicates skewness in the data. The whiskers represent the sample minimum and maximum values. Results of Kruskal-Wallis ANOVA on ranks followed by Tukey post-hoc analysis showed statistically significant differences ($H(4) = 106.290$, $p < 0.001$). Different letters indicate statistically significant differences. 59

Figure 2.15. Box plots summarize the distributions of PPFD within the vertical layers. The horizontal line within the box represents the median. The boundaries of each box represent the lower 25th and upper 75th percentiles. The spacing of components within the box indicates skewness in the data. The whiskers represent the sample minimum and maximum values. Results of Kruskal-Wallis ANOVA on ranks followed by Tukey post-hoc analysis showed statistically significant differences ($H(5) = 524.876$, $p < 0.001$). Different letters indicate statistically significant differences. 60

Figure 2.16. A 3D surface plot shows influence of time of the day (x-axis) and vertical layer (y-axis) on PPFD (z-axis) within the VFS. PPFD data are displayed on a pseudo-colour intensity scale; in which 'red' corresponds to the highest light intensity, whereas 'deep blue' represents lowest light intensity. 61

Figure 2.17. Linear regression analysis of shoot fresh weight versus PPFD in the VFS. The regression equation, adjusted R^2 values, and significance of the regression (p-value) are reported at the top of the panel. Each point is an individual plant. 62

Figure 2.18. Differences in NO_3^- concentration between incoming (black bars) and effluent (white bars) nutrient solution. Values indicated with different letters indicate statistically significant differences according to one-way ANOVA test; $F(7,32) = 214.1$, $p < 0.001$, followed by Tukey post-hoc analysis. Bars represent means \pm SE (n=6). 63

Figure 2.19. Floor plan of the CE room at Lancaster Environment Centre. The yellow rectangles represent the exact position of the 400 W metal halide lamps. The white and grey circles represent the exact position of the six layered (6L) and single layer (SL) VFS within the CE room, respectively. The black circles show the position of the three dummy (6L) VFS. The white and black rectangles 64

represent the exact position of the water tank contain incoming and effluent nutrient solution, respectively. VFS are superimposed above the lamps for clarity.

Figure 2.20. Shoot fresh weight per vertical layer within the VFS. Values indicated with different letters indicate statistically significant differences (one-way ANOVA test; $F(2,35)= 68.5$, $p<0.001$, followed by Tukey post-hoc analysis. Bars are means of 12 plants \pm SE. 65

Figure 2.21. Shoot fresh weight versus layer in the within the six layered VFS. The regression equation, adjusted R^2 values and significance of the regression (p-value) are reported at the top of the panel. Each point is an individual plant. 66

Figure 2.22. PPFD within all layers of the VFS. The horizontal line within the box represents the median. The boundaries of each box represent the lower 25th and upper 75th percentiles. The spacing of components within the box indicates skewness in the data. The whiskers represent the sample minimum and maximum values. Kruskal-Wallis ANOVA on ranks followed by Dunn's method showed statistically significant differences ($H(6) = 550.573$, $p<0.001$). Differences were indicated by different letters. 67

Figure 2.23. Barplot shows changes in incident light intensity (PPFD) between weeks 1 and 4 caused by a shading effect within the VFS as a result of plant growth. White bars represent PPFD measured during the first week of the experiment, whereas black bars represent PPFD measured four weeks after. Error bars represent SE (n=6). Values indicated with asterisk indicate statistically significant differences between week 1 and 4 (t-test, $p < 0.05$). 68

Figure 2.24. Shoot fresh weight versus PPFD in the VFS. The regression equation, adjusted R^2 values, and significance of the regression (p-value) are reported at the top of the panel. Each point is an individual plant. 69

Figure 2.25. Changes in root zone temperature of top (closed symbols) and bottom (open symbols) layers within six layered VFS in the CE room and glasshouse as they increased during the transition from the dark (light grey background) to the light (white background) period. In the glasshouse, each circle represents the mean of 2 data loggers through the period of 4 days. Error bars represent SE. In the CE room, each circle represents the mean of 3 data loggers through the period of 8 days. Error bars represent SE. Values indicated with asterisk indicate statistically significant differences (t-test, $p < 0.05$). 70

Figure 2.26. Canopy temperature of plants grown within the top (black bars) and bottom (white bars) layers of the VFS and SL VFS (grey bar). Values indicated with different letters indicate statistically significant differences ($t = 13.445$ with 22 degrees of freedom, $p < 0.001$) in the glasshouse study and one-way ANOVA 72

test; $F(2,71)= 30.924$, $p<0.001$, followed by Tukey post-hoc analysis in the CE room study. Bars represent means of \pm SE (n=12).

Figure 2.27. Photographs of harvested lettuce (*Lactuca sativa* L. cv. 'Frank') plants grown within the uppermost layers affected by tipburn symptoms (A-C) and within the bottom layer of six layered VFS (D-F) which were not affected by tipburn. White arrows show tipburn symptoms located at the edges of leaves. Scale bars are 1 cm. 73

Figure 2.28. Photographs of harvested lettuce plants grown within the VFS in the CE room study. A and B, lettuce plants grown within the top layers of the VFS affected by tipburn symptoms. C and D, lettuce plants grown within the bottom layer of the VFS which were not affected by tipburn. Black arrows show tipburn symptoms located at the edges of young leaves within the developing head. Scale bars are 1 cm. 74

CHAPTER 3

Figure 3.1. (A) Side view of the Deep Flow Hydroponics System (DFTS) shows shoots and roots of lettuce plants 29 days after they were transferred to the DFTS. The growth system consisted of 16 litre independent black plastic boxes. Four lettuce plants were grown in each hydroponic box. The rockwool block and the plastic lid of the hydroponic box supported the plants. The crop's roots were submerged in continuously aerated half-strength Hoagland's solution. Scale bar is 10 cm. (B) Top view of the DFTS shows lettuce plants 15 days after they were transferred to the DFTS. The air pump used to continuously oxygenate the nutrient solution in the hydroponic box through the 5 ml pipette tip in the centre of the lid. Scale bar is 3 cm. 87

Figure 3.2. Shows the CE room floor plan in scale. The black rectangular shapes represent the hydroponic boxes, which comprised the DFTS. Yellow and red circles represent data points from where light quantity and quality measurements were obtained using a Macam Q203 Quantum radiometer and the SR9110-V7 spectroradiometer, respectively. Measured lines (in metres) show the CE room's exact dimensions. 89

Figure 3.3. Flow diagram shows the steps followed to separate tipburn affected leaf area from total leaf area. Picture (A) shows the original photograph, picture (B) shows total leaf area, picture (C) shows tipburn affected leaf area, picture (D) the 8-bit image, and picture (E) the binary image. Each leaf was assessed 93

separately for visual tipburn symptoms.

Figure 3.4. Shows the four different growth cabinet's floor plans in scale. The black rectangular shapes represent the hydroponic boxes, which comprised the DFTS. Yellow represent data points from where light quantity measurements were obtained using a Macam Q203 Quantum radiometer. Measured lines (in metres) show the chamber's exact dimensions. 95

Figure 3.5. Shoot fresh weight of lettuce cultivars (cv. 'Frank' and cv. 'Sunstar') grown under high (HL) and low (LL) PPFD treatments. Values are mean \pm SE (n=3). Different letters indicate statistically significant differences ($p < 0.05$). Statistical analysis was performed on log-transformed data using a two-way ANOVA, followed by Tukey's post-hoc analysis. 97

Figure 3.6. Contour map projection on the floor plan of the CE room shows PPFD distribution on the DFTS displayed on a pseudo-colour intensity scale; in which 'red' corresponds to the highest PPFD, whereas 'deep blue' represents absolute shade. 98

Figure 3.7. Frequency distributions of PPFD within the DFTS under two light treatments; HL (black bars) and LL (white bars) treatments. Data were normally distributed for both HL and LL (Shapiro–Wilk-test: $p=0.113$ and 0.562 , respectively) however they showed different patterns of symmetry and pointiness (skewness: -0.81 and 0.310 ; kurtosis: 0.838 and -0.298 , respectively). 99

Figure 3.8. Incident spectral irradiance of HL (red line) and LL (blue line) treatments. Lines represent means of 8 measurement points of light irradiances over the spectral range of 290-800 nm \pm SD (dotted lines). 100

Figure 3.9. Changes in HL and LL surface temperature of the DFTS (red and black diagonal cross symbols, respectively), root zone temperature (red and black grey circle symbols, respectively) and air temperature (red and black diamond symbols, respectively) during the transition from the dark (grey background) to the light (white background) period. Each diagonal cross and circle represents the mean of three data loggers through the period of 26 days, whereas air temperature was recorded with one data logger in each treatment through the period of 26 days. Error bars represent SE. 101

Figure 3.10. HL and LL canopy and root zones temperature data separated between the dark (light grey background) and the light (white background) periods. The horizontal line within the box represents the median. Results of 102

Kruskal-Wallis ANOVA on ranks followed by Dunn's Method showed statistically significant differences between the medians of the 8 different temperature series ($H(7) = 5013.87$, $p < 0.001$). Different letters indicate statistically significant differences.

Figure 3.11. Canopy temperature of cv. 'Frank' crops grown under HL (black bars) and LL (white bars) and cv. 'Sunstar' crops grown under LL (dark grey bars) and LL (light grey bars). Values indicated with different letters indicate statistically significant ($p < 0.05$) differences according to two-way ANOVA test followed by Tukey post-hoc analysis. Bars represent means of \pm SE ($n=3$). 103

Figure 3.12. Light response curves of photosynthetic CO_2 assimilation rate A ($\mu\text{mol m}^{-2} \text{s}^{-1}$) of HL (diagonal cross symbols) and LL-grown (circle symbols) butterhead lettuce varieties (*L. sativa* cv. 'Frank' and 'Sunstar') determined 15 DAT. Each point is the mean of different leaves from three different plants. Vertical bars represent the standard errors ($n=3$). 104

Figure 3.13. Lettuce plants 29 DAT. (A) and (B), *Lactuca sativa* cv. 'Frank'. (C) and (D), *Lactuca sativa* cv. 'Sunstar'. LL (A/C) – non-affected by tipburn symptoms. HL (B/D) – affected by tipburn symptoms; white arrows show tipburn symptoms located at the edges of leaves within the developing head. Scale bars are 3 cm. 106

Figure 3.14. Leaves of lettuce plants (*L. sativa* cv. 'Frank') 30 DAT. White arrows show tipburn symptoms located at the edges of lettuce leaves. These lesions were visible only after harvest, when leaves were separated. Scale bar is 1 cm. 107

Figure 3.15. Tipburn affected leaf area ratio of lettuce, *L. sativa* cv. 'Frank' and cv. 'Sunstar', grown at HL. cv. 'Sunstar' exhibited significantly more ($t(4) = 14.01$, $p < 0.001$) symptoms of tipburn than the 'Frank' cv. Asterisk (*) indicates significance. Bars represent means of 3 plants \pm SE. 106

Figure 3.16. PPFD within the growth cabinets (cabinet 1 - HL and HT, cabinet 2 - HL and LT, cabinet 3 - LL and HT, and cabinet 4 - LL and LT.). The horizontal line within the box represents the median. Results of Kruskal-Wallis ANOVA on ranks followed by Dunn's method showed statistically significant ($H(3) = 71.511$, $p < 0.001$). Different letters indicate statistically significant differences. 108

Figure 3.17 Contour map projection on the floor plan of the CE room shows PPF distribution on the DFTS displayed on a pseudo-colour intensity scale; in which 'red' corresponds to the highest PPF, whereas 'deep blue' represents absolute shade. 109

Figure 3.18. Shoot fresh weight (g) of lettuce plants (*Lactuca sativa* L. cv. 'Frank') grown in 4 growth cabinets (cabinet 1 - HL and HT, cabinet 2 - HL and LT, cabinet 3 - LL and HT, and cabinet 4 - LL and LT). Values indicated with different letters indicate statistically significant differences (Two-way ANOVA test followed by Tukey post-hoc analysis). Bars represent means of 3 plants \pm SE. 110

Figure 3.19. Light response curves of photosynthetic CO₂ assimilation rate A ($\mu\text{mol m}^{-2} \text{s}^{-1}$) of lettuce plants (*Lactuca sativa* cv. 'Frank') in 4 growth cabinets determined 15 DAT. Each point is the mean of different leaves from three different plants. Vertical bars represent the standard errors (n=3). 111

Figure 3.20. Lettuce plants (*L. sativa* L. cv. 'Frank') 30 DAT. (A) HL and HT (cabinet 1), (B) HL and LT (cabinet 2), (C) LL and HT (cabinet 3), (D) LL and LT (cabinet 4). Plants only developed tipburn symptoms under combined conditions of HL and HT (cabinet 1). White arrows in picture (A) show tipburn symptoms located at the edges of leaves within the developing head. Scale bars are 3 cm. 113

CHAPTER 4

Figure 4.1. Plant leaf tissue was on a sterilized tile, and approximately a 2 mm strip dissected from the edge of the leaf; henceforth denoted as tip (white arrows). Scale bar is 1 cm. 123

Figure 4.2. Development of visual tipburn symptoms in a lettuce plant (*Lactuca sativa* cv. 'Frank') grown under the stress treatment. The first visual symptoms of tipburn appeared 16 days after the stress treatment was applied, as small, circular, necrotic spots (A). Panel (B) shows tipburn development on the same plant, 23 days after the stress treatment was applied. Panel (C) shows expansion of tipburn region of panel (A). White arrows indicate tipburn symptoms on plants in both panels. Scale bar in 3 cm in (A) and (B), and 0.5 cm in (C). 132

Figure 4.3. Time-course of changes in total Ca concentration of seedlings (days 0 – 5) and tips of developing leaves (days 7 – 15) of *Lactuca sativa* cv. 'Frank' (A) and cv. 'Sunstar' (B) under stress (closed symbols, black letters) and control (open symbols, grey letters) treatments. One-way ANOVA results for the cv. 'Frank' and cv. 'Sunstar' were $F(17, 36) = 2.79, p < 0.001$ and $F(17, 36) = 2.5, p < 0.01$, 134

respectively. Values are means \pm SE (n=3). Means denoted by the same letter did not significantly differ at $p < 0.05$ according to Duncan's multiple range test. The dotted line indicates the different sampling techniques (Days 0 to 5; whole seedlings, Days 7 to 15; two fully expanded leaves).

Figure 4.4. Time-course of changes in MDA equivalents of seedlings (days 0 – 5) and tips of developing leaves (days 7 – 15) of *Lactuca sativa* cv. ‘Frank’ (A) and cv. ‘Sunstar’ (B) under stress (closed symbols, black letters) and control (open symbols, grey letters) treatments. One-way ANOVA results for the cv. ‘Frank’ and cv. ‘Sunstar’ were $F(17, 36) = 3.56$, $p < 0.001$ and $F(17, 36) = 3.56$, $p < 0.001$, respectively. Values are means \pm SE (n=3). Means denoted by the same letter did not significantly differ at $p < 0.05$ according to Duncan's multiple range test. The dotted line indicates the different sampling techniques (Days 0 to 5; whole seedlings, Days 7 to 15; two fully expanded leaves). 136

Figure 4.5. Time-course of changes in SOD activity of seedlings (days 0 – 5) and tips of developing leaves (days 7 – 15) of *Lactuca sativa* cv. ‘Frank’ (A) and cv. ‘Sunstar’ (B) under stress (closed symbols, black letters) and control (open symbols, grey letters) treatments. One-way ANOVA results for the cv. ‘Frank’ and cv. ‘Sunstar’ were $F(17, 36) = 15.45$, $p < 0.001$ and $F(17, 36) = 11.6$, $p < 0.001$, respectively. Values are means \pm SE (n=3). Means denoted by the same letter did not significantly differ at $p < 0.05$ according to Duncan's multiple range test. The dotted line indicates the different sampling techniques (Days 0 to 5; whole seedlings, Days 7 to 15; two fully expanded leaves). 138

Figure 4.6. Time-course of changes in CAT activity of seedlings (days 0 – 5) and tips of developing leaves (days 7 – 15) of *Lactuca sativa* cv. ‘Frank’ (A) and cv. ‘Sunstar’ (B) under stress (closed symbols, black letters) and control (open symbols, grey letters) treatments. One-way ANOVA results for cv. ‘Frank’ and cv. ‘Sunstar’ were $F(17, 36) = 3.17$, $p < 0.05$ and $F(17, 36) = 3.57$, $p < 0.001$, respectively. Values are means \pm SE (n=3). Means denoted by the same letter did not significantly differ at $p < 0.05$ according to Duncan's multiple range test. The dotted line indicates the different sampling techniques (Days 0 to 5; whole seedlings, Days 7 to 15; two fully expanded leaves). 140

Figure 4.7. Time-course of changes in APX activity of seedlings (days 0 – 5) and tips of developing leaves (days 7 – 15) of *Lactuca sativa* cv. ‘Frank’ (A) and cv. ‘Sunstar’ (B) under stress (closed symbols, black letters) and control (open symbols, grey letters) treatments. One-way ANOVA results for the cv. ‘Frank’ and cv. ‘Sunstar’ were $F(17, 36) = 6.88$, $p < 0.001$ and $F(17, 36) = 2.5$, $p < 0.01$, respectively. Values are means \pm SE (n=3). Means denoted by the same letter did not significantly differ at $p < 0.05$ according to Duncan's multiple range test. The dotted line indicates the different sampling techniques (Days 0 to 5; whole seedlings, Days 7 to 15; two fully expanded leaves). 142

Figure 4.8. Time-course of changes in GR activity of seedlings (days 0 – 5) and tips of developing leaves (days 7 – 15) of *Lactuca sativa* cv. ‘Frank’ (A) and cv. ‘Sunstar’ (B) under stress (closed symbols, black letters) and control (open symbols, grey letters) treatments. One-way ANOVA results for the cv. ‘Frank’ and cv. ‘Sunstar’ were $F(17, 36) = 4.22, p < 0.01$ and $F(17, 36) = 3.05, p < 0.01$, respectively. Values are means \pm SE (n=3). Means denoted by the same letter did not significantly differ at $p < 0.05$ according to Duncan's multiple range test. The dotted line indicates the different sampling techniques (Days 0 to 5; whole seedlings, Days 7 to 15; two fully expanded leaves). 143

Figure 4.9. Schematic representation indicating which antioxidant enzyme pathways were enhanced (green arrows; pointing upwards) or depressed (red arrows; pointing downwards) under stress through the experiment, overall for both cultivars. Numbers indicate days after the treatment was applied. 150

CHAPTER 5

Figure 5.1. Venn diagram shows the number of DEGs that were uniquely expressed in cv. ‘Sunstar’ and cv. ‘Frank’ within the yellow (left) and blue (right) circles, respectively. FPKM and DESeq estimated the level of gene expression and the number of DEGs, respectively. The overlapping region (green) shows the number of genes that were expressed in both groups. 163

Figure 5.2. Heat map showing the overall results of FPKM cluster analysis, clustered using the $\log_{10}(\text{FPKM}+1)$ value. Three main groups were identified which are represented by the three high-level numbered clusters in the dendrogram. The intensity of the colour represents expression levels of DEGs. Red denotes genes with high expression levels, and blue denotes genes with low expression levels. Scale bar represents the $\log_{10}(\text{FPKM}+1)$ value from large to small. 165

Figure 5.3. Volcano plots obtained by pairwise comparison of cv. ‘Frank’ (A) and cv. ‘Sunstar’ (B) between treatments (stress and control). The x-axis shows the fold-change in gene expression between different samples, and the y-axis shows the statistical significance of the differences. Significantly up and down-regulated genes are highlighted in red and green, respectively. No significant difference in gene expression is shown in blue. 166

Figure 5.4. Gene ontology (GO) classifications of DEGs in cv. ‘Frank’ (A) and cv. ‘Sunstar’ (B). The x-axis shows the enriched GO terms and the y-axis is the 168

number of DEGs. Different colours are used to distinct biological process (green), cellular component (orange) and molecular function (blue). Asterisk (*) indicates significantly enriched GO terms according to corrected p-value < 0.05

Figure 5.5. The 20 most enriched KEGG pathways in cv. ‘Frank’ (A) and cv. ‘Sunstar’ (B) are shown together with their q-value (colour), rich factor (vertical ordinate) and number of genes (size of circles). Up regulated and down regulated KEGG pathways are highlighted in green and red, respectively. 170

List of tables Page

CHAPTER 1

Table 1.1. Non-enzymatic antioxidant defence mechanisms functions and subcellular location. 15

Table 1.2. Enzymatic antioxidant defence mechanisms, reaction catalysed and subcellular location. 19

CHAPTER 2

Table 2.1. Comparison of the productivity of the Vertical Farming System (VFS) and Horizontal Hydroponic System (HHS). 52

CHAPTER 3

Table 3.1. Photosynthetic parameters of two butterhead lettuce cultivars (cv. ‘Frank’ and cv. ‘Sunstar’) derived from the Mitscherlich equation. A_{max} is the maximum net photosynthetic rate, k is the initial slope of the curve, and x_0 is light compensation point. Data were compared using two-way ANOVA test, followed by Tukey post-hoc analysis. Values indicated with different letters indicate statistically significant differences, whereas those marked with the same letters show statistically similar values. 105

Table 3.2. Photosynthetic parameters of lettuce plants (*Lactuca sativa* L. cv. ‘Frank’) grown under contrasting PPFD and temperature conditions. Values represent means of 3 plants \pm SE. For k statistical analysis was performed on log-transformed data using a two-way ANOVA, followed by Tukey’s post-hoc analysis. Values indicated with different letters indicate statistically significant differences, whereas those marked with the same letters show statistically similar values. 112

CHAPTER 4

Table 4.1. F and p values of three-way ANOVA examining the effects of the nine sampling periods (Time; T), the control and stress treatments (Treatment; Tr), and the two lettuce cultivars *Lactuca sativa* cv. ‘Frank’ and cv. ‘Sunstar’ (Cultivar; C) on Calcium (Ca) concentration, Malondialdehyde equivalents (MDA eq), superoxide dismutase (SOD), catalase (CAT), ascorbate peroxidase (APX) and glutathione reductase (GR). 145

CHAPTER 5

Table 5.1. Overview of Mapping Status. Clean reads were obtained by removing low quality reads from raw reads. Q20 and Q30 represent the percentages of bases whose correct base recognition rates are greater than 99% and 99.9% in total bases, respectively. GC represents the percentages of G and C in total bases. Total mapped represents total number of reads that was mapped to the reference genome. Multiple mapped is the number of reads that was mapped to multiple sites in the reference genome and uniquely mapped is number of reads that was uniquely mapped to the reference genome. 162

CHAPTER 1

GENERAL INTRODUCTION

1.1 Context.

The global population is expected to reach nine billion by 2050, a significant proportion of which will be urban dwellers, requiring more than a 70% increase in agricultural productivity (Corvalan et al., 2005; Tilman et al., 2011; Rotter et al., 2011). Agricultural land is increasingly becoming a scarce resource due to the expansion of urban landscapes, which can accelerate the loss of cultivated land surrounding cities e.g. in China (Tan et al., 2005; Jiang et al., 2013), the United States of America (Healy and Rosenberg, 2013), and India (Pandey and Seto, 2015). In addition, land-use intensification and climate change have further contributed to land degradation and loss of soil fertility (Foley et al., 2011; Lambin et al., 2013). Creating new agricultural land is becoming increasingly costly due to competition from other human activities (Godfray et al., 2010), in addition to being a threat for many ecosystem services (Chaplin-Kramer et al., 2015). The need for innovation in land-use efficiency for crop production is therefore increasingly important (Lambin and Meyfroidt, 2011).

1.2 Urbanization and the emergence of urban agriculture.

Urbanization is the expansion of urban populations, including the process of population migration from rural to urban areas (Pacione, 1999). By leading the conversion of natural landscapes to urban areas, urbanization is posing both direct and indirect challenges to global food security (Chen, 2007). In addition, rapid urbanization is a significant contributor to species extinctions (Goddard et al., 2010) and is thus a major threat to biodiversity and to fundamental ecosystem services (Sol et al., 2014). Furthermore, in large urban settlements natural landscapes are

marginalized and scarce (Jim, 2012). This contributes to the development of chronic human health issues such as stress, depression and cardiovascular disease, which may be improved through interaction with the natural world (Warber et al., 2015). Spatial and financial pressures mean that many cities today also contain ‘food deserts’, defined as urban neighbourhoods with limited access to fresh, healthy and affordable food (Short et al., 2007; Thomas, 2010; Shannon, 2014). In addition, cities currently account for 70% of global energy use and for approximately 50% of global greenhouse gas emissions (newsroom.unfccc, 2015; Papa et al., 2016) even though they cover less than 3% of the global terrestrial surface (Grimm et al., 2008).

In response to these challenges, Urban Agriculture (UA) has been expanding in both the developed (Lin et al., 2015) and the developing world (Orsini et al., 2013). UA is an umbrella term which encompasses the production, processing and distribution of food, fuel and fibre on urban and peri-urban land (Tornaghi, 2014). As such, UA can be a source of food and supplementary income for urban dwellers (Gómez-Baggethun and Barton, 2013). UA initiatives can bring fresh, locally grown food to deprived urban areas and potentially relieve some of the issues associated with ‘food deserts’ (Block et al., 2011; Wang et al., 2014) by using vacant lots, parks, community farms, rooftop gardens, and other productive features of the urban environment to produce food (Knight and Riggs, 2010; Lovell, 2010). In addition, UA creates food producing landscapes within urban environments which can provide refuge for native biodiversity (Goddard et al., 2010) and may potentially free up existing rural agricultural land or allow for alternative landscape use e.g. bioenergy production and ecosystem restoration (Specht et al., 2014). It can promote the physical activity of urban dwellers (Wolch et al., 2014; Warber et al., 2015), facilitate the development of

important social values, such as community building and re-skilling around food related activities (La Rosa et al., 2014), and reduce the carbon footprint and costs of food transport; due to the proximity of production and consumption locations (Beatley, 2007; Bougherara et al., 2009; Grewal and Grewal, 2012; Specht et al., 2014).

UA has been implemented to improve the sustainability of urban environments (Badami and Ramankutty, 2015; Huang and Drescher, 2015), to promote urban food security (Sanyé-Mengual et al., 2015), and as an alternative for urban land use (Lovell, 2010; Mogk et al., 2010) via a wide variety of methods. These vary from small-scale urban horticulture for self-consumption to commercial vertical farming systems (Eigenbrod and Gruda, 2014).

1.3 Vertical farming as a tool for urban agriculture.

Vertical farming has been proposed as an engineering solution to increase productivity per unit area of crop available land, by extending plant cultivation into the vertical dimension (Despommier, 2013; Eigenbrod and Gruda, 2014; Thomaier et al., 2015). To date, there are few examples of the large-scale implementation of vertical farming. These comprise growth spaces (e.g. glasshouses) stacked on top of each other to construct vertical farm skyscrapers built specifically for food production (Despommier, 2011). The only real-world examples of the large scale vertical farming concept being currently implemented are building-integrated agriculture (Eigenbrod and Gruda, 2014) or zero-acreage farming (Specht et al., 2014). These approaches involve the incorporation of food production in and on existing buildings, e.g. on rooftop gardens, edible green walls and indoor farms (Specht et al., 2015). A similar

concept of stacked crop production units can be seen on a smaller scale through Vertical Farming Systems (VFS), which are growth systems that expand crop production into the vertical dimension (Hochmuth and Hochmuth, 2001; Resh, 2012). Examples of VFS are presented in Figure 1.1 and include: column-type VFS (Liu et al., 2004; Linsley-Noakes et al., 2006; Ramírez-Gómez et al., 2011; Rius-Ruiz et al., 2014; Chandra et al., 2014; Lee et al., 2015), pyramid-like shaped A-frame designs (El-Behairy et al., 2000; Hayden, 2006), conveyor driven stacked growth systems (Bayley et al., 2010; Mahdavi et al., 2012), and plant factory approaches (Morimoto et al., 1995; Hahn et al., 1996; Kato et al., 2010; Kozai et al., 2015; Sago, 2016).



Figure 1.1. Vertical Farming Systems (VFS) currently used in the food production industry: (A) column-type VFS (www.towergarden.com) in which plants are grown in upright vertical columns or pipes, (B) Pyramid like A-frame designs (www.skygreens.com/about-skygreens) which grow plants across the sides of the pyramid, (C) Conveyor driven stacked growth systems (www.verticrop.com) that rotate crop growing platforms to increase uniformity of light distribution within the

VFS, (D) Plant factory approaches (farmedhere.com) which entail enclosed and fully controlled systems which grow crops in stacked shelves under artificial lighting, with a dedicated lighting system for each crop producing shelf.

As VFS offer the potential to maximise space use efficiency for crop production, they have been exploited to produce food in rather unconventional urban settings in which space is limited (Schnitzler, 2013). For example, VFS have been used as the main production system within an abandoned (plastics) factory by Green Spirit Farms in Michigan, USA (Figure 1.2.A), to grow leafy vegetables and herbs within a café space of the Farm: London- a based Farm project in Hackney, London (Figure 1.2.B), and within glasshouses and on shipping containers located on rooftops such as in the Growup project in London, UK (Figure 1.2.C) and the Bell Book & Candle restaurant in New York, USA (Figure 1.2.D). In all these examples, the distance between production and consumption is minimized (Kozai, Niu and Takagaki, 2015), demonstrating how urban use of VFS may provide environmental benefits by reducing “food miles” and consequently the carbon footprint of food production (Eigenbrod and Gruda, 2014).



Figure 1.2. Vertical Farming Systems (VFS) within different urban environments: (A) Stacked growing shelves of a plant factory VFS within a previously abandoned factory (www.greenspiritfarms.com) (B) Vertical columns and plant factory set-up within a cafe space (farmlondon.weebly.com/index.html) (C) Protected (growup.org.uk) and (D) unprotected vertical columns on urban rooftops (bbandcnyc.com).

1.4 Cultivation methods in vertical farming systems.

The majority of VFS employ soilless growing methods such as aeroponics, hydroponics and semi-hydroponics. All systems use a defined nutrient solution to meet plant nutritional needs (Jones, 1982; Ritter et al., 2001). In aeroponics, the roots of plants are suspended in a sprayed fine mist of nutrient solution (Christie and Nichols, 2004). In hydroponics, the roots are immersed in aerated nutrient solution in a method commonly known as a Deep Flow Technique System (DFTS) (Goto et al., 1996; Park and Kurata, 2009). Alternatively, the roots are suspended in a thin flowing

stream of nutrient solution along a water-tight channel usually made from PVC pipes or guttering, as in the case with Nutrient Film Technique System (NFTS) (Cooper 1978; Jones, 2004; Resh, 2012). Semi-hydroponics systems use soilless media such as perlite, expanded clay pebbles, rockwool or sand with a nutrient solution (Eltrop and Marschner, 1996; Mateus-Rodriguez et al., 2013) and have been primarily exploited to grow crops such as tomatoes, cucumbers and peppers (Jensen, 1997).

Soilless production systems have been reported to enhance crop growth rates and to deliver up to 75% increase in production yields (Steinberg et al., 2000; Norén et al., 2004; Manzocco et al., 2011). In addition, they have been reported to utilise land and water more efficiently in comparison to conventional soil-based cultivation (Lages Barbosa et al., 2015), to avoid soil-borne pathogens and contaminants, and to provide standardised, reproducible growing practises (Falovo et al., 2009). However, energy availability has been identified as a key limitation to the sustainability and adoption of hydroponic methods (Lages Barbosa et al., 2015). The high start-up costs of hydroponic installations, and the increased technical skill required to operate these systems may also restrict their expansion (Savvas, 2003). Furthermore, vertical gradients in light distribution and nutrient availability may influence crop productivity within VFS (Liu et al., 2004; Ramírez-Gómez et al., 2012; Jones, 2014). Nevertheless, simplified hydroponic approaches have been successfully implemented as a low-cost alternative to overcome some of these barriers within commercial intensive hydroponics (Fecondini et al., 2010; Orsini et al., 2010, 2013; Eigenbrod and Gruda, 2014).

1.5 Lettuce cultivation in vertical farming systems.

Lettuce (*Lactuca sativa L.*) is classified as a 'fourth range' product, which is a category that includes fresh vegetables that are cleaned, cut and placed into sealed plastic containers, often in a modified atmosphere, to be consumed raw (Bevilacqua et al., 2009). It is an annual herbaceous plant of the *Compositae* family (Chon et al., 2005), a major food crop in the EU (Baslam et al., 2011), and a widely grown leafy vegetable in hydroponics and VFS (Kimura and Rodriguez-Amaya, 2003; Lee et al., 2006; Bayley, Yu, and Frediani 2011; Lin et al., 2013). Therefore, lettuce provides an ideal model crop for studying plant growth and resource use efficiency within VFS.

In hydroponic systems, the frequent monitoring of nutrient solution temperature, pH, electrical conductivity (EC) and dissolved oxygen (DO) concentration is imperative to maintain optimal growing conditions (Brechner and Both, 2016). Lettuce is a cool season crop, with average optimum temperature for growth of 18°C (Jenni, 2005). Nutrient solution pH can affect nutrient availability even if it doesn't directly affect crop growth, with pH 5.8 reported to provide optimal nutrient availability in hydroponic growth systems (Bugbee, 2003). Electrical conductivity of the nutrient solution is recommended to not exceed 2.0 dS m⁻¹ due to lettuce's high sensitivity to salinity (Andriolo et al., 2005). DO concentration values below 2.1 mg l⁻¹ can inhibit lettuce growth and an average of 8.4 mg l⁻¹ (saturated) is considered optimal (Goto et al., 1996). Optimal and supra-optimal growing conditions lead to luxuriant growth and are often employed in VFS to accelerate growth rates (Gruda, 2005; Koyama et al., 2012; Sago, 2016).

However, lettuce crops grown under luxuriant growth conditions in VFS, such as

excessive light intensities, high temperatures, elevated CO₂ levels and supra-optimal nitrogen supply, often develop a physiological disorder called tipburn (Saure, 1998; Barta and Tibbitts, 2000; Gruda, 2005; Wien and Villiers, 2005; Koyama et al., 2012; Lee et al., 2013; Kozai, Niu, and Takagaki, 2015; Sago, 2016). This represents a potential limitation to the commercial exploitation of VFS. It is therefore important to gain an understanding of the mechanisms underlying the development and amelioration of tipburn in VFS-grown lettuce in order to optimise this approach as a commercially viable production system.

1.6 Tipburn of lettuce.

1.6.1 An unpredictable and irreversible physiological disorder.

Tipburn of lettuce is an irreversible physiological disorder that decreases plant quality (Wissemeier and Zühlke, 2002; Hartz et al., 2007; Corriveau et al., 2010; Jenni and Hayes, 2010), resulting in significant economic losses (Koyama et al., 2012). Visible symptoms of tipburn include the collapse and necrosis of margins and the apex of developing leaves (Collier and Tibbitts, 1982; Saure, 1998; Barta and Tibbitts, 2000; Corriveau et al., 2010) (Figure 1.3).



Figure 1.3. Tipburn of lettuce significantly affects crop quality and marketability. The disorder is characterised by dark black-brown necrotic leaf lesions starting at the margins of developing leaves, as indicated by the white arrows. Scale bar is 5 cm.

Tipburn occurrence is unpredictable and although the underlying mechanisms of the disorder are not fully understood (Saure, 1998; Kerton et al., 2009; Carassay et al., 2012), a localized Calcium (Ca) deficiency has been implicated (Collier and Tibbitts, 1982, 1984; Saure, 1998; Frantz et al., 2004). Ca deficiencies can promote general disintegration of the plasma membrane structure, as Ca is essential for membrane stability and selective permeability and the maintenance of cell integrity (Kirkby and Pilbeam, 1984). It has been suggested that tipburn occurs when lettuce growth rates exceed Ca supply to the tissue (Seginer et al., 2006).

A link between tipburn of lettuce and Ca was first established by experiments that used foliar Ca sprays to prevent symptoms (Kruger 1966; Thiobodeau and Minotti, 1969). Similarly, Ashkar and Ries (1971) showed that increasing the Ca concentration

of the nutrient solution also prevented tipburn. Subsequent studies quantifying Ca concentration of comparable but differently located tissues in lettuce heads have provided insights into the causal relationship between tipburn and Ca deficiency. Ca content progressively decreased from the outer to inner leaves of developing lettuce heads, with the inner leaves being more susceptible to the disorder (Thiobodeau and Minotti, 1969). Similarly, the water-soluble Ca concentration in the inner and middle leaves was lower than the outer leaves of mature lettuce heads, with lower Ca concentration in the heads of tipburn-sensitive lettuce cultivars in comparison to tipburn-resistant cultivars (Misaghi and Grogan, 1978; Collier and Huntington, 1983). As Ca is predominately xylem mobile, and thus distributed by the transpiration stream, low transpiration rates can result in insufficient Ca delivery to the enclosed young leaves within developing lettuce heads (White and Broadley, 2003; Gilliham et al., 2011). In a separate study, artificially enclosing the inner leaves using aluminized polyethylene sheaths (to reduce their transpiration rate) significantly decreased Ca concentration and produced a high incidence of tipburn (53% of leaves) compared to the almost symptom-less (<1% tipburn incidence) non-enclosed inner leaves (Gilliham and Tibbitts, 1986). Therefore, increasing the transpiration rate of the meristem to enhance Ca delivery can obviate tipburn incidence (Gilliham et al., 2011).

Electron microprobe x-ray analysis, allowing mineral analysis of individually separate and distinct leaf areas, provides strong evidence that tipburn of lettuce is caused by localised Ca deficiency (Barta and Tibbitts, 1991; 2000). Tissue Ca concentrations were significantly lower in tipburn affected areas of leaves compared to similar areas of non-affected leaves, whilst tissue magnesium concentration was negatively correlated with Ca concentration (Barta and Tibbitts, 1991). In addition, tissue Ca

concentrations decreased (from 1.0 to 0.7 mg g⁻¹ DW) during leaf enlargement (from 5 mm to 30 mm in length) in enclosed lettuce leaves, but increased in freely transpiring leaves (Barta and Tibbitts, 2000). Thus critical low Ca levels between 0.2 to 0.4 mg g⁻¹ DW in enclosed leaves are needed for tipburn development (Barta and Tibbitts, 2000).

Importantly, however, reduced Ca content can also be found in marginal areas of non-affected tissue (Ryder, 2012) and supplying the plant with additional Ca is not always effective in ameliorating the disorder (Dayod et al., 2010). Interestingly, a survey of 15 commercial romaine lettuce fields found no relationship between tipburn severity and leaf Ca concentration or soil Ca availability (Hartz et al., 2007) whilst in another study no relation between total leaf Ca concentration and tipburn symptoms was observed (Cresswell, 1991). Taken together, these results suggest that other factors in addition to Ca may also contribute to the induction of tipburn of lettuce symptoms.

1.6.2 Links between oxidative stress and Ca related disorders.

Tipburn symptoms can be induced in lettuce by factors that promote rapid and luxuriant growth such as excessive light intensities (Gaudreau et al., 1994; Seginer et al., 2006); high temperature (Jenni and Hayes, 2010) and supra-optimal nitrogen supply (Brumm and Schenk, 1992), and by adverse growing conditions such as root restriction (Olle, 2012), salinity (Carassay et al., 2012) and drought (Aroca, 2012; Périard et al., 2015). Interestingly, all of these environmental conditions may also evoke reactive oxygen species (ROS) accumulation and oxidative stress in plants (Suzuki and Mittler, 2006; Almeselmani et al., 2006; Sharma et al., 2012) suggesting that ROS might play a role in the induction of tipburn in lettuce. However, to date

there is little empirical evidence for a role of ROS in mediating the disorder (Carassay et al., 2012).

ROS are produced continuously in plants during electron transport and as by-products of aerobic metabolism within the chloroplasts, mitochondria and peroxisomes (Apel and Hirt, 2004; Gill and Tuteja, 2010). They include free radicals such as superoxide anions ($O_2^{\cdot-}$), hydroxyl radicals ($\cdot OH$), and non-radical molecules like hydrogen peroxide (H_2O_2) and singlet oxygen (1O_2) (Sharma et al., 2012). ROS are highly reactive and they can damage proteins, lipids, carbohydrates and DNA, resulting in oxidative stress and cell death (Ramel et al., 2012). Under steady state conditions, ROS levels are controlled by a complex system of non-enzymatic and enzymatic antioxidative defense mechanisms (Miller et al., 2010). These work synergistically to protect plant cells against free radical damage by scavenging excess ROS (Gill and Tuteja, 2010). Non-enzymatic antioxidative defense mechanisms include the major cellular redox buffers ascorbate (AsA) and glutathione (GSH), as well as tocopherols, polyphenols and carotenoids (Apel and Hirt, 2004; Sharma et al., 2012) (Table 1.1).

Table 1.1. Non-enzymatic antioxidant defence mechanisms functions and subcellular location.

Antioxidant	Functions	Subcellular location
Ascorbate (Asa)	Reduces H ₂ O ₂ to water via APX. Scavenges ROS generated by oxygen photoreduction and photorespiration. Regenerates α -tocopherol.	Detected in the majority of plant cell types, organelles and apoplast in plants. Abundant in photosynthetic tissues.
Glutathione (GSH)	Substrate of glutathione peroxidase (GPX) reactions. Participates in the regeneration of AsA as an electron donor, via the AsA-GSH cycle. Free radical scavenger.	Chloroplasts, endoplasmic reticulum, vacuoles and mitochondria.
Tocopherols (α , β , γ , and δ)	Principal role is the scavenging of lipid peroxyradicals. Scavengers of oxygen free radicals and ¹ O ₂ .	α -Tocopherol is mostly present in the chloroplasts of plant cells, while β , γ , and δ -homologues are usually found outside these organelles.

Antioxidant	Functions	Subcellular location
Carotenoids	Scavenges $^1\text{O}_2$ and minimizes the production of triplet chlorophyll.	In the thylakoid membranes of chloroplasts in the green, photosynthetic plant tissue and in chromoplasts in non photosynthetic tissues
Polyphenols	Direct ROS scavengers. Chelates metals that generate ROS via the Fenton reaction. Inhibits lipid peroxidation by trapping the lipid alkoxyl radical.	Polyphenols can be found in hydrophilic regions such as vacuoles and apoplasts and in lipophilic regions such as oil glands and waxy layers.

References: Erdman et al., 1993; Kamal-Eldin and Appelqvist, 1996; Noctor and Foyer, 1998; Smirnoff, 2000; Sakihama et al., 2002; Mittler et al., 2004; Ramel et al., 2012; Sharma et al., 2012; Ahmad, 2014.

Enzymatic antioxidative mechanisms include both enzymes that scavenge and detoxify ROS (e.g. superoxide dismutase, catalase, ascorbate peroxidase, guaiacol peroxidase), and enzymes that regenerate the active forms of the non-enzymatic antioxidants (e.g. monodehydroascorbate reductase, dehydroascorbate reductase, glutathione reductase) (Blokhina, Virolainen, and Fagerstedt, 2003) (Figure 1.4).

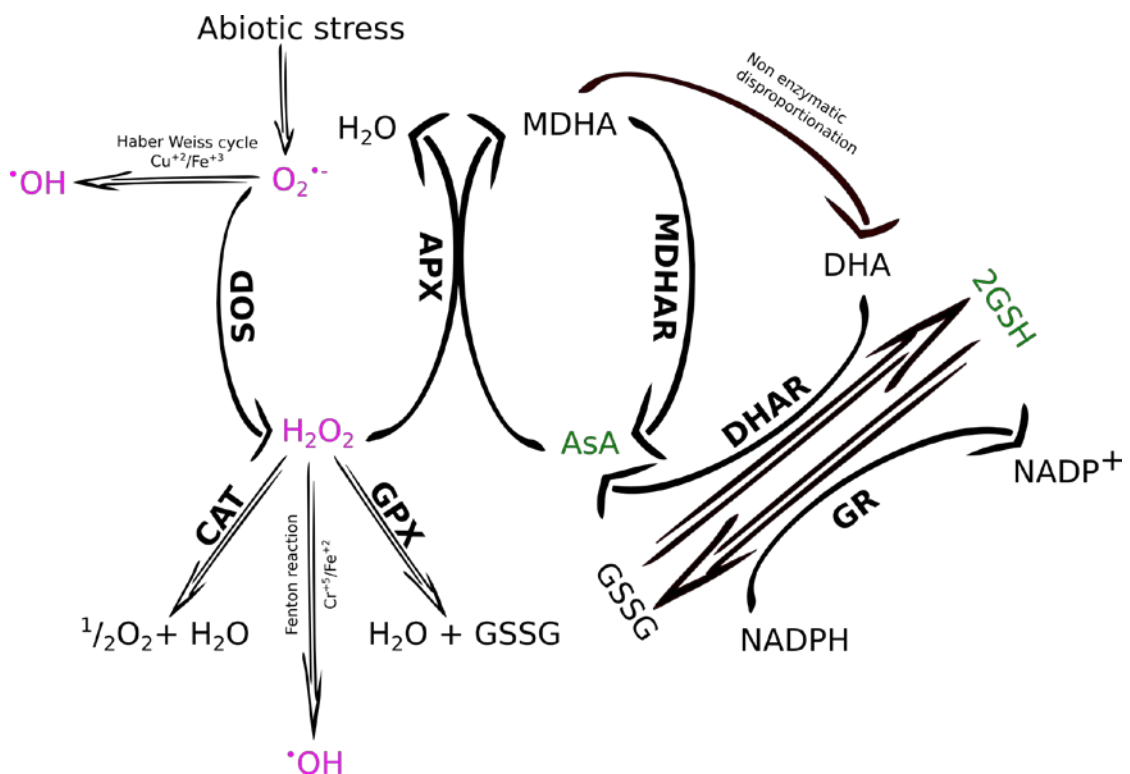


Figure 1.4. Schematic representation of antioxidant metabolic pathways in plants. Superoxide radical ($O_2^{\bullet-}$) is dismutated by superoxide dismutases (SOD) to hydrogen peroxide (H_2O_2). This is catalyzed to H_2O by catalase (CAT), ascorbate peroxidase (APX) or glutathione peroxidase (GPX). The hydroxyl radical ($\bullet OH$) is generated by $O_2^{\bullet-}$ in the presence of Cu^{+2} or Fe^{2+} ions (Haber Weiss cycle) or by H_2O_2 in the presence of Cr^{+5} and Fe^{+2} (Fenton reaction). In the ascorbate-glutathione cycle H_2O_2 is reduced to water by APX, ascorbate (AsA) is utilised as an electron donor. The monodehydroascorbate (MDHA) that is produced is regenerated by monodehydroascorbate reductase (MDAR). In addition, MDHA is non-enzymatically

disproportionated into dehydroascorbate (DHA). DHA is recycled to AsA by dehydroascorbate reductase (DHAR) using glutathione (GSH) as the reducing substrate. Oxidized glutathione (GSSG) is reduced by glutathione reductase (GR) using NADPH as electron donor. Antioxidant enzymes are represented by bold characters, ROS by magenta characters and non-enzymatic antioxidants by green characters (Adapted from Gill and Tuteja, 2010; Miller et al., 2010).

These enzymes function in concert to maintain an intercellular steady state-level of ROS in a range of subcellular compartments. The subcellular localization of antioxidant enzymes and the reaction catalysed by each enzyme are presented in Table 1.2 (Gaur and Sharma, 2013).

Table 1.2. Enzymatic antioxidant defence mechanisms, reaction catalysed and subcellular location.

Antioxidant enzyme	Reaction catalysed	Subcellular location
Superoxide dismutase (SOD, EC 1.15.1.1)	$O_2^{\bullet-} + O_2^{\bullet-} + 2H^+ \rightarrow 2H_2O_2 + O_2$	Chloroplasts, mitochondria, cytosol.
Catalase (CAT, EC 1.11.1.6)	$H_2O_2 \rightarrow H_2O + \frac{1}{2}O_2$	Peroxisomes.
Ascorbate peroxidase (APX, EC 1.1.11.1)	$H_2O_2 + AsA \rightarrow 2H_2O + DHA$	Chloroplasts, mitochondria, cytosol, peroxisomes.
Guaiacol peroxidase (GPX, EC 1.11.1.7)	$H_2O_2 + GSH \rightarrow 2H_2O + GSSG$	Chloroplasts, mitochondria, cytosol.
Monodehydroascorbate reductase (MDHAR, EC 1.6.5.4)	$MDHA + NAD(P)H \rightarrow AsA + NAD(P)^+$	Chloroplasts, mitochondria, cytosol, peroxisomes.
Dehydroascorbate reductase (DHAR, EC 1.8.5.1)	$DHA + 2GSH \rightarrow AsA + GSSG$	Chloroplasts, mitochondria, cytosol, peroxisomes.
Glutathione reductase (GR, EC 1.6.4.2)	$GSSG + NAD(P)H \rightarrow 2GSH + NAD(P)^+$	Chloroplasts, mitochondria, cytosol, peroxisomes.

References: Blokhina, Virolainen, and Fagerstedt, 2003; Miller et al., 2010; Gill and Tuteja, 2010; Gupta, 2010; Sharma et al., 2012; Gaur and Sharma, 2013

Although there is currently little empirical evidence for a role of ROS in mediating tipburn in lettuce (Carassay et al., 2012), a number of studies link ROS accumulation and oxidative stress with blossom-end rot (BER) of tomato and pepper. Like tipburn in lettuce, BER has been viewed as a Ca-related disorder (Adams and Ho, 1993; de Freitas et al., 2012). However, it has recently been proposed that increased ROS production leading to oxidative stress, ion leakage, and eventually to cell death, rather than Ca deficiency, might be the cause of BER (Saure, 2014). Oxidative stress was involved in initiating BER symptoms in two bell pepper cultivars with contrasting susceptibility to salinity, whereas fruit Ca content was not affected in both cultivars (Aktas et al., 2003). However, H₂O₂ and ¹O₂ production, as well as NADPH oxidase activity, were all increased in the salt-sensitive cultivar, which also exhibited significantly more BER symptoms (Aktas et al., 2003).

Enhanced BER symptoms were observed in bell pepper plants grown under high salinity, along with increased apoplastic ROS production, and enhanced NADPH oxidase activity in the pericarp when fruit were most sensitive to BER (Aktas et al., 2005). Although salinity did not affect fruit Ca concentrations, foliar and fruit manganese concentrations were significantly reduced. Since manganese serves as a ROS scavenger, this might be related to the observed apoplastic ROS accumulation (Aktas et al., 2005). Similarly, BER-affected pepper fruits had significantly increased H₂O₂ concentrations and apoplast-associated peroxidase activity, compared to healthy fruits when grown under salinity stress (Turhan et al., 2006). Apoplast-associated peroxidase activity, ascorbic acid and apoplastic ROS levels were significantly higher in a BER-susceptible cultivar compared to a BER-resistant cultivar. These results suggest that apoplastic antioxidant mechanisms may mitigate salinity damage and

BER expansion in pepper fruit (Turhan et al., 2006). BER symptoms, together with increased peroxidase activity and malondialdehyde (MDA) content, and decreased tocopherol content and SOD activity were observed in leaves of hydroponically-grown tomato (Schmitz-Eiberger et al., 2002). Similarly, an increase in the proteins participating in the ascorbate–glutathione cycle and the pentose phosphate pathway were observed in tomato fruits with BER symptoms, suggesting that these two biochemical pathways restrained the spread of the necrotic lesions to the whole fruit via ROS scavenging (Casado-Vela, Sellés, and Bru Martínez, 2005). Mestre et al. (2012) compared the oxidative metabolism of BER affected and healthy tomato fruit grown in Ca-deficient medium, concluding that the visual symptoms of BER resulted from a massive lipid peroxidation event following the breakdown of cellular glutathione homeostasis, as demonstrated by the inhibition of glutathione reductase (GR) in healthy tissue adjacent to BER lesions. Taken together, these findings suggest that ROS and oxidative stress play an important role in mediating the symptoms of Ca related disorders in *Solanaceae* crops.

Environmental factors that have the potential to cause tipburn of lettuce, as well as ROS accumulation and oxidative stress, are commonly found in hydroponics and VFS. These include high light intensities, high temperature, salinity and nutrient imbalances (Shi et al., 2007; Resh, 2012; Koyama et al., 2012; Kozai, Niu, and Takagaki, 2015; Sago, 2016). This raises the intriguing possibility that excessive ROS accumulation and the consequent oxidative stress may contribute to tipburn development in both VFS and hydroponic systems.

1.7 Environmental factors inducing tipburn of lettuce.

Environmental factors inducing tipburn that can also lead to localised Ca deficiency, ROS accumulation and oxidative stress, are commonly found in VFS and hydroponics (Figure 1.5).

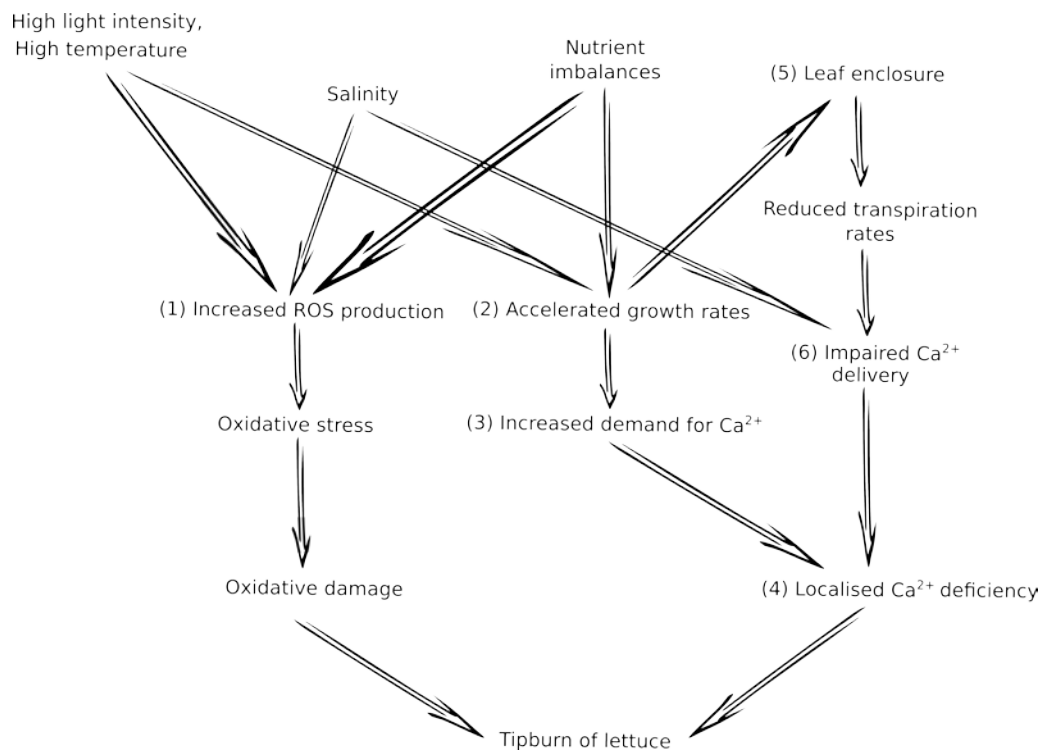


Figure 1.5. Flow chart summarizing mechanisms of common tipburn inducing factors in VFS and hydroponics. High light intensity and high temperature can increase ROS production and oxidative damage, if not controlled by the plant's antioxidant machinery (1). Both conditions can significantly accelerate lettuce growth rates (2), thereby increasing shoot's demand for Ca (3) which may lead to localised Ca deficiency (4). Rapidly growing lettuce plants can enclose young leaves within the lettuce head (5), leading to reduced transpiration rates, and impaired Ca delivery (6) and localised Ca deficiency (4). Salinity stress can impair Ca transport to young

developing leaves (6) and enhance ROS accumulation in plants (1). Nutrient imbalances can accelerate growth rates (2) if nutrients are provided in supra-optimal levels which can increase the shoot's demand for Ca (3), impair Ca delivery to the shoot via competition with other elements (6) and enhance ROS in cells (1).

1.7.1 Light intensity affects tipburn of lettuce induction.

Light intensity has a profound affect on lettuce growth and development in both protected (Ferentinos et al., 2000; Richards et al., 2004; Sago, 2016) and field growing conditions (Wolff and Coltman, 1990; Wissemeier and Zühlke, 2002). However, exposure of plants to light intensities, far exceeding the light saturation point of photosynthesis, results in high light stress (Demmig-Adams and Adams, 1992).

High light intensities created with the use of supplementary lighting in glasshouse trials can result in higher tipburn incidence in hydroponically grown lettuce (Gaudreau et al., 1994). Similarly, the use of supplementary lighting by high pressure sodium (HPS) and metal halide (MH) lamps, both of which increased photosynthetic photon flux density (PPFD) by $50 \mu\text{mol m}^{-2} \text{s}^{-1}$ at crop height, significantly enhanced lettuce tipburn symptoms in comparison to plants grown under natural glasshouse illumination (Chadjaa et al., 2001). Previously, high light intensity has been linked to tipburn symptoms via the acceleration of growth rates (Read and Tibbits, 1970; Sago, 2016) thereby increasing the demand for Ca in the developing meristems (Frantz et al., 2004). However, plants grown under low light intensity are not always free from tipburn (Saure, 1998). Therefore, it has been proposed that the underlying mechanisms of light-induced tipburn may not be restricted to accelerated growth rates but could

potentially involve other mechanisms such as oxidative stress driven by combined nutrient deficiencies and high light stress (Wissemeier and Zühlke, 2002).

High light intensity is one of the most common causes of oxidative stress in plants (Dat et al., 2000). It can enhance ROS production in cells (Suzuki and Mittler, 2006) and increases antioxidant enzyme activity (SOD, CAT and APX) and MDA content (Zhou et al., 2009; Fu et al., 2012) in lettuce plants. High light intensity inhibits the activity of photosystem II (PSII), leading to oxidative damage of its reaction center in a process known as photoinhibition (Aro, Virgin and Andersson, 1993). Photoinhibition occurs when incident light intensity exceeds a plant's capacity of CO₂ assimilation (Apel and Hirt, 2004). The extent of photoinhibition depends on the balance between the rate of light-dependent damage (photodamage) to PSII and the rate of its repair (Takahashi and Badger, 2011), which requires protein synthesis (Nishiyama et al., 2006). The rate of photodamage to PSII is linearly proportional to the intensity of incident light (Allakhverdiev and Murata, 2004; Takahashi and Murata, 2008) and the rate of PSII repair is susceptible to ROS inhibition (Nishiyama et al., 2006).

Photoinhibition leads to increased ¹O₂ concentrations in leaves (Nooden, 2003) which are produced mainly in PSII from ground-state oxygen interacting with triplet excited P680 and other triplet excited chlorophyll molecules within the PSII (Takahashi and Murata, 2005; Triantaphylidès and Havaux, 2009). ¹O₂ is a strong electrophile agent that can readily oxidize macromolecules such as lipids, proteins and DNA (Triantaphylidès and Havaux, 2009; Ramel et al., 2012) if not quenched by carotenoids or tocopherol (Krieger-Liszkay, 2005). According to Triantaphylidès et al.

(2008), $^1\text{O}_2$ is likely the primary cause of photodamage to PSII, and it may act as a signalling molecule provoking changes in gene expression which may lead to programmed cell death (Danon et al., 2005; Ramel et al., 2012). Photosystem I (PSI) is more resistant to high light stress in comparison to PSII (Scheller and Haldrup, 2005). However, PSI components also respond to high light intensities. In PSI, molecular oxygen (O_2) is reduced to $\text{O}_2^{\cdot-}$ through a process called the Mehler reaction (Triantaphylidès et al., 2008; Karuppanapandian et al., 2011). $\text{O}_2^{\cdot-}$ are disproportionate to H_2O_2 and O_2 catalysed by SOD (Asada, 2006). The H_2O_2 generated by SOD is detoxified to water by APX (Makino, Miyake, and Yokota, 2002). If not converted to water, H_2O_2 can oxidize a wide range of molecules inside the chloroplast or can diffuse outside the chloroplast envelope via aquaporins (Borisova et al., 2012). Therefore, the probability of oxidative stress mediated tipburn induction under high light intensity is highly likely.

1.7.2 High temperature and tipburn severity.

Heat or high temperature stress, defined as an increase in temperature beyond a critical threshold causing irreversible damage (Wahid et al., 2007; Gill and Tuteja, 2010), can affect plants both at the whole-plant and cellular level, altering growth and development (Gruda, 2005). This is particularly important for lettuce, a temperate crop, especially in regions with persistent high temperatures such as the tropics (He et al., 2001). High temperatures are usually coupled with high light intensities which may further enhance the adverse effects of the stress (Suzuki and Mittler, 2006). Adverse visual symptoms of high temperatures on plant growth include leaf senescence and abscission (Wahid et al., 2007).

High temperatures can promote the development of tipburn symptoms in lettuce (Yanagi et al., 1983; Jenni, 2005; Cancellier et al., 2010; Lee et al., 2013) and BER in tomato crops (Taylor and Locascio, 2004; Ho and White, 2005). Temperature increases from 0°C up to 36°C were positively correlated with tipburn severity (Misaghi and Grogan, 1978) and lowering leaf temperature by average 0.9°C using water-cooled high pressure sodium (HPS) lamps significantly reduced tipburn symptoms compared to conventionally air-cooled HPS lamps (Mankin and Walker, 1987). In addition, the combined effects of elevated temperatures (up to 37°C) and high humidity (> 90%) promoted tipburn development in tipburn resistant and susceptible lettuce cultivars, with resistant cultivars losing their ability to control tipburn development under extreme temperatures (Nagata and Stratton, 1994). Furthermore, tipburn incidence was positively correlated with air temperature over a three-year field study (Wissemeier and Zühlke, 2002). It is believed that high temperatures may promote tipburn by increasing growth rates (Yanagi et al., 1983; Saure, 1998; Choi et al., 2000).

Cellular changes induced by heat stress may lead to increased accumulation of ROS in PSI, PSII and in the Calvin–Benson cycle and may decrease the radical scavenging ability of the cell (Asada, 2006; Suzuki et al., 2012; Hasanuzzaman et al., 2013). Under high temperature (38°C), the enzyme ribulose-1,5-bisphosphate carboxylase/oxygenase (RuBisCO, EC 4.1.1.39) loses its specificity toward CO₂ *versus* O₂, producing H₂O₂ as a side reaction of its oxygenation (Kim and Portis, 2004). Loss of photosynthetic electron transport due to the thermolability of PSII can increase ¹O₂ accumulation within chloroplasts under high temperature stress (Ali et al., 2005). Interestingly, moderately high temperatures (35°C - 45°C) inhibit PSII repair

but do not impose serious PSII damage (Allakhverdiev et al., 2008). In contrast, PSI appears to be heat resistant in comparison to PSII (Haldimann and Feller, 2004). However, due to the very slow recovery rate of PSI, PSI photoinhibition is regarded as more dangerous than PSII photoinhibition (Kudoh and Sonoike, 2002). Higher NADPH/ATP ratio, due to increased ATP demand for photosynthetic CO₂ assimilation during high temperature stress (Yamori and Shikanai, 2016), can lead to PSI photoinhibition (caused by increased ROS generation) due to enhanced electron transfer to the Mehler reaction (Yan et al., 2013). Furthermore, ROS accumulation may occur in mitochondria as heat-induced impaired mitochondrial metabolism and may evoke oxidative bursts and induce oxidative damage (Suzuki and Mittler, 2006; Sun and Guo, 2016).

Interestingly, light-mediated heat-induced oxidative damage in *Arabidopsis thaliana* increased after the application of Ca channel blockers and calmodulin inhibitors, whereas adding exogenous CaCl₂ decreased oxidative damage (Larkindale and Knight, 2002). In addition, CaCl₂ pre-treatments increased SOD activity in *Agrostis stolonifera* under heat stress (Larkindale and Huang, 2004). This indicates that protection against heat-induced oxidative damage in *A. thaliana* requires Ca and calmodulin (Larkindale and Knight, 2002). Taken together, these studies suggest that tipburn induction under high temperature stress could be related to insufficient Ca delivery to the affected tissue, although it may also be mediated by increased ROS production and the consequent oxidative stress.

1.7.3 The role of plant nutrition in tipburn induction.

Cation imbalances in hydroponic nutrient solutions can often cause tipburn symptoms

in lettuce and other crops (Napier and Combrink, 2006). Root Ca^{2+} uptake can be stimulated by the presence of high levels of ions such as NO_3^- , and depressed by high levels of NH_4^+ , K^+ , Mg^{2+} and Al^{3+} in the nutrient solution (Kirkby, 1979; Ehret and Ho, 1986; Ryan and Kochian, 1993; Lieten, 2004; Frantz et al., 2004; Saure, 2005; Meriño-Gergichevich et al., 2010). With high levels of K^+ and Mg^{2+} in the nutrient solution, Ca^{2+} can be replaced by K^+ and Mg^{2+} on binding sites at the plasma membrane, leading to leaky membranes and tipburn symptoms (de Freitas and Mitcham, 2012). In hydroponically grown lettuce, tipburn symptoms were prevented by reducing the K/Ca ratio in the hydroponic solution from 3.5/1.0 to 1.25/1.0 (Huett, 1994). Interestingly, in hydroponically grown lettuce higher tipburn incidence was reported when K was added to the nutrient solution in the form of K_2SO_4 rather than KCl (Inthichack et al., 2012), an effect that was more evident at high K concentrations (643.7 mg l^{-1}), indicating a direct effect of K form and concentration on tipburn occurrence.

In field grown lettuce, supra-optimal N supply (up to 400 kg/ha) increased tipburn symptoms, possibly because of excessively high growth rates (Brumm and Schenk, 1992). In lettuce grown in NFTS, tipburn incidence was increased by the partial replacement of $\text{NO}_3\text{-N}$ in the nutrient solution with urea combined with NH_4Cl (Gunes et al., 1995). In contrast, increased N supply in crisphead lettuce alleviated tipburn symptoms in the external, older leaves (Sørensen et al., 1994). Tipburn was also induced in Chinese cabbage through the application of high levels of $\text{NH}_4^+\text{-N}$ fertilizer (Imai, 1990; Yu et al., 2002) whilst increased rates of urea and urea-ammonium nitrate decreased tipburn symptoms (Vavrina et al., 1993). Thus, nitrogen form and rate of supply can modulate tipburn occurrence.

Importantly, nutrient imbalances can also evoke oxidative stress in plants. For example, spinach plants grown in Ca deficient Hoagland's nutrient solution showed increased plasma membrane permeability, MDA and enhanced ROS accumulation, in addition to decreased activities of the antioxidant enzymes and glutathione content (Chao et al., 2009). Similarly, lipid peroxidation and inhibition of cellular glutathione homeostasis occurred in tomato plants grown in Ca-deficient medium (Mestre et al., 2012). Taken together, these studies suggest that tipburn symptoms may be induced through reduced Ca availability (caused by competition with other nutrients), by accelerated growth rates (caused by supra-optimal nutrient supply, in particularly NPK fertilisers) and nutrient-induced oxidative stress.

1.7.4 Salinity stress and tipburn.

Salinity stress results from the presence of solutes (ions) in the growing medium at concentrations that adversely affect plant growth (de Oliveira et al., 2013), and is commonly encountered in closed-loop soilless systems (Savvas et al., 2007). High solute concentrations in the rhizosphere decrease osmotic potential thereby limiting plant water uptake (Taiz and Zeiger, 2010). In addition to having osmotic effects, salinity can affect crops through specific ion toxicity and nutritional disorders (Läuchli and Grattan, 2007). For example, Ca transport to young developing leaves can be reduced by salinity (Lazof and Bernstein, 1999). A high salt concentration in the root zone appears to inhibit Ca loading to the xylem and consequently decreases shoot Ca content. This may cause Ca-related disorders, such as tipburn in lettuce (DePascale and Barbieri, 1995; Halperin et al., 1997; Volkmar et al., 1998; Lazof and Bernstein, 1999; Neves-Piestun and Bernstein, 2005; Läuchli and Grattan, 2007).

Lettuce is a moderately salt-tolerant crop (De Pascale and Barbieri, 1995) with a threshold of 1.1 dS/m soil salinity (Ünlükara et al., 2008). In hydroponic lettuce, moderate nutrient solution EC (2 dS/m) has been linked to tipburn occurrence (Cresswell, 1991; Huett, 1994) and EC levels above 2.6 dS/m result in decreased growth and yield (Andriolo et al., 2005).

Salinity stress enhances ROS accumulation in plants, increases lipid peroxidation, and the activities of antioxidant enzymes (Nor'aini et al., 1997; Sairam et al., 2002). Interestingly, it has been reported that tipburn symptoms in lettuce during high salinity conditions were mediated by increased ROS activity (Carassay et al., 2012). Therefore, salinity may promote tipburn of lettuce symptoms by inhibiting Ca uploading to the xylem but symptoms may also be mediated by increased ROS production and the consequent oxidative stress.

1.8 Control and prevention of tipburn of lettuce.

Although tipburn has been widely researched, there are few effective and practical solutions to prevent the disorder in lettuce (Hartz et al., 2007; Corriveau et al., 2012). Moreover, little attention has been given to other mechanisms that could contribute to tipburn development, which could potentially facilitate the development of novel approaches to ameliorate tipburn symptoms (Carassay et al., 2012).

1.8.1 Foliar Calcium applications.

Foliar Ca sprays have been used to prevent Ca-related disorders in crops (Amarante et al., 2001; Lanauskas and Kvikliene, 2006; Lötze et al., 2008; Olle and Bender, 2009). Although this could be extended to lettuce, the morphology and phyllotaxy of this

species may limit the effectiveness of this approach, preventing the sprayed solution from reaching the enclosed young leaves within the developing lettuce head, which are highly prone to tipburn due to their reduced transpiration rates (Misaghi et al., 1981; Barta and Tibbitts, 1986; Leclerc et al., 1992; Hartz et al., 2007; Torres et al., 2009; Jenni and Hayes, 2010). Nevertheless, foliar Ca applications significantly reduced tipburn symptoms and increased the Ca content of inner and outer leaves of saline-stressed butterhead lettuce plants (Saleh, 2009). Similarly, foliar applications of Ca (90, 180 and 360 mg l⁻¹ Ca twice a week) significantly decreased the total lettuce leaf area of romaine lettuce affected by tipburn, although there was no difference in the incidence of tipburn prevention between the three treatments (Corriveau et al., 2012). Thus, responses to Ca spraying may depend on lettuce leaf architecture, which determines whether the sprayed solution reaches the plant's centre (Corriveau et al., 2012). Direct application of Ca (1 mM Ca solution along with the Ca ionophore A23187) to leaves has also been shown to prevent tipburn symptoms in butterhead lettuce (Carassay et al., 2012), by facilitating the movement of Ca across cell membranes thereby increasing the Ca²⁺ concentration within cells (Ochwang'i et al., 2013; Sohn et al., 2013). Importantly, factors such as plant genotype, foliar spray concentration and application timing and frequency may significantly affect the efficacy of foliar applications in preventing Ca-deficiency symptoms (Chang et al., 2004).

Interestingly, foliar Ca applications can also benefit the plants in other ways. For example, CaCl₂ sprays increased antioxidant activity of *Camellia sinensis*, thereby improving post-drought recovery (Upadhyaya et al., 2011). Similarly, SOD activity in *Agrostis stolonifera* under heat stress was enhanced by CaCl₂ pre-treatments

(Larkindale and Huang, 2004).

1.8.2 Ventilation to prevent tipburn.

Tipburn often appears in tissues with low transpiration rates (Gilliham et al., 2011). In lettuce, leaf enclosure (overlapping of expanding leaves) is a primary reason for reduced transpiration rates of young leaves (Barta and Tibbitts, 1986; Chang and Miller, 2004). One way to increase the transpiration rates of enclosed leaves, and by extension prevent Ca-related disorders, is by blowing air directly into the folded leaves. Tipburn symptoms were prevented by blowing air directly into the inner leaves of developing lettuce heads, thereby ameliorating the effects of leaf enclosure, increasing transpiration rates and consequently transpiration-driven Ca delivery to the tissues (Goto and Takakura, 1992; Kossowski et al., 1994; Shibata et al., 1994; Both et al., 1994). A similar approach in which air was blown directly into the meristem was subsequently used to prevent tipburn of lettuce in high light ($1000 \mu\text{mol m}^{-2} \text{s}^{-1}$) and high CO_2 ($1200 \mu\text{mol mol}^{-1}$) conditions (Frantz et al., 2004).

Overhead fans have also been shown to significantly ameliorate upper leaf necrosis, a Ca deficiency disorder, of *Lilium* plants (Chang and Miller, 2004). Increasing the air flow over transgenic lettuce expressing a recombinant pharmaceutical protein, Stx2eB, increased leaf number and eliminated tipburn, irrespective of whether the air flow was from the side, above or below (Takahashi et al., 2011). More recently, Lee et al. (2013) exposed tipburn-sensitive cultivars to three different air temperatures and three different air flow conditions in a closed plant factory system, to establish a practical method of ameliorating tipburn in a commercial-scale VFS. Air flow applications

were more effective than controlling the air temperature to decrease tipburn symptoms in VFS (Lee et al., 2013).

1.8.3 Tipburn resistant lettuce cultivars.

Breeding and selecting tipburn-resistant lettuce cultivars can be a viable long-term solution for preventing tipburn symptoms (Nagata and Stratton, 1994; Jenni and Hayes, 2009). Lettuce cultivars vary considerable in terms of their susceptibility to tipburn (Ryder and Waycott, 1998; Choi and Lee, 2008; Ferriol et al., 2009; Koyama et al., 2012).

Interestingly, it has been suggested that red lettuce varieties show higher resistance to tipburn symptoms, possibly due to their higher antioxidant capacity, when compared to green lettuce varieties (Llorach et al., 2008; Mulabagal et al., 2010; Carassay et al., 2012). However, although a study of 70 different romaine, crisphead, green leaf and red leaf lettuce varieties reported significant effects of genotype on tipburn incidence, the results were not replicable over time, indicating that different environmental conditions influence the relative susceptibilities of lettuce cultivars to tipburn (Jenni and Hayes, 2009).

1.8.4 Modifications of relative air humidity.

High relative humidity (RH) during daylight hours can increase tipburn incidence in leafy vegetables (Barta and Tibbitts, 1986; Saure, 1998), potentially by impeding leaf transpiration and subsequently inhibiting Ca transport to the shoot (Gilliham et al., 2011; White, 2012). In contrast, high RH during the dark period can encourage root pressure flow, thereby enhancing Ca transport towards low transpiring tissue in leafy

vegetables and strawberries, inhibiting tipburn occurrence (Palzkill et al., 1976; Tibbitts and Palzkill, 1979; Guttridge et al., 1981; Cox and Dearman, 1981; Berkel, 1988; Kerton et al., 2009). Tipburn was completely eliminated when lettuce was grown at 40% RH during the daytime and 80% RH during the dark period (Choi and Lee, 2008). Furthermore, sprinkler irrigation used to mist the crop canopies thereby reducing the air temperature from above 28°C to 11°C, significantly reduced tipburn incidence of endive plants (Jenni et al., 2008). In contrast, fogging romaine lettuce plants in greenhouse conditions had no significant effect on tipburn occurrence (Corriveau et al., 2010). However, agronomic approaches that offer the potential to increase RH on a large scale, such as misting or fogging crop canopies, have not been yet adopted on a commercial level, possibly due to the high associated costs and potential encouragement of pest and disease caused by a higher humidity (Jenni and Hayes, 2010).

1.9 Thesis aims.

The aim of this thesis was to characterise a novel VFS and to identify limitations to crop growth in the VFS. Consequently, fundamental and applied plant science investigations were primarily planned to contribute to the successful establishment of VFS as commercially feasible means to increase crop productivity per area.

The objectives of this thesis are:

1. To compare the column-type VFS to a conventional Horizontal Hydroponic System (HHS), to test whether the VFS represents a viable alternative to HHS.
2. To elucidate the underlying mechanisms of tipburn of lettuce under luxuriant

growth conditions (high light intensity and high temperature), which were present within the upper layers of the VFS and are often employed to maximize the efficiency of VFS.

3. To elucidate the presymptomatic links between tipburn, oxidative stress and Ca.
4. To elucidate the molecular basis of tipburn of lettuce.
5. To identify potential novel approaches for the remediation of tipburn of lettuce.

To the authors knowledge, this study represents a first example where a commercial VFS was empirically scrutinized, a plant physiological issue was identified as a key limitation of the VFS and a research strategy was designed to explore plant science based solutions to enhance commercial exploitation of the VFS.

CHAPTER 2

CHARACTERISING A VERTICAL FARMING SYSTEM

2.1 Introduction.

Vertical Farming Systems (VFS) have been proposed as an engineering solution to increase crop production per unit area of available land (Despommier, 2013; Eigenbrod and Gruda, 2014; Thomaier et al., 2015). They achieve this by expanding crop production into the vertical dimension to produce a higher yield per unit area in comparison to conventional horizontal growth systems (Hochmuth and Hochmuth, 2001; Resh, 2012).

Recent studies have focused on column-type VFS (Liu et al., 2004; Linsley-Noakes et al., 2006; Ramírez-Gómez et al., 2012; Rius-Ruiz et al., 2014; Chandra et al., 2014; Lee et al., 2015). Although these studies have quantified crop production of column-type VFS, there have been few direct comparisons with horizontal hydroponic systems of similar cropping density. Thus, little information is available on whether column-type VFS present a viable alternative to horizontal crop production systems. In addition, previous yield comparisons of column-type VFS with horizontal systems have confounded other factors with crop orientation. For example, Liu et al. (2004) showed an increase in yields (up to 2-fold) and profits (3.6-5.5 US dollar m⁻²) in a soilless VFS compared to conventional soil cultivation, however the comparison failed to take account of the use of different growing media in both systems. Similarly, significantly higher yields have been reported for strawberry grown in a vertical column-type VFS compared to either conventional grow bags or multi-tiered stacked VFS (Ramírez-Gómez et al., 2012), although no information was provided regarding the root zone volume of the growth systems, a factor which can considerably influence the availability of below-ground resources and consequently crop growth (Poorter et al., 2012).

Column-type VFS are prone to marked gradients in the growing environment. Light intensity declines from top to base of different vertical column systems and affects the overall productivity of the system (Liu et al., 2004; Ramírez-Gómez et al., 2012). In addition, it has been proposed that nutrient concentration gradients within the gully of NFTS influence crop uniformity (Winsor, 1978; Puerta et al., 2007; Mavrogianopoulos, 2011) and it has been suggested that similar gradients exist along the vertical column of VFS (Jones, 2014).

Nitrate (NO_3^-) is the main source of nitrogen (N), the nutrient that plants need in greatest abundance (Crawford, 1995; Lérán et al., 2015), and large inputs of nitrogenous mineral fertilizers are required in agricultural systems to maintain plant growth and yield (Broadley et al., 2003). In hydroponic systems, the concentration of N in the nutrient solution is a key factor determining crop yield and quality (Jones, 2014) and low NO_3^- concentrations can decrease yield (Demšar et al., 2004).

The objective of this chapter was to characterise a prototype column-type VFS developed by the BBSRC CASE industrial partner, Saturn Bioponics Ltd (Birmingham, UK), which was patented under the trade name Saturn Grower. The research aimed to identify solutions to the industrial partner's challenges and fill existing gaps in the knowledge of plant behaviour in column-type VFS. Specifically, the chapter aims were to:

1. Compare the Saturn Grower column-type VFS to a conventional Horizontal Hydroponic System (HHS) with similar fertigation regimes, root zone volumes and planting densities, in which the systems only differ in their spatial orientation of the growth environment.

2. To identify and quantify putative light and NO_3^- concentration gradients within the Saturn Grower VFS.
3. To disentangle the effects of light intensity and NO_3^- concentration gradients within the VFS as key determinants of yield in column-type VFS. These studies identified additional areas of research required to optimize crop productivity and resource use efficiency in VFS.

2.2 Materials and methods.

2.2.1 Plant material.

Lettuce was used as a model plant as it is widely grown in hydroponics as a leafy vegetable (Kimura and Rodriguez-Amaya, 2003; Lee et al., 2006) with a fast growth rate (Lin et al., 2013) and avoids some of the complexities of changes in crop biomass allocation during the reproductive process (Heller et al., 2014). Romaine lettuce (*Lactuca sativa* L. cv. 'Little Gem') and butterhead lettuce (*L. sativa* L. cv. 'Frank') seeds were purchased from Moles Seeds (Essex, UK). Seeds were sown in 84-cell plug trays (Length 52 cm x Width 32 cm x Depth 5 cm, plug size 3.8 cm square) containing Levington M3 peat-based substrate (Scotts UK, Ipswich, UK) and germinated in a 3.4 m x 4.15 m walk-in Controlled Environment room (CE room) at 17°C (60-80% relative humidity). Photosynthetic Photon Flux Density (PPFD) was maintained at approximately $170 \mu\text{mol m}^{-2} \text{s}^{-1}$ at bench height under a 16 hour photoperiod (06:00 hrs to 22:00 hrs). Room temperature and humidity were recorded by Ektron II C sensor (HortiMaX B.V. Pijnacker, Netherlands), which was located in the middle of the CE room, at 1.83 m above the ground. Plants were transplanted at the four true-leaf stage, 20 days after sowing.

2.2.2 The Saturn Grower Vertical Farming System (VFS).

The VFS used in this study was a prototype column-type grower (Saturn Bioponics LTD, Birmingham, UK). Plants were grown vertically in upright cylindrical columns comprised of individual modular units stacked on top of each other to reduce the system footprint (Figure 2.1). Each modular unit comprised two stackable elements: a growing container (10.5 cm high and 7.5 cm radius) and a spacing collar (20 cm high and 7.5 cm radius).



Figure 2.1. The Saturn Grower VFS. The growing container formed from a single unit of moulded opaque plastic (dark green) incorporating a central core/airspace. The spacing collar formed from transparent plastic with four anti-diametrical planting apertures. When constructing the vertical column, the spacing collar was placed on the rim of the pot, allowing the installation of an additional growing container on top. Each VFS was sealed at both the top and bottom to create a vertical airspace within the core of each growing column. Scale bar is 5 cm.

The VFS's growing containers and spacing collars were sterilized in TriGene

disinfectant (MediChem International Ltd., UK) prior to filling the containers with 130 ± 0.5 g medium grade perlite (LBS Horticulture Ltd, Lancashire, UK). Highly porous perlite was the substrate of choice to minimize the risk of root-zone hypoxia and the resultant accumulation of ethylene (Geisler-Lee et al., 2010) within the airspace of the vertical column. The perlite was held in place by horticultural frost fleece (LBS Horticulture Ltd, Lancashire, UK) placed at the bottom of each growing container. The perlite in each container was levelled and seedlings were placed on the perlite at 90 degrees to the horizontal (Figure 2.2). This planting approach was followed, according to the designer's instructions, in an attempt to reduce labour effort during planting and harvest (A. Fisher, personal communication).



Figure 2.2. The Saturn Grower VFS's modular growth unit. Seedlings were planted within the VFS by gently placing the dark coloured peat block on top of, rather than planting into, the granular white perlite. Scale bar is 2 cm.

Each vertical column was supplied with half-strength Hoagland's solution (Hoagland

and Arnon, 1950) from a re-circulating 18 litre Titan PC4R Tank (Kingspan Environmental Ltd, Armagh, UK) through a 1.27 cm double walled PVC hose (LBS Horticulture Ltd, Lancashire, UK). The composition of the nutrient solution was 0.5 mM NH_4NO_3 , 1.75 mM $\text{Ca}(\text{NO}_3)_2 \cdot 4\text{H}_2\text{O}$, 2.01 mM KNO_3 , 1.01 mM KH_2PO_4 , 0.5 mM $\text{MgSO}_4 \cdot 7\text{H}_2\text{O}$, 1.57 μM $\text{MnSO}_4 \cdot 5\text{H}_2\text{O}$, 11.3 μM H_3BO_3 , 0.3 μM $\text{CuSO}_4 \cdot 5\text{H}_2\text{O}$, 0.032 μM $(\text{NH}_4)_6\text{Mo}_7\text{O}_{24} \cdot 4\text{H}_2\text{O}$, 1.04 μM $\text{ZnSO}_4 \cdot 7\text{H}_2\text{O}$ and 0.25 mM NaFe EDTA. Nutrient solution electrical conductivity (EC) was $1 \pm 0.2 \text{ dS m}^{-1}$. In closed-loop hydroponic systems, the concentration and pH of the nutrient solution is progressively modified by the effluent discharge (Guidi et al., 1997). Therefore, the pH of the nutrient solution was checked daily and maintained at $\text{pH } 5.8 \pm 0.2$ with the dropwise addition of 2 M H_3PO_4 and the nutrient solution in the tank was replaced weekly.

The nutrient solution was delivered to the top layer of the VFS via Hozelock 360 degree Micro Jet micro-sprinklers (Hozelock limited, Aylesbury, UK) allowing gravity driven drip-irrigation of plants in growing modules lower down the column. The effluent from the bottom layer of the VFS was subsequently returned to the tank and re-circulated around the growing system using a submersible aquarium water pump (All Pond Solutions Ltd, Middlesex, UK). The pump was capable of delivering a maximum of 3100 l h^{-1} . All hoses and pumps were connected using Hozelock Coupling 13 mm hose connectors (Hozelock limited, Aylesbury, UK) (Figure 2.3).



Figure 2.3. The closed-loop irrigation system of the Saturn Grower VFS. The white arrows indicate the route of the nutrient solution within the VFS. Nutrient solution was pumped to the top of the column, sprayed within the top layer by micro-sprinklers, dripped through the vertical layers and returned to the water tank to be re-circulated around the growing system. Scale bar is 10 cm.

Each pump was programmed using a multi-purpose electronic digital programmable timer (JoJo Waterproof Digital Outdoor Electrical Timer, Auction Z Ltd, Bradford, UK) allowing the micro-sprinklers to spray nutrient solution within the top layer of the VFS for 1 minute every hour. This watering frequency was adequate to ensure that all plants within the VFS were well watered (visual assessment).

2.2.3 Modifications of the VFS for experimental purposes.

Putative nutrient concentration gradients within the Saturn Grower VFS were investigated using a ten column six layered VFS. One blank column was used to evaluate the effect of perlite on the nutrient solution in the absence of plants within the VFS. The nine remaining columns were divided into three treatment groups, with three replicates per treatment. These were: columns with two planted layers (2L), columns with four planted layers (4L) and columns with six planted layers (6L), with layers 1 and 2, layers 1-4, and all layers being planted, respectively; numbering from the top of the column (Figure 2.4).



Figure 2.4. The different treatments representing four different planting densities: blank column (A), columns with two planted layers (2L) (B), columns with four planted layers (4L) (C) and columns with six planted layers (6L) (D). The photograph was taken 3 weeks after the plants were transferred to the VFS. Scale bars are 10 cm.

The relative effects of PPFD and NO_3^- concentration gradients on yield within the VFS were investigated by comparing crop productivity of columns with six planted

layers (6L) and single layer (SL) VFS. In total, three 6L and four SL VFS were planted. Each SL VFS was positioned to receive similar PPFD to the bottom layer of the 6L VFS and similar nutrient solution concentration to the top layer of the 6L VFS. Therefore, putative differences in yield between the SL VFS and the top layer of the 6L VFS would be attributed to the difference in PPFD, whereas putative differences in yield between the SL VFS and the bottom layer of the 6L VFS would be attributed to differences in NO_3^- concentration. To ensure that both the top layer of the 6L VFS and the SL VFS received comparable nutrient solutions, an open-loop system was used in which fresh nutrient solution was provided to the top of the VFS and the effluent from the bottom of the VFS was collected and later discharged (Figure 2.5).

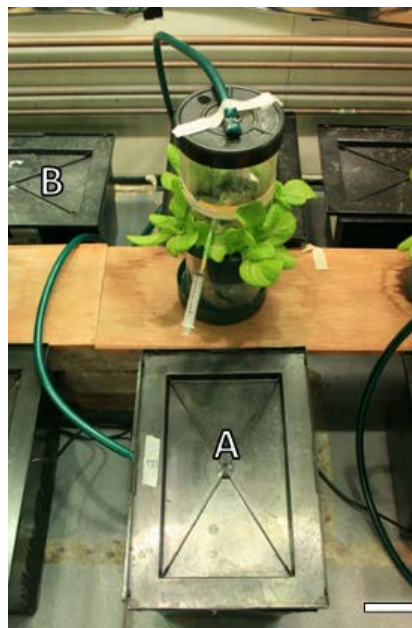


Figure 2.5. The open-loop irrigation system of the VFS, demonstrated on the SL VFS. The water tank at the bottom of picture (A) contained the submersible pump and provided fresh nutrient solution to the VFS. The water tank at the top of the picture (B) collected the effluent nutrient solution. The same approach was applied to all VFS of the study. Scale bar is 7.5cm.

2.2.4 The Horizontal Hydroponic System (HHS).

The Horizontal Hydroponic System (HHS) comprised five cylindrical PVC pipes (45.5 cm high and 3.6 cm radius), which were sterilized in TriGene disinfectant (MediChem International Ltd., UK). Each pipe was filled with 130 ± 0.5 g of perlite (LBS Horticulture Ltd, Lancashire, UK) and placed in parallel at 20 cm apart, centre to centre. Horticultural frost fleece (LBS Horticulture Ltd, Lancashire, UK) was placed in the outlet of each pipe to hold the perlite in place. Each pipe held four plants placed in 4.4 cm square holes, in rows. To minimise algal growth, black nylon fabric was used to cover the outlet channel of the system (Gibeaut et al., 1997). Each HHS contained 20 lettuce plants in total. The PVC pipes were mounted on commercial growth benches (90 cm from ground and 130 cm from lights). The height of commercial growth benches was equivalent to VFS's layer 2 (Figure 2.6).

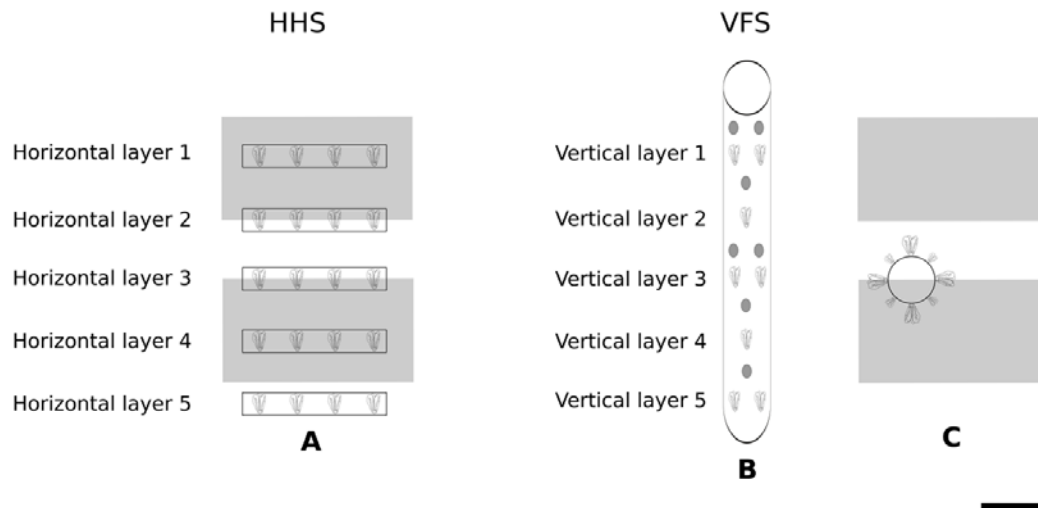


Figure 2.6. Schematic shows planting densities within the HHS and VFS. Overhead view of HHS (A). Side-view of VFS (B). Overhead view of VFS (C). The HHS occupied 0.4 m^2 of growing floor area, whereas the VFS occupied 0.02 m^2 per column of floor area. The grey rectangles show the exact position of the 400 W metal halide lamps above the growth systems. Scale bar is 20 cm.

2.2.5 Location of the studies.

Studies were performed either exclusively under artificial lighting in a CE room, or in a natural lit (with supplementary lighting) glasshouse to investigate the influence of natural illumination on light distribution within the VFS. Artificial lighting is the dominant approach found in most urban vertical farming projects (Kozai, 2015; He et al., 2015; Sago, 2016), and allows more precise control of environmental conditions (Poorter et al., 2012).

Specifically, two studies (Sections 2.3.1 and 2.3.3) were conducted in a 3.4 m x 4.15 m walk-in CE room at the Lancaster Environment Centre (LEC, Lancaster University, UK). Illumination was provided by twelve 400 W metal halide lamps (HQI-T 400N, Osram, St Helens, UK) for a 16 hour photoperiod (06:00 hrs to 22:00 hrs). Highly reflective plastic film (LBS Horticulture Ltd, Lancashire, UK) was placed on the walls of the room to increase the diffusion of light. Room air temperature ranged between 16°C and 18°C and relative humidity ranged from 60% to 80%.

A third study (Section 2.3.2) was conducted in a 3.20 m x 5.50 m heated and passively ventilated glasshouse at LEC. The glasshouse was naturally lit with supplementary lighting supplied by ten high-pressure sodium lamps (600 W Greenpower, Osram, St Helens, UK) for a 16 hour photoperiod (06:00 hrs to 22:00 hrs). Room air temperature ranged between 13.5°C and 26.9°C and relative humidity ranged from 25% to 60%.

2.2.6 Light intensity.

Photosynthetic Photon Flux Density (PPFD) measurements were obtained using a

Macam Q203 Quantum radiometer (Macam Photometrics LTD, Livingstone, UK). The quantum sensor was placed in the middle of the spacing collar, in a 10 cm radius zone around the vertical column in the VFS, and was placed 20 cm above the PVC pipes in the HHS. In the VFS and HHS comparison (Section 2.3.1), PPFD measurements were obtained one and five weeks after the plants were transferred to the growth systems. In the glasshouse study (Section 2.3.2), 3 6L VFS were used for PPFD measurements during three different days on week 2, 3 and 4, respectively. Measurements were performed with 3 hour sampling intervals and 5 time points, starting at 06:00 hrs and completing the measurements at approximately 18:30 hrs, to investigate diurnal PPFD changes within the VFS in the glasshouse (Figure 2.7).

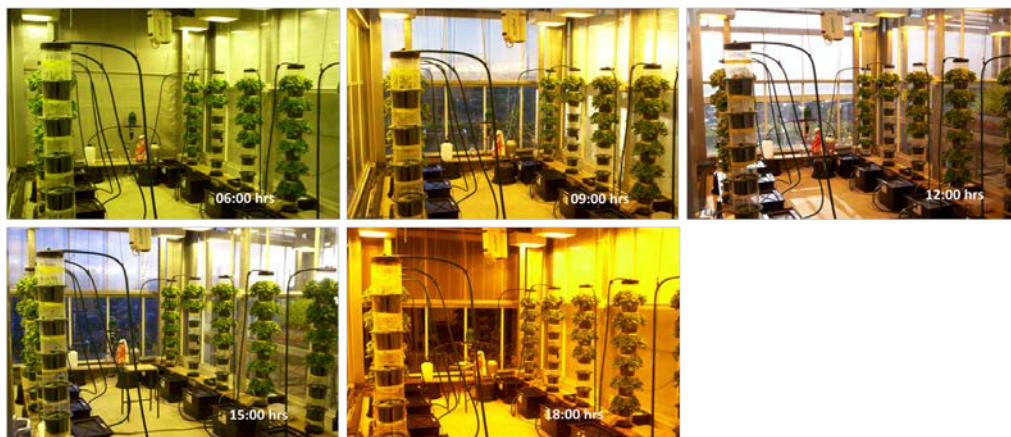


Figure 2.7. Color photographs taken at 06:00 hrs, 09:00 hrs, 12:00 hrs, 15:00 hrs, 18:00 hrs on the 5th of December 2012 (Week 4) show diurnal changes in light in the greenhouse (See Figure 2.11 for position of supplementary lighting from top of column.) That day was sunny, according to a weather report (www.metoffice.gov.uk).

In the second study in the CE room (Section 2.3.3), all vertical columns were used for measurements on two different days on the first and final weeks of the study, respectively. These dates were chosen to investigate the effect of plant growth on light distribution within the VFS in the absence of natural illumination.

2.2.7 System temperatures.

System diurnal root zone temperatures were recorded at 30 min intervals using the EL-USB-1 temperature data logger (Lascar Electronics Ltd., Salisbury, UK). The data loggers were buried within the perlite in the top and bottom layers of the VFS. Canopy temperature of plants grown with the top and bottom layers of the VFS were measured using a handheld infrared thermometer (model 39750-20, Cole Parmer Instruments Co., Chicago, IL) with a measurement area of 7.07 cm² at 5 cm distance from the canopy.

2.2.8 Crop yield.

Plants were harvested using a knife, starting from the top layer and moving downward. Shoot fresh weight was measured immediately after harvest using a 2 decimal point scientific balance.

2.2.9 Nitrate (NO₃⁻) concentration of the nutrient solution.

NO₃⁻ concentration was measured using a compact NO₃⁻ ion meter (Horiba LAQUA twin Model B-343, Kyoto, Japan). A two-point calibration (150 ppm and 2000 ppm) was conducted before measuring NO₃⁻ concentration and between every 3 measurements. NO₃⁻ content of the incoming solution was measured directly from within the tank of each column, and effluent was collected using 30 ml containers (SLS; Nottingham, UK).

2.2.10 Data analysis

To compare average shoot fresh weight per growth system using Student's t test, the data were square root transformed, as they were not normally distributed (Table 2.1). Yield and number of plants per occupied growing floor area for growth systems was used to calculate the ratio of VFS to HHS (Table 2.1). Linear regression analysis analyzed the relationship between shoot fresh weight and layers within growth system (Figures 2.9, 2.13 and 2.21) and between shoot fresh weight and PPFD (Figures 2.11, 2.17 and 2.24). Significant differences in PPFD within the VFS and the HHS were detected using one-way ANOVA followed by Tukey post-hoc analysis (Figure 2.10). Kruskal-Wallis ANOVA on ranks followed by Tukey post-hoc analysis was used to compare diurnal changes in PPFD (Figure 2.14) and differences in PPFD between vertical layers (Figure 2.15), as the distributions had unequal variances and this was not solved by transforming the data. The 3D surface plot in Figure 2.16 was assessed visually to explore the influence of time of the day and vertical layer on incident light intensity within the VFS. One-way analysis of variance (ANOVA) followed by Tukey post-hoc analysis investigated differences in NO_3^- concentration between incoming and effluent nutrient solution (Figure 2.18) and shoot fresh weight between top and bottom layers of the VFS (Figure 2.20). Kruskal-Wallis ANOVA on ranks followed by Dunn's method was used to compare PPFD between vertical layers and the single layered VFS because the data violated ANOVA assumption of normality and this was not solved by transforming the data (Figure 2.22). Student's t test was performed to ascertain statistical significance in PPFD between weeks 1 and 4 per plant within the VFS (Figure 2.23), differences in crop productivity between layers within the VFS in Section 2.3.2.1 and significant changes in NO_3^- concentration of the effluent

compared to the incoming nutrient solution in the blank column (Section 2.3.2.6). changes in root zone temperature of top and bottom layers within the VFS (Figure 2.25). One-way analysis of variance (ANOVA) and Student's t test were used to compare canopy temperature (Figure 2.26). Probability values less than 0.05 ($p < 0.05$) were considered to indicate a statistically significant difference. All statistical tests were performed on R version 3.1.2 software (R Development Core Team, 2014).

2.3 Results.

2.3.1 Comparing the VFS with a HHS.

To determine whether VFS represents a viable alternative to HHS, a VFS with five vertical layers was compared to a conventional HHS with similar fertigation regimes, root zone volumes and planting densities. Thus, the growth systems only differed in their spatial orientation. The CE room accommodated 2 VFS and 2 HHS, with one of each arranged on each side of the room (Figure 2.8). Plants were grown for 32 days.

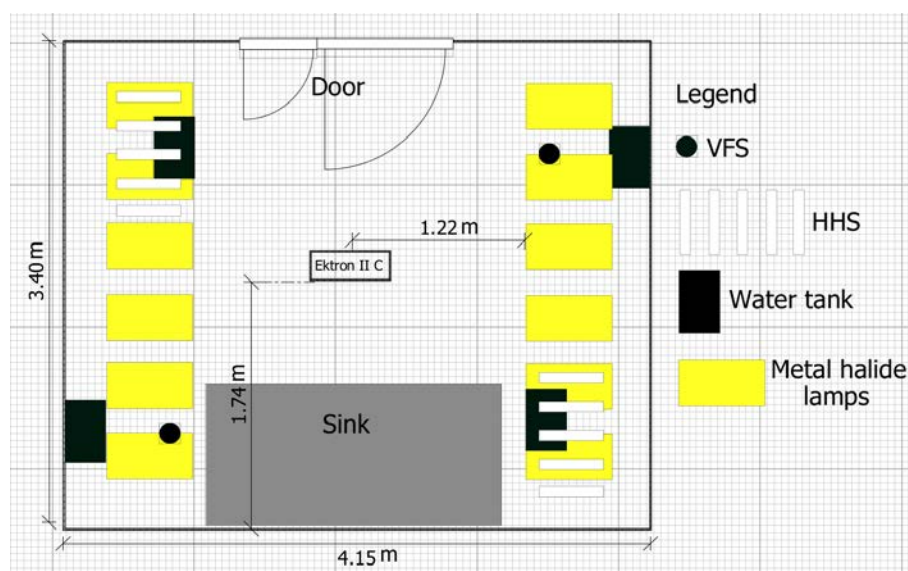


Figure 2.8. Floor plan of the controlled environment facility (CE room) at Lancaster Environment Centre. The yellow rectangles represent the exact position of the 400 W

metal halide lamps. The black circles and parallel five white rectangles represent the exact positions of the VFS and HHS respectively. The black rectangles represent the exact positions of the water tank. Measured lines (in metres) show the exact position of the Ektron II C sensor in relation to the metal halide lamps and sink and the CE room's exact dimensions. VFS and HHS are superimposed above the lamps for clarity.

2.3.1.1 The VFS produced more crop per unit area compared to the HHS

The VFS produced 13.8 times more crop, calculated as a ratio of yield (kg FW) to occupied growing floor area (m²) (Table 2.1). However, average FW (g) for lettuce crops grown within the HHS was significantly higher than of those grown within the VFS. Therefore, although the same number of plants was grown in each system, the HHS produced 1.7 kg more crop compared to the VFS (5.5 kg and 3.8 kg of crop in total, respectively). Consequently, the higher productivity of the VFS, in terms of kg FW m⁻² growing floor area, can be attributed to the 20 times higher number of plants per growing floor area achievable in the VFS over the HHS.

Table 2.1. Comparison of the productivity of the Vertical Farming System (VFS) and Horizontal Hydroponic System (HHS).

Parameter	HHS	VFS	Result
Shoot fresh weight (g) Average \pm SE (n=40)	138 \pm 6	95 \pm 6	p < 0.001 ^a
Yield per occupied floor area ^b (kg FW m ⁻²)	6.9	95	VFS/HHS = 13.8
Number of plants per occupied floor area ^b	50	1000	VFS/HHS = 20

^a Student's t-test on square root transformed data, t (78) = 5.66

^b HHS growing floor area: 0.4 m², VFS growing floor area: 0.02 m²

2.3.1.2 Yield decreased from top to base of VFS but was uniform within the HHS.

Shoot fresh weight decreased from top to base of vertical columns of the VFS, whereas there was no difference in productivity between the horizontal layers of the HHS (Figure 2.9). Crop productivity was normally distributed and uniform in the HHS with a range of 133 g, whereas in the VFS crop productivity had a range of 180 g within a non-normal distribution with positive skewness ($Sk=1.035$). Plants grown within the top layer of the VFS and within all layers of the HHS were of similar shoot fresh weight. However, in the middle and bottom layers (Layers 2-5) of the VFS, productivity decreased. As a result, the bottom layer of the VFS produced 43% less shoot fresh weight, in total, than the top layer of the VFS.

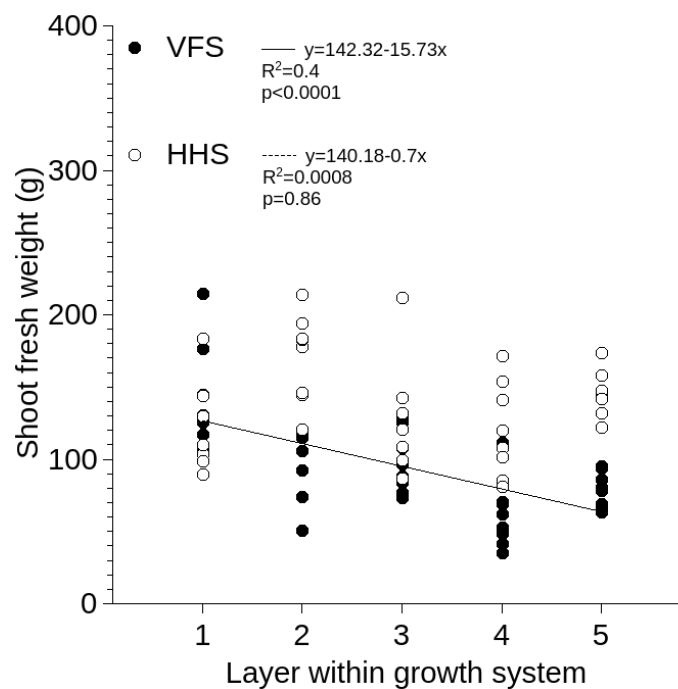


Figure 2.9. Shoot fresh weight of lettuce plants (*Lactuca sativa L.* cv. ‘Little Gem’) versus vertical layer in the VFS (solid line; closed symbols) and HHS (open symbols) respectively. The regression equation, adjusted R^2 values and significance of the regression (p-value) are reported at the top of the panel.

2.3.1.3 PPFD decreased from top to base of VFS

PPFD decreased significantly from top to base of vertical columns within the VFS, whereas no significant difference in PPFD was observed within the horizontal layers of the HHS (Figure 2.10). PPFD values varied between 491 and 134 $\mu\text{mol m}^{-2} \text{s}^{-1}$ from top to base of vertical column of the VFS and between 570 and 340 $\mu\text{mol m}^{-2} \text{s}^{-1}$ within the horizontal layers of the HHS. The top layer of the VFS received similar PPFD to all the horizontal layers of the HHS. However, there was no significant difference in PPFD between layers 2 and 3 and between layers 3, 4 and 5.

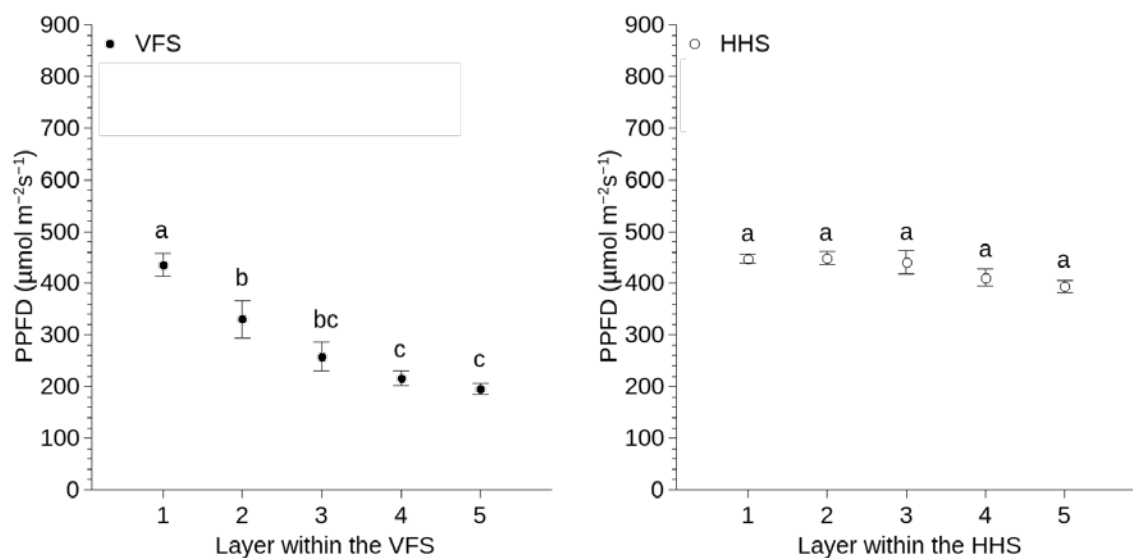


Figure 2.10. PPFD within the Vertical Farming System (VFS; closed symbols) and the Horizontal Hydroponic System (HHS; open symbols) plotted against layers in the growth systems. Values indicated with different letters indicate statistically significant differences (one-way ANOVA test; $F(4, 35) = 16.68$, $p < 0.01$ for the VFS and $F(4, 35) = 2.25$, $p = 0.06$ for the HHS, followed by Tukey post-hoc analysis), whereas those marked with the same letters show statistically similar values. Error bars represent SE ($n=8$).

2.3.1.4 PPFD influenced growth in the VFS but not in the HHS.

Shoot fresh weight increased significantly with PPFD in the VFS, indicating that as PPFD increased so did crop productivity. In contrast, there was no significant relationship between yield and PPFD within the HHS (Figure 2.11).

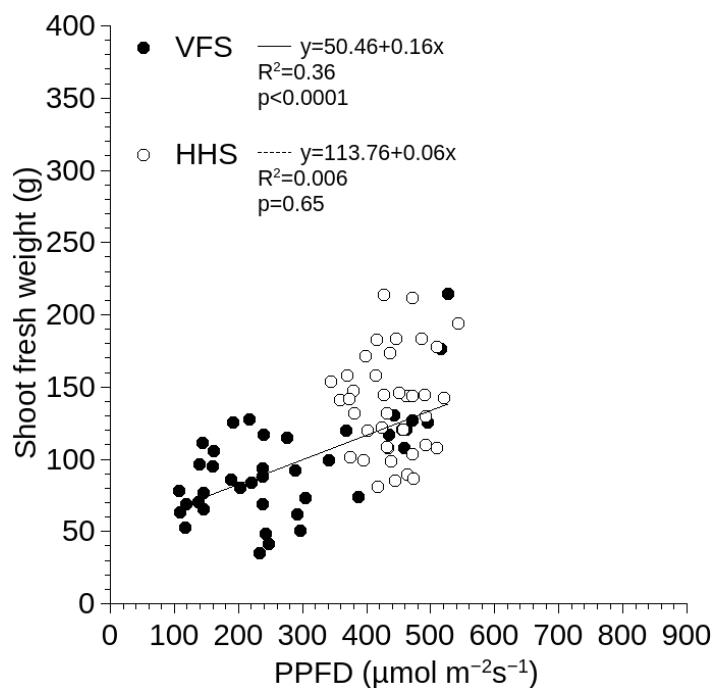


Figure 2.11. Shoot fresh weight of lettuce plants (*Lactuca sativa L.* cv. ‘Little Gem’) versus PPFD in the Vertical Farming System (VFS; solid line; closed symbols) and Horizontal Hydroponic System (HHS; open symbols) respectively. The regression equation, adjusted R^2 values, and significance of the regression (p-value) are reported at the top of the panel.

2.3.2 Identifying PPFD and nutrient concentration gradients within the VFS.

Putative nutrient concentration gradients within the VFS were investigated using a ten column six layered Saturn Grower VFS situated in the glasshouse in LEC (see Section 2.2.4). The vertical columns were positioned randomly (using the research randomizer

application (<http://www.randomizer.org>) and equally distant from each other (75 cm) on wooden benches. The exact positions of the treatments within the glasshouse are shown in Figure 2.12.

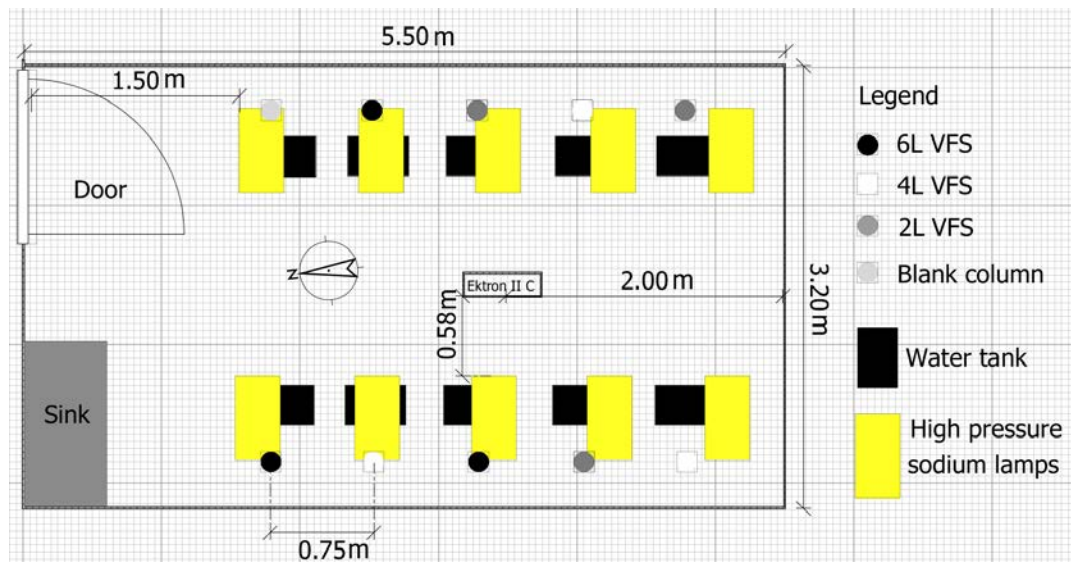


Figure 2.12. Floor plan of the experimental set up at Lancaster Environment Centre's glasshouse facility. The black, white, dark grey and light grey circles represent the exact position of the columns with six planted layers (6L), four planted layers (4L) and two planted layers (2L) and blank column within the glasshouse, respectively. The yellow rectangles represent the exact position of the 600 W HPS lamps. The Ektron II C sensor was positioned approximately in the middle of the glasshouse. Compass indicator shows the position of the glasshouse in relation to the North. Measured lines (in metres) show the exact position of the sensor in relation to the glasshouse's walls, distance between vertical columns and the glasshouse's exact dimensions. VFS are superimposed above the lamps for clarity.

2.3.2.1 Yield decreased from top to base of VFS in all planting density treatments.

Shoot fresh weight significantly decreased from top to base of the VFS in all

treatments (Figure 2.13). In all cases, the top layer of the VFS produced a higher yield than the remaining vertical layers. More specifically, within the 2L VFS the top layer produced 33% more crop compared to the bottom layer and within the 4L VFS and the 6L VFS the top layer produced 51% and 62% more crop than the bottom layer, respectively. Comparing the top to the second layer of the 4L VFS ($t = 3.78$ with 22 degrees of freedom, $p < 0.001$) and the 6L VFS ($t = 5.11$ with 22 degrees of freedom, $p < 0.001$) indicated differences in crop productivity that were evident from the very first transition between layers within the VFS.

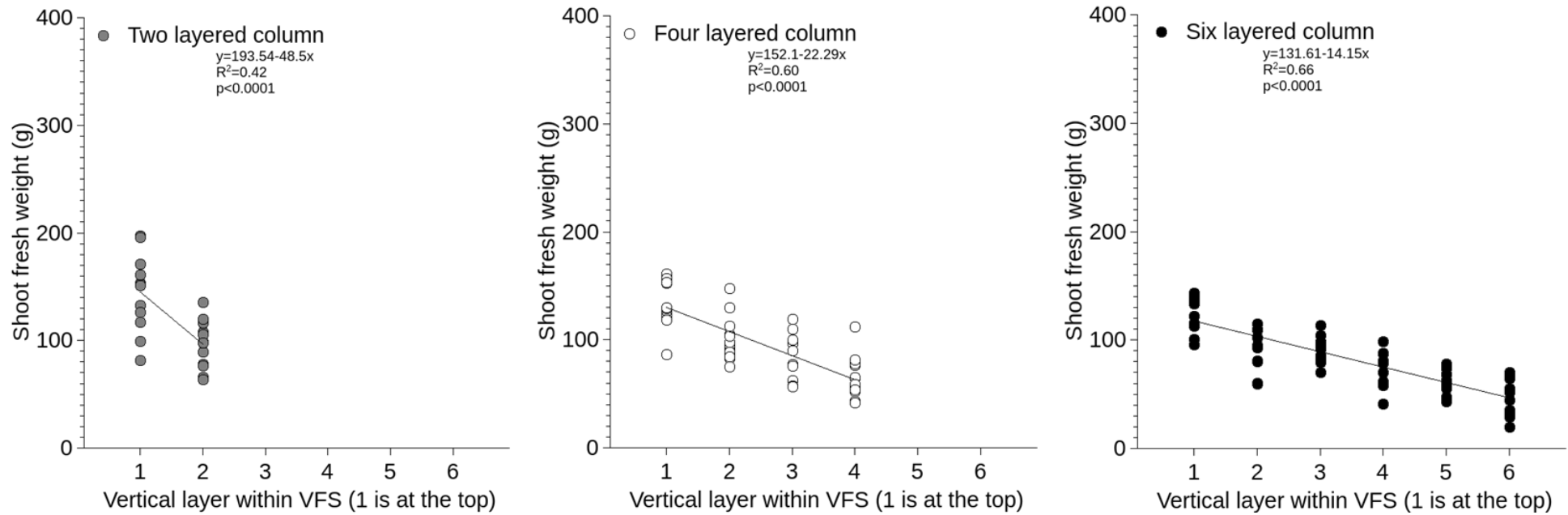


Figure 2.13. Linear regression analysis of shoot fresh weight versus layer in the 2L VFS (grey symbols), 4L VFS (open symbols) and 6L VFS (closed symbols). The regression equation, adjusted R^2 values and significance of the regression (p-value) are reported at the top of the panel.

2.3.2.2 PPFD peaked at 12:00 pm in the glasshouse.

PPFD within the VFS was measured at 5 time points with 3 hour sampling intervals; between 6:00 hrs and 18:30 hrs. PPFD was maximal at 12:00 hrs with no significant differences during the rest of the day (Figure 2.14). Although diurnal differences in PPFD occurred, artificial illumination may have contributed to the stability of light levels at 6:00 hrs, 9:00 hrs, 15:00 hrs and 18:00 hrs.

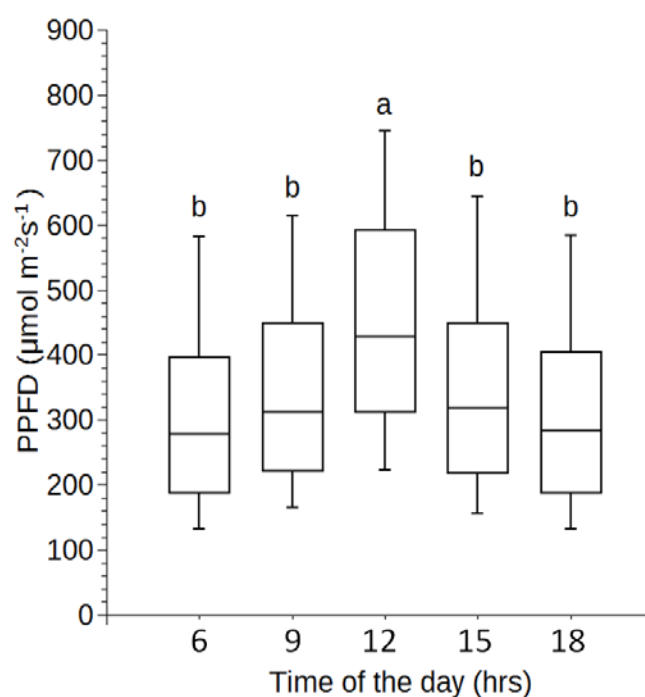


Figure 2.14. Diurnal distributions of light intensity within all layers of the VFS in the glasshouse. The horizontal line within the box represents the median. The boundaries of each box represent the lower 25th and upper 75th percentiles. The spacing of components within the box indicates skewness in the data. The whiskers represent the sample minimum and maximum values. Results of Kruskal-Wallis ANOVA on ranks followed by Tukey post-hoc analysis showed statistically significant differences ($H(4) = 106.290, p < 0.001$). Different letters indicate statistically significant differences.

2.3.2.3 PPF_D declined from top to base of VFS in the glasshouse.

PPFD decreased from top to base of the VFS (Figure 2.15). Interestingly, although light intensity between the three bottom layers (layers 4, 5 and 6) was not significantly different it was nevertheless significantly lower than the higher layers of the VFS.

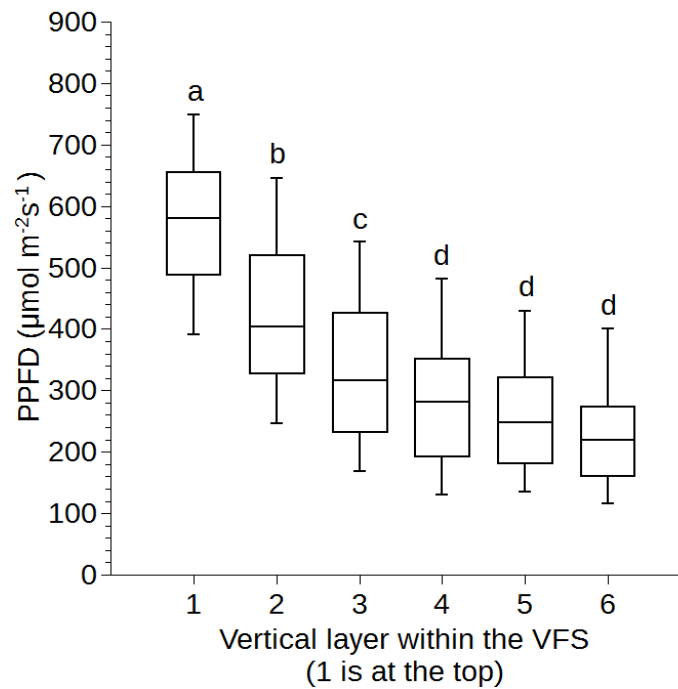


Figure 2.15. Box plots summarize the distributions of PPF_D within the vertical layers. The horizontal line within the box represents the median. The boundaries of each box represent the lower 25th and upper 75th percentiles. The spacing of components within the box indicates skewness in the data. The whiskers represent the sample minimum and maximum values. Results of Kruskal-Wallis ANOVA on ranks followed by Tukey post-hoc analysis showed statistically significant differences ($H(5) = 524.876$, $p < 0.001$). Different letters indicate statistically significant differences.

2.3.2.4 Natural illumination did not alleviate PPFD gradient within the VFS.

A 3D surface plot was generated to visually assess the influence of time of the day and vertical layer on PPFD within the VFS, simultaneously (Figure 2.16). Visual inspection of the 3D plot showed that PPFD declined from top to base of vertical column in all time points and that PPFD plateaued when approaching the three bottom layers. This was confirmed statistically in Figure 2.15. Importantly, the surface plot clearly shows that PPFD was higher at 12:00 hrs than other time-points in all vertical layers, as demonstrated by the ridge of the surface plot. Furthermore, at all times the top layer of the VFS received the highest PPFD in comparison to the other vertical layers. Thus, natural illumination did not alleviate the PPFD gradient within the VFS at any time-point.

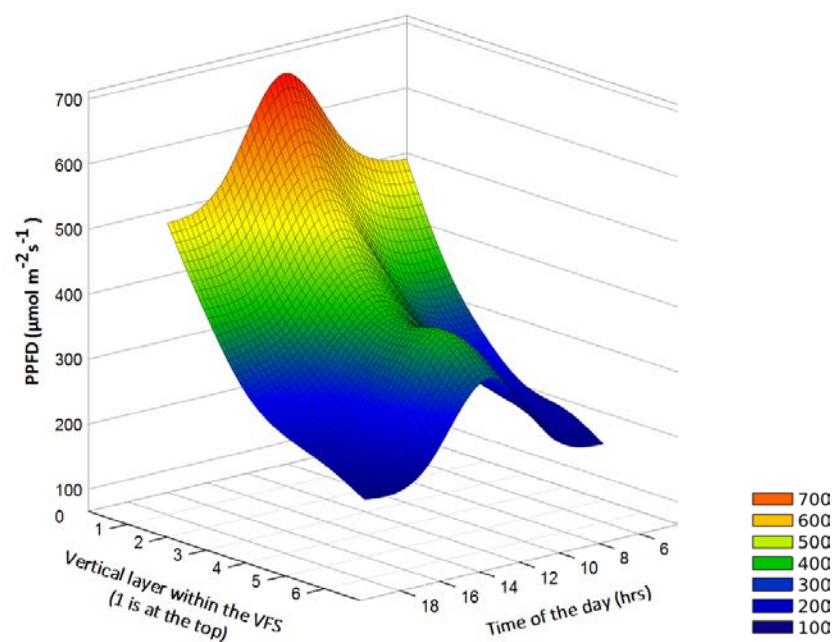


Figure 2.16. A 3D surface plot shows influence of time of the day (x-axis) and vertical layer (y-axis) on PPFD (z-axis) within the VFS. PPFD data are displayed on a pseudo-colour intensity scale; in which 'red' corresponds to the highest light intensity, whereas 'deep blue' represents lowest light intensity.

2.3.2.5 PPFD within the VFS significantly influenced yield.

Shoot fresh weight increased linearly with increased PPFD, indicating that as PPFD increased so did crop productivity, with PPFD explaining 49% of the variation in crop productivity (Figure 2.17).

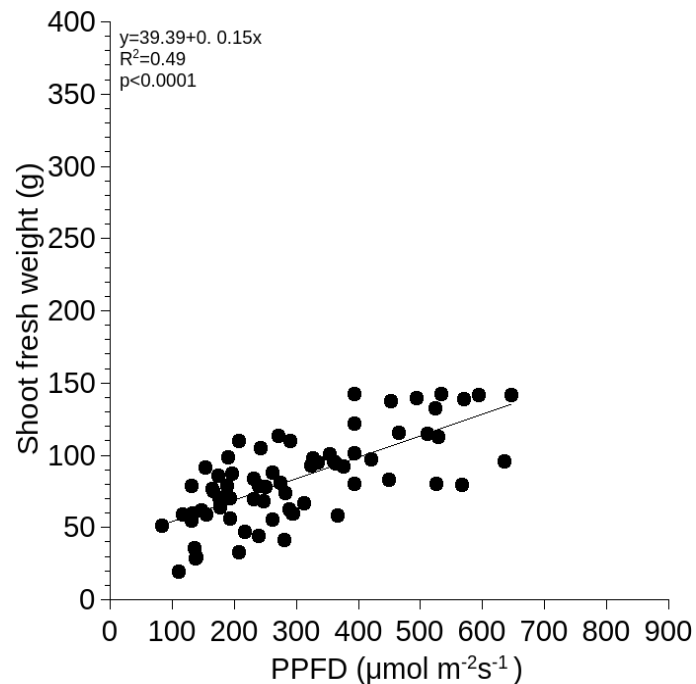


Figure 2.17. Linear regression analysis of shoot fresh weight (*Lactuca sativa L. cv. 'Frank'*) versus PPFD in the VFS. The regression equation, adjusted R^2 values, and significance of the regression (p-value) are reported at the top of the panel. Each point is an individual plant.

2.3.2.6 A nitrate concentration gradient within the VFS.

Nutrient solution NO_3^- concentrations decreased significantly as the number of planted vertical layers increased. Consequently, the effluent of the 2L VFS contained a significantly higher concentration of NO_3^- compared to the effluent of the 4L and 6L VFS (1.8-fold and 3.7-fold, respectively). The effluent of the 4L VFS contained a

significantly higher (2-fold) concentration NO_3^- concentration compared to the 6L VFS (Figure 2.18). There were no significant changes in NO_3^- concentration of the effluent solution in the blank column (without plants), according to student's t-test ($t = -1.974$ with 4 degrees of freedom, $p = 0.123$).

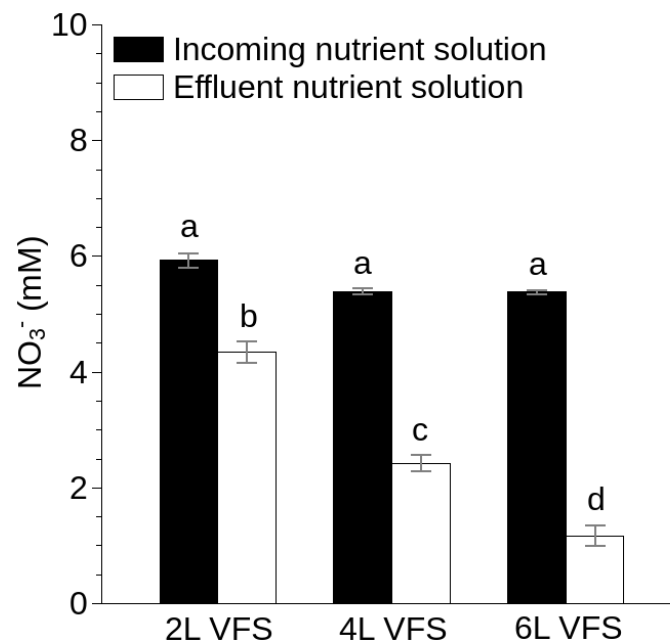


Figure 2.18. Differences in NO_3^- concentration between incoming (black bars) and effluent (white bars) nutrient solution. Values indicated with different letters indicate statistically significant differences according to one-way ANOVA test; $F(7,32) = 214.1$, $p < 0.001$, followed by Tukey post-hoc analysis. Bars represent means \pm SE ($n=6$).

2.3.3 Separating the effects of PPFD and NO_3^- concentration on yield.

The relative effects of PPFD and nutrient concentration gradients within the VFS on yield were investigated by comparing crop productivity in six layered (6L) and single layer (SL) VFS. The study was conducted under similar conditions to those described

in Section 2.3.1. The exact positions of the treatments within the CE room are shown in Figure 2.19.

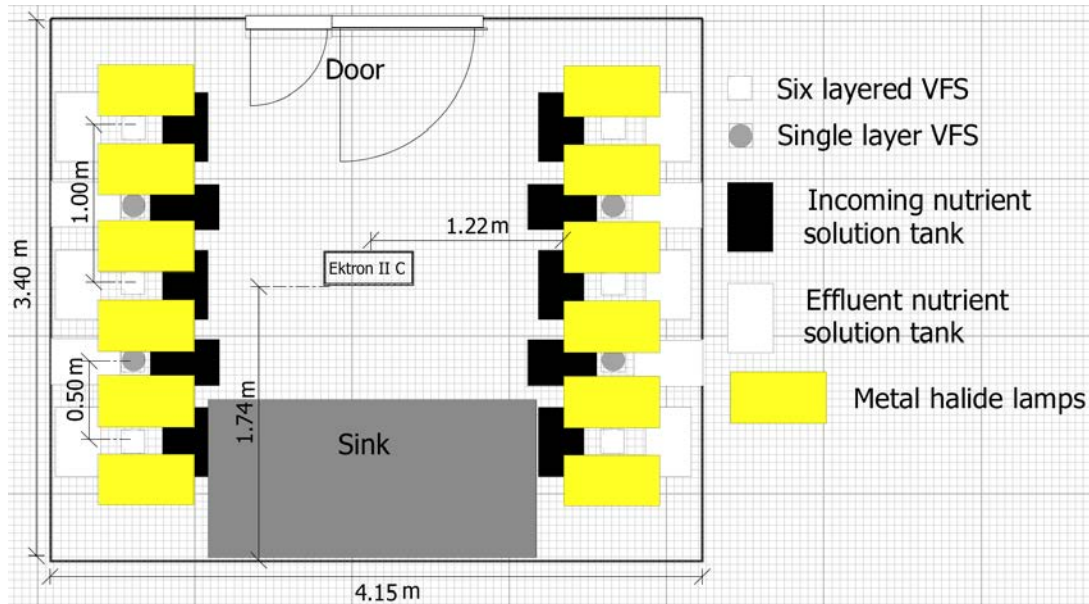


Figure 2.19. Floor plan of the CE room at Lancaster Environment Centre. The yellow rectangles represent the exact position of the 400 W metal halide lamps. The white and grey circles represent the exact position of the six layered (6L) and single layer (SL) VFS within the CE room, respectively. The white and black rectangles represent the exact position of the water tank contain incoming and effluent nutrient solution, respectively. VFS are superimposed above the lamps for clarity.

2.3.3.1 Nutrient concentration gradient did not affect yield under low PPFD.

The SL VFS produced 2.2-fold significantly lower yield than the top layer of the 6L VFS, even though the two vertical layers received nutrient solution of similar EC and pH. However, there was no significant difference in yield between the bottom layer of the VFS and the SL VFS (Figure 2.20).

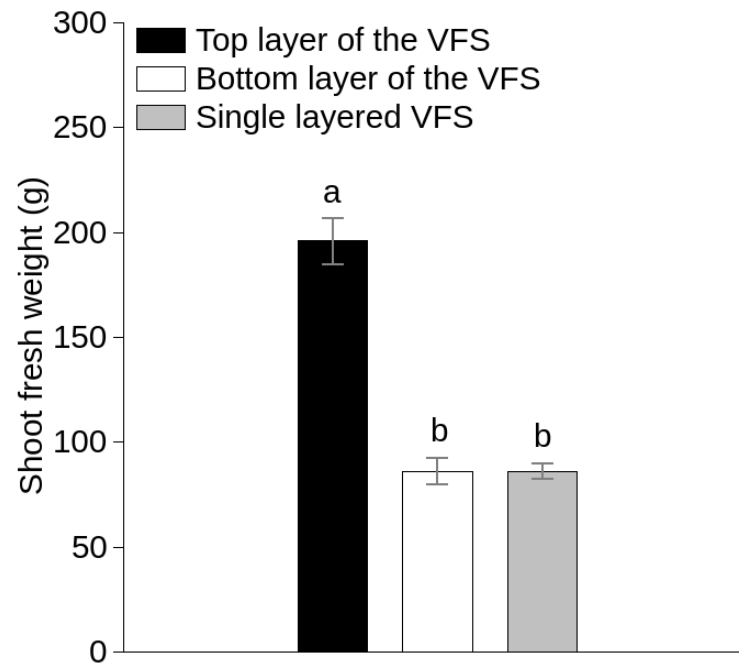


Figure 2.20. Shoot fresh weight (*Lactuca sativa* L. cv. 'Frank') per vertical layer within the VFS. Values indicated with different letters indicate statistically significant differences (one-way ANOVA test; $F(2,35) = 68.5$, $p < 0.001$, followed by Tukey post-hoc analysis). Bars are means of 12 plants \pm SE.

Crop productivity within the VFS showed a similar pattern to that observed previously (see Figures 2.9 and 2.13), exhibiting a significant decline in shoot fresh weight from top to base of the vertical column (Figure 2.21).

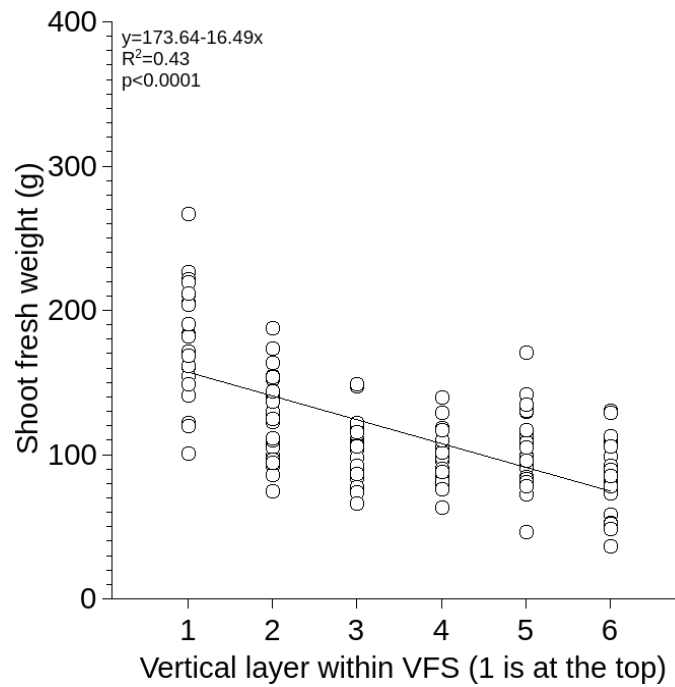


Figure 2.21. Shoot fresh weight (*Lactuca sativa* L. cv. ‘Frank’) versus layer in the within the six layered VFS. The regression equation, adjusted R^2 values and significance of the regression (p-value) are reported at the top of the panel. Each point is an individual plant.

2.3.3.1 Single layered VFS received similar PPFD to the bottom layer of the VFS.

PPFD decreased from top to base of vertical columns (Figure 2.22), with the top layer receiving significantly higher PPFD than all the other vertical layers. The SL VFS received similar PPFD to the fifth and sixth layers of the 6L VFS which was significantly different to all the remaining vertical layers and, importantly, significantly lower than the top layer of the 6L VFS. Taken together with Section 2.3.3.1, this indicates that PPFD, but not NO_3^- , was the main factor influencing crop productivity within the VFS.

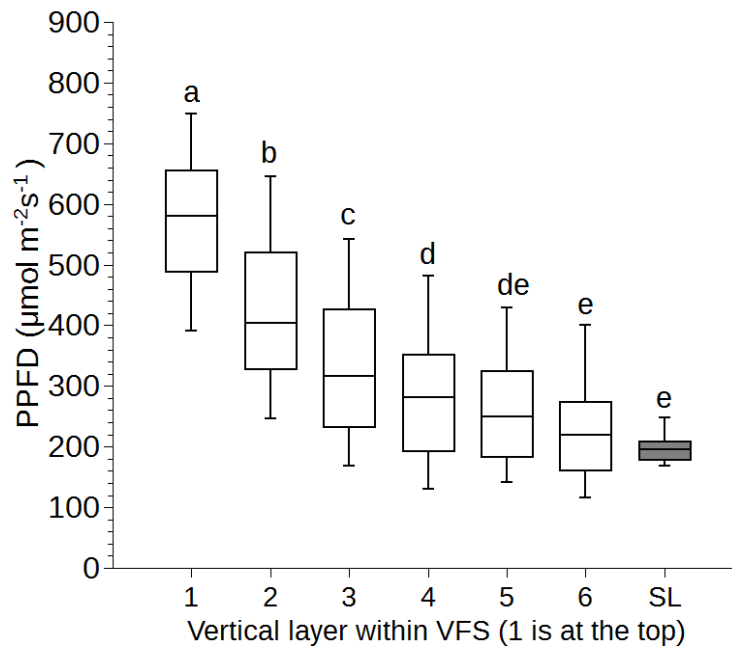


Figure 2.22. PPFD within all layers of the VFS. The horizontal line within the box represents the median. The boundaries of each box represent the lower 25th and upper 75th percentiles. The spacing of components within the box indicates skewness in the data. The whiskers represent the sample minimum and maximum values. Kruskal-Wallis ANOVA on ranks followed by Dunn's method showed statistically significant differences ($H(6) = 550.573$, $p < 0.001$). Differences were indicated by different letters.

2.3.3.2 Plants obscured lower positioned plants from light source.

There was no significant change in incident PPFD within layer 1 of the VFS between weeks 1 and 4 of the experiment. However, PPFD varied over time within the middle and bottom layers of the VFS. PPFD decreased significantly between weeks 1 and 4 in plants grown at layers 2 to 6 (Figure 2.23). This reduction was due to the larger plants in layer 1 of the VFS, as seen by their greater shoot fresh weight (see Figure 2.21), obscuring lower positioned plants from the light source.

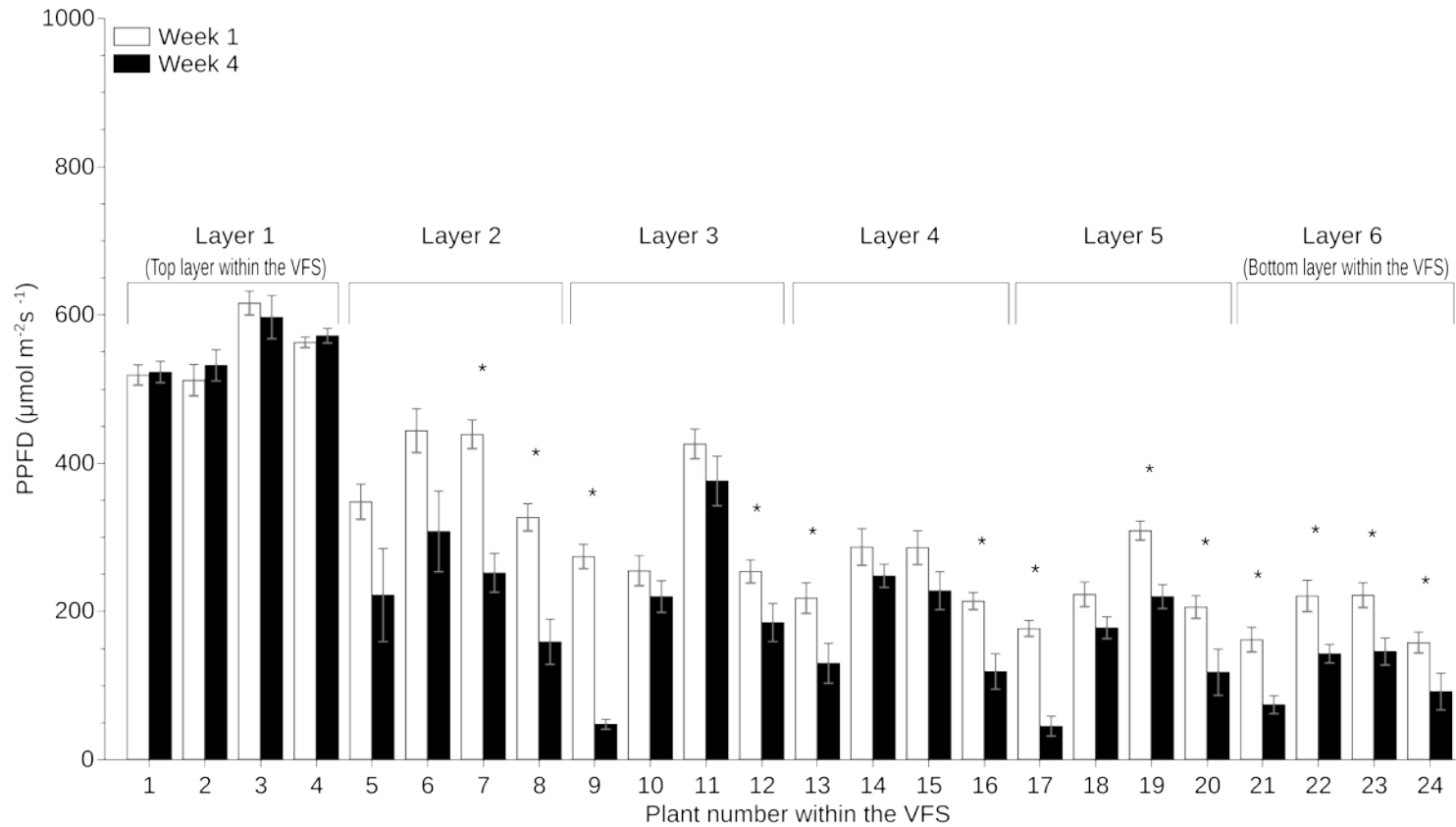


Figure 2.23. Barplot shows changes in incident light intensity (PPFD) between weeks 1 and 4 caused by a shading effect within the VFS as a result of plant growth. White bars represent PPFD measured during the first week of the experiment, whereas black bars represent PPFD measured four weeks after. Error bars represent SE (n=6). Values indicated with asterisk indicate statistically significant differences between week 1 and 4 (t-test, $p < 0.05$).

2.3.3.3 Yield was significantly correlated with PPFD.

Shoot fresh weight increased linearly with increased PPFD, with PPFD explaining 52% of the variation in crop productivity of 6L VFS (Figure 2.24).

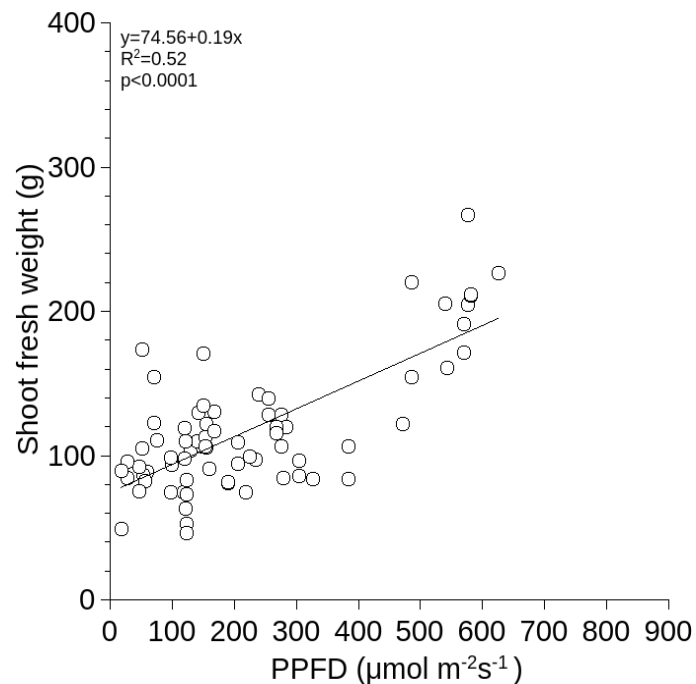


Figure 2.24. Shoot fresh weight (*Lactuca sativa* L. cv. 'Frank') versus PPFD in the VFS. The regression equation, adjusted R^2 values, and significance of the regression (p-value) are reported at the top of the panel. Each point is an individual plant.

2.3.4 Identification of temperature gradients.

Root zone temperatures within the VFS in both glasshouse (Section 2.3.2) and CE room (Section 2.3.3) environments were influenced by distance from the light source and photoperiod (Figure 2.25). In both cases, the top layers of the VFS had higher root zone temperature than the bottom layers. In the glasshouse study, the root zone temperatures in the top and bottom layers increased during the light period and were equalised when approaching the dark period. In contrast, in CE room studies, the

difference in root zone temperature between the top and bottom layers was maintained during the dark period and root zone temperature of the bottom layer was not influenced by the lights during the light period. This may be due to the CE room's air conditioning system blowing directly into the bottom layers of the VFS.

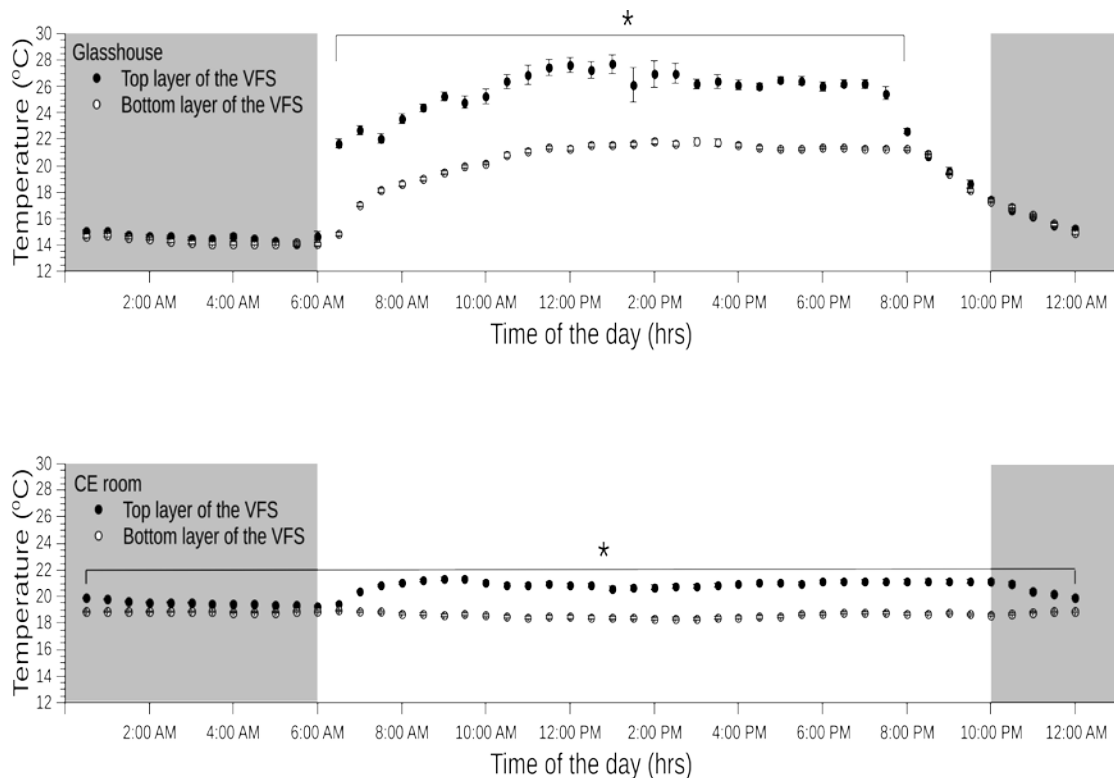


Figure 2.25. Changes in root zone temperature of top (closed symbols) and bottom (open symbols) layers within six layered VFS in the CE room and glasshouse as they increased during the transition from the dark (grey background) to the light (white background) period. In the glasshouse, each circle represents the mean of 2 data loggers through the period of 4 days. Error bars represent SE. In the CE room, each circle represents the mean of 3 data loggers through the period of 8 days. Error bars represent SE. Values indicated with asterisk indicate statistically significant differences (t-test, $p < 0.05$).

Canopy temperature was significantly higher in plants grown within the top layer and

closer to the light source, than those of plants grown within the bottom layer of the VFS. Interestingly, canopy temperatures of plants grown at the same vertical layer ranged within similar levels across both the glasshouse and CE room studies ($\pm 1^\circ\text{C}$). Specifically, average canopy temperature of glasshouse and CE room grown plants within the top layers of the VFS were $21 \pm 0.2^\circ\text{C}$ and $20.3 \pm 0.2^\circ\text{C}$ and for plants grown within the bottom layers were $16.6 \pm 0.2^\circ\text{C}$ and $17.5 \pm 0.34^\circ\text{C}$, respectively. There was no significant difference in canopy temperature between the bottom layer of the 6L VFS and the SL VFS in the CE room (Figure 2.26).

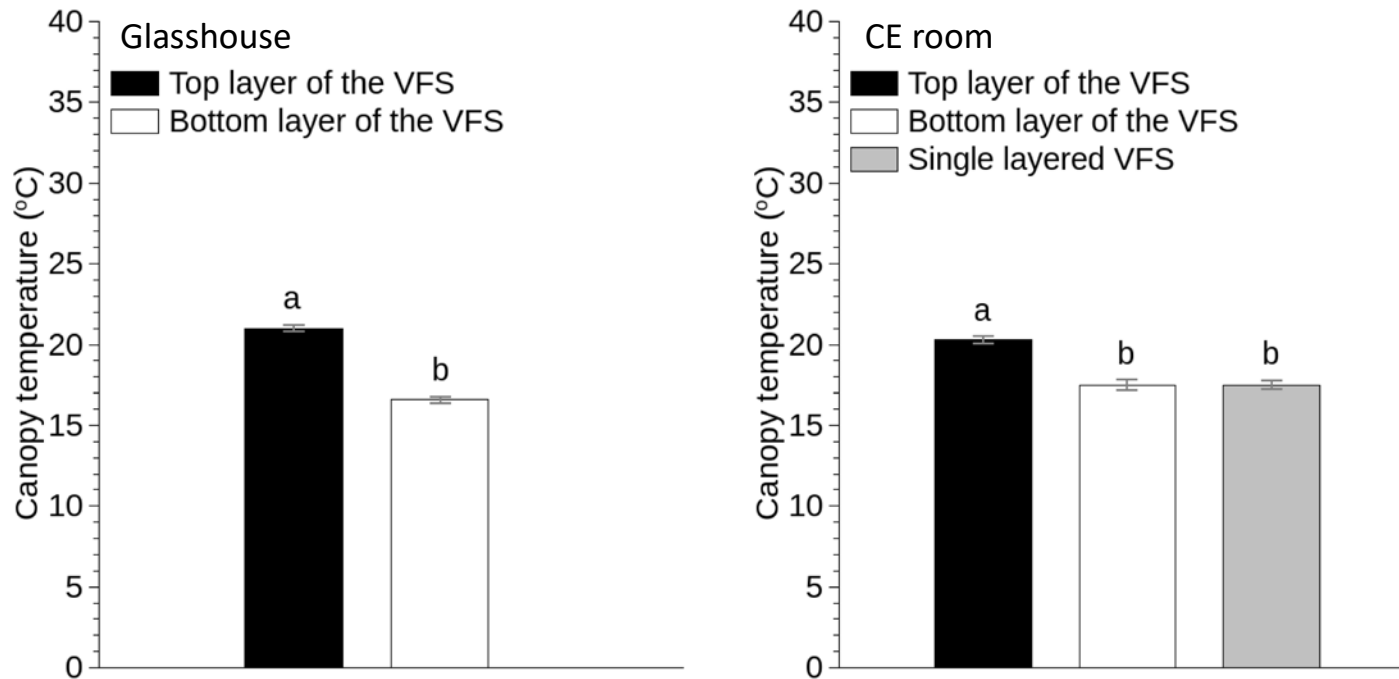


Figure 2.26. Canopy temperature of plants grown within the top (black bars) and bottom (white bars) layers of the VFS and SL VFS (grey bar). Values indicated with different letters indicate statistically significant differences ($t = 13.445$ with 22 degrees of freedom, $p < 0.001$) in the glasshouse study and one-way ANOVA test; $F(2,71) = 30.924$, $p < 0.001$, followed by Tukey post-hoc analysis in the CE room study. Bars represent means of \pm SE ($n=12$).

2.3.5 Tipburn of lettuce symptoms were observed in plants in the top layer of the VFS

Although the plants within the top layers of the VFS in both glasshouse (Section 2.3.2) and CE room (Section 2.3.3) environments produced the highest yields (Figures 2.9, 2.13 and 2.21) they also developed a physiological disorder called tipburn of lettuce (Barta and Tibbits, 2000; Frantz et al., 2004; Gilliam et al., 2011), which makes them unsuitable commercially as hearting lettuce (Figure 2.27 and 2.28). Plants grown at the top layers of the VFS in the glasshouse (Figure 2.27 a-c) developed tipburn symptoms, whereas plants grown within the bottom layers of the VFS (Figure 2.27 d-f) did not develop the disorder.

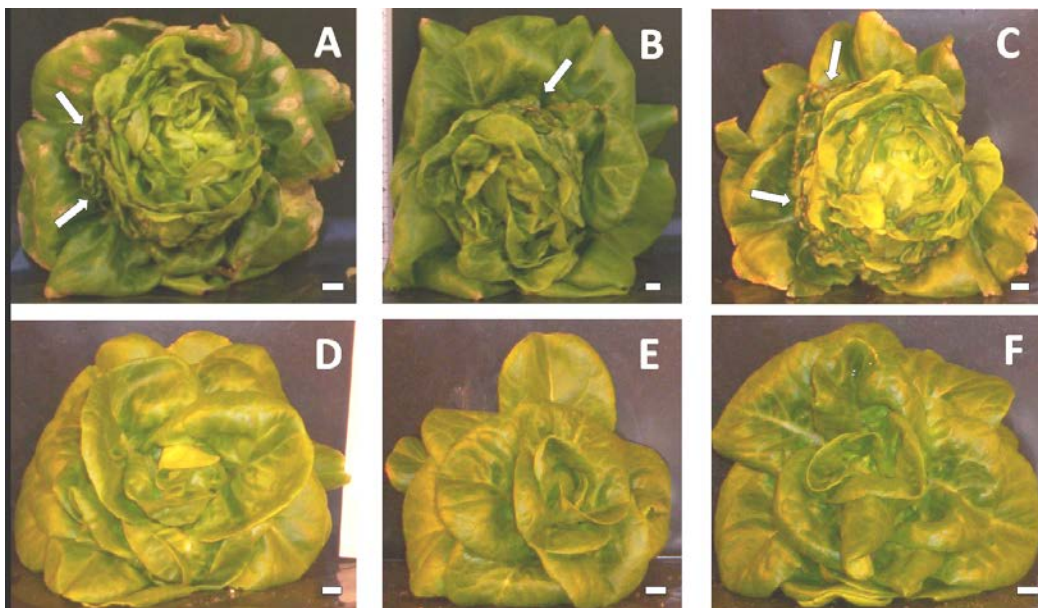


Figure 2.27. Photographs of harvested lettuce (*Lactuca sativa* L. cv. 'Frank') plants grown within the uppermost layers affected by tipburn symptoms (A-C) and within the bottom layer of six layered VFS (D-F) which were not affected by tipburn. White arrows show tipburn symptoms located at the edges of leaves. Scale bars are 1 cm.

Plants grown within the uppermost layers of the VFS in the CE room (Figure 2.28) developed what is known as internal tipburn (Sørensen et al., 1994) during which the inner leaves of developing lettuce heads show marginal necrosis (Figure 2.28.A and 2.29.8). However, plants grown within the bottom layers of the VFS did not develop the disorder (Figure 2.28.C and 2.28.D).



Figure 2.28. Photographs of harvested lettuce plants (*Lactuca sativa* L. cv. 'Frank') grown within the VFS in the CE room study. A and B, lettuce plants grown within the

top layers of the VFS affected by tipburn symptoms. C and D, lettuce plants grown within the bottom layer of the VFS which were not affected by tipburn. Black arrows show tipburn symptoms located at the edges of young leaves within the developing head. Scale bars are 1 cm.

2.5 Discussion.

This study aimed to characterize the growing environment of the Saturn Grower VFS, identify issues and challenges in the system, and propose interventions to optimise its use and resource use efficiency. To this end, three consecutive studies were conducted in two different growing environments to characterise plant growth and environmental variables.

The initial study (Section 2.3.1) investigated whether column-type VFS present a viable alternative to a horizontal hydroponic system (HHS) to increase yield per growing area by extending plant cultivation into the vertical dimension (Despommier, 2013; Eigenbrod and Gruda, 2014; Al-Chalabi, 2015; Thomaier et al., 2015). To date, there is no conclusive evidence that VFS can produce a higher yield per area compared to conventional HHS. This study showed that crop productivity, defined as a ratio of yield to occupied growing floor area, was 13.8 times higher in VFS than the HHS. This is most likely due to the potential of a 20-fold higher planting density achievable in the VFS compared to the HHS by incorporating the vertical dimension into the growth environment (Table 2.1). However, these calculations are based on independent vertical columns and do not consider the effect of column spacing on yield per occupied growing floor area. For example, in high wire crop training

systems high planting densities imposed intense competition for light within the growth system (Pettersenet et al., 2010). This is an important factor that needs to be considered in future studies, as spacing between vertical columns influenced crop productivity in VFS glasshouse trials (Liu et al., 2004). In contrast, the absolute yield of the HHS, in terms of shoot fresh weight, was higher than the VFS (Table 2.1). This can be explained by the significant causal relationship between shoot fresh weight and PPFD within the VFS (Figure 2.11); there was a significant decrease in PPFD from top to base of the vertical columns in the VFS, compared to the uniform light distribution in the HHS (Figure 2.10), thereby limiting growth in the lower layers.

Light intensity is one of the primary variables affecting lettuce yield and quality (Ferentinos et al., 2000; Son and Oh, 2013; Ouzounis et al., 2015) and it is has been well documented that lettuce yield increases with increasing light intensity (Knight and Mitchell, 1988; Masson et al., 1991; Frantz and Bugbee, 2005; Qin et al., 2008; Johkan et al., 2012; Kang et al., 2014). Since yield decreased from top to base of the vertical column and yield was uniform within the HHS (Figure 2.9), it was anticipated that the VFS would produce less crop in total than the HHS. Light intensity and shoot fresh weight were highly correlated and both decreased from top to base of vertical columns in a glasshouse (Liu et al., 2004). Light gradients from top to base of vertical column-type VFS were also reported by Linsley-Noakes et al. (2006) and Ramírez-Gómez et al. (2011) in glasshouse vertical strawberry cultivation. Similarly, significant causal relationships between shoot fresh weight and PPFD within the Saturn Grower VFS (Figures 2.17 and 2.24) and significant decreases in PPFD and yield from top to base of vertical columns were also observed in the glasshouse and in the CE room, respectively (Figures 2.13; 2.15; 2.21; 2.22). Therefore, basipetal

gradients in PPFD limit plant growth in vertical column VFS in both indoor and glasshouse settings.

In glasshouse trials with a vertical column-type VFS, PPFD decreased from top to base of vertical columns, with lower PPFD values being recorded towards the northern side of columns compared to the southern side (Liu et al., 2004). Thus, natural illumination introduced an additional gradient in light distribution within the VFS. In the glasshouse studies presented in Section 2.3.2, vertical PPFD gradients were not altered by natural illumination (Figure 2.16), which significantly increased light intensity within the VFS only at 12:00 hrs (Figure 2.14), but did not diminish the PPFD gradient within the VFS (Figure 2.15). However, since the glasshouse received low levels of natural illumination during the study (e.g. the maximum PPFD recorded in December during the study was $470 \mu\text{mol m}^{-2}\text{s}^{-1}$, whereas in June maximum PPFD within the same greenhouse was $840 \mu\text{mol m}^{-2}\text{s}^{-1}$), further studies are required to test whether natural illumination alters PPFD gradients within the VFS between different seasons and locations.

PPFD in growth chambers decreases as distance from the light source increases (Poorter et al., 2012). This phenomenon likely contributed to the large variance in PPFD observed in vertical layers 2 to 6 (Figure 2.15). In addition, higher positioned plants shaded lower positioned plants within the VFS (Figure 2.23). Side-on rather than top-down illumination could potentially ameliorate the shading effect within the VFS, eliminating the downward gradient in PPFD and consequently mitigating the gradient in crop productivity within the VFS. Side-on illumination, also known as inter-lighting, improved uniformity of light distribution within tall canopies and, in

some cases increased crop yield and light use efficiency (Olle and Viršile, 2013). Inter-lighting with light emitting diodes (LEDs) ameliorated mutual shading within tomato plants in high planting density and increased tomato yield by 12-14% in comparison to the control (Lu et al., 2012). Overhead illumination combined with intra-canopy lighting using HPS lamps increased cucumber yield in high wire crop training system by 11% compared to traditional overhead illumination (Pettersen et al., 2010). In contrast, Gomez et al. (2013) found no differences in productivity when comparing LED inter-lighting against overhead HPS in high-wire tomato cultivation. Similarly, inter-lighting by fluorescent tubes did not increase yield in high-wire cucumber production in the glasshouse (Heuvelink et al., 2006). Thus, variation in crop responses to inter-lighting may be due to the different environmental conditions (especially natural illumination) and crop management applied. However, since column-type VFS share similar light distribution properties within the vertical plane to plants grown in high wire crop training systems (Hovi et al., 2004), side-on illumination could potentially mitigate observed PPFD within the VFS.

An important difference between the VFS and the HHS study in Section 2.3.1 was that each layer of the HHS received nutrient solution directly from the tank, whereas in the VFS nutrient solution was delivered to the top layer and dripped to vertical layers beneath. This induced basipetal gradients in nutrient availability within the VFS (Figure 2.18). However, this concentration gradient didn't appear to alter plant growth within the VFS since there was no significant difference in yield in a SL VFS and the bottom layers of a 6L VFS (Figure 2.20), both receiving similar PPFD (Figure 2.23) but different nitrate concentrations. Thus, the significant difference in yield between the top layer of the 6L and the SL VFS was attributed to the difference in PPFD (Figures 2.20 and 2.22). Interestingly, lettuce dry matter production significantly

decreased when plants were grown in NO_3^- deprived conditions under high light intensity, whereas it was slightly affected under low light intensity (Henriques and Marcelis, 2000). Thus, future studies with inter-lighting, aimed at increasing PPFD within the lower layers of the VFS, should consider these light-dependent effects as they could exacerbate yield reductions within the lower layers of the VFS which received lower NO_3^- concentrations than the top layers.

High pressure sodium and metal halide lamps emit significant amounts of heat (Gupta and Jatothu, 2013). Interestingly, HPS lamps convert only ~30% of the electricity provided to light and the remaining 70% is emitted as radiant heat energy (Gómez et al., 2013). This can explain the significantly higher root-zone and canopy temperatures within the top layers of the VFS in comparison to the bottom layers of the VFS, as the top layers were closer to the lamps (Figures 2.25 and 2.26). LEDs used in inter-lighting applications generate low heat and could potentially reduce canopy and root-zone temperature gradients within the VFS (Hovi et al., 2004; Jokinen et al., 2012). Future studies should aim to disentangle the effects of light intensity and heat on crop growth in VFS.

Importantly, although plants within the top layers of the VFS produced more biomass, they developed a physiological disorder commonly known as tipburn of lettuce (Figures 2.27 and 2.28). Plants grown within the remaining 5 layers of the VFS did not develop the disorder, at least at the same time as the plants within the top layers. Tipburn is an irreversible quality defect that decreases marketable yields and causes significant economic losses (Hartz et al., 2007; Corriveau et al., 2010). Tipburn has been linked to a localised calcium deficiency (Lee et al., 2013) and can be a key defect

of crop quality of plants grown in controlled environments and vertical farming set-ups where luxuriant growth conditions (e.g. high PPFD, high temperature and optimal nutrient availability) are often employed to accelerate growth rates (Saure, 1998; Wien and Villiers, 2005; Koyama et al., 2012; Sago, 2016).

2.6 Conclusions.

This chapter suggests that column-type VFS present a viable alternative to conventional horizontal growth systems by optimizing growing space use efficiency. Specifically, the Saturn Grower VFS produced more crop per unit area than the HHS. Gradients of PPFD (together with temperature and NO_3^- concentration gradients) may nevertheless affect system usability and resource use efficiency. Further increases in yield could be achieved by incorporating artificial lighting within the VFS, such as inter-lighting, to mitigate these PPFD gradients. From a commercial perspective, crop utilization and marketability will dictate whether VFS can provide an alternative to HHS. For example, if lettuce is grown to be sold as individual heads, then the non-uniform productivity of the VFS would be a potential weakness of the VFS over the HHS. Alternatively, if the crop is destined for pre-cut salad bags then crop uniformity may be irrelevant while increased yield per unit area could be a significant advantage of the VFS. Ultimately, further research is required to compare organoleptic properties of crops grown within the two systems e.g. sensory analysis (Oliveira et al., 2013) and quality markers such as texture, color, dry matter and water content (Martín-Diana et al. 2007; Gutierrez et al., 2008)

The engineering and design solutions required to optimise PPFD, system temperatures and nutrient distribution within the Saturn Grower VFS fall beyond the scope of the

present study. However, tipburn of lettuce was also identified as a key limitation to the quality of lettuce to be sold as either individual heads or bagged cut salad when grown within the top layers of the VFS. Subsequent chapters therefore focus on the elucidation of the underlying mechanisms of tipburn of lettuce with the aim of preventing this disorder in VFS.

CHAPTER 3

DISENTANGLING THE CONTRIBUTION OF LIGHT INTENSITY AND TEMPERATURE TO LETTUCE TIPBURN

3.1 Introduction.

Chapter 2 characterized a prototype VFS in which PPFD, substrate temperature and NO_3^- availability significantly decreased from the top layer to the bottom layer. Although the top layer of the column-type VFS produced the higher yield, plants in this layer developed a physiological disorder commonly known as tipburn of lettuce. Tipburn of lettuce is a major limitation to productivity in VFS where luxuriant growth conditions (high PPFD and high temperature) are often employed to increase yields (Koyama et al., 2012; Sago, 2016).

Visible symptoms of tipburn are collapse and necrosis of the margins and the apex of developing leaves (Collier and Tibbitts, 1982; Saure, 1998; Barta and Tibbitts, 2000; Corriveau et al., 2010). High PPFD and high temperatures were reported to induce tipburn symptoms in lettuce by enhancing growth rates and consequently Ca demand of young, rapidly growing tissues (Frantz et al., 2004; White, 2012; Sago, 2016). Thus it is generally accepted that tipburn results from a localized Ca deficiency (Barta and Tibbitts, 2000; Frantz et al., 2004), but there is still little definitive evidence that Ca deficiency induces the disorder (Kerton et al., 2009).

Interestingly, tipburn symptoms also appear under adverse growing conditions, during which growth is usually retarded, including root restriction (Olle, 2012), salinity (Carassay et al., 2012) and drought (Aroca, 2012). High PPFD and high temperature, as well as salinity and drought, can enhance the production of ROS which, if not quenched by the antioxidant machinery of the plant, may result in oxidative stress and damage to lipids, proteins, nucleic acids and carbohydrates (Scandalios, 1993; Mittler, 2002; Suzuki et al., 2014). Thus, recent studies of the mechanistic basis for tipburn

have explored links between oxidative stress and tipburn of lettuce (Carassay et al., 2012). Similarly, the involvement of ROS in inducing BER, another Ca related disorder of pepper and tomato fruits (Aktas et al., 2005; Casado-Vela et al., 2005; Mestre et al., 2012), has also been studied. However, to date there is no consensus regarding the relative importance of Ca deficiency and ROS in inducing tipburn symptoms.

The presence of multiple environmental gradients and confounding factors within column-type VFS (Liu et al., 2004; Linsley-Noakes et al., 2006; Ramírez-Gómez et al., 2012; Rius-Ruiz et al., 2014; Chandra et al., 2014; Lee et al., 2015) makes the contribution of individual factors to the generation of tipburn symptoms difficult to study. In contrast, Deep Flow Hydroponic Systems (DFTS), in which the roots are submerged in aerated nutrient solution, eliminate the environmental gradients present in column-type VFS and allow the individual contributions of PPF and temperature to tipburn to be studied. The advantages of DFTS are that they provide a uniform root zone environment with tight control of solution pH, nutrient composition and dissolved oxygen concentration (Chow et al., 1992; Jensen, 2002; Vimolmangkang et al., 2010; Sengupta and Banerjee, 2012). Consequently, DFTS have been used widely in plant science research and particularly for lettuce crops, for example, to study the effects of different nutrient solution aeration approaches on yield (Goto et al., 1996; Kratky, 2005; Park and Kurata, 2009), the influence of shoot and root temperature on yield (Thompson et al., 1998), how different growing substrates (Assimakopoulou et al., 2013) and different air flow rates (Lee et al., 2013) influenced tipburn occurrence, and the effect of different ratios of blue to red LED illumination on growth, ascorbic acid and anthocyanins in lettuce (Lee et al., 2014).

This chapter established a DFTS as a model system for studying the contributions of ROS and localised Ca deficiency to the induction of tipburn symptoms of lettuce, when plants were grown under luxuriant growth conditions of high PPFD and high temperature. This system allowed the contribution of PPFD and temperature to the induction of tipburn to be disentangled thereby contributing to understanding the causes of tipburn.

3.2 Materials and methods.

3.2.1 Plant material.

Two varieties of butterhead lettuce, the tipburn resistant (*Lactuca sativa* L. cv. 'Frank') and susceptible (*L. sativa* L. cv. 'Sunstar') lettuce were purchased from Moles Seeds (Essex, UK) and Hazera Seeds (Lincolnshire, UK), respectively. Seeds were individually sown into 2 cm x 2 cm x 4 cm rockwool cubes (Grodan, Fargro Ltd., UK) and germinated in a CE room (see Chapter 2) at 17°C. PPFD was maintained at approximately 170 $\mu\text{mol m}^{-2} \text{s}^{-1}$ under a 16 hour photoperiod (06:00 hrs to 22:00 hrs). The seedlings were incubated in aerated deionized water for 15 days and then in one-quarter-strength Hoagland's solution (EC: $0.25 \pm 0.1 \text{ dS m}^{-1}$, pH: 5.8 ± 0.2). DO concentration was maintained at $8.4 \pm 0.2 \text{ mg l}^{-1}$ by an aquarium air pump (All Pond Solutions Ltd, Middlesex, UK). Plants were transferred to the DFTS 28 days after sowing and were grown for a further 30 days.

3.2.2 The Deep Flow Hydroponics System (DFTS).

The DFTS consisted of individual 16 litre clear storage boxes and lids (Wilkinsons Stores, Lancaster, UK) of 17.2 cm height, 42.7 cm width and 32.8 cm depth. The

boxes and lids were painted black using gloss enamel spray paint (B&Q, Lancaster, UK) to restrict light penetration and discourage the growth of algae (Gibeaut et al., 1997). No growing medium other than the nutrient solution was used in the DFTS. Mechanical support for the plants was provided by the lid of the hydroponic box (Figure 3.1.A). The hydroponic boxes were sterilized in TriGene disinfectant (MediChem International Ltd., UK) prior to filling with 15 litre of half-strength Hoagland's solution (Hoagland and Arnon, 1950). The composition of the nutrient solution was 0.5 mM NH_4NO_3 , 1.75 mM $\text{Ca}(\text{NO}_3)_2 \cdot 4\text{H}_2\text{O}$, 2.01 mM KNO_3 , 1.01 mM KH_2PO_4 , 0.5 mM $\text{MgSO}_4 \cdot 7\text{H}_2\text{O}$, 1.57 μM $\text{MnSO}_4 \cdot 5\text{H}_2\text{O}$, 11.3 μM H_3BO_3 , 0.3 μM $\text{CuSO}_4 \cdot 5\text{H}_2\text{O}$, 0.032 μM $(\text{NH}_4)_6\text{Mo}_7\text{O}_{24} \cdot 4\text{H}_2\text{O}$, 1.04 μM $\text{ZnSO}_4 \cdot 7\text{H}_2\text{O}$ and 0.25 mM NaFe EDTA. The box lids were also painted black and four 2.5 cm diameter holes, one in each quadrant, were cut in the lids to hold seedlings. As demonstrated in Figure 3.1.B, a fifth hole was cut in the centre of the lid to accommodate a 5 ml pipette tip (Sarstedt AG & Co, Nümbrecht, Germany). The pipette tip was connected through a 4 mm internal diameter tube to an aquarium air pump (All Pond Solutions Ltd, Middlesex, UK), which continuously delivered 3.2 l min^{-1} ambient air directly into the nutrient solution, maintaining a DO concentration of $8.4 \pm 0.2 \text{ mg l}^{-1}$; this has been reported to be within optimum levels for lettuce growth (Goto et al., 1996).

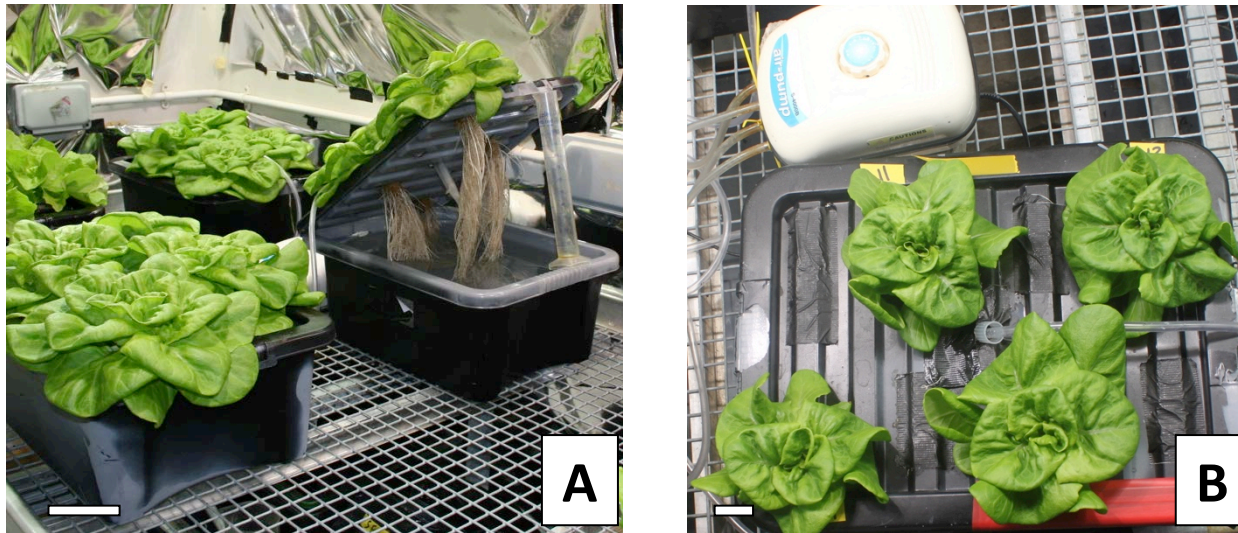


Figure 3.1. (A) Side view of the Deep Flow Hydroponics System (DFTS) shows shoots and roots of lettuce plants (*Lactuca sativa* cv. 'Frank') 29 days after they were transferred to the DFTS. The growth system consisted of 16 litre independent black plastic boxes. Four lettuce plants were grown in each hydroponic box. The rockwool block and the plastic lid of the hydroponic box supported the plants. The crop's roots were submerged in continuously aerated half-strength Hoagland's solution. Scale bar is 10 cm. (B) Top view of the DFTS shows lettuce plants 15 days after they were transferred to the DFTS. An air pump was used to continuously oxygenate the nutrient solution in the hydroponic box through the 5 ml pipette tip in the centre of the lid. Scale bar is 3 cm.

The initial EC of the nutrient solution was $1 \pm 0.2 \text{ dS m}^{-1}$. The nutrient solution was replaced weekly and 2M H_3PO_4 was added dropwise to maintain pH of 5.8 ± 0.2 . A DO700 hand-held multi-parameter instrument (Extech Instrument, MA, USA) was used to monitor daily changes of pH, EC, DO levels of the nutrient solution.

The DFTS was illuminated by 400 W metal halide lamps (HQI-T 400N, Osram, St Helens, UK). The height of lighting units above the DFTS was adjusted to reproduce the light environment within the top and bottom layers of the VFS (see Chapter 2), thereby establishing a model system to provide reproducible tipburn symptoms. Two contrasting light environments were created; high light (HL) and low light (LL) treatments, by distancing the DFTS at 70 cm and 120 cm, respectively from the lighting units. Within each treatment, the hydroponic boxes were rotated randomly every two days to minimize positional effects.

3.2.3 Light intensity and spectral wavelength.

Light intensity measurements were taken, using a Macam Q203 Quantum radiometer (Macam Photometrics LTD, Livingstone, UK), at the top of the hydroponic boxes, with lids closed and across a 17 x 6 grid to evaluate PPFD uniformity under the two contrasting light treatments. A SR9110-V7 Spectroradiometer (Macam Photometrics LTD, Livingstone, UK) fitted with a fibre optic probe was used to determine the light irradiances over the spectral range of 290-800 nm to investigate whether adjusting the height of the lighting units influenced the spectral wavelength within the two light treatments (Figure 3.2).

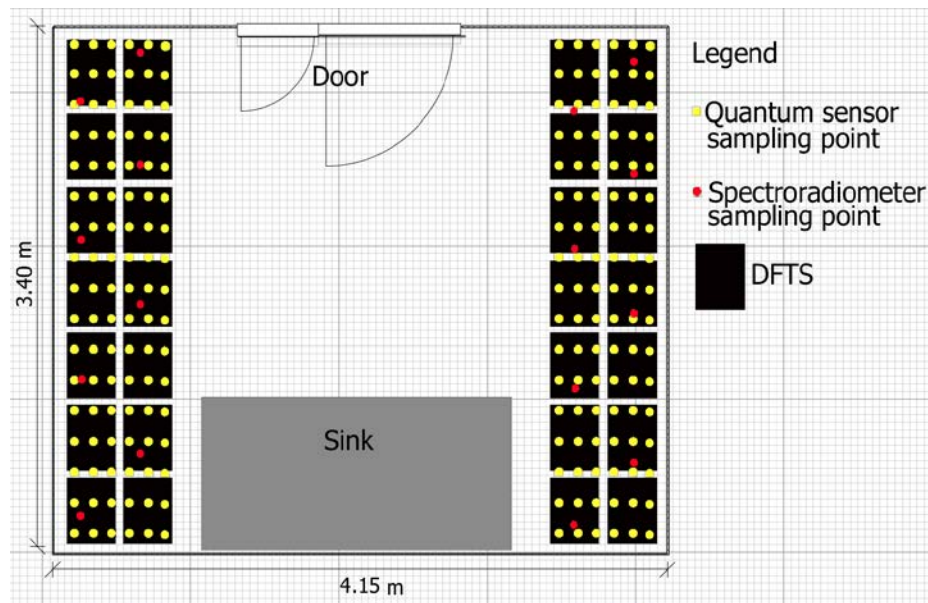


Figure 3.2. Shows the CE room floor plan in scale. The black rectangular shapes represent the hydroponic boxes, which comprised the DFTS. Yellow and red circles represent data points from where light quantity and quality measurements were obtained using a Macam Q203 Quantum radiometer and the SR9110-V7 spectroradiometer, respectively. Measured lines (in metres) show the CE room's exact dimensions.

3.2.4 DFTS, air and leaf temperatures.

Lid surface temperature of the DFTS was recorded hourly using the EL-USB-1 temperature data logger (Lascar Electronics Ltd., Salisbury, UK). Three data loggers were placed on top of three different and randomly selected hydroponic boxes and were subsequently rotated randomly in different positions across the growth area every two days. Similarly, three EL-USB-1 temperature data loggers, enclosed within EL-USB-CASE submersible metal cases, were submerged into three different hydroponic boxes, at the bottom of the box, per treatment to record nutrient solution temperature (root zone temperature). Air temperature was recorded by Ektron II C

sensor (HortiMaX B.V. Pijnacker, Netherlands) equipped with two Pt1000 temperature sensors. Each Pt1000 sensor was mounted 40 cm above the centre of the growth bench which accommodated the DFTS. Crop canopy temperature was measured using a handheld infrared thermometer (model 39750-20, Cole Parmer Instruments Co., Chicago, IL) with a measurement area of 7.07 cm² at 5 cm distance from the canopy. Measurements of canopy temperature were made at 18:00 hrs in six different per treatment and cultivar randomly selected plants.

3.2.5 Gas exchange measurements.

Leaf gas exchange measurements assessed the influence of the two contrasting light environments on plant responses within the DFTS. Photosynthetic light-response curves were constructed as a function of incident PPFD using a portable Li-6400XT photosynthesis system (Li-Cor, Lincoln, USA) coupled with a standard 6400-40 leaf-chamber fluorometer (Li-Cor, Lincoln, USA). The following PPFD levels were used: 0, 20, 40, 80, 100, 200, 400, 800, 1000, 1200 and 1400 $\mu\text{mol m}^{-2} \text{s}^{-1}$ provided by the built-in red and blue LED light sources, with 10% blue light. Conditions within the leaf chamber were maintained constant for 3 minutes, for equilibration, before data were logged. Ambient CO₂ concentration in the leaf chamber was maintained at 389.5 \pm 0.3 ppm and block temperature was set at 19.8 \pm 0.02°C. All gas-exchange measurements were performed 15 days after transfer (DAT) of plants to the DFTS, on three randomly selected plants from each light treatment and cultivar. The fourth fully expanded leaf counting from the outermost fully expanded leaf was sampled. Measurements started at 10:00 hrs and were completed at 18:00 hrs. To quantitatively compare the photosynthetic light-response curves, the data were fitted to the Mitscherlich equation (Potvin et al., 1990; Marino et al., 2010) of the form:

$$A(\text{PPFD}) = A_{\text{max}} [1 - e^{-k(x - x_0)}]$$

where A is net photosynthesis, A_{max} is the maximum net photosynthetic rate, k is the initial slope of the curve at low light levels, x represents PPFD and x_0 is the light compensation point (where photosynthetic uptake and respiratory CO_2 release are equal). This model was preferred over the other two model types mostly used by physiologists to fit photosynthetic light-response curves (the non-rectangular hyperbola and the modified Michaelis–Menten function (Heschel et al., 2004)) since it is:

- i) typically used to model yield responses to fertilizer input, since CO_2 and in this case light can be perceived as “fertilizer” for photosynthesis (Potvin et al., 1990)
- ii) a phenomenological and not a mechanistic description of photosynthesis and because the equation consists of only three parameters (A_{max} , k and x_0), which are linked to distinct biological processes, it is easier to fit to observed responses in comparison to other approaches (e.g. quadratic models (Peek et al., 2002; Heschel et al., 2004; Marino et al., 2010; Lachapelle et al., 2012)).

The Mitscherlich model was significantly fitted for each photosynthetic light-response curve ($R^2 > 0.90$, $p < 0.001$, for all photosynthetic parameters).

3.2.6 Quantifying tipburn injury by digital image analysis.

Digital image analysis was used to compare the ratio between total leaf area and tipburn-affected leaf area between the two lettuce cultivars. After harvest, lettuce leaves were placed on black polyethylene material with the abaxial side facing down to be photographed. All photographs were taken using a Canon EOS 100D Digital SLR Camera with a Canon 18-55mm II DC Lens (Canon Inc., Tokyo, Japan). The image files (in JPEG compression) were loaded to gimp 2.8 image analysis software

(The GIMP team, GIMP 2.8.10, www.gimp.org) to separate the different leaf areas using the GIMP Magic Wand tool. Both the total leaf areas and tipburn affected leaf areas were calculated using Image J software (version 1.46r; National Institutes of Health, Bethesda, USA). Image J was calibrated using a ruler, which was placed next to the photographed lettuce leaves. To measure leaf area with Image J the digital colour images were transformed stepwise to 8-bit and then into binary images (black and white pixels), with white pixels representing leaf area, whereas black pixels representing the background (Figure 3.3). The tipburn-affected leaf area ratio was calculated according to the following formula:

$$\text{Tipburn-affected LA ratio (\%)} = \text{LA}_{\text{tipburn-affected}} (\text{LA}_{\text{total}})^{-1} 100$$

where LA is leaf area, $\text{LA}_{\text{tipburn-affected}}$ is total tipburn affected leaf area and LA_{total} is total leaf area.

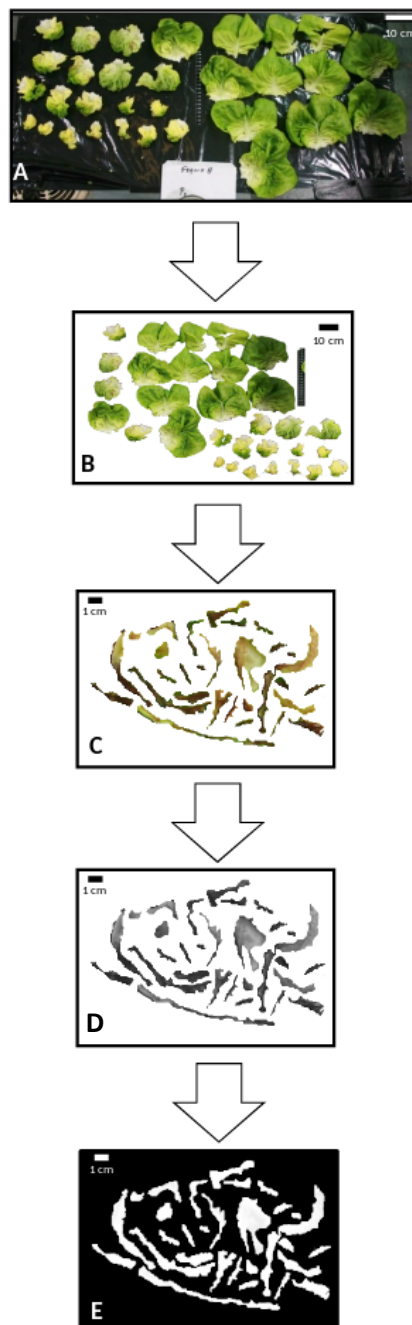


Figure 3.3. Flow diagram shows the steps followed to separate tipburn affected leaf area from total leaf area. Picture (A) shows the original photograph, picture (B) shows total leaf area, picture (C) shows tipburn affected leaf area, picture (D) the 8-bit image, and picture (E) the binary image. Each leaf was assessed separately for visual tipburn symptoms.

3.2.7 Growth chambers studies: PPFD and temperature treatments.

To separate the effects of PPFD and temperature on tipburn induction, lettuce plants (*Lactuca sativa L. cv. 'Frank'*) were grown for 30 days in four different growth cabinets (Microclima 1750, Snijders scientific, the Netherlands), which allowed tight regulation of environmental variables. Four treatments were employed: two PPFD (high (HL), $450 \mu\text{mol m}^{-2}\text{s}^{-1}$; low (LL), $170 \mu\text{mol m}^{-2}\text{s}^{-1}$) and two ambient temperature regimes (high (HT), 27 / 17°C; low (LT), 21 / 17 °C; light / dark period) under a 16 hour photoperiod (06:00 hrs to 22:00 hrs). These conditions simulated the PPFD and an approximate average of the three different temperatures recorded within the two treatments of the model DFTS. Treatments were: cabinet 1 - HL and HT, cabinet 2 - HL and LT, cabinet 3 - LL and HT, and cabinet 4 - LL and LT. Six hydroponic boxes, containing four plants each, were placed in each growth cabinet. Temperature was programmed electronically, whereas incident PPFD was modified by adjusting the distance of the plants from the light sources. Illumination was provided by a combination of 46 daylight fluorescent tubes (20 x Sylvania T5 FHO 54W 840 1149mm, 20 x Sylvania T5 FHO 24W 840 549mm, 6 x Sylvania Brite Grow T8 58W 1200mm (Osram, St Helens, UK)). Relative humidity within the growth chambers was programmed at 70%. PPFD measurements were taken, using a Macam Q203 Quantum radiometer (Macam Photometrics LTD, Livingstone, UK), at the top of the hydroponic boxes, with lids closed and across an 8 x 3 grid (Figure 3.4). The hydroponic boxes were rotated randomly within each treatment every two days to minimize positional effects.

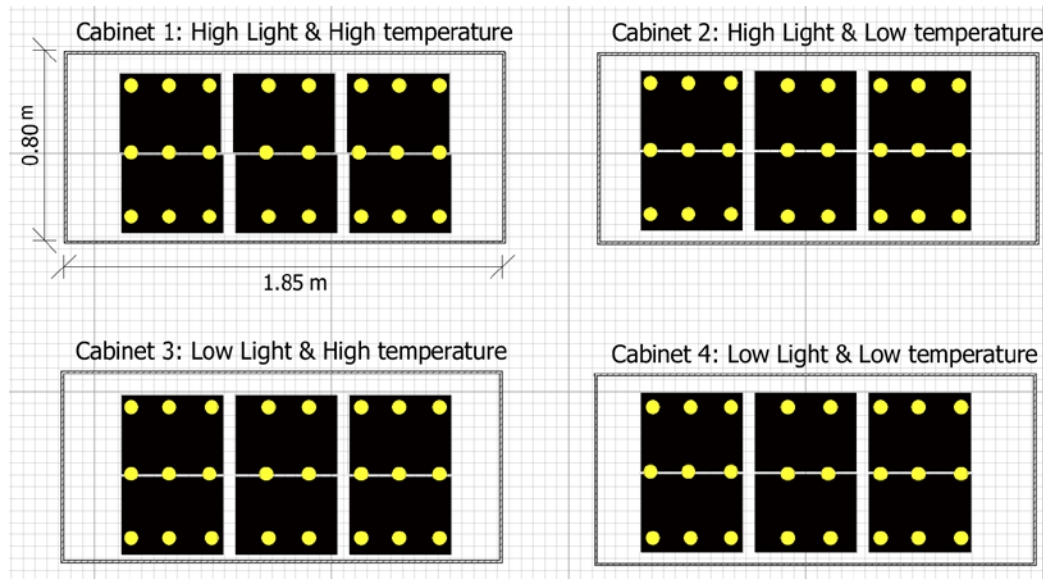


Figure 3.4. Shows the four different growth cabinet's floor plans in scale. The black rectangular shapes represent the hydroponic boxes, which comprised the DFTS. Yellow represent data points from where light quantity measurements were obtained using a Macam Q203 Quantum radiometer. Measured lines (in metres) show the chamber's exact dimensions.

Gas exchange measurements were performed using the same portable Li-6400XT photosynthesis system and same settings as in Section 3.2.5. All gas-exchange measurements were performed 15 DAT on three randomly selected plants from each growth chamber. Measurements started at 10:00 hrs and were completed at 18:00 hrs.

3.2.8 Data analysis.

Effects of PPFD treatments and cultivar on shoot fresh weight (g) were assessed using two-way ANOVA on log-transformed data to better approximate normality (Tables 3.1 and 3.2). Descriptive statistics were used to assess the pattern of PPFD distribution between treatments in Figure 3.8. In addition, the data were overlaid on to a contour

map to visually inspect light distribution to identify potential hotspots (Figure 3.9). Putative differences in light quality between treatments were assessed visually in Figure 3.10. Root and canopy zone temperatures were assessed visually in Figure 3.11 and the data were pooled and compared with Kruskal-Wallis ANOVA on Ranks in order to identify significant differences between treatments and time zones (Figure 3.12). Photosynthetic light response curves were assessed visually in Figures 3.13 and 3.19. Following this, a nonlinear mixed model with 3 parameters known as the Mitscherlich equation was fitted to the net photosynthesis rate of single leaves A ($\mu\text{mol CO}_2 \text{ m}^{-2} \text{ s}^{-1}$) against PPFD ($\mu\text{mol photons m}^{-2} \text{ s}^{-1}$) using the nonlinear least squares regression function (nls) of R version 3.1.2 and the empirical parameters were compared using two-way ANOVA, followed by Tukey post-hoc analysis (Tables 3.3, 3.4, 3.6 and 3.7). Tipburn damage was compared between the two varieties using Student's t-test (Figure 3.16). Kruskal–Wallis ANOVA on Ranks test followed by Tukey post-hoc analysis was employed to compare PPFD between the 4 growth cabinets in Figure 3.17. Two-way ANOVA, followed by Tukey post-hoc analysis was used to examine the effects of PPFD and temperature on shoot fresh weigh within the growth cabinets (Table 3.5). Probability values less than 0.05 ($p < 0.05$) were considered to indicate a statistically significant difference. All statistical tests were performed on R version 3.1.2 software (R Development Core Team, 2014).

3.3 Results.

3.3.1 DFTS as a model system for studying tipburn of lettuce.

The model DFTS was designed to mimic the conditions within the top and bottom layers of the VFS in which tipburn was observed (see Section 2.4). The mean PPFD

value for each treatment was $448 \pm 11 \mu\text{mol m}^{-2} \text{s}^{-1}$ (HL) and $173 \pm 5 \mu\text{mol m}^{-2} \text{s}^{-1}$ (LL). These values were comparable to those observed in the VFS (Figure 2.16).

3.3.1.1 PPFD and cultivar both affected yield.

Shoot FW was significantly ($p < 0.001$) higher in HL in both cultivars. Although there was no significant difference in the shoot FW between cultivars under HL, the shoot FW of the cv. 'Sunstar' was significantly ($p < 0.05$) less than the cv. 'Frank' under LL (Figure 3.5). Thus the cultivars tended to respond differently to the light treatments ($p = 0.06$ for cultivar x light interaction).

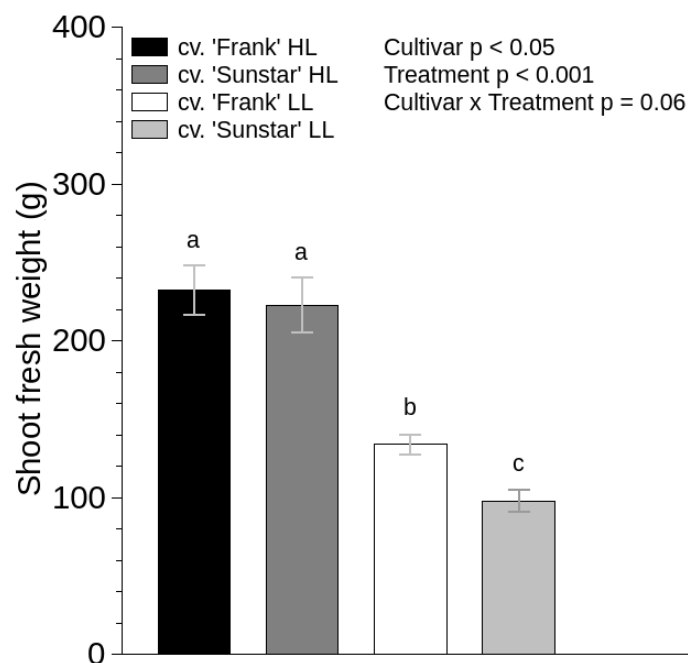


Figure 3.5. Shoot fresh weight of lettuce cultivars (cv. 'Frank' and cv. 'Sunstar') grown under high (HL) and low (LL) PPFD treatments. Values are mean \pm SE ($n=3$). Different letters indicate statistically significant differences ($p < 0.05$). Statistical analysis was performed on log-transformed data using a two-way ANOVA, followed by Tukey's post-hoc analysis.

3.3.1.2 Light treatment didn't affect spatial distribution of PPFD.

The spatial distribution of PPFD within the DFTS was analysed to evaluate the potential of the model DFTS to grow plants under uniform environmental conditions. Although visual inspection of the contour map of the light distribution (Figure 3.6) revealed an area of low PPFD (between $100 \mu\text{mol m}^{-2} \text{s}^{-1}$ and $150 \mu\text{mol m}^{-2} \text{s}^{-1}$) at the top right corner of the LL treatment, overall the light distribution was reasonably uniform in this treatment despite “patches” of reduced PPFD (Figure 3.7). PPFD distribution across the HL treatment was more uniform, which was also demonstrated by the lower coefficient of variation (HL, 14%; LL, 16%), with higher PPFD values (between $450 \mu\text{mol m}^{-2} \text{s}^{-1}$ and $550 \mu\text{mol m}^{-2} \text{s}^{-1}$) dispersed across the largest part of the growth bench of the DFTS. Lower PPFD values (between 250 and $400 \mu\text{mol m}^{-2} \text{s}^{-1}$) were observed around the edge of the growth bench.

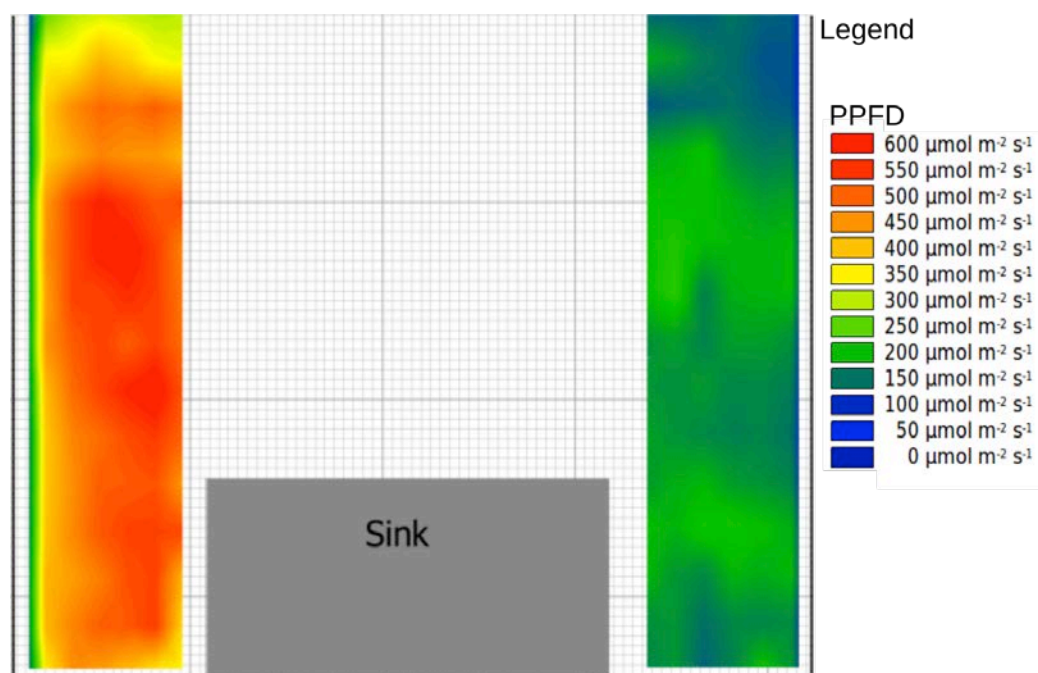


Figure 3.6. Contour map projection on the floor plan of the CE room shows PPFD distribution on the DFTS displayed on a pseudo-colour intensity scale; in which 'red' corresponds to the highest PPFD, whereas 'deep blue' represents absolute shade.

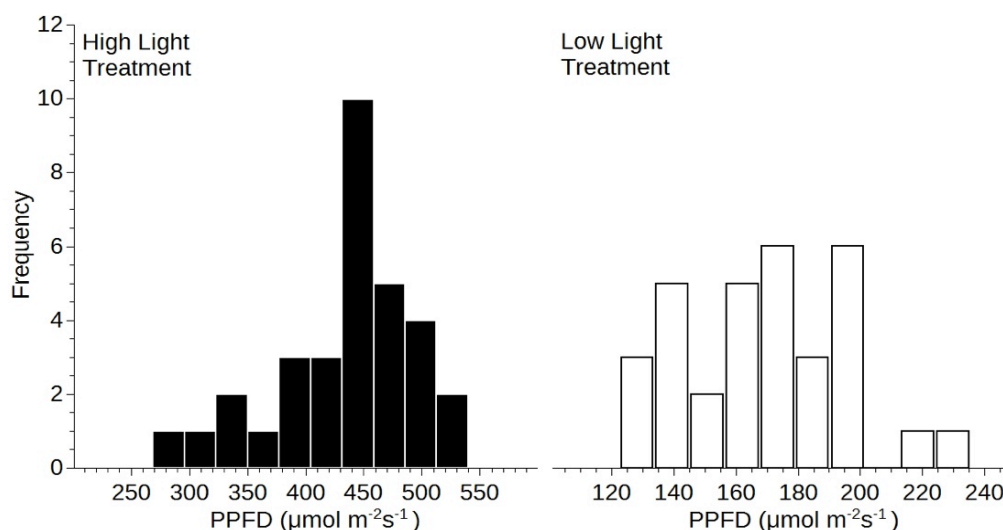


Figure 3.7. Frequency distributions of PPFD within the DFTS under two light treatments; HL (black bars) and LL (white bars) treatments. Data were normally distributed for both HL and LL (Shapiro–Wilk-test: $p=0.113$ and 0.562 , respectively) however they showed different patterns of symmetry and pointiness (skewness: -0.81 and 0.310 ; kurtosis: 0.838 and -0.298 , respectively).

3.3.1.3 Both HL and LL had similar light quality.

Adjusting the height of the lighting units to modify PPFD between the two light treatments had no effect on light quality. Both treatments showed similar patterns of incident spectral irradiance whilst, at different intensity levels (Figure 3.8). Thus, putative differences in plant responses of crops grown within the two light treatments of the model DFTS can be attributed to differences in light intensity rather than light quality.

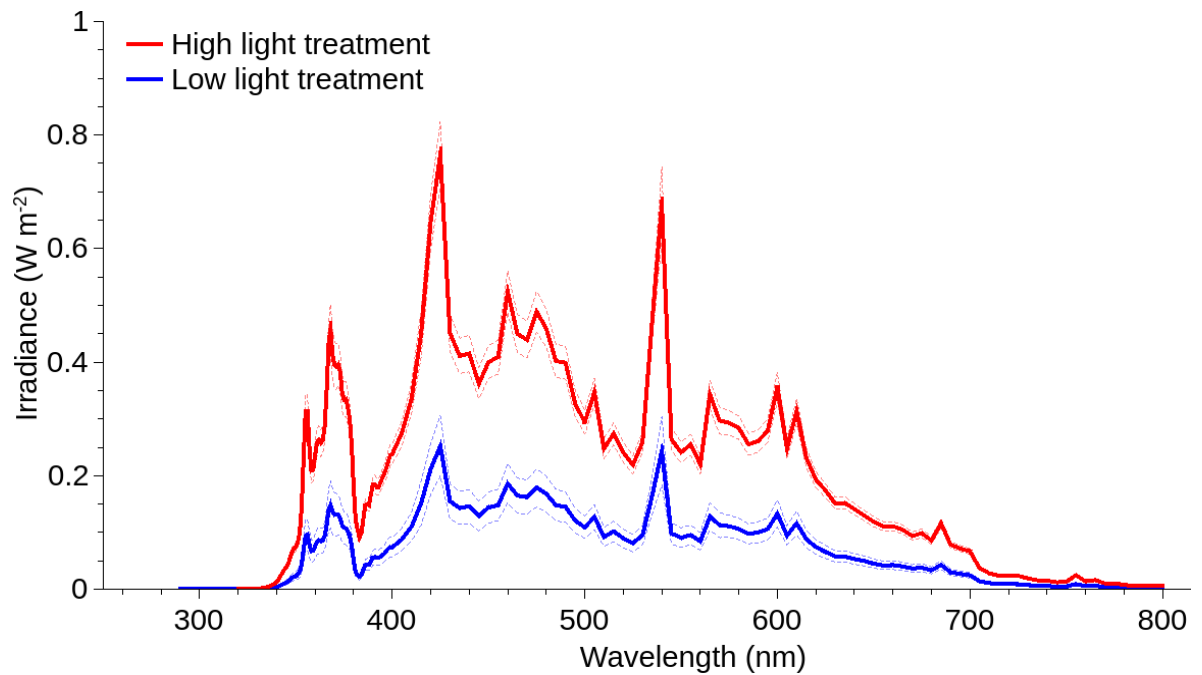


Figure 3.8. Incident spectral irradiance of HL (red line) and LL (blue line) treatments. Lines represent means of 8 measurement points of light irradiances over the spectral range of 290-800 nm \pm SD (dotted lines).

3.3.1.4 Air and plant canopy temperatures were affected by PPFD.

Surface temperature on the lid of the DFTS and air temperature of both light treatments increased from 06:00 hrs onwards after the lights were turned on (Figure 3.9). In contrast, only the root zone temperature of HL increased with that of LL remaining stable between light and dark periods.

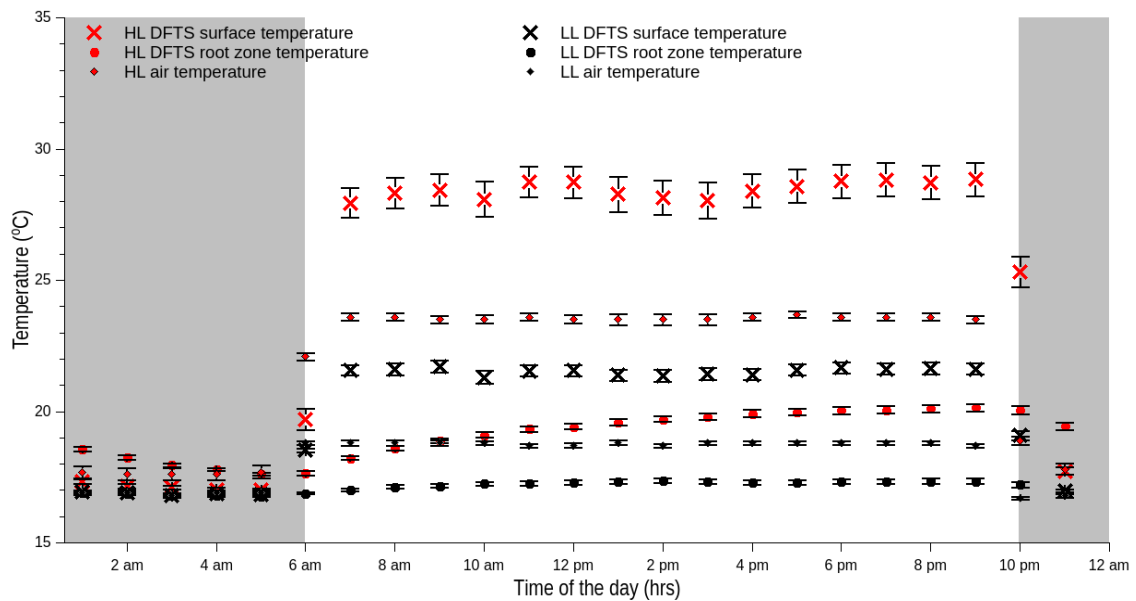


Figure 3.9. Changes in HL and LL surface temperature of the DFTS (red and black diagonal cross symbols, respectively), root zone temperature (red and black circle symbols, respectively) and air temperature (red and black diamond symbols, respectively) during the transition from the dark (grey background) to the light (white background) period. Each diagonal cross and circle represents the mean of three data loggers through the period of 26 days, whereas air temperature was recorded with one data logger in each treatment through the period of 26 days. Error bars represent SE.

DFTS surface temperature under HL was significantly ($p < 0.001$) higher than other temperatures within the DFTS. HL root zone temperature was significantly ($p < 0.001$) higher than the LL root zone temperature during light period but not during the dark period. Interestingly, only HL root zone temperature was significantly ($p < 0.001$) higher than the other temperatures, which were not significantly different to each other, during the dark period (Figure 3.10). Between 00:00 hrs and 6:00 hrs, HL root zone temperature decreased at a slower rate than the other three temperatures (Figure 3.9) resulting in a significantly ($p < 0.001$) higher median value compared to LL root

zone temperature.

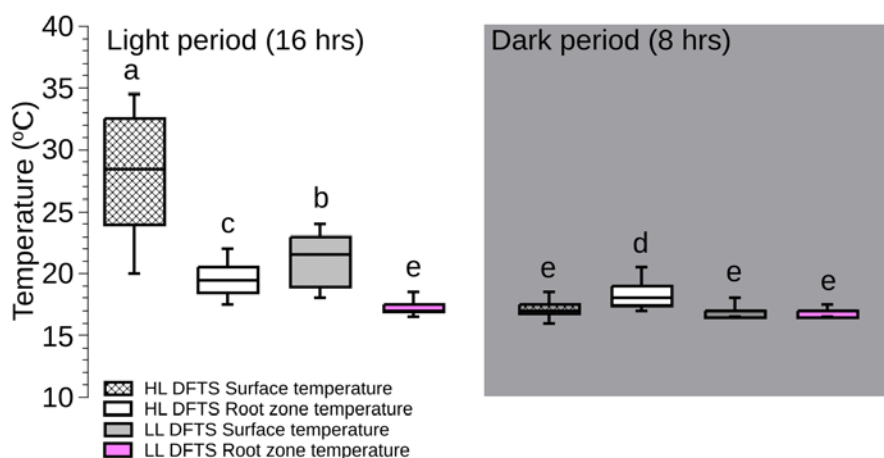


Figure 3.10. HL and LL canopy and root zones temperature data separated between the light (white background) and the dark (grey background) periods. The horizontal line within the box represents the median. Results of Kruskal-Wallis ANOVA on ranks followed by Dunn's Method showed statistically significant differences between the medians of the 8 different temperature series ($H(7) = 5013.87, p < 0.001$). Different letters indicate statistically significant differences.

Canopy temperature of both cultivars responded similarly to the light treatments (no significant cultivar effect, and no cultivar x PPFD interaction – Figure 3.11), Canopy temperature was significantly ($p < 0.01$) higher in plants of both cultivars grown under HL, compared to those grown under LL.

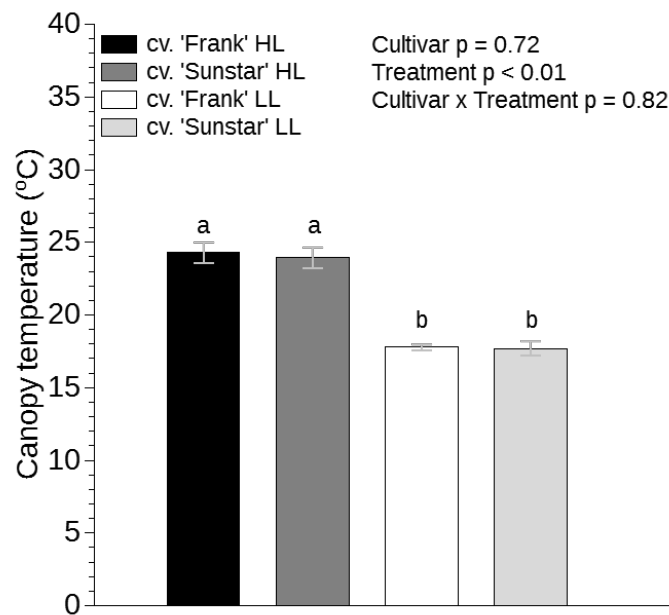


Figure 3.11. Canopy temperature of *L. sativa* cv. 'Frank' crops grown under HL (black bars) and LL (white bars) and cv. 'Sunstar' crops grown under HL (dark grey bars) and LL (light grey bars). Values indicated with different letters indicate statistically significant ($p < 0.05$) differences according to two-way ANOVA test followed by Tukey post-hoc analysis. Bars represent means of \pm SE ($n=3$).

3.3.1.5 Both cultivars responded similarly to the different PPFD environments.

The light response curves demonstrated that both cultivars responded in a similar way to the light treatments. In addition, the curves clearly demonstrated that LL plants reached the light saturation point at a lower PPFD than HL plants (Figure 3.12). There were significant differences in A_{\max} , x_0 and k between plants grown under different PPFD, but no differences between cultivars when grown under the same PPFD (Table 3.1). Both cultivars grown at HL had significantly higher A_{\max} ($p < 0.001$) than LL-grown plants, and there was no significant effect of cultivar on A_{\max} ($p = 0.26$). x_0 was significantly affected by PPFD ($p < 0.001$) but not by cultivar ($p = 0.34$). Similarly,

there was a significant effect of PPFD on k ($p = 0.003$) but no effect of cultivar ($p = 0.88$). There was no interaction between cultivar and PPFD in any of the three parameters of the Mitscherlich equation (Table 3.1).

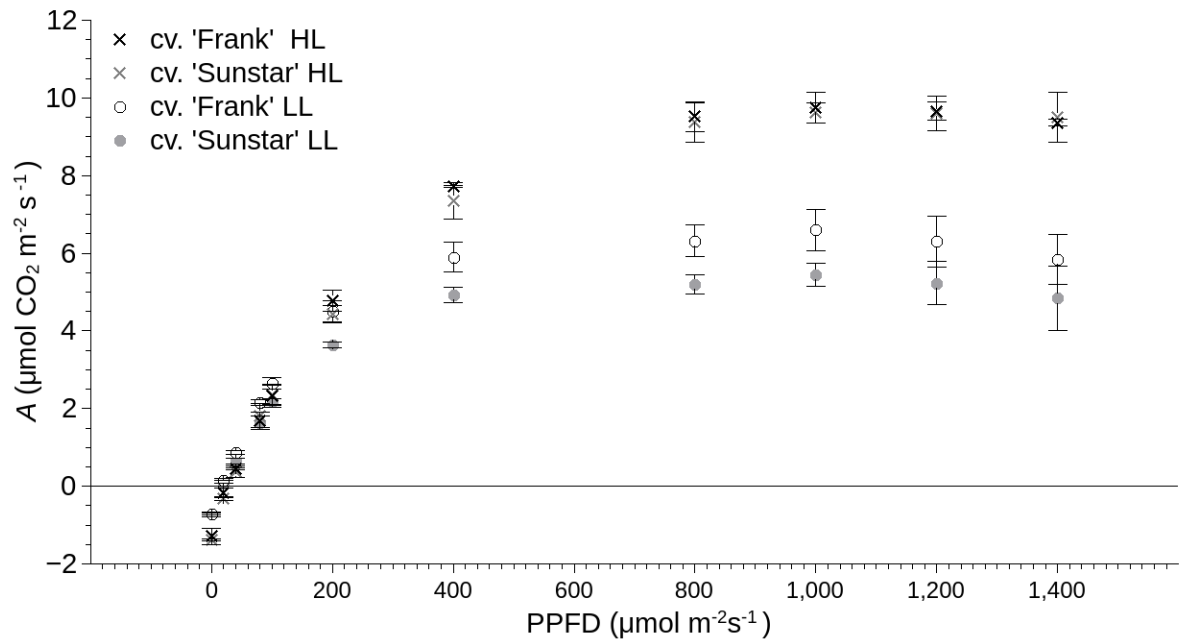


Figure 3.12. Light response curves of photosynthetic CO₂ assimilation rate A ($\mu\text{mol m}^{-2} \text{ s}^{-1}$) of HL (diagonal cross symbols) and LL-grown (circle symbols) butterhead lettuce varieties (*L. sativa* cv. 'Frank' and 'Sunstar') determined 15 DAT. Each point is the mean of different leaves from three different plants. Vertical bars represent the standard errors ($n=3$).

Table 3.1. Photosynthetic parameters of two butterhead lettuce cultivars (cv. ‘Frank’ and cv. ‘Sunstar’) derived from the Mitscherlich equation. A_{\max} is the maximum net photosynthetic rate, k is the initial slope of the curve, and x_0 is light compensation point. Data were compared using two-way ANOVA test, followed by Tukey post-hoc analysis. Values indicated with different letters indicate statistically significant differences, whereas those marked with the same letters show statistically similar values.

Cultivar	PPFD treatment					
	High			Low		
	A_{\max}	x_0	k	A_{\max}	x_0	k
cv. ‘Frank’	9.76 ± 0.17^A	28.68 ± 1.6^a	0.0041 ± 0.0002^x	6.3 ± 0.25^B	16.84 ± 0.45^b	0.0068 ± 0.0002^y
cv. ‘Sunstar’	9.74 ± 0.32^A	31.04 ± 1.34^a	0.0039 ± 0.0002^x	5.23 ± 0.26^B	19.51 ± 0.8^b	0.0069 ± 0.0007^y

3.3.1.6 Tipburn was greater in the susceptible cultivar 'Sunstar'.

Tipburn symptoms first appeared 16 DAT in both cultivars under the HL treatments, whereas none of the plants grown under the LL developed tipburn. Tipburn symptoms appeared as dark coloured necrotic leaf areas of deformed leaves enclosed within the developing head (Figure 3.13). Although plants grown at HL had significantly higher yields (Figure 3.5), these symptoms can decrease marketability of the crop.



Figure 3.13. Lettuce plants 29 DAT. (A) and (B), *Lactuca sativa*. cv. 'Frank'. (C) and (D), *Lactuca sativa* cv. 'Sunstar'. LL (A/C) – non-affected by tipburn symptoms. HL (B/D) – affected by tipburn symptoms; white arrows show tipburn symptoms located at the edges of leaves within the developing head. Scale bars are 3 cm.

Evaluating the extent of tipburn symptoms post-harvest revealed that lesions were scattered throughout the leaf blade, irrespective of whether the affected part had been enclosed within the developing head or not (Figure 3.14).



Figure 3.14. Leaves of lettuce plants (*L. sativa* cv. 'Frank') 30 DAT. White arrows show tipburn symptoms located at the edges of lettuce leaves. These lesions were visible only after harvest, when leaves were separated. Scale bar is 1 cm.

Digital image analysis ascertained that cv. 'Sunstar' exhibited significantly more ($p < 0.001$) tipburn damage than cv. 'Frank' (Figure 3.15).

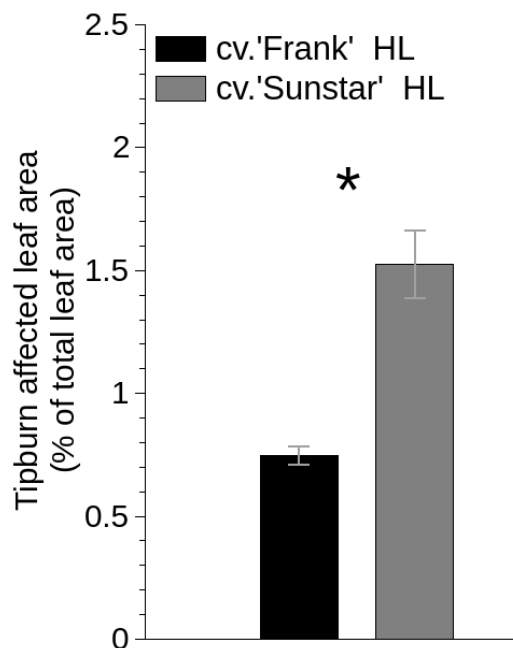


Figure 3.15. Tipburn affected leaf area ratio of lettuce, *L. sativa* cv. 'Frank' and cv. 'Sunstar', grown at HL. cv. 'Sunstar' exhibited significantly more ($t(4) = 14.01$, $p < 0.001$) symptoms of tipburn than the 'Frank' cv. Asterisk (*) indicates significance. Bars represent means of 3 plants \pm SE.

3.3.2 Disentangling the contribution of PPFD and temperature to tipburn.

Cabinets that received HL had significantly ($p < 0.001$) higher PPFD (Cabinet 1: $444 \pm 14.8 \mu\text{mol m}^{-2} \text{s}^{-1}$ (at $27^\circ\text{C}/17^\circ\text{C}$); Cabinet 2: $437 \pm 8.7 \mu\text{mol m}^{-2} \text{s}^{-1}$, (at $21^\circ\text{C}/17^\circ\text{C}$)) than cabinets that received LL (Cabinet 3: $158.6 \pm 3.6 \mu\text{mol m}^{-2} \text{s}^{-1}$ (at $27^\circ\text{C}/17^\circ\text{C}$); Cabinet 4: $163.3 \pm 2.8 \mu\text{mol m}^{-2} \text{s}^{-1}$ (at $21^\circ\text{C}/17^\circ\text{C}$). Importantly, there were no significant differences between cabinets receiving the same treatment (cabinets 1 and 2 - HL; cabinets 3 and 4 - LL) confirming the robust nature of the experimental design (Figure 3.16).

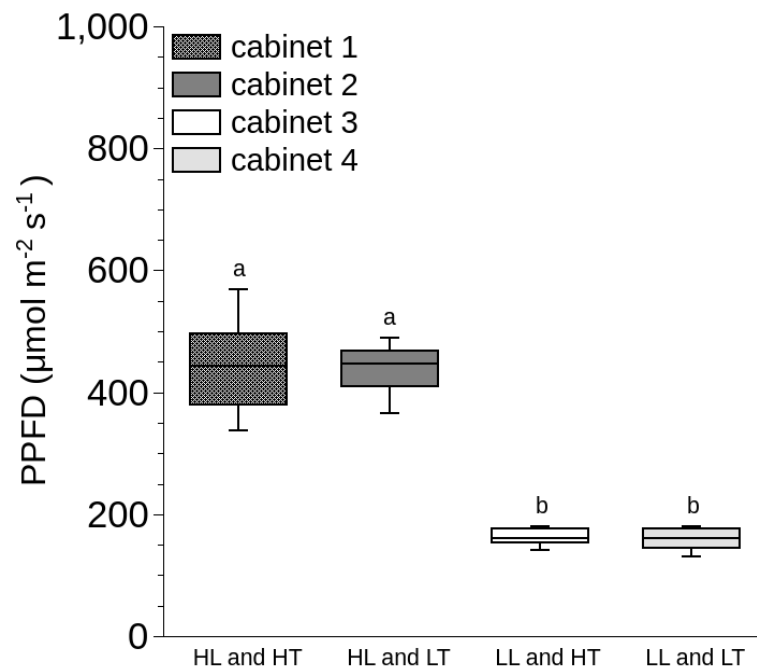


Figure 3.16. PPFD within the growth cabinets (cabinet 1 - HL and HT, cabinet 2 - HL and LT, cabinet 3 - LL and HT, and cabinet 4 - LL and LT). The horizontal line within the box represents the median. Results of Kruskal-Wallis ANOVA on ranks followed by Dunn's method showed statistically significant ($H(3) = 71.511$, $p < 0.001$). Different letters indicate statistically significant differences.

The spatial distribution of PPFD within the growth chambers was assessed to evaluate the potential of the system to grow plants under uniform environmental conditions. Visual inspection of the contour maps of the light distribution shown in Figure 3.17 revealed overall uniform PPFD distribution within the central part of the cabinets ($444 \pm 14.8 \mu\text{mol m}^{-2} \text{s}^{-1}$) under HL treatment (cabinets 1 and 2) and lower PPFD (between $200 \mu\text{mol m}^{-2} \text{s}^{-1}$ and $350 \mu\text{mol m}^{-2} \text{s}^{-1}$) at the margins of the cabinets. Similarly, PPFD distribution was uniform across the centre of the cabinets ($168.2 \pm 11.2 \mu\text{mol m}^{-2} \text{s}^{-1}$) under LL treatments (cabinets 3 and 4) and slightly decreased at the margins of the cabinets (between $120 \mu\text{mol m}^{-2} \text{s}^{-1}$ and $140 \mu\text{mol m}^{-2} \text{s}^{-1}$).

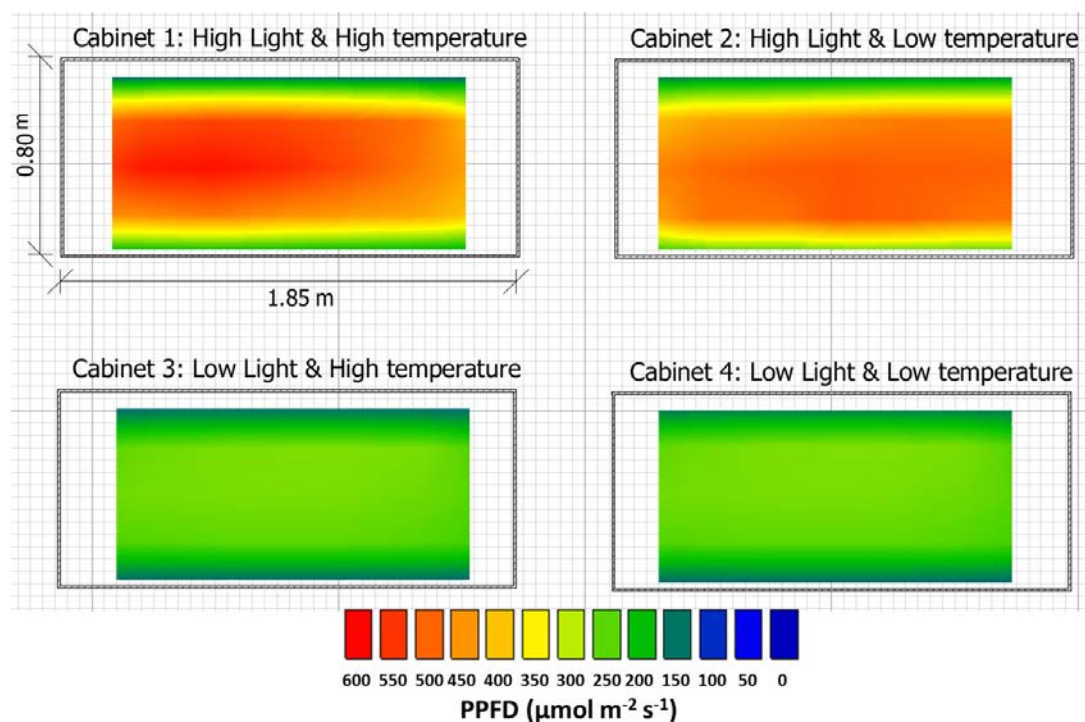


Figure 3.17 Contour map projection on the floor plan of the CE room shows PPFD distribution on the DFTS displayed on a pseudo-colour intensity scale; in which 'red' corresponds to the highest PPFD, whereas 'deep blue' represents absolute shade.

3.3.2.1 HL and HT combined gave the highest yield.

HL significantly ($p < 0.001$) increased shoot FW, especially when combined with HT. At low temperature, PPFD had no significant effect on shoot FW. LL combined with HT in cabinet 3 significantly ($p < 0.05$) decreased growth compared to growth in the other cabinets. Thus the growth response to PPFD depended on cabinet temperature (Figure 3.18), as indicated by a significant ($p < 0.001$) PPFD x temperature interaction.

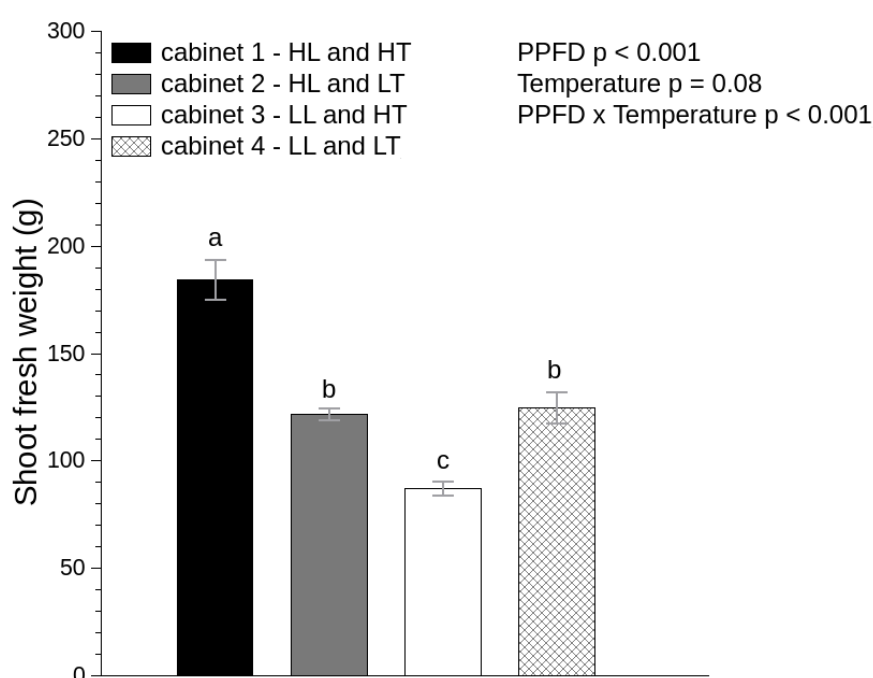


Figure 3.18. Shoot fresh weight (g) of lettuce plants (*Lactuca sativa* L. cv. 'Frank') grown in 4 growth cabinets (cabinet 1 - HL and HT, cabinet 2 - HL and LT, cabinet 3 - LL and HT, and cabinet 4 - LL and LT) and harvested 30 DAT. Values indicated with different letters indicate statistically significant differences (Two-way ANOVA test followed by Tukey post-hoc analysis). Bars represent means of 3 plants \pm SE.

3.3.2.2 A_{\max} was differentially affected within each cabinet.

PPFD and temperature within the growth environment had a marked effect on photosynthetic light response curves. The curves clearly demonstrated that plants grown in cabinet 1 (HL and HT) reached the light saturation point at lower PPFD compared to the plants in cabinet 2 (HL and LT), and similarly for plants grown in cabinet 3 (LL and HT) compared to the plants in cabinet 4 (LL and LT) (Figure 3.19). As such, both PPFD ($p < 0.001$) and temperature ($p < 0.001$) had a significant effect on A_{\max} . x_0 was significantly affected by PPFD ($p < 0.01$), plants under HL had higher x_0 . Similarly, k was significantly affected by PPFD ($p < 0.001$); plants under HL demonstrated significantly lower k compared to plants grown in cabinet 4 (LL and LT) (Table 3.2).

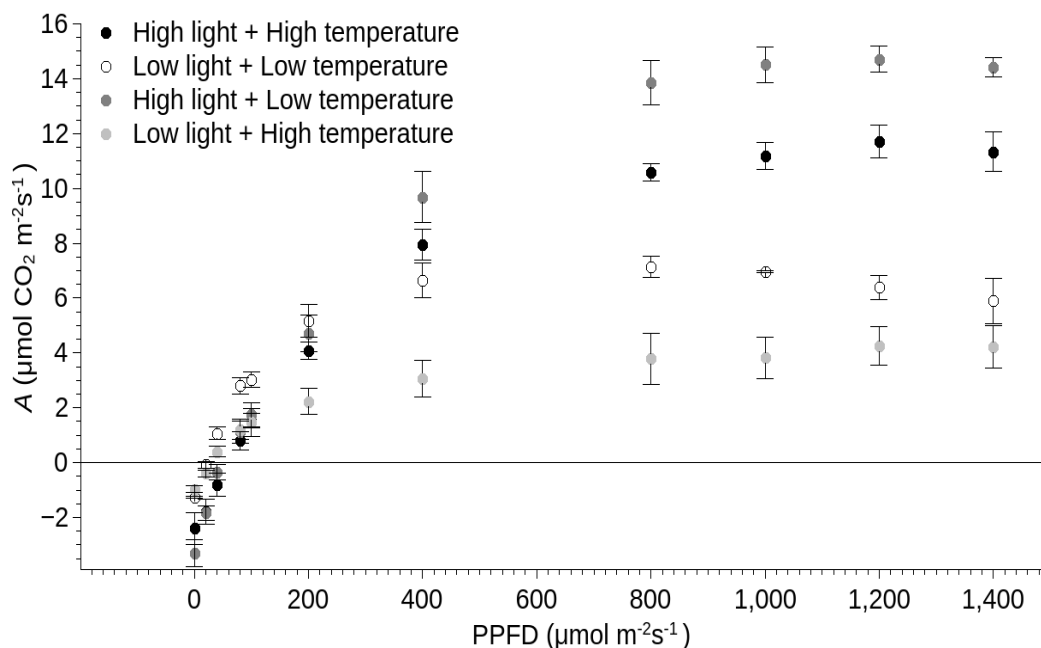


Figure 3.19. Light response curves of photosynthetic CO_2 assimilation rate A ($\mu\text{mol m}^{-2} \text{s}^{-1}$) of lettuce plants (*Lactuca sativa* cv. 'Frank') in 4 growth cabinets determined 15 DAT. Each point is the mean of different leaves from three different plants. Vertical bars represent the standard errors ($n=3$).

Table 3.2. Photosynthetic parameters of lettuce plants (*Lactuca sativa L.* cv. ‘Frank’) grown under contrasting PPFD and temperature conditions. Values represent means of 3 plants \pm SE. For k statistical analysis was performed on log-transformed data using a two-way ANOVA, followed by Tukey’s post-hoc analysis. Values indicated with different letters indicate statistically significant differences, whereas those marked with the same letters show statistically similar values.

Temperature	PPFD treatment					
	High			Low		
	A_{max}	x_0	k	A_{max}	x_0	k
High	11.8 ± 0.62^B	58.2 ± 6.6^a	0.003 ± 0.0004^b	4 ± 0.76^D	34.3 ± 9^b	0.005 ± 0.003^{ab}
Low	15.2 ± 0.52^A	60.1 ± 8.5^a	0.003 ± 0.0003^b	6.7 ± 0.13^C	20.7 ± 2.03^b	0.008 ± 0.0017^a

3.3.2.3 Tipburn was induced by combined HL and HT.

Visual tipburn symptoms were observed only in plants grown under combined HL and HT (Figure 3.20). Symptoms appeared as dark coloured necrotic areas of deformed leaves enclosed within the developing head.

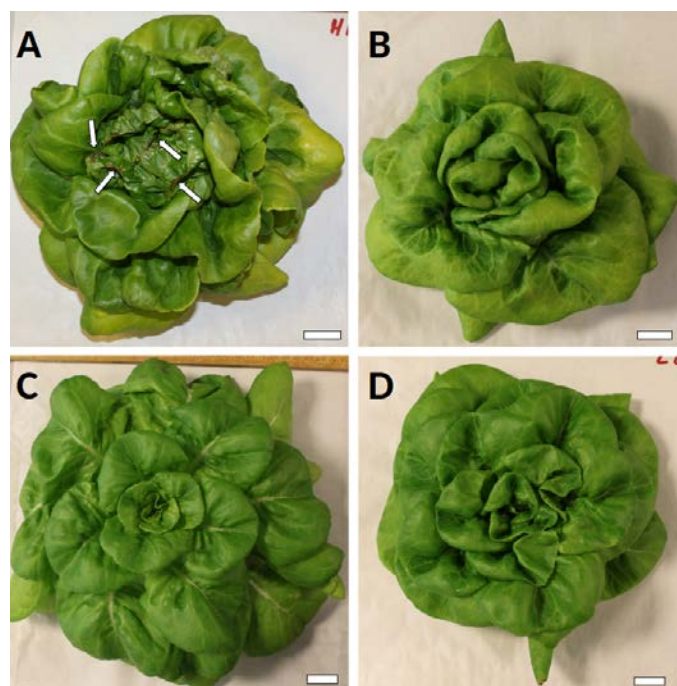


Figure 3.20. Lettuce plants (*L. sativa* L. cv. 'Frank') 30 DAT. (A) HL and HT (cabinet 1), (B) HL and LT (cabinet 2), (C) LL and HT (cabinet 3), (D) LL and LT (cabinet 4). Plants only developed tipburn symptoms under combined conditions of HL and HT (A). White arrows in picture (A) show tipburn symptoms located at the edges of leaves within the developing head. Scale bars are 3 cm.

3.4 Discussion.

Uniform distribution of PPFD within a growth system is necessary to achieve consistent and reproducible plant responses (Yano et al., 2012). Although PPFD of both HL and LL treatments was moderately uniform, fragmentation of the LL

treatment was also evident in the contour map of Figure 3.6 with “blue” patches of lower light intensity within the higher light intensity “green” landscape, due to every other lighting unit being turned off to achieve the desired PPFD. There was no observed difference in incident spectral irradiance between the two light treatments (Figure 3.8), suggesting that plant responses within the DFTS were due to light intensity and not quality. Taken together, these findings suggest that the DFTS provided a uniform and consistent lighting environment.

Metal-halide lights have been widely documented as heat sources since they produce large amounts of infrared energy (Barradas et al., 1994; Borgeraas and Hessen, 2000; Seddon and Cheshire, 2001; Weerakoon et al., 2002; Hughes et al., 2005). When lights were turned on (at 06:00 hrs), surface temperature on the lid of the DFTS and air temperature of both light treatments increased, whereas when lights were turned off (at 22:00 hrs) all system temperatures decreased. This indicates a strong link between the operating time of the lights and system temperatures. Under the HL treatment and during the light period, the median surface temperature on the lid of the DFTS was 28.4°C and it peaked in several cases at 34°C (Figure 3.10), which was 10°C higher than the upper limit of the optimal temperature range for lettuce growth (between 7°C to 24°C) (Jenni and Hayes, 2009). Mean air temperature ($23.6 \pm 0.04^\circ\text{C}$) peaked in several cases above supra-optimal levels ($> 24^\circ\text{C}$). These temperature levels promote luxuriant growth and the development of tipburn symptoms in lettuce (Misaghi and Grogan, 1978; Collier and Tibbitts, 1984; Nagata and Stratton, 1994; Choi et al., 2000; Frantz et al., 2004; Lee et al., 2013). In contrast, under the LL treatment and during the light period, the median surface temperature on the lid of the DFTS was 21.5°C, whereas air temperature fluctuated within the optimal range for lettuce growth (19°C)

(Jenni and Hayes, 2009). Similarly, mean canopy temperature at 18:00 hrs was 1.36-fold higher under HL ($24.1 \pm 0.5^{\circ}\text{C}$) compared to LL ($17.7 \pm 0.7^{\circ}\text{C}$) for both cultivars, indicating that plants under HL were grown at supra-optimal temperatures.

Root zone temperature also increased during the light period and gradually decreased during the dark period in HL (Figures 3.9 and 3.10). Values peaked at 21°C with a median value of 19.5°C during the light period. When the lights were turned off temperatures gradually declined from 21°C to 17°C . However, in LL, root zone temperature was not affected by the lights and fluctuated between 18°C to 16.5°C . According to Collier and Tibbitts (1984), lettuce plants grown under higher root zone temperature ($25.1 \pm 2^{\circ}\text{C}$ / $21.8 \pm 2^{\circ}\text{C}$ light/dark period) developed tipburn symptoms earlier compared to the control ($15.9 \pm 1^{\circ}\text{C}$ / $13.9 \pm 1^{\circ}\text{C}$ light/dark period). Consequently, it is likely that the higher root zone temperatures in HL contributed to tipburn development in this treatment. In the tropics, lowering root zone temperature to 20°C promoted lettuce growth compared to a fluctuating ambient root zone temperature (23°C to 40°C), whilst allowing the aerial parts to be maintained at supra-optimal, growth-inhibiting temperatures (36°C) (He and Lee, 2004). Future studies are therefore required to separate the individual effects of canopy and root zone temperature in the induction of tipburn, either of which might prove to be more cost-effective and feasible to manipulate in certain environments.

When plants were grown in HL and LL in combination with either HT or LT (Section 3.3.2), plants grown at HL and HT produced higher yields than the three other treatments. This is consistent with previous reports that lettuce productivity generally increases with higher PPFD and temperatures (Frantz and Bugbee, 2005; Qin et al.,

2008; Johkan et al., 2012; Kang et al., 2014; Sago, 2016). In contrast, plants grown at LL and HT produced significantly lower yield compared to the three other treatments (Figure 3.18). This might result from enhanced respiration rates, due to HT (Lambers et al., 2013), which can rapidly deplete available stored energy in plants under low PPFD (Kubatsch et al., 2007).

Importantly, tipburn symptoms were only observed in plants grown at HL and HT (Figure 3.20). This is consistent with studies that have linked increased growth rates to tipburn development (Cox et al., 1976; Frantz et al., 2004; Sago, 2016). Interestingly, lowering system temperatures may ameliorate tipburn symptoms in DFTS and VFS. Nevertheless, accelerated growth rates are particularly desirable in VFS, for example in plant factories, to maximize the efficiency of the growth facilities by permitting more crops in a fixed period of time (Sago, 2016). Therefore, the lower yields associated with this approach run counter to the requirements of high productivity VFS.

Plants grown within the DFTS showed light-response curves typical of either sun (HL) or shade (LL) -grown plants (Figure 3.12) (Von Caemmerer and Farquhar, 1981; Singhal, 1999; Larcher, 2003; Lambers et al., 2008). Higher A_{\max} and x_0 are often observed in sun-grown compared to shade-grown plants, as the latter photosynthesize more slowly compared to the former (Heschel et al., 2004). In contrast, k values are usually similar (Lambers et al., 2008) as the efficiency of the light reactions remains the same irrespectively of PPFD (McDonald, 2003). Plants grown under the HL treatment reached the x_0 and A_{\max} at higher PPFD compared to plants grown under the LL (Figure 3.12). However, k values were significantly lower in plants under HL

compared to LL. This is an important observation since a reduction in k is associated primarily with the effects of photoinhibition (Burgess et al., 2015) suggesting that plants grown under the HL exhibited photoinhibition. This process occurs when incident light intensity exceeds a plant's capacity of CO₂ assimilation (Apel and Hirt, 2004). This can inhibit photosystem II (PSII) activity (Murata et al., 2007) and may lead to photooxidative destruction of the photosynthetic apparatus (Long et al., 1994) via the overproduction of ROS, which can decrease the repair rate of photodamaged PSII (Nishiyama et al., 2006).

Photosynthesis is one of the processes most sensitive to heat (Camejo et al., 2005); high temperatures can both enhance photorespiration (Sharkey, 2005) and intensify photoinhibition (Long et al., 1994). Thus, the observed decrease in k could be attributed to the synergistic effects of HL and HT imposed on the HL-grown plants, as these two factors combined have a more profound negative effect on photosynthesis than they have separately (Leverenz et al., 1990). Photoinhibition has also been linked to, although not always accompanied by, reductions in A_{\max} (Demmig-Adams et al., 1998; Murchie and Niyogi, 2011). In agreement, significant changes in A_{\max} occurred when the effects of PPFD and temperature were separated. A_{\max} of plants grown at 27°C (HT) was significantly lower than plants grown at 21°C (LT), declining from 15.2 $\mu\text{mol CO}_2 \text{ m}^{-2} \text{ s}^{-1}$ to 11.8 $\mu\text{mol CO}_2 \text{ m}^{-2} \text{ s}^{-1}$ and from 6.7 $\mu\text{mol CO}_2 \text{ m}^{-2} \text{ s}^{-1}$ to 4 $\mu\text{mol CO}_2 \text{ m}^{-2} \text{ s}^{-1}$ for the HL (cabinets 1 and 2) and the LL (cabinets 3 and 4) PPFD treatments, respectively (Table 3.2). Taken together, these results suggest that HL and HT can synergistically induce oxidative stress-related responses. Crucially, since leaf gas exchange measurements were performed one day before the appearance of first visual tipburn symptoms, these findings lend additional credence to the hypothesis

that increased photoinhibition under luxuriant growth conditions, leading to oxidative stress, may induce tipburn in lettuce. This hypothesis will be tested empirically in the following chapters.

3.5 Conclusions.

Tipburn of lettuce is a key limitation of productivity and crop quality, particularly in VFS, making it imperative to establish commercially viable approaches to mitigate the disorder. This requires a detailed understanding of the underlying mechanisms. This chapter established a model DFTS in which both light and temperature treatments were independently manipulated, and in which tipburn symptoms in lettuce were reproducibly observed. This allowed tipburn development, which was observed under luxuriant growth conditions in the prototype VFS (Chapter 2), to be studied independently of the other environmental gradients present in the system. The DFTS revealed that changes in the photosynthetic performance of plants grown under luxuriant growth conditions precede the first visible symptoms of tipburn, suggesting a causative link between increased photoinhibition, leading to oxidative stress, and tipburn. This model DFTS will be used in subsequent chapters to test whether this hypothesis can explain tipburn occurrence of lettuce within VFS, under luxuriant growth conditions.

CHAPTER 4

DO OXIDATIVE STRESS AND CALCIUM DEFICIENCY PRECEDE
THE DEVELOPMENT OF LETTUCE TIPBURN?

4.1 Introduction.

In Chapter 3, plants grown under high PPFD and temperature exhibited reproducible tipburn symptoms. These conditions can lead to ROS over-accumulation and inevitably oxidative stress (Suzuki and Mittler, 2006; Almeselmani et al., 2006; Sharma et al., 2012). Plants exhibited photoinhibition, as demonstrated in photosynthetic light-response curves, one day before visual symptoms appeared (Figure 3.12). Photoinhibition occurs when incident PPFD exceeds the plant's capacity for CO₂ assimilation (Apel and Hirt, 2004), and can be further intensified by high temperatures (Long et al., 1994). This can result in increased ¹O₂ concentrations in leaves causing oxidative damage to lipids, proteins, nucleic acids and loss of PSII activity (Nooden, 2003; Takahashi and Murata, 2005; Krieger-Liszkay et al., 2008; Triantaphylidès and Havaux, 2009). Excess PPFD can also enhance the generation of O₂⁻ in PSI via the Mehler reaction (Triantaphylidès et al., 2008; Karuppanapandian et al., 2011). O₂⁻ can be converted to the toxic molecules H₂O₂, and [•]OH, further damaging cellular components (Nishiyama et al., 2006; Miller et al., 2010). In addition, high temperatures can exacerbate oxidative stress through the loss of specificity of RuBisCO towards CO₂ *versus* O₂, producing H₂O₂ (Kim and Portis, 2004). This raises two key questions concerning the physiological events preceding the appearance of tipburn symptoms: 1) is the observed photoinhibition linked to ROS over-accumulation, causing oxidative stress prior to visual symptoms? and 2) is this putative oxidative stress causally related to the development of the disorder?

To date, there has been only a single study linking oxidative stress and tipburn in lettuce (Carassay et al., 2012). Therefore, in this chapter, a presymptomatic investigation (Christakis, 2001) empirically tested whether oxidative stress occurs

prior to the appearance of the visual tipburn symptoms using membrane lipid peroxidation (Sharma et al., 2012) and the activity of antioxidant enzymes (Bestwick et al., 2001; Sudhakar et al., 2001; Suzuki and Mittler, 2006; Gusman et al., 2013) as indicators of ROS over-accumulation. Specifically, the extent of lipid peroxidation was quantified by measuring Malondialdehyde (MDA) concentration. MDA is a three-carbon aldehyde which is the cytotoxic product of radical attack on polyunsaturated fatty acids (Zhang et al., 2007; Sharma et al., 2012) and consequently indicates the extent of lipid peroxidation and, indirectly, of ROS production (Havaux et al., 2005; Møller et al., 2007; Zhang et al., 2007; Alboresi et al., 2009; Kong et al., 2016). In addition, the activities of the major ROS-scavenging enzymes: SOD, CAT, APX and GR were investigated presymptomatically (for a detailed description of the role of antioxidant enzymes in plant cell protection from oxidative damage, see Section 1.6.2).

Previously, Carassay et al. (2012) locally modified leaf Ca concentration using EGTA, verapamil and LaCl_3 or Ca^{2+} ionophore (A 23187) to decrease or increase Ca concentration, respectively, to study the link between oxidative stress and tipburn. Oxidative stress was reduced locally using Tiron (a ROS scavenger) and DPI (a suicide inhibitor of NADPH oxidase). All treatments were applied locally by painting the edge of lettuce leaves. The plants were grown under high ambient temperature (up to 36°C) within saline nutrient solution (stress) or in control, and the nutrient solution of both treatments contained low Ca concentration (0.5 mM) to induce tipburn symptoms. Stress and EGTA treatment significantly increased O_2^- and MDA concentrations, and significantly enhanced tipburn symptoms. On the other hand, Tiron application significantly ameliorated tipburn symptoms.

Although providing useful insights into the development of the disorder, the plants were not grown under commercial production settings and pharmacological approaches were used to promote tipburn symptoms (Carassay et al., 2012). Consequently, in this chapter, the total Ca concentration in lettuce seedlings and leaf tips was also measured presymptomatically to investigate whether Ca deficiency, in addition to oxidative stress, is associated with the development of tipburn symptoms (Collier and Tibbitts, 1982, 1984; Saure, 1998; Barta and Tibbitts, 2000; Frantz et al., 2004, Sago, 2016). Plants were grown in a (commercially) relevant environment and tipburn symptoms were induced in a non-invasive manner.

4.2 Materials and methods.

4.2.1 Plant material and treatments.

Two varieties of butterhead lettuce, with contrasting susceptibility to tipburn, were used to investigate the contribution of oxidative stress and Ca deficiency to the development of lettuce tipburn. Seeds of tipburn resistant (*Lactuca sativa* L. cv. 'Frank') and susceptible (*L. sativa* L. cv. 'Sunstar') lettuce were purchased from Moles Seeds (Essex, UK) and Hazera Seeds (Lincolnshire, UK), respectively. The seeds were sown into 2 cm x 2 cm x 4 cm rockwool cubes (Grodan, Fargro Ltd., UK) and germinated in the CE room described in Chapter 2 at 17°C. PPFD was maintained at approximately 170 $\mu\text{mol m}^{-2} \text{s}^{-1}$ under a 16 hour photoperiod (06:00 hrs to 22:00 hrs). The seedlings were incubated in aerated deionized water for 15 days and then in one-quarter-strength Hoagland's solution (EC: $0.25 \pm 0.1 \text{ dS m}^{-1}$, pH: 5.8 ± 0.2) for 13 days. DO concentration was maintained at $8.4 \pm 0.2 \text{ mg l}^{-1}$ by aerating the solution with an aquarium air pump (All Pond Solutions Ltd, Middlesex, UK). Uniform

seedlings were transferred to a DFTS 28 days after sowing and were subsequently acclimated for 7 days under PPFD of $170 \mu\text{mol m}^{-2} \text{s}^{-1}$ and air temperature of $19/17^{\circ}\text{C}$; light/dark period. The DFTS contained half-strength Hoagland's solution (EC: $1 \pm 0.2 \text{ dS m}^{-1}$, pH: 5.8 ± 0.2). The nutrient solution was replaced every 7 days. Each hydroponic box (17.2 cm height, 42.7 cm width and 32.8 cm depth) contained two cv. 'Frank' and two cv. 'Sunstar' plants.

Two previously characterised combinations of PPFD and air temperature (see Chapters 2 and 3) were applied as experimental treatments a week after the plants were transferred to the DFTS. These were a stress (PPFD at $450 \mu\text{mol m}^{-2} \text{s}^{-1}$ and $24/18^{\circ}\text{C}$ air temperature, $20/19^{\circ}\text{C}$ root zone temperature; light/dark period) and a control (PPFD at $170 \mu\text{mol m}^{-2} \text{s}^{-1}$ and $19/17^{\circ}\text{C}$ and $17/17^{\circ}\text{C}$ root zone temperature; light/dark period) treatment. The position of the hydroponic boxes was rotated randomly every 2 days to minimize positional effects.

4.2.2 Collection of plant material.

Leaf tissue samples were collected between 18:00 hrs and 19:00 hrs (12 hours after the start of the photoperiod) prior to the application of the treatments (Day 0; on the seventh day of the acclimation period), on Day 1 following the start of the treatments and subsequently on every second day (Days 3, 5, 7, 9, 11, 13, 15) during the experiment. The shoots of whole seedlings were sampled on Days 0 to 5. Thereafter, the two youngest, fully expanded leaves were chosen for sampling, since these were the first to show tipburn symptoms in previous trials (see Chapter 3). Leaves were detached from the plant and placed on a sterilized tile (90% EtOH for 2 min, followed

by a wash with distilled water) to be dissected using a single edge blade. Approximately 2 mm strips were cut from the edge of the leaf tissue, henceforth denoted as tips (Figure 4.1).



Figure 4.1. Plant leaf tissue was on a sterilized tile, and approximately a 2 mm strip dissected from the edge of the leaf; henceforth denoted as tip (white arrows). Scale bar is 1 cm.

Leaf samples were placed into different eppendorf tubes, then immediately flash frozen into liquid nitrogen and stored at -80°C . Specifically, 0.2 g fresh weight of tissue was collected to analyse antioxidant enzymes activity, total protein (Bradford assay) and lipid peroxidation. Also, ≥ 0.2 g fresh weight of tissue was collected, washed with milliQ water and stored at -80°C in eppendorf tubes to determine Ca concentration using inductively coupled plasma optical emission spectrometry (ICP-OES).

4.2.3 Antioxidant enzymes activity analysis.

4.2.3.1 Sample handling and extraction.

Leaf tissue (0.2 g) was ground into fine powder using a pre-chilled mortar and pestle in liquid nitrogen and then homogenized with 1.2 ml ice-cold extraction buffer (0.2 M potassium phosphate buffer, pH 7.8, 0.1 mM EDTA). The homogenate was centrifuged at 15,000 g for 20 min at 4°C. The supernatant was collected and stored in 2 ml eppendorf tubes on ice. The pellet was re-suspended in 0.8 ml ice-cold extraction buffer (0.2 M potassium phosphate buffer, pH 7.8, 0.1 mM EDTA) and a second supernatant was obtained after spinning the homogenate for 15 min at 15,000 g at 4°C. The two supernatants were combined and stored on ice (Elavarthi and Martin, 2010). The combined supernatants were used as crude extract for enzyme activity and lipid peroxidation assays, which were assessed photometrically using an Ultrospec 2100 Pro UV/visible spectrophotometer (GE Healthcare UK Ltd, Little Chalfont, UK).

4.2.3.2 Superoxide dismutase (SOD) (EC 1.15.1.1) assay.

Total SOD activity was determined by measuring its ability to inhibit the photochemical reduction of nitro blue tetrazolium chloride (NBT), as described by Giannopolitis and Ries (1977). The method was based on the reduction of the yellow dye NBT by O_2^- to produce purple-coloured formazan. O_2^- were generated with illumination of riboflavin in the presence of the electron donor L-methionine and O_2 . SOD in the leaf extract competed with NBT for O_2^- and the inhibition of NBT reduction was proportional to the amount of SOD in sample (Weydert and Cullen, 2010). Each 2 ml assay reaction mixture contained 100 μ l leaf extract, 1.88 ml 50 mM potassium phosphate buffer (pH 7.8, containing 2 mM EDTA, 9.9 mM L-methionine, 0.025% Triton-X100, 55 μ M NBT), and 20 μ l of 1 mM Riboflavin which was added

last. The reactions were performed in glass vials with tightly closed rubber stopper (ThermoFisher Scientific, Dublin, Ireland). The tubes were shaken and placed in a polystyrene box lined with aluminium foil at room temperature. The reaction was initiated by illuminating, using two fluorescent tubes, with $80 \pm 2 \mu\text{mol m}^{-2} \text{s}^{-1}$ PPFD. The reaction was allowed to proceed for 10 min after which the lights were switched off and the box was covered with a polystyrene lid. Two identical tubes containing 100 μl of 50 mM potassium phosphate buffer (pH 7.8) were used either as control (10 min illuminated with samples) or blank (10 min kept in dark). The reduction of the tetrazolium salts to purple coloured formazan was then determined by measuring absorbance at 560 nm. The blank was used to zero the spectrophotometer at 560 nm. One unit of SOD activity (U) was defined as the amount of enzyme required to cause 50% photoinhibition of the NBT photo reduction rate in comparison to the control. Results were expressed as units of SOD activity per mg of total protein in the sample.

4.2.3.3 Catalase (CAT) (EC 1.11.1.6) assay.

Total CAT activity was determined according to Aebi and Lester (1984) by following the consumption of H_2O_2 as a decrease in absorbance at 240 nm for 3 min. The method is based on the ability of catalase to scavenge H_2O_2 by converting two molecules of H_2O_2 to H_2O and O_2 (Ahmad, 2014). Each 3 ml assay mixture contained 10 μl leaf extract, 1.49 ml of 50 mM potassium phosphate buffer (pH 7) and 1.5 ml of 10 mM H_2O_2 in potassium phosphate buffer (pH 7). The extinction coefficient of H_2O_2 ($40 \text{ mM}^{-1} \text{ cm}^{-1}$ at 240 nm) was used to calculate CAT activity that was expressed in terms of mmol of H_2O_2 per minute per mg of total protein in the sample.

4.2.3.4 Ascorbate Peroxidase (APX) (EC 1.11.1.11) assay.

Total APX activity was determined according to Nakano and Asada (1981) by monitoring the rate of consumption of ascorbate (AsA) as a decrease in absorbance at 290 nm for 3 min. The method is based on the ability of ascorbate peroxidase to utilize AsA as specific electron donor to catalyse the decomposition of H₂O₂ into H₂O and O₂ (Caverzan et al., 2012). Each 1 ml reaction mixture contained 100 µl leaf extract, 600 µl 50 mM potassium phosphate buffer (pH 7.0), 100 µl of 5 mM ascorbate, 100 µl of 1 mM EDTA, and 100 µl of 1 mM H₂O₂. The reaction was initiated by adding H₂O₂. The extinction coefficient for reduced AsA (2.8 mM⁻¹ cm⁻¹ at 290 nm) was used to calculate APX activity that was expressed in terms of mmol of AsA per minute per mg of total protein in the sample.

4.2.3.5 Glutathione Reductase (GR) (EC 1.6.4.2) assay.

Total GR activity was determined according to Foyer and Halliwell (1976) by monitoring the oxidation of NADPH to NADP⁺ as a decrease in absorbance at 340 nm for 3 min. The method is based on the ability of GR to catalyse the NADPH-dependent reduction of oxidized glutathione (GSSG) to reduced glutathione (GSH). GR is present at rate-limiting concentrations therefore; the rate of NADPH oxidation is directly proportional to the GR activity in the sample (Ahmad, 2014). Each 1 ml reaction mixture contained 100 µl leaf extract, 700 µl 25 mM potassium phosphate buffer (pH 7.8), 100 µl of 1.2 mM NADPH-Na₄, and 100 µl of 5 mM GSSG. The reaction was initiated by adding the leaf extract. The extinction coefficient for NADPH (6.2 mM⁻¹ cm⁻¹ at 340 nm) was used to calculate GR activity that was expressed in terms of mmol of NADPH per minute per mg of total protein in the

sample.

4.2.3.6 Total protein quantification.

Total protein content of all leaf extracts was determined according to Bradford (1976) using bovine serum albumin (BSA) as a standard. The method is based on the binding of the dye Coomassie brilliant blue G250 to protein, which causes a shift in absorbance from 465 nm to 595 nm (Kruger, 1994). BSA stock solution was prepared daily by dissolving lyophilized BSA powder (Sigma-Aldrich, Dorset, UK) in milliQ water. The quality of stock solution was assessed by measuring the absorbance of 1 mg ml⁻¹ BSA stock solution at 280 nm ($A_{280} = 0.66$). BSA standards were prepared in duplicates using the same extraction buffer as the samples in the following concentrations: 0 (Blank), 10, 20, 30, 40, 50, 60, 70, 80, 90, 100 µl ml⁻¹. The blank was used to zero the spectrophotometer at 595 nm. Each 1 ml reaction mixture contained 10 µl leaf extract, 90 µl extraction buffer (0.2 M potassium phosphate buffer, pH 7.8, 0.1 mM EDTA), and 900 µl of Bradford reagent (Sigma, Cat no. B6916-500 ml). The reaction mixture was left at room temperature in the dark for 30 min and the absorbance was recorded at 595 nm.

4.2.4 Lipid peroxidation assay.

Lipid peroxidation is a free-radical-mediated chain of reactions which has been widely used to indicate oxidative stress in cells and tissues (Mittler, 2002; Ayala et al., 2014). A common method for measuring lipid peroxidation products, also known as Malondialdehyde (MDA) equivalents, is the thiobarbituric acid reactive substances (TBARS) assay (Hodges et al., 1999). MDA is a biomarker of general lipid

peroxidation as it is a secondary end product of the oxidation of polyunsaturated fatty acids (Møller et al., 2007). MDA equivalents were determined according to the corrected TBARS method (Hodges et al. 1999). This method improves the basic protocol of Heath and Packer (1968) by correcting for compounds other than MDA which absorb at 532 nm, by subtracting the absorbance at 532 nm of a solution containing the plant extract incubated without thiobarbituric acid (TBA) from an identical solution containing TBA (Hodges et al., 1999). The method is based on the acid catalyzed nucleophilic addition reaction of MDA with two molecules of TBA yielding a red chromagen, which peaks at 532 nm absorbance (Hodges et al, 1999). Each 2 ml reaction mixture contained 500 μ l leaf extract, 1 ml 20% Trichloroacetic Acid (TCA) and 500 μ l 0.65% TBA. Identical solutions were prepared containing 500 μ l leaf extract and 1.5 ml 20% TCA without TBA, representing the zero control. To initiate the reaction the tubes were heated for 30 min in a heating block at 95°C. After 30 min the tubes were placed on ice to stop the reaction. The samples were centrifuged for 10 min at 15000 g and absorbance was read at 440 nm, 532 nm and 600 nm.

MDA equivalents were calculated according to Hodges et al. (1999):

$$1) A = [(A_{532+TBA} - A_{600+TBA}) - (A_{532-TBA} - A_{600-TBA})]$$

$$2) B = [(A_{440+TBA} - A_{600+TBA}) \times 0.0571]$$

$$3) \text{MDA equivalents (nmol ml}^{-1}\text{)} = ((A - B)/157000) \times 10^6$$

where 532 nm represents maximum absorbance of the TBA-MDA complex, 600 nm the correction for nonspecific turbidity, 440 nm represents maximum sucrose absorbance and 157000 $\text{m}^{-1} \text{cm}^{-1}$ the molar extinction coefficient for MDA. 0.0571 is the ratio of molar absorbance of sucrose at 532 nm and molar absorbance of sucrose at 440 nm.

4.2.5 Determination of total Ca concentration in leaf samples.

Samples were lyophilized at -52°C and 0.05 mbar for 48 hours in an Alpha1-2 LD Plus freeze dryer (Martin Christ, Osterode, Germany) prior to analysis. The lyophilized samples were weighed in glass conical flasks, then 10 ml of concentrated trace metal grade HNO_3 (Sigma-Aldrich, Dorset, UK) was added and the conical flasks allowed to stand in a fume hood while the initial reaction subsided (approximately 30 min). The conical flasks were then covered and heated on a hot plate up to 100°C and then maintained at this temperature overnight. After cooling, the conical flasks were opened and placed on a hot plate at 250°C and evaporated to incipient dryness, but not baked. The residue was then dissolved by adding 10 ml of 5% HNO_3 and 10 ml of milliQ water. To prepare samples for analysis, the acid digestate was filtered through a $0.45\ \mu\text{m}$ syringe filter. Blank digests were carried out in a similar manner. Ca concentration was determined using Inductively Coupled Plasma - Optical Emission Spectrometry (ICP-OES; iCAP 6300, Thermo Scientific, Massachusetts, USA). Samples were compared against standards of a known range of concentrations and the results were expressed as mg g^{-1} dry weight (DW).

4.2.6 Statistical analysis.

One-way ANOVA, followed by Duncan's multiple range test, was used to analyze all independent variables on a day-to-day basis for the two cultivars separately between treatments, and across the duration of the experiment in Figures 4.3-4.8. Log transformations were performed when the data violated ANOVA assumptions of normality and homoscedasticity of variances, in Figures 4.3.A, 4.4.B and 4.7.A. Log transformed means were not back transformed prior to display for consistency

between figures. Further, three-way ANOVA was used to examine differences in the independent variables (Ca concentration, MDA equivalents, and SOD, CAT, APX and GR activities) for main effects (cultivar, treatment and time), three first-order interactions (cultivar x time, treatment x time, cultivar x treatment) and one second-order interaction (cultivar x treatment x time). Duncan's multiple range test was used to highlight differences between the cultivar and treatment factors when main effects were significant and when there were no interactions. The results of the three-way ANOVA are presented in Table 4.1. Probability value less than 0.05 ($p < 0.05$) was considered to indicate a statistically significant difference. All statistical tests were performed on R version 3.1.2 software (R Development Core Team, 2014).

4.3 Results.

4.3.1 Visual symptoms of tipburn occurred on day 16.

The first visual symptoms of tipburn under stress (but not under the control treatment) developed 16 days after treatments were applied (Figure 4.2). Both cultivars, 'Frank' and 'Sunstar', developed tipburn symptoms although damage was more severe in the latter. (For a quantitative representation of tipburn affected area between cultivars, see Figure 3.15).

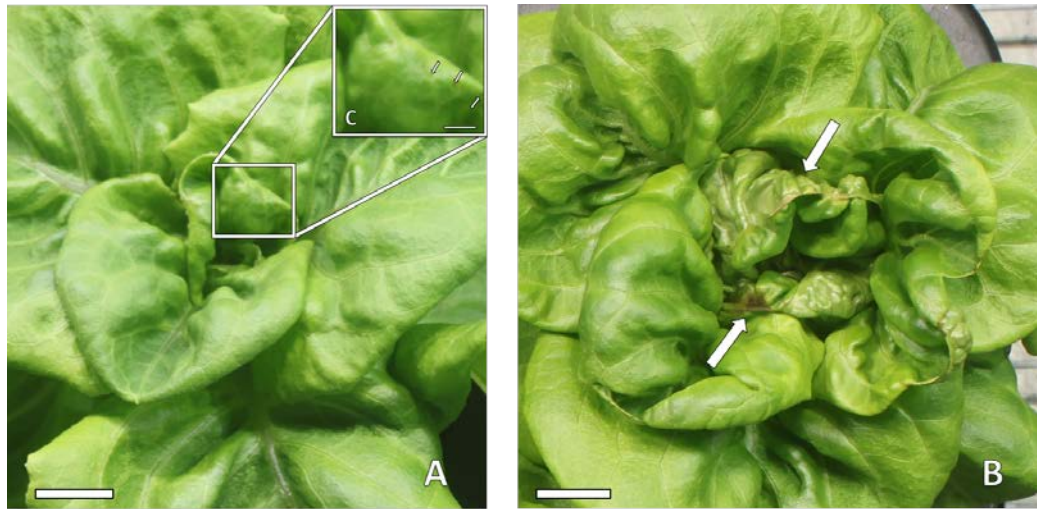


Figure 4.2. Development of visual tipburn symptoms in a lettuce plant (*Lactuca sativa* cv. 'Frank') grown under the stress treatment. The first visual symptoms of tipburn appeared 16 days after the stress treatment was applied, as small, circular, necrotic spots (A). Panel (B) shows tipburn development on the same plant, 23 days after the stress treatment was applied. Panel (C) shows expansion of tipburn region of panel (A). White arrows indicate tipburn symptoms on plants in both panels. Scale bar in 3 cm in (A) and (B), and 0.5 cm in (C).

4.3.2 There was no presymptomatic link between Ca and tipburn.

In cv. 'Frank', Ca concentration was maintained within similar levels in both treatments throughout the experiment (Figure 4.3.A). Under control treatment, Ca concentration on day 15 was significantly ($p < 0.05$) less than half of that on days 5 and 9, whilst in the stress treatment Ca concentration didn't change significantly over time (average Ca concentration was $8.2 \pm 0.6 \text{ mg g}^{-1} \text{ DW}$) (Figure 4.3.A).

In cv. 'Sunstar' however, Ca concentration decreased significantly ($p < 0.05$) by 1.5-fold on day 1 in both treatments in comparison to day 0 and then fluctuated over the

first 7 days of the experiment (Figure 4.3.B). In control plants, Ca concentration subsequently dropped significantly ($p < 0.05$) from day 9 onwards. In contrast, stressed plants showed a significant ($p < 0.05$), 1.5-fold increase in Ca concentration, after the nutrient solution was changed on day 7 following which Ca concentration also decreased significantly ($p < 0.05$) from day 9 to day 15 (Figure 4.3.B). Therefore, there doesn't appear to be a link between presymptomatic concentrations of Ca and the development of tipburn symptoms in either cv. 'Frank' or cv. 'Sunstar'.

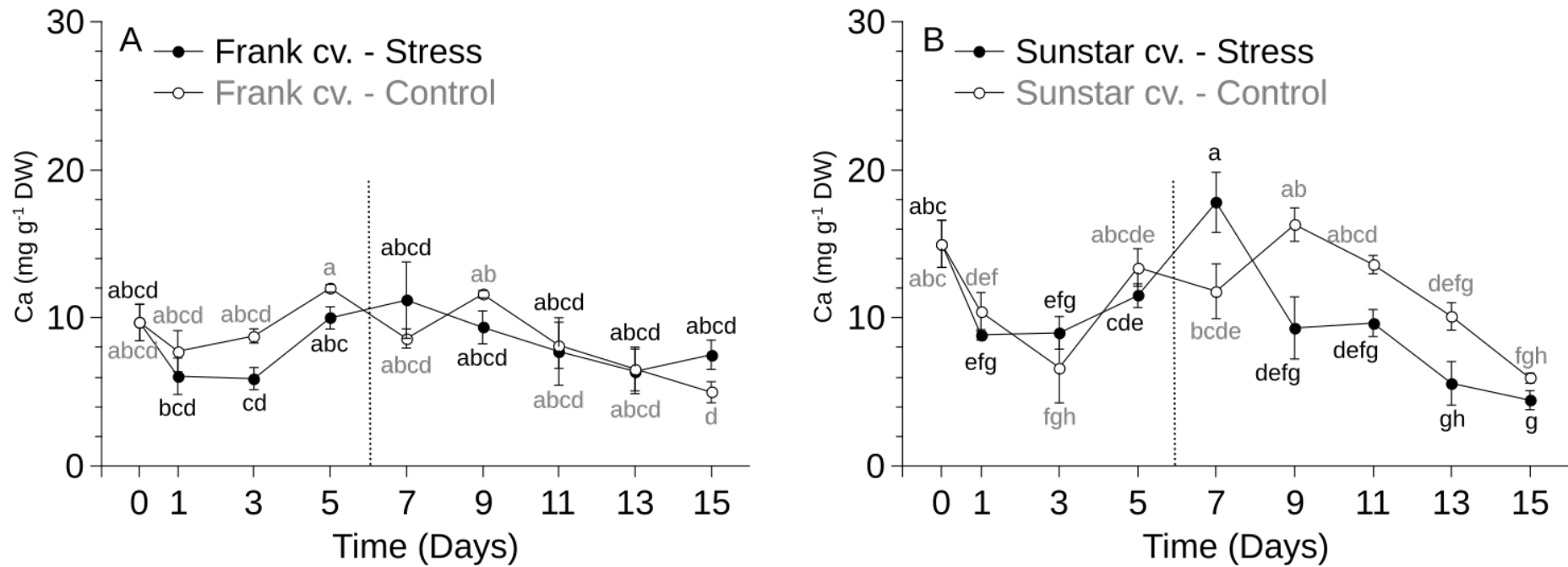


Figure 4.3. Time-course of changes in total Ca concentration of seedlings (days 0 – 5) and tips of developing leaves (days 7 – 15) of *Lactuca sativa* cv. ‘Frank’ (A) and cv. ‘Sunstar’ (B) under stress (closed symbols, black letters) and control (open symbols, grey letters) treatments. One-way ANOVA results for the cv. ‘Frank’ and cv. ‘Sunstar’ were $F(17, 36) = 2.79$, $p < 0.001$ and $F(17, 36) = 2.5$, $p < 0.01$, respectively. Values are means \pm SE ($n=3$). Means denoted by the same letter did not significantly differ at $p < 0.05$ according to Duncan's multiple range test. The dotted line indicates the different sampling techniques (Days 0 to 5; whole seedlings, Days 7 to 15; two fully expanded leaves)

4.3.3 Lipid peroxidation levels were higher under stress.

MDA levels were relatively stable in both the cv. 'Frank' and cv. 'Sunstar' (except for a transient increase in cv. 'Sunstar' on day 9) in control plants. However, stress significantly ($p < 0.001$) increased MDA. Treatment duration did not affect these responses, as indicated by the non-significant time x cultivar or time x treatment interactions (Table 4.1). In cv. 'Frank', MDA levels increased significantly ($p < 0.05$), by 2.5-fold on Day 1 and thereafter remained elevated throughout the rest of the experiment. MDA concentration was significantly ($p < 0.05$) higher under stress on days 1, 7, and 15 compared to the control in cv. 'Frank' (Figure 4.4.A). In cv. 'Sunstar', stress doubled MDA after 3 days and remained elevated throughout the remainder of the experiment (Figure 4.4.B). These data indicate that increased lipid peroxidation preceded the occurrence of tipburn (day 16) in both the cv. 'Frank' and cv. 'Sunstar'.

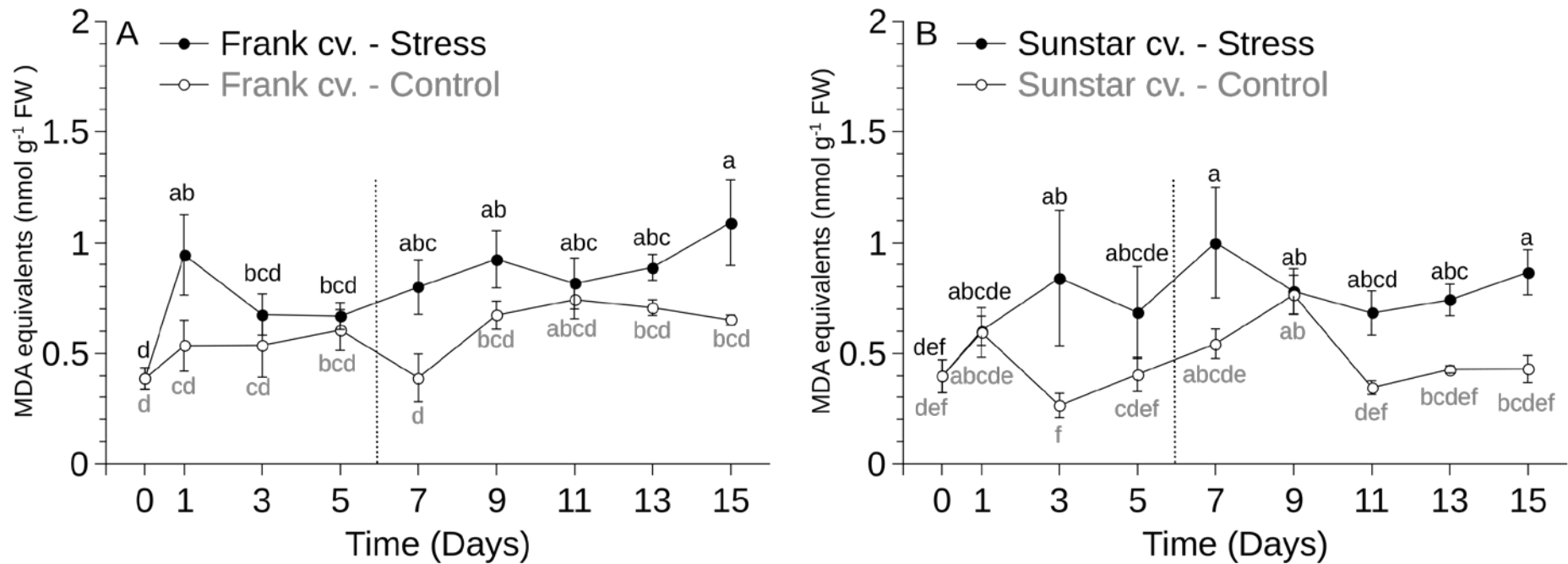


Figure 4.4. Time-course of changes in MDA equivalents of seedlings (days 0 – 5) and tips of developing leaves (days 7 – 15) of *Lactuca sativa* cv. ‘Frank’ (A) and cv. ‘Sunstar’ (B) under stress (closed symbols, black letters) and control (open symbols, grey letters) treatments. One-way ANOVA results for the cv. ‘Frank’ and cv. ‘Sunstar’ were $F(17, 36) = 3.56, p < 0.001$ and $F(17, 36) = 3.56, p < 0.001$, respectively. Values are means \pm SE (n=3). Means denoted by the same letter did not significantly differ at $p < 0.05$ according to Duncan's multiple range test. The dotted line indicates the different sampling techniques (Days 0 to 5; whole seedlings, Days 7 to 15; two fully expanded leaves)

4.3.4 SOD activity transiently peaked under stress.

Differences in SOD activity between cultivars and between treatments were directly related to treatment duration, as indicated by significant cultivar x time ($p < 0.05$) and treatment x time ($p < 0.01$) interactions (Table 4.1). In cv. 'Frank', SOD activity fluctuated in the control treatment throughout the experiment. Under stress, however, SOD activity increased significantly ($p < 0.05$) on Days 1, 3 and 13 (Figure 4.5.A). In contrast, in cv. 'Sunstar', SOD activity fluctuated in both treatments, with a 2.3-fold increase observed in stressed plants on day 3 (Figure 4.5.B). This suggests a protective response to oxidative stress in both cv. 'Frank' and 'Sunstar', which was more evident at the beginning of the experiment.

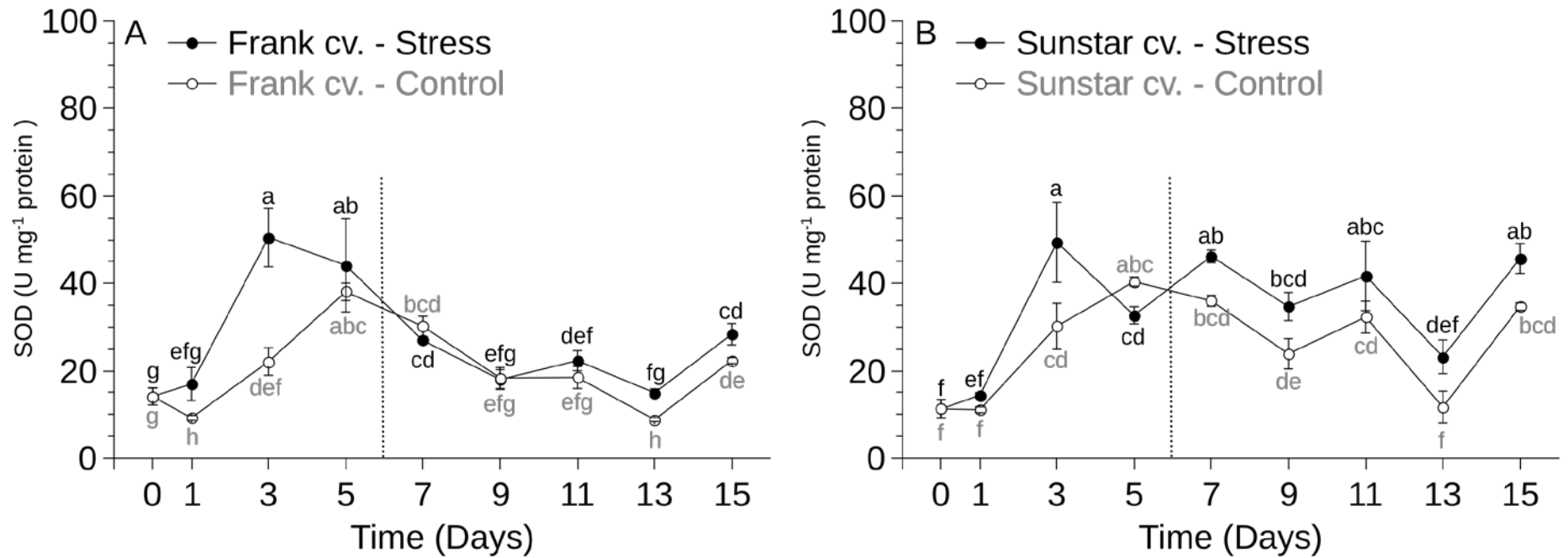


Figure 4.5. Time-course of changes in SOD activity of seedlings (days 0 – 5) and tips of developing leaves (days 7 – 15) of *Lactuca sativa* cv. ‘Frank’ (A) and cv. ‘Sunstar’ (B) under stress (closed symbols, black letters) and control (open symbols, grey letters) treatments. One-way ANOVA results for the cv. ‘Frank’ and cv. ‘Sunstar’ were $F(17, 36) = 15.45$, $p < 0.001$ and $F(17, 36) = 11.6$, $p < 0.001$, respectively. Values are means \pm SE ($n=3$). Means denoted by the same letter did not significantly differ at $p < 0.05$ according to Duncan's multiple range test. The dotted line indicates the different sampling techniques (Days 0 to 5; whole seedlings, Days 7 to 15; two fully expanded leaves)

4.3.5 CAT activity peaked in cv. 'Sunstar' but not in cv. 'Frank'.

Treatment effects on CAT activity varied significantly over time as indicated by the significant treatment x time ($p < 0.01$) interaction (Table 4.1). In cv. 'Frank', with one notable exception (a 2.5-fold drop in CAT activity on day 7), CAT activity in the control treatment remained stable during the experiment (average CAT activity from days 0 to 15, excluding day 7, was 0.093 ± 0.004 mmol H₂O₂ min⁻¹ mg⁻¹ protein). Under stress, CAT activity was similarly stable from day 5 onwards (average CAT activity from days 5 to 15 was 0.12 ± 0.004 mmol H₂O₂ min⁻¹ mg⁻¹ protein). Taken together, these data provide little indication of a link between H₂O₂-induced oxidative stress and tipburn of lettuce in the cv. 'Frank' (Fig. 4.6.A). In the cv. 'Sunstar', CAT activity in control plants also remained fairly stable through the duration of the experiment (average CAT activity from days 0 to 15 was 0.072 ± 0.005 mmol H₂O₂ min⁻¹ mg⁻¹ protein). However, in stressed plants CAT activity levels were significantly ($p < 0.05$) enhanced on day 5 compared to previous days, as well as in comparison to control on the same day, and remained elevated throughout the experiment being significantly ($p < 0.05$) higher on days 9 and 11 compared to control plants. These data are consistent with a protective response of CAT to H₂O₂ overproduction due to the stress treatment (Fig. 4.6.B).

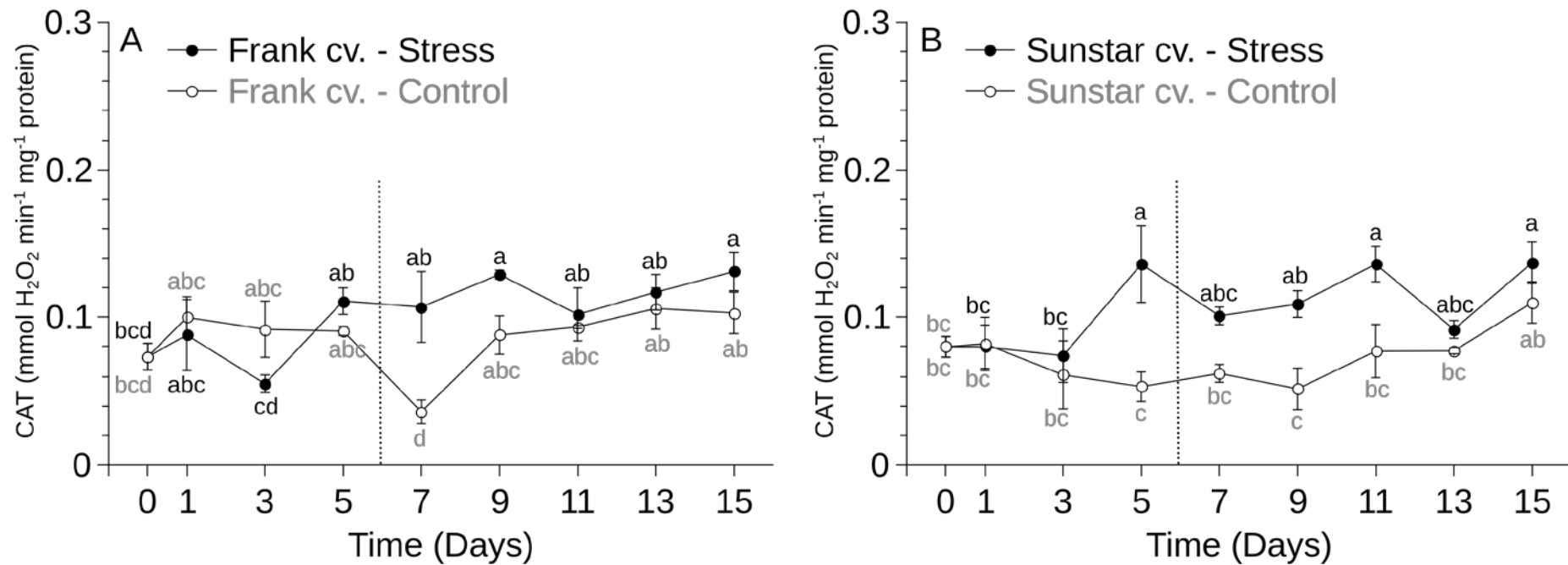


Figure 4.6. Time-course of changes in CAT activity of seedlings (days 0 – 5) and tips of developing leaves (days 7 – 15) of *Lactuca sativa* cv. ‘Frank’ (A) and cv. ‘Sunstar’ (B) under stress (closed symbols, black letters) and control (open symbols, grey letters) treatments. One-way ANOVA results for cv. ‘Frank’ and cv. ‘Sunstar’ were $F(17, 36) = 3.17, p < 0.05$ and $F(17, 36) = 3.57, p < 0.001$, respectively. Values are means \pm SE (n=3). Means denoted by the same letter did not significantly differ at $p < 0.05$ according to Duncan's multiple range test. The dotted line indicates the different sampling techniques (Days 0 to 5; whole seedlings, Days 7 to 15; two fully expanded leaves).

4.3.6 APX activity fluctuated under stress.

There was no cultivar difference in response to the two treatments, as indicated by the non-significant interactions between cultivar x treatment interaction (Table 4.1). Nevertheless, there was a significant interaction between time and treatment ($p < 0.05$) influencing APX activity, suggesting that the differences between treatments increased with time (Table 4.1). In cv. 'Frank', stress significantly ($p < 0.05$) decreased APX activity more than two-fold on day 1 in comparison to day 0, indicating an immediate plant response. After this initial decrease, APX activity recovered gradually and was significantly ($p < 0.05$) higher on day 7 (1.6-fold) and day 13 (1.7-fold) compared to control on the same day (Figure 4.7.A). In contrast, in cv. 'Sunstar', APX activity remained fairly stable in both treatments from day 0 to 13, only increasing on day 15. Although values were not significantly different between the control and stressed plants, stress significantly increased APX activity by 1.9-fold on day 15 compared to the average APX activity from day 0 to 13 (average APX activity was $0.82 \pm 0.07 \text{ mmol AsA min}^{-1} \text{ mg}^{-1} \text{ protein}$) (Figure 4.7.B).

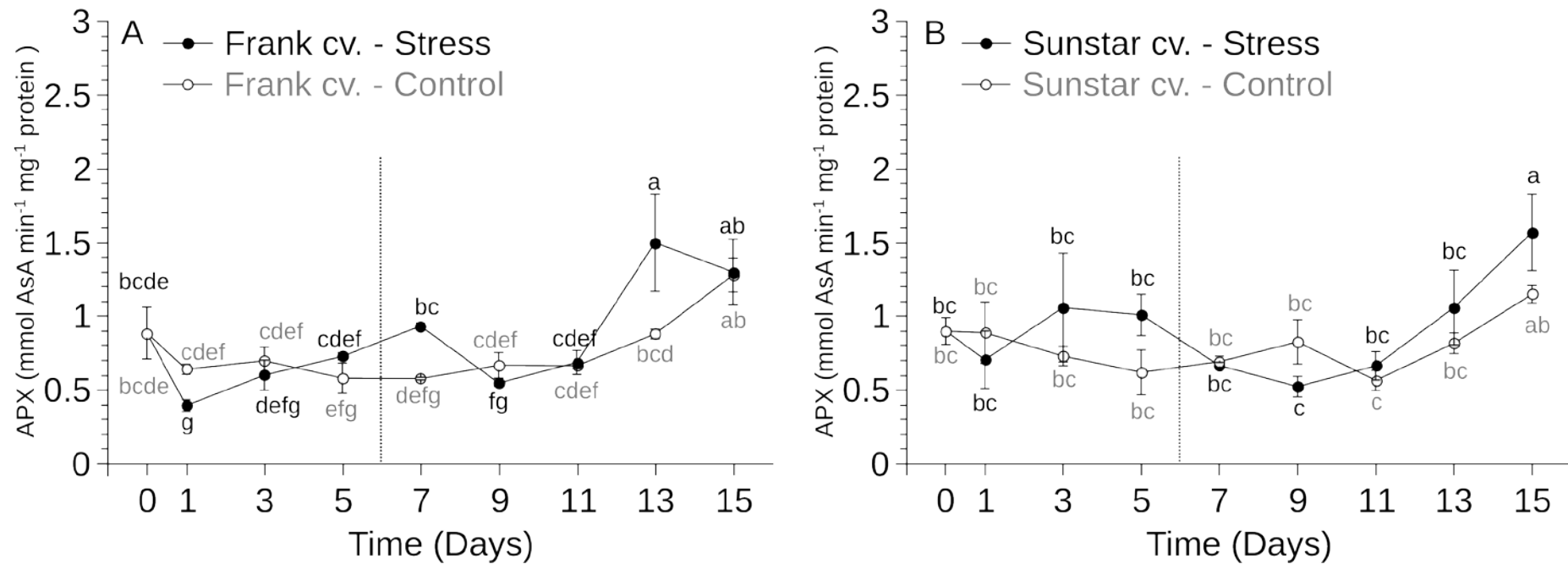


Figure 4.7. Time-course of changes in APX activity of seedlings (days 0 – 5) and tips of developing leaves (days 7 – 15) of *Lactuca sativa* cv. ‘Frank’ (A) and cv. ‘Sunstar’ (B) under stress (closed symbols, black letters) and control (open symbols, grey letters) treatments. One-way ANOVA results for the cv. ‘Frank’ and cv. ‘Sunstar’ were $F(17, 36) = 6.88, p < 0.001$ and $F(17, 36) = 2.5, p < 0.01$, respectively. Values are means \pm SE ($n=3$). Means denoted by the same letter did not significantly differ at $p < 0.05$ according to Duncan's multiple range test. The dotted line indicates the different sampling techniques (Days 0 to 5; whole seedlings, Days 7 to 15; two fully expanded leaves).

4.3.7 GR activity peaked towards the end the treatments.

Treatment duration significantly influenced GR activity, as indicated by significant interactions between treatment and time ($p < 0.01$) (Table 4.1). GR activity remained stable with no significant differences in both cv. 'Frank' and cv. 'Sunstar', for up to day 9 in both treatments. There was a 1.5-fold significant ($p < 0.05$) increase cv. 'Frank' under stress on day 11 compared to day 0 followed by an increase in GR activity which peaked on day 13. In cv. 'Sunstar', GR activity also increased significantly ($p < 0.05$) by 1.6-fold on day 13 (Fig. 4.8.B). However, increases in GR activity were also observed in both cultivars under control suggesting a growth-related increase in GR activity during the final days of the treatments (Fig. 4.8.A).

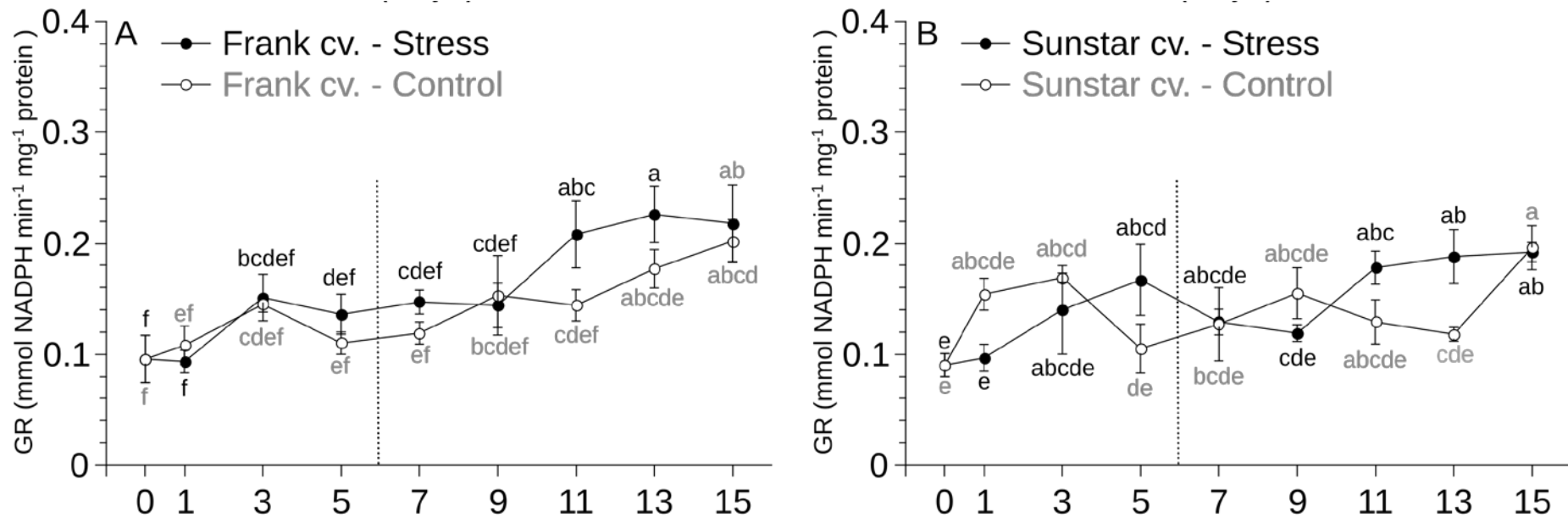


Figure 4.8. Time-course of changes in GR activity of seedlings (days 0 – 5) and tips of developing leaves (days 7 – 15) of *Lactuca sativa* cv. ‘Frank’ (A) and cv. ‘Sunstar’ (B) under stress (closed symbols, black letters) and control (open symbols, grey letters) treatments. One-way ANOVA results for the cv. ‘Frank’ and cv. ‘Sunstar’ were $F(17, 36) = 4.22, p < 0.01$ and $F(17, 36) = 3.05, p < 0.01$, respectively. Values are means \pm SE ($n=3$). Means denoted by the same letter did not significantly differ at $p < 0.05$ according to Duncan's multiple range test. The dotted line indicates the different sampling techniques (Days 0 to 5; whole seedlings, Days 7 to 15; two fully expanded leaves).

Table 4.1. F and p values of three-way ANOVA examining the effects of the nine sampling periods (Time; T), the control and stress treatments (Treatment; Tr), and the two lettuce cultivars *Lactuca sativa* cv. 'Frank' and cv. 'Sunstar' (Cultivar; C) on Calcium (Ca) concentration, Malondialdehyde equivalents (MDA eq), superoxide dismutase (SOD), catalase (CAT), ascorbate peroxidase (APX) and glutathione reductase (GR).

	Effects						
	T	C	Tr	C x T	Tr x T	C x Tr	C x Tr x T
Df	8	1	1	8	8	1	8
Variables							
Ca	14.36 ***	28.24 ***	4.17 *	2.41 *	3.46 **	0.96 n.s.	1.8 n.s.
MDA eq	3.96 ***	5.5 *	39.22 ***	1.4 n.s.	1.52 n.s.	0.42 n.s.	1.2 n.s.
SOD	33.16 ***	25.42 ***	30.05 ***	4.49 ***	3.74 **	0.35 n.s.	1.5 n.s.

	Effects						
	T	C	Tr	C x T	Tr x T	C x Tr	C x Tr x T
Df	8	1	1	8	8	1	8
Variables							
CAT	5.05 ***	1.51 n.s.	25.28 ***	1.08 n.s.	3.45 **	3.63 n.s.	1.19 n.s.
APX	10.27 ***	0.97 n.s.	3.78 n.s.	1.35 n.s.	2.2 *	0.098 n.s.	1.09 n.s.
GR	10.68 ***	1.12 n.s.	3.3 n.s.	1.1 n.s.	2.8 **	0.74 n.s.	0.41 n.s.

Df: degrees of freedom

Significance codes: *** $p < 0.001$, ** $p < 0.01$, * $p < 0.05$, n.s. Non significant

4.4 Discussion.

Several studies provided evidence that a localised Ca deficiency is the main cause of tipburn. These include correlations of tissue Ca concentration with tipburn symptoms (Misaghi and Grogan, 1978; Collier and Huntington, 1983; Barta and Tibbitts, 1991; 2000), amelioration of tipburn via Ca spraying (Thiobodeau and Minotti, 1969; Corriveau et al., 2012) or meristem aeration to increase Ca delivery (Goto and Takakura, 1992; Kossowski et al., 1994; Shibata et al., 1994; Both et al., 1994; Frantz et al., 2004), and promotion of tipburn symptoms via artificial leaf enclosure (Barta and Tibbitts, 1986) to reduce transpiration rates and thus Ca delivery (White and Broadley, 2003; Gilliam et al., 2011). However, to date few alternative aetiologies for the induction of the disorder have been proposed (Saure, 1998; Carassay et al., 2012). The present study is the first to show that oxidative stress indicators, but not foliar Ca concentrations, change prior to the appearance of visual tipburn symptoms in lettuce plants grown under luxuriant growth conditions of high PPFD and temperature.

Foliar Ca concentration did not significantly differ between the stress and control treatments in the cv. 'Frank' over time (Figure 4.3.A), suggesting that the observed differences in tipburn severity and yield between the two treatments (see Chapter 3; Figures 3.15 and 3.5) were independent of foliar Ca concentration. Similarly, there were no significant differences in Ca concentration between the inner leaves of butterhead lettuce (*Lactuca sativa* cv. 'capitata L.') grown under four continuous PPFD treatments of 150, 200, 250, and 300 $\mu\text{mol m}^{-2} \text{s}^{-1}$ even though the number of tipburned leaves, as well as yield, increased with increasing PPFD (Sago, 2016). Conversely, Ca concentration in the cv. 'Sunstar' significantly decreased on day 9

under stress compared to the control. This drop initiated a non-significant difference in Ca concentration between the two treatments, starting from day 11 up to day 15 (Figure 4.3.B). These data suggest that the cv. 'Sunstar' exhibited a presymptomatic growth-related decrease in Ca concentration. Interestingly, foliar applications of CaCl₂ enhanced the ability of several plant species such as *Arabidopsis thaliana* (10 mM CaCl₂) (Larkindale and Knight, 2002) and *Agrostis stolonifera* (10 mM CaCl₂) (Larkindale and Huang, 2004) to cope with heat-induced oxidative stress, as well as post-drought recovery of *Camellia sinensis* (50 and 100 µM CaCl₂) (Upadhyaya et al., 2011). Thus, decreased foliar Ca concentration was related to the greater sensitivity of cv. 'Sunstar' to tipburn, compared to cv. 'Frank' (see also Section 3.3.1.6). However, as this response was observed in both stress and control treatments, it does not provide evidence of presymptomatic links between Ca and tipburn in cv. 'Sunstar'. In contrast, tipburn development was linked to decreased Ca concentrations of inner (enclosed within the developing head) lettuce leaves over time (Barta and Tibbitts 2000). Since, in the current study the lettuce heads did not develop enough to enclose the inner leaves (Figure 4.2), Ca transport to these tissues may not have been inhibited (Chang and Miller, 2004; Frantz et al., 2004; Gilliham et al., 2011) to a similar degree as in the Barta and Tibbitts (2000) study. Therefore, future investigations should explore the contribution of leaf enclosure to presymptomatic Ca depression in cv. 'Sunstar' by using aluminized polyethylene sheaths to artificially enclose the inner lettuce leaves (Barta and Tibbitts, 1986) or meristem aeration to increase Ca delivery to the enclosed leaves (Frantz et al., 2004).

The level of lipid peroxidation, which was quantified via MDA concentration measurements, is considered to indicate plant oxidative stress (Hodges et al., 1999;

Gupta, 2010; Sharma et al., 2012). Stress increased MDA concentration (Table 4.1) consistently, although not always significantly (Figures 4.4.A and 4.4.B), showing a higher degree of lipid peroxidation compared to the control, and thus indirectly higher ROS accumulation under stress (Havaux et al., 2005; Alboresi et al., 2009; Ahammed et al., 2012). These results agree with reports of significantly higher MDA values in lettuce plants grown under 700-900 $\mu\text{mol m}^{-2} \text{s}^{-1}$ compared to 200-350 $\mu\text{mol m}^{-2} \text{s}^{-1}$ PPFD at 27/20°C (air temperature; day/night) (Zhou et al., 2009), under 400 and 800 $\mu\text{mol m}^{-2} \text{s}^{-1}$ compared to 100, 200 and 400 $\mu\text{mol m}^{-2} \text{s}^{-1}$ PPFD at 20/16°C (air temperature; day/night) (Fu et al., 2012), and under increasing daytime air temperature treatments (starting from 25°C, 30°C, 38°C, up to 42°C; PPFD data not provided) (Han et al., 2013). Importantly, one day prior to the appearance of visual tipburn symptoms under stress, MDA concentrations of both cultivars significantly increased compared to the control. This was not unexpected, since these plants were simultaneously photoinhibited (Chapter 3; Tables 3.1. and 3.2), which has been related to increased MDA concentration, mainly via ROS over-accumulation leading to photooxidative damage (Cui et al., 2006; Zhou et al., 2009; Jbir-Koubaa et al., 2015). Crucially however, these elevated MDA values preceded the appearance of visual tipburn symptoms, thus highlighting that increased lipid peroxidation and the initiation of the disorder are temporally linked.

In addition to the changes in lipid peroxidation levels, the treatments induced marked variations in antioxidant enzyme responses (Figure 4.9).

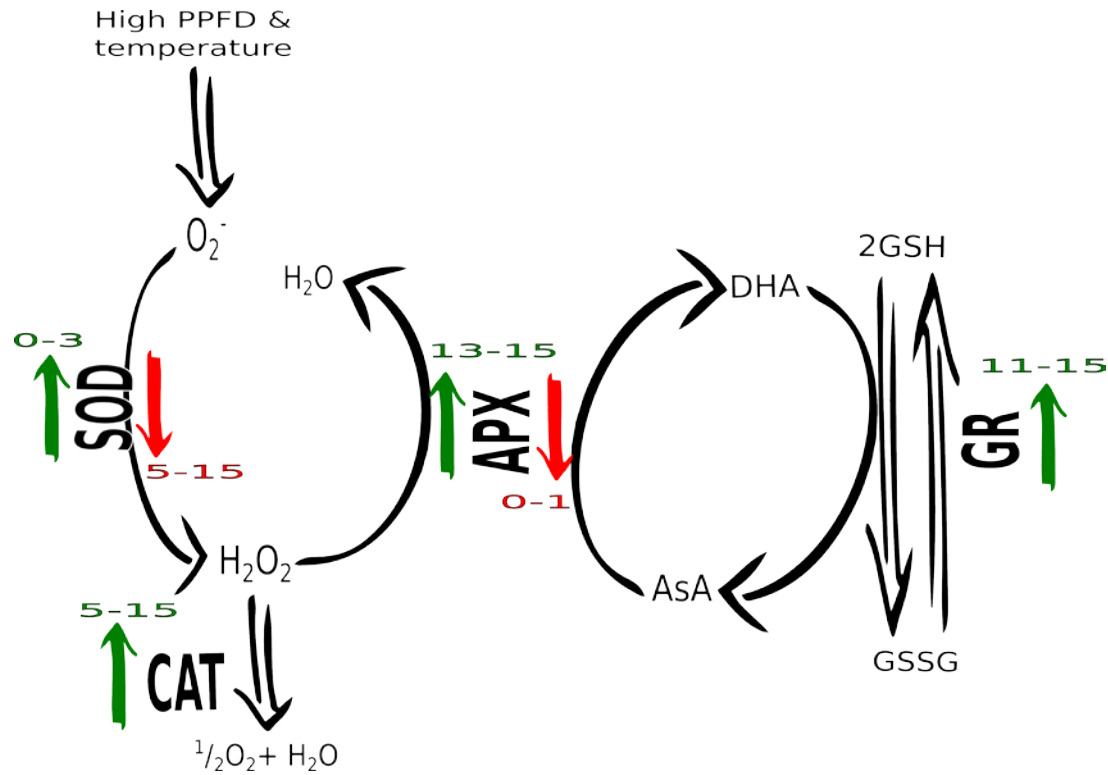


Figure 4.9. Schematic representation indicating which antioxidant enzyme pathways were enhanced (green arrows; pointing upwards) or depressed (red arrows; pointing downwards) under stress through the experiment, overall for both cultivars. Numbers indicate days after the treatment was applied.

The first enzymatic line of defence against ROS is SOD, which dismutates the highly reactive O_2^- to produce the more stable H_2O_2 (Bowler et al., 1992). SOD activity significantly increased under stress almost immediately (day 3) after treatment (Figures 4.5.A and 4.5.B) in both cultivars, suggesting higher O_2^- generation under oxidative stress which can increase SOD activity (Calatayud et al., 2002; Gill and Tuteja, 2010). These transient peaks in SOD activity may enhance the ability of plants to detoxify O_2^- but also may have increased H_2O_2 levels, which if not effectively quenched by the plant's antioxidant machinery, can intensify lipid peroxidation (Eraslan et al., 2007). H_2O_2 is reduced to H_2O in the cytosol and chloroplasts through the ascorbate-glutathione cycle by APX and GR, and in peroxisomes by CAT (Foyer and Halliwell, 1976; Miller et al. 2010; Gill and Tuteja, 2010; Gupta 2010; Sharma et al., 2012). In cv. 'Sunstar' under stress, the peak in SOD activity on day 3 coincided with the onset of elevated MDA concentration and with the subsequent increase in CAT activity two days later. Increased MDA and CAT activity persisted in stressed plants throughout the remainder of the experiment, although they were not always significantly different to the control (Figure 4.4.B).

Similar increases in lipid peroxidation coupled with enhanced SOD and CAT activities occurred in lettuce under high PPFD stress (400 and 800 $\mu\text{mol m}^{-2} \text{s}^{-1}$) (Fu et al., 2012), and in tomato plants under heat stress (40/30°C; day/night) (Ogweno et al., 2008). In cv. 'Frank' under stress, the peak in SOD activity on day 3 succeeded a significant drop in APX activity on day 1. This could be attributed to H_2O_2 over-production, via spontaneous disproportionation of O_2^- (Ksas et al., 2015) and is consistent with the MDA peak on day 1 depleting AsA pools and consequently inactivating APX (Shikanai et al., 1998), as AsA is used as substrate by APX (Conklin and Barth, 2004).

Alternatively, it could be due to the transfer of plants from low control temperature (experienced during the seven day acclimation period) to the higher temperature of the DFTS stress treatment. This is because high temperature can diminish AsA regeneration and pool size by inhibiting the activities of the AsA/glutathione cycle enzymes MDHAR, DHAR and GR (Massot et al., 2013). GR activity, which was measured in this study, maintains the pool of GSH in the reduced state allowing its consumption by DHAR to regenerate AsA (Noctor et al., 1998). Interestingly, GR activity did not change significantly on day 1 (Figure 4.8.A) and thus was not causing a putative reduction in AsA pool size. The gradual increase over time in GR activity (Figures 4.8.A and 4.8.B), which was particularly evident during the later stages of the experiment, coincided with APX peaks in both cultivars. This mutual relationship consistently occurs in several species under different abiotic stresses (Anjum et al., 2010), implying that GR contributed to antioxidant protection by regenerating the GSH pool for AsA recycling (Noctor et al., 1998; Sharma et al., 2012). Therefore, future studies should investigate AsA concentration and MDHAR and DHAR activities on day 1 to elucidate the influence of the treatment on the AsA/glutathione cycle.

Following the transient depression of APX under stress on day 1, there were no significant differences in APX activity between treatments in cv. 'Frank', with the exception of a noticeable significant peak on day 7. However, on day 13 APX activity was 1.7-fold higher under stress than the control and there was no significant change in SOD activity on the same day. This was possible because O_2^- is used in spontaneous disproportion reactions, producing H_2O_2 with or without the aid of SOD in chloroplasts (Thompson et al., 1987; Karuppanapandian et al., 2011; Ksas et al., 2015)

stimulating APX activity (Noctor and Foyer, 1998). In fact, in cv. 'Frank' SOD activity decreased from day 7 onwards, which coincided with a significant increase, compared to day 0, in MDA concentration from day 7 onwards. It is possible that O_2^- generation exceeded the scavenging ability of SOD in cv. 'Frank', and that over-accumulation of O_2^- and other ROS may have inactivated and degraded the SOD protein (Casano et al., 1997; Panda and Khan, 2004; Ahammed et al., 2012). Decreased SOD activity and increased MDA concentration occur in parallel during senescence of tobacco leaves (Dhindsa et al., 1981), and in wheat plants under combined UV-B and high temperature (40°C) stress (Dawar et al., 1998). CAT activity in cv. 'Frank' was stable during the experiment, which explains why APX activity peaked more often in cv. 'Frank' compared to cv. 'Sunstar', as the latter enzyme would scavenge peroxisomal H_2O_2 under conditions when CAT is unable to control H_2O_2 accumulation (Inze and Montagu, 2003).

Taken together, the stress treatment induced significant oxidative stress in both cultivars before the visual appearance of tipburn. Stress markedly increased MDA concentration throughout the experiment, and was more prominent one day prior to visual tipburn symptoms. Plants responded to the treatments with marked changes in the antioxidant enzyme machinery. Ca concentration did not appear to be related to presymptomatic tipburn induction. The findings suggest links between the induction of tipburn of lettuce and oxidative stress under luxuriant growth conditions.

4.5 Conclusions

Saure (1998, 2005) argued that plant scientists' fixation on Ca deficiency as the main cause of tipburn of lettuce impeded a better understanding of the underlying mechanisms of the disorder. The results described herein indicate that the induction of tipburn on day 16 of the stress treatment was not related to presymptomatic changes in Ca concentration, but instead provide evidence that enhanced oxidative stress contributed to the induction of the disorder. This is the first study, to our knowledge, to examine an alternative to the Ca hypothesis for the induction of lettuce tipburn in a non-invasive manner, whilst mimicking a "realistic" growing environment similar to that present in commercial hydroponic production units. This study may contribute to the inception of novel approaches in ameliorating the disorder via antioxidant pathways. Furthermore, day 15 appeared to be a significant time point since plants under stress exhibited photoinhibition (see Chapter 3) and increased lipid peroxidation levels prior to the appearance of tipburn symptoms. To investigate the underlying mechanisms of tipburn induction, Chapter 5 will elucidate the genetic basis of tipburn of lettuce induction via transcriptomic RNA sequencing analysis of plants sampled on day 15.

CHAPTER 5

ELUCIDATING THE MOLECULAR BASIS OF LETTUCE TIPBURN

5.1 Introduction.

Chapter 4 revealed that under luxuriant growth conditions of high PPFD and high temperature, the induction of lettuce tipburn symptoms was associated with presymptomatic oxidative stress. Therefore, to acquire a deeper mechanistic insight into the events leading to the development of tipburn symptoms a whole transcriptome sequencing study using RNA sequencing (RNAseq) was performed. RNAseq analysis provides a snapshot of the transcriptome, which is the complete set of transcripts in a cell and thus, a momentary reflection of cellular activity (Twine et al., 2011; Martin et al., 2014). Furthermore, RNAseq allows gene expression profiling with high sensitivity and low background noise (Wang et al., 2009) providing an unbiased analysis of RNA transcripts (Arbona et al., 2013).

Lettuce is a diploid ($2n = 18$) species with genome size of 2.5 Gb (Truco et al., 2013). The lettuce genome was recently sequenced (Reyes-Chin-Wo et al., 2017) and utilised as the reference sequence in this RNAseq investigation. RNAseq analyses have previously explored circadian oscillations in the lettuce transcriptome under constant light and light–dark conditions in a plant factory system (Higashi et al., 2016), investigated gene clusters related to resistance to *Bremia lactucae* and the hypersensitive response to *Pseudomonas syringae* (Christopoulou et al., 2015), and elucidated the lettuce – *Botrytis cinerea* interaction (De Cremer et al., 2013).

The genetic basis of lettuce tipburn has been studied using recombinant inbred lines (RILs), revealing three major clusters of quantitative trait loci (QTLs) showing tight linkage between tipburn incidence and severity, and lettuce head morphology (Jenni et

al. 2013). In the present study, RNAseq has been used to investigate the underlying mechanisms leading to the induction of lettuce tipburn prior to the appearance of visual symptoms. As far as the author is aware, this is the first RNAseq investigation on presymptomatic to lettuce tipburn transcriptome changes under luxuriant growth conditions of high PPFD and temperature. Plants were grown under luxuriant growth conditions using the experimental system established in Chapter 3 providing reproducible tipburn symptoms, thereby circumventing issues associated with the unpredictability of the disorder (Olle and Bender, 2009). Whole genome comparative gene expression analysis was performed to provide data on the differentially expressed genes (DEGs). Study of DEGs related to presymptomatic tipburn induction furthers the understanding of the underlying mechanisms of the disorder and may contribute to the investigation of novel approaches to mitigating the disorder.

5.2 Materials and methods.

5.2.1 Plant material and treatments.

A tipburn resistant (*L. sativa* cv. 'Frank') and a tipburn susceptible (*L. sativa* cv. 'Sunstar') butterhead lettuce cultivars were grown for 15 days under tipburn-inducing (stress) and tipburn-free (control) treatments, within the DFTS and CE room previously described in detail in Chapters 2 and 3.

5.2.2 Collection of plant material.

Leaf tissue samples were collected between 18:00 hrs and 19:00 hrs (12 hours after the start of the photoperiod) on day 15 after the start of the treatments, prior to the visual appearance of tipburn symptoms. The two youngest, fully expanded leaves

were chosen for sampling since they were the first to show tipburn symptoms (see Chapter 3) and for consistency with previous measurements of antioxidant enzyme activity, Ca concentration and MDA equivalents (Chapter 4). Leaves were detached from the plant and placed on a sterilized tile (90% EtOH for 2 min, followed by a wash with distilled water) to be dissected using a single edge blade. Approximately 2 mm strips, weighing 0.1 g fresh weight, were cut from the edge of the leaf tissue (Figure 4.1). Leaf samples were placed into different eppendorf tubes, then immediately flash frozen into liquid nitrogen and stored at -80°C.

5.2.3 RNA extraction.

RNA was extracted using the RNeasy Plant Mini Kit (Qiagen, Manchester, UK), following the Qiagen protocol; DNase treatment was applied to reduce DNA contamination. The RNA concentration was measured by NanoDrop 2000 Spectrophotometer (Thermo Fisher Scientific, DE, USA) and the ratio between A_{260} and A_{280} was used to establish adequate RNA purity, in addition to monitoring for RNA degradation and contamination on 1% agarose gels.

5.2.4 Library Preparation and Transcriptome Sequencing.

RNA samples were sent on dry ice to Beijing Novogene Bioinformatics Technology Co., Ltd. (Beijing, China) for RNA sequencing analysis. Upon delivery, RNA integrity was assessed using the RNA Nano 6000 Assay Kit of the Bioanalyzer 2100 system (Agilent Technologies, CA, USA) and RNA purity was checked using the NanoPhotometer spectrophotometer (IMPLEN, CA, USA). Sequencing libraries were generated using NEBNext Ultra™ RNA Library Prep Kit for Illumina (NEB, USA)

following manufacturer's recommendations and index codes were added to attribute sequences to each sample. The clustering of the index-coded samples was performed on a cBot Cluster Generation System using HiSeq PE Cluster Kit cBot-HS (Illumina) according to the manufacturer's instructions. After cluster generation, the library preparations were sequenced on an Illumina HiSeq platform and 125 bp/150 bp paired-end reads were generated.

Raw data (raw reads) of fastq format were processed through in-house perl scripts. Clean reads were obtained by removing reads containing adapter, poly-N and low quality reads from raw data. At the same time, Sequencing Quality Scores (Q) were calculated based on the equation:

$$Q = -10\log_{10}(e)$$

where e is the estimated probability of the base call being wrong (Ewing et al., 1998; Richterich, 1998). Specifically, Q20 and Q30 were utilized as quality scores having an incorrect base call probability of 1 in 100 times and 1 in 1000 times, respectively. Guanine-cytosine (GC) content was calculated and was used for normalization of read counts, as GC abundance is heterogeneous across the genome making it difficult to separate the GC effect from true expression signal, and thus it may influence RNAseq quantification (Pickrell et al., 2010; Risso et al., 2011; Benjamini and Speed, 2012). All the downstream analyses were based on the clean reads which were determined by their error rate, Q20, Q30, and GC contents.

5.2.5. Data analysis

Reference genome and gene model annotation files were downloaded from the

Lettuce Genome Resource website (lgr.genomecenter.ucdavis.edu). Index of the reference genome was built using Bowtie v2.2.3 (Broad Institute, Cambridge, MA, USA) according to Langmead et al. (2009) and paired-end clean reads were aligned to the reference genome using TopHat v2.0.12 (Broad Institute, Cambridge, MA, USA), according to Trapnell et al. (2012). HTSeq v0.6.1 (California Institute of Technology, Pasadena, CA, USA) was used to count the numbers of reads mapped to each gene (Table 5.1). The expression metric: expected fragments per kilobase of transcript per million fragments sequenced (FPKM) of each gene was calculated based on the length of the gene and reads count mapped to this gene. FPKM was chosen because it is currently the most commonly used method for estimating gene expression levels and for evaluating the sequencing depth and gene length of the reads, and it is conceptually analogous to the reads per kilobase per million reads sequenced (RPKM) (Trapnell et al., 2010).

Differential expression analysis (DEA) to identify differentially expressed genes (DEGs) for the two lettuce cultivars (cv. 'Frank and cv. 'Sunstar') separately, and across the two treatments (stress and control) was performed using the DESeq R package (1.18.0) using a model based on the negative binomial distribution. Genes with an adjusted p-value less than 0.05 ($p < 0.05$) found by DESeq were assigned as differentially expressed. DEGs overlap between conditions was assessed using a Venn diagram (Figure 5.1). Hierarchical cluster analysis based on $\log_{10}(\text{FPKM}+1)$ values is presented in Figure 5.2. The resulting p-values were adjusted using Benjamini and Hochberg's approach for controlling the false discovery rate and were presented as volcano plots in Figure 5.3.

The GOseq R package was utilised to perform Gene Ontology (GO) enrichment

analysis of DEGs, in which gene length bias was corrected. GO terms with corrected p-value less than 0.05 were considered significantly enriched by DEGs (Figures 5.4.A and B). Kyoto Encyclopedia of Genes and Genomes Pathway (KEGG; www.genome.jp/kegg) annotations were assigned according to the KEGG database using KOBAS software (Peking University, Beijing, China) to test the enrichment of DEGs in particular KEGG pathways (Figures 5.5.A and B). Enrichment degree of KEGG was measured via the rich factor, q-value and genes counts enriched to this pathway. Rich factor is the ratio of DEGs in the related pathway divided by the number of all the annotated genes in this pathway. The higher the rich factor is, the greater the degree of enrichment. q-value is the adjusted p-value after multiple hypothesis testing. The closer the q-value is to zero, the more significant the enrichment.

5.3 Results.

5.1 RNA Sequencing data generation.

A total of ~ 500 million raw sequencing reads were generated and after processing the raw reads (Section 5.2.4), approximately 400 million high-quality clean reads were obtained. The average percentages of bases whose correct base recognition rates are greater than 99% (Q20) and than 99.9% (Q30) in total bases were 97% and 92.5%, respectively, and the average GC content was 45.4%. Approximately 77% of the clean reads were mapped to the reference genome and ~ 3% of the clean reads were mapped to multiple sites in the reference genome (Table 5.1).

Table 5.1. Overview of Mapping Status. Clean reads were obtained by removing low quality reads from raw reads. Q20 and Q30 represent the percentages of bases whose correct base recognition rates are greater than 99% and 99.9% in total bases, respectively. GC represents the percentages of G and C in total bases. Total mapped represents total number of reads that was mapped to the reference genome. Multiple mapped is the number of reads that was mapped to multiple sites in the reference genome and uniquely mapped is number of reads that was uniquely mapped to the reference genome.

cv 'Frank'	Raw reads	Clean reads	Q20 (%)	Q30 (%)	GC (%)	Total mapped	Multiple mapped	Uniquely mapped
stress rep 1	40158976	38075672	97.03	92.55	44.92	31459795 (82.62%)	1142948 (3%)	30316847 (79.62%)
stress rep 2	45457948	42400710	97.02	92.53	45.73	33946307 (80.06%)	1347701 (3.18%)	32598606 (76.88%)
stress rep 3	39996088	37405106	96.92	92.35	45.11	30205865 (80.75%)	1109722 (2.97%)	29096143 (77.79%)
control rep 1	40716150	38595760	96.95	92.38	45.48	31912548 (82.68%)	1153722 (2.99%)	30758826 (79.69%)
control rep 2	45485434	42606968	97	92.49	45.63	34661492 (81.35%)	1330184 (3.12%)	33331308 (78.23%)
control rep 3	44832574	41769824	96.79	92.03	45.68	33843307 (81.02%)	1221278 (2.92%)	32622029 (78.1%)

cv 'Sunstar'	Raw reads	Clean reads	Q20 (%)	Q30 (%)	GC (%)	Total mapped	Multiple mapped	Uniquely mapped
stress rep 1	44819388	42427422	96.86	92.21	45.43	34363730 (80.99%)	1416523 (3.34%)	32947207 (77.66%)
stress rep 2	38388328	35649604	96.95	92.41	45.69	28445740 (79.79%)	1367170 (3.84%)	27078570 (75.96%)
stress rep 3	41273360	38298600	97.14	92.83	45.74	30726008 (80.23%)	1303611 (3.4%)	29422397 (76.82%)
control rep 1	45721084	43181274	97.08	92.66	45.31	36120467 (83.65%)	1288929 (2.98%)	34831538 (80.66%)
control rep 2	50273830	46532940	97.1	92.8	45.29	38219217 (82.13%)	1596847 (3.43%)	36622370 (78.7%)
control rep 3	45599408	41140808	96.92	92.34	45.05	32681043 (79.44%)	1170026 (2.84%)	31511017 (76.59%)

5.2. 30% of total DEGs were commonly expressed in both cultivars.

To elucidate the underlying molecular mechanisms leading to the induction of lettuce tipburn, the gene expression profiles of two lettuce cultivars (cv. 'Frank' and cv. 'Sunstar') under tipburn inducing (stress) and tipburn free (control) conditions were compared, and the significant DEGs identified. A total of 2694 DEGs were identified between the two cultivars and treatments, with 806 genes (29.9% of the total DEGs) commonly expressed in both conditions (Figure 5.1). In cv. 'Frank' and in cv. 'Sunstar', 340 DEGs (12.6% of the total DEGs) and 742 DEGs (27.5% of the total DEGs) were uniquely expressed, respectively (Figure 5.1).

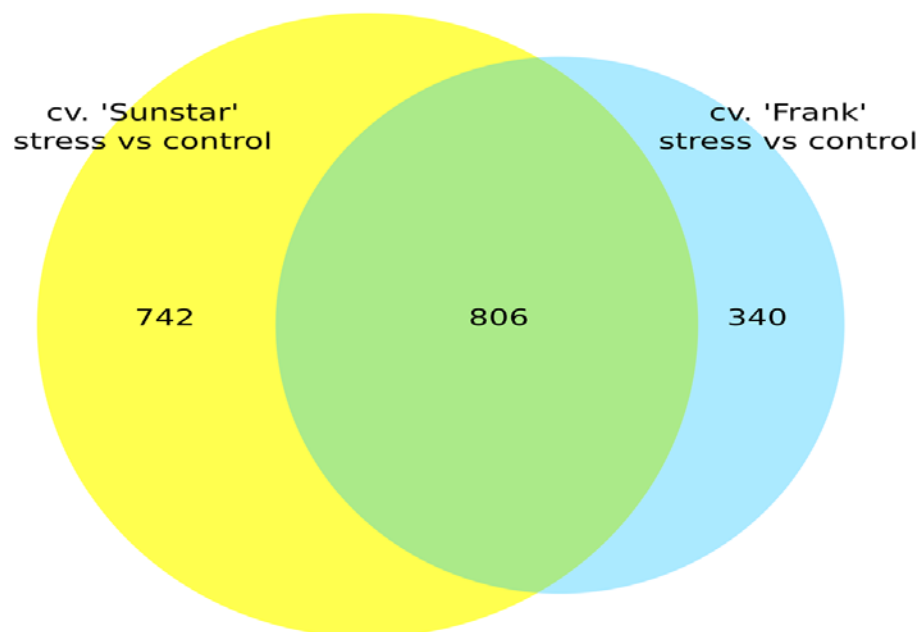


Figure 5.1. Venn diagram shows the number of DEGs that were uniquely expressed in cv. 'Sunstar' and cv. 'Frank' within the yellow (left) and blue (right) circles, respectively. FPKM and DESeq estimated the level of gene expression and the number of DEGs, respectively. The overlapping region (green) shows the number of genes that were expressed in both groups.

5.3 Hierarchical clustering of DEGs revealed marked differences across treatments.

To assess the effects of the two treatments separately on gene expression in each lettuce cultivar, all DEGs from each treatment were arranged using hierarchical clustering of expression patterns based on the $\log_{10}(\text{FPKM}+1)$ (Figure 5.2). Visual inspection of the value heat map showed marked differences in expression levels between treatments within the same cultivar. In contrast, differences in expression levels between different cultivars when grown under the same treatment were far less pronounced. When comparing control and stress treatments, relatively distinct gene clusters and expression patterns were observed in both cultivars. Specifically, in cluster 1, the DEGs in both control treatments showed $\log_{10}(\text{FPKM}+1)$ values > 0 (red coloured), indicating that DEGs had high expression level within this cluster, whereas DEGs in the stress treatments had lower expression values (blue coloured). In contrast, in clusters 2 and 3, DEGs in both control treatments showed low expression levels whereas the inverse relationship tended to be observed in stress treatments (Figure 5.2). Therefore, a differential expression analysis was performed separately for each cultivar between the stress and control treatments (Section 5.4).

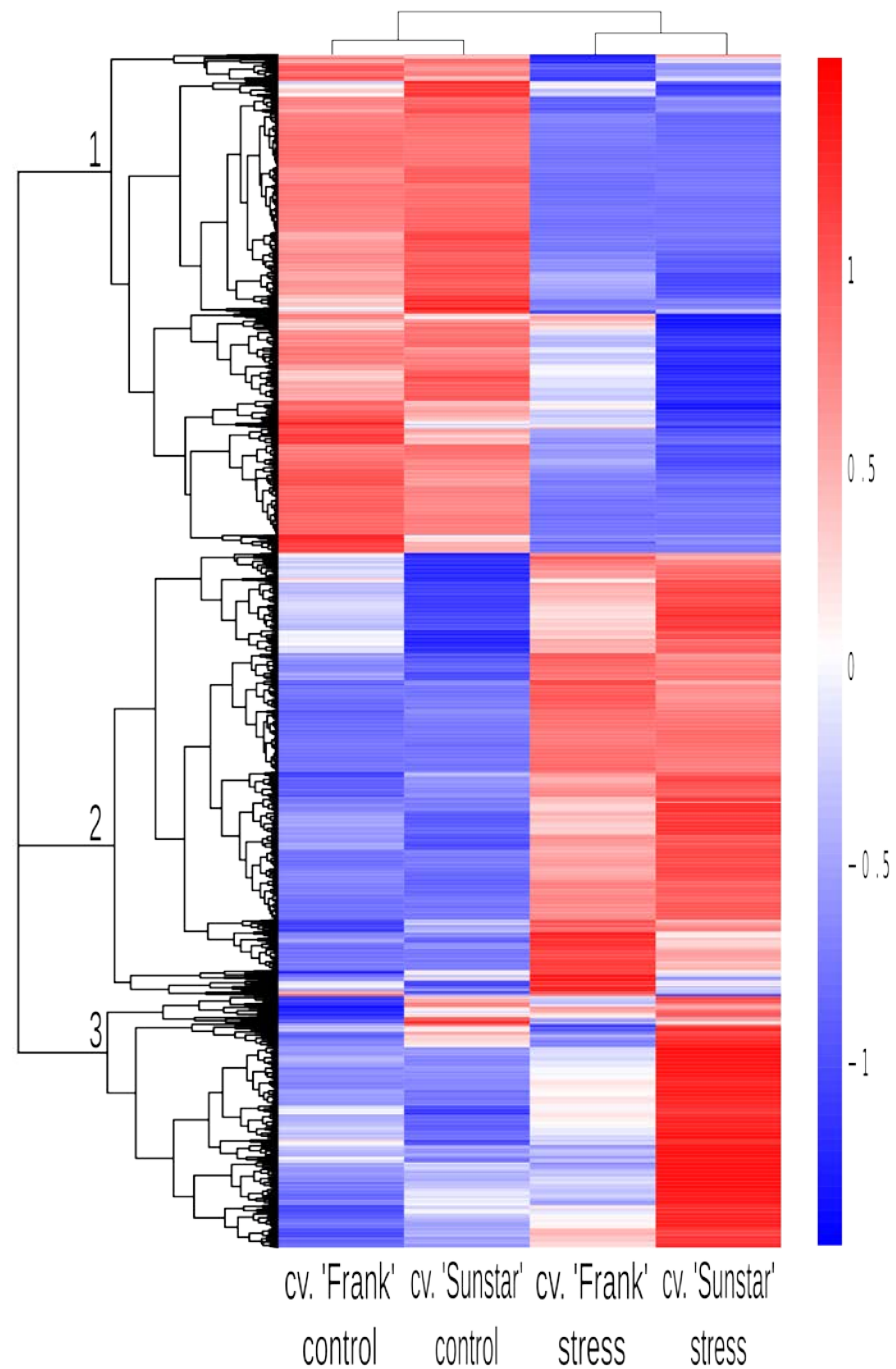


Figure 5.2. Heat map showing the overall results of FPKM cluster analysis, clustered using the $\log_{10}(\text{FPKM}+1)$ value. Three main groups were identified which are represented by the three high-level numbered clusters in the dendrogram. The intensity of the colour represents expression levels of DEGs. Red denotes genes with high expression levels, and blue denotes genes with low expression levels. Scale bar represents the $\log_{10}(\text{FPKM}+1)$ value from large to small.

5.3 More DEGs were observed in cv. 'Sunstar'.

Comparing stress and control for cv. 'Frank', 1146 DEGs were observed, of which 512 (44.7%) were up-regulated genes and 634 (55.3%) were down-regulated genes (Figure 5.3.A). In contrast, a similar comparison between stress and control in the cv. 'Sunstar' revealed a higher number of DEGs (1548 genes) than in cv. 'Frank', of which 930 (60.1%) were up-regulated genes and 618 (39.9%) were down-regulated genes (Figure 5.3.B).

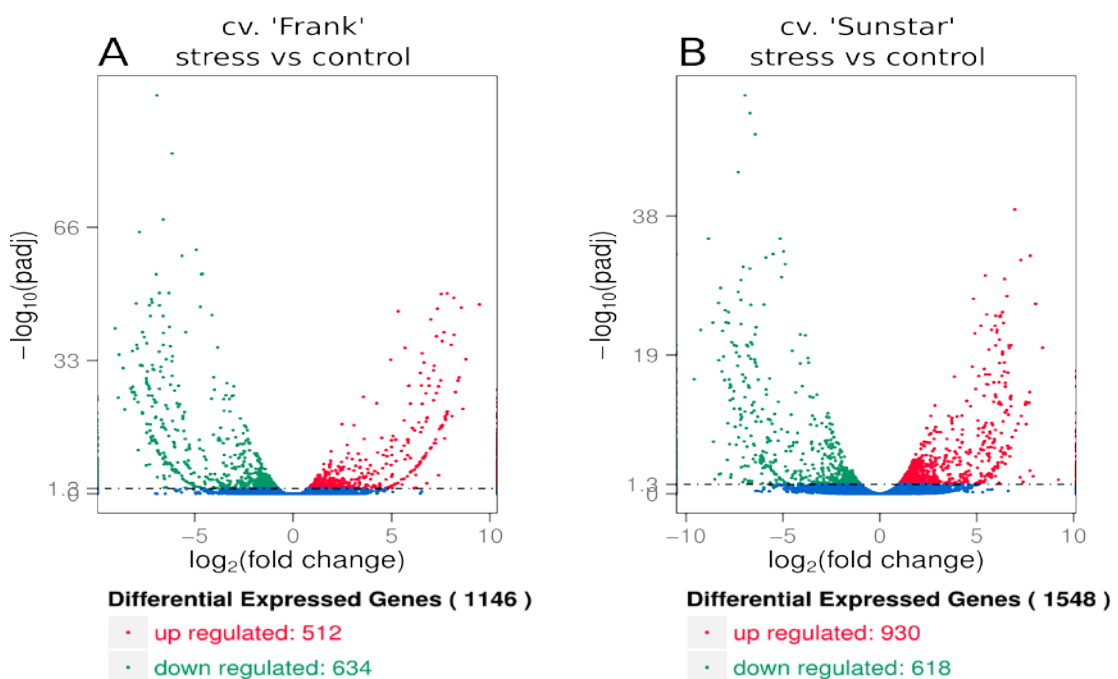


Figure 5.3. Volcano plots obtained by pairwise comparison of cv. 'Frank' (A) and cv. 'Sunstar' (B) between treatments (stress and control). The x-axis shows the fold-change in gene expression between different samples, and the y-axis shows the statistical significance of the differences. Significantly up and down-regulated genes are highlighted in red and green, respectively. No significant difference in gene expression is shown in blue.

5.4 GO enrichment of DEGs

Gene ontology (GO) analysis was used to obtain functional information for the DEGs identified in Section 5.3, to assist in understanding the distribution of gene functions at a macro level. In tipburn-susceptible cv. ‘Sunstar’ 22 significant GO terms were detected whereas, there were no-significant GO terms in tipburn-resistant cv. ‘Frank’. A large proportion of the enriched lettuce DEGs in cv. ‘Sunstar’ fell into the categories of “oxidation–reduction process” (GO:0055114), “photosynthesis” (GO:0015979), “biological process” (GO:0008150), “metabolic process” (GO:0008152), and “single-organism metabolic process” (GO:0044710). In the cellular components category, “photosynthetic membrane” (GO:0034357), “photosystem” (GO:0009521), “thylakoid” (GO:0009579), “thylakoid part” (GO:0044436), “thylakoid membrane” (GO:0042651), “photosystem I” (GO:0009522), “photosystem I reaction center” (GO:0009538), “photosystem II oxygen evolving complex” (GO:0009654), were the most enriched terms. In the molecular function category, “oxidoreductase activity” (GO:0016616), “oxidoreductase activity, acting on paired donors, with incorporation or reduction of molecular oxygen” (GO:0016705), “oxidoreductase activity, acting on paired donors, with incorporation or reduction of molecular oxygen, NAD(P)H as one donor, and incorporation of one atom of oxygen” (GO:0016709), “oxidoreductase activity, acting on CH-OH group of donors” (GO:0016616), “iron ion binding” (GO:0005506), “heme binding” (GO:0020037), “cofactor binding” (GO:0048037) and “coenzyme binding” (GO:0050662) and “tetrapyrrole binding” (GO:0046906) showed significant proportions.

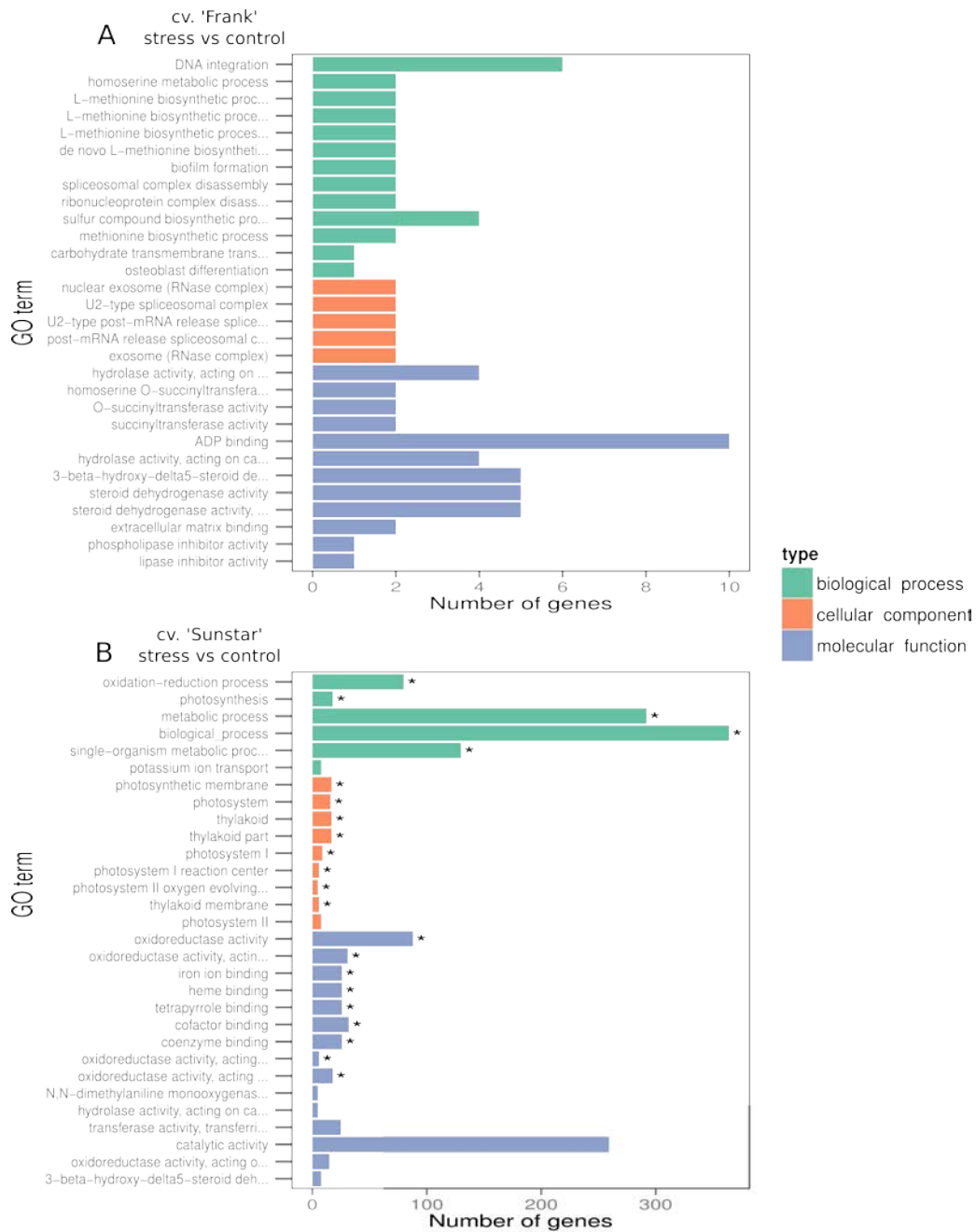


Figure 5.4. Gene ontology (GO) classifications of DEGs in cv. 'Frank' (A) and cv. 'Sunstar' (B). The x-axis shows the enriched GO terms and the y-axis is the number of DEGs. Different colours are used to distinct biological process (green), cellular component (orange) and molecular function (blue). Asterisk (*) indicates significantly enriched GO terms according to corrected p-value < 0.05.

5.5 KEGG Pathway Enrichment Analysis of DEGs.

KEGG enrichment pathway analysis, providing classifications for studying the complex biological functions of genes, showed that DEGs in the “flavonoids biosynthesis” (ath00941) pathway were down regulated in both cv. ‘Frank’ and cv. ‘Sunstar’. The following KEGG pathways were significantly enriched only in cv. ‘Sunstar’: “photosynthesis-antenna proteins” (ath00196), “photosynthesis” (ath00195), “glyoxylate and dicarboxylate metabolism” (ath00630), “carbon metabolism” (ath01200), “carbon fixation in photosynthetic organisms” (ath00710) and “brassinosteroids biosynthesis” (ath00905) (Figure 5.5).

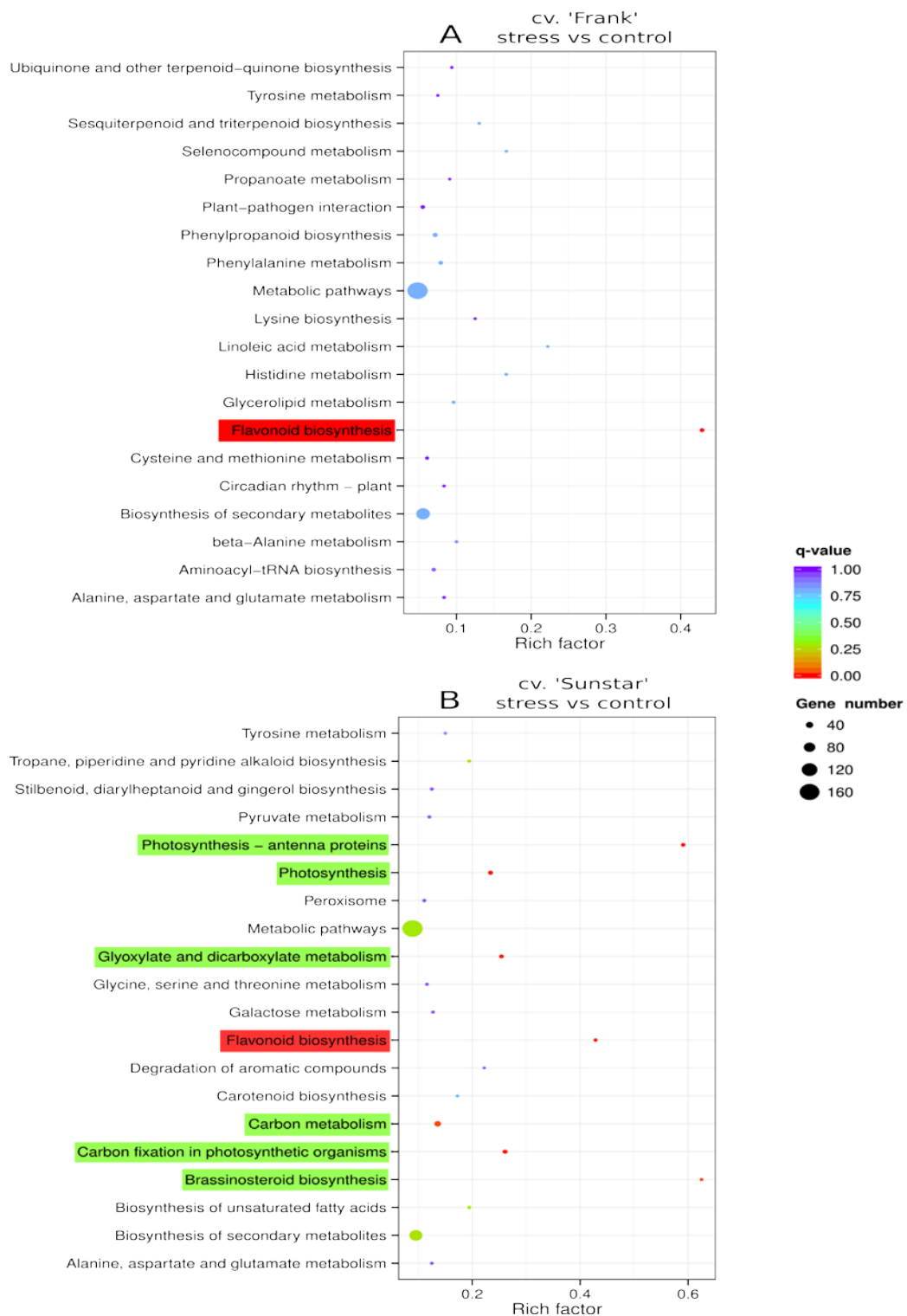


Figure 5.5. The 20 most enriched KEGG pathways in cv. 'Frank' (A) and cv. 'Sunstar' (B) are shown together with their q-value (colour), rich factor (vertical ordinate) and number of genes (size of circles). Up regulated and down regulated KEGG pathways are highlighted in green and red, respectively.

5.4 Discussion.

Analysis of transcriptional changes which occur prior to the appearance of visible tipburn symptoms may contribute to understanding the underlying mechanisms of the disorder. This chapter has analysed changes in the lettuce transcriptome in response to tipburn-inducing conditions of high PPFD and temperature (Chapter 3). In total, 77% of the clean reads could be assigned to lettuce genes and were used for gene expression profiling (Table 5.1), indicating that the sequencing quality and depth was sufficient for transcriptome coverage (Zhang et al., 2016). A total of 2694 DEGs were identified in cv. ‘Frank’ and cv. ‘Sunstar’ of which 12.6% and 27.5% were uniquely expressed in each cultivar, respectively (Figure 5.1). Interestingly, RNAseq analysis of *Brassica oleracea* lines derived from tipburn susceptible and tipburn resistant cabbages (*B. oleracea* cv. capitata), as well as kale (*B. oleracea* cv. acephala) identified 1844 DEGs as tipburn-related phenotype-specific genes. GO annotation revealed these DEGs were involved in regulatory metabolic processes or stress responses and were differentially expressed in response to increasing intracellular Ca^{2+} and K^{+} concentrations (Lee et al., 2016). This raised the intriguing possibility that the approximately 2-fold higher uniquely DEGs in cv. ‘Sunstar’ compared to cv. ‘Frank’ (Fig 5.1) may have contributed to the significantly higher sensitivity to tipburn of the former cultivar compared to the latter (Section 3.3.1.6).

The DEGs detected in this chapter were enriched into GO terms to identify putative underlying mechanisms and pathways leading to the induction of lettuce tipburn under the luxuriant growth conditions experienced. Unexpectedly, there were no significant GO enrichment terms for cv. ‘Frank’ (Figure 5.4), possibly since there were fewer DEGs in cv. ‘Frank’ than cv. ‘Sunstar’ (Figures 5.1, 5.2 and 5.3). In addition, this

might also be attributed to limitations of the specific GO enrichment tool (GOseq) utilised in the investigation, as different implementations and algorithms between GO platforms may yield different results (Blake, 2013). GO annotations can help explain the physiological meaning of different experimental conditions, based on the over-representation of DEGs which are part of specific molecular or biological pathways (Conesa et al., 2005). However, conclusions drawn from GO enrichment become less useful as the investigations diverge from well-annotated model systems (Clark and Greenwood, 2016) as in novel sequenced species (Kumar et al., 2013) such as lettuce. Whilst web-based GO analysis toolkits focused on agricultural species exist, such as AgriGO (Du et al., 2010), that may facilitate further GO investigations in the current study, at the time of writing (April 2017) no methods are available to convert the obtained data into a suitable format for further analysis via AgriGO. However, following the recent publication of the lettuce genome (Reyes-Chin-Wo et al., 2017) an additional round of functional annotations will be widely available to the scientific community (Sebastian Reyes-Chin-Wo, personal communication). Furthermore, GO annotations reflect the current state of knowledge and changes to improve their accuracy are frequent (Gaudet and Dessimoz, 2017), although this does not imply that previous annotations are incorrect (Huntley et al., 2014). Thus, future investigations should explore ways to utilise the capabilities of agriGO, in addition to making use of novel GO annotations.

In contrast to the GO results of cv. 'Frank', in cv. 'Sunstar' a large number of DEGs were significantly enriched into different GO terms. The majority of GO terms that were enriched were related to various aspects of photosynthesis, such as "oxidation-reduction process", "photosynthesis" "photosynthetic membrane", "photosystem" and

“photosystem reaction center”. These findings were consistent with the higher photosynthetic rates of cv. ‘Sunstar’ under stress compared to the control (Figure 3.12 and Table 3.1). Photosynthesis is a source of ROS in leaves (Foyer and Shigeoka, 2011) thus increased photosynthetic rates may also lead to higher oxidative stress (Pieterse et al., 2014) and lipid peroxidation (Sharma et al., 2012), which agree with the observed higher MDA levels in cv. ‘Sunstar’ under stress (Figure 4.4.B).

A commonly shared GO term in the molecular function categories was “oxidoreductase activity” (Figure 5.4.B). Oxidoreductase proteins have been widely reported to hold a crucial role in plant responses to oxidative stress (Jacquot, 2009). Oxidoreductases catalyze reactions which can scavenge ROS, as in the case of CAT, APX, POD, and SOD (Sharma et al., 2012) but may also generate ROS in cells. For example, NADPH oxidase catalyses the transfer of electrons from cytoplasmic NADPH to reduce molecular O₂ to form O₂⁻ (Gestelen et al., 1997). However, whilst ROS over accumulation can cause oxidative damage to cells, they may also act as signalling molecules, since cells can regulate rapid changes in ROS levels under normal conditions (Mittler et al., 2011). In this context, the NADPH oxidase *RbohD* had a central role in cell-to-cell communication and stress signalling in *A. thaliana* plants, which were exposed to different abiotic stresses (high light, heat, wounding, salt and cold stress) (Miller et al., 2009; Sewelam et al., 2016). Similarly, studies of high light stress in *A. thaliana* demonstrated that *RbohD* was required for ROS signal amplification which regulated expression of the cytosolic ascorbate peroxidase (APX1) gene (Mullineaux et al., 2006). Thus, in cv. ‘Sunstar’ under stress, NADPH oxidase activation may have enhanced ROS over accumulation and increased presymptomatic levels of MDA (Figure 4.4.B). However, this may have also triggered

a signalling cascade that enhanced APX activity under stress (Figure 4.7.B). Interestingly, Carrassay et al. (2012) reported that foliar application of diphenyleneiodonium chloride (DPI), which is a suicide inhibitor of the NADPH oxidase and other apoplastic peroxidases, mitigated tipburn symptoms in salt-stressed lettuce plants in comparison to untreated plants, suggesting that NADPH oxidase-derived ROS contributes to lettuce tipburn induction. Thus, further research is required to investigate the contributions of NADPH oxidase to lettuce tipburn induction under luxuriant growth conditions, and to assess whether manipulating NADPH oxidase activity, via DPI applications, could potentially ameliorate tipburn symptoms.

Additional GO terms that were significantly enriched in the molecular function categories in cv. 'Sunstar' were "tetrapyrrole binding", "heme binding", and the term "iron ion binding" as well as other binding-related terms ("cofactor binding" and "coenzyme binding"). "Tetrapyrrole binding" and "iron ion binding", as well as "oxidoreductase activity", have previously been reported to be significantly enriched in *A. thaliana* under nine abiotic stress conditions (cold, osmotic stress, salt, drought, genotoxic stress, ultraviolet light, oxidative stress, wounding, and high temperature) (Swindell, 2006). This further indicates a general plant stress response to luxuriant growth conditions which occurs prior to the induction of first visual tipburn symptoms.

Following the GO investigation, KEGG enrichment analysis identified pathways that play important roles to presymptomatic tipburn induction. Similarly to GO annotations, there were more pathways enriched in cv. 'Sunstar' compared to cv.'

Frank'. In cv. 'Sunstar' the "Photosynthesis—antenna proteins" pathway was significantly enriched by upregulated DEGs indicating that stress induced protective mechanisms against the effects of high PPF via non photochemical quenching (Han et al., 2016). Furthermore, upregulated DEGs were involved in metabolic pathways related to carbon metabolism, such as "carbon metabolism", "carbon fixation in photosynthetic organisms", and "glyoxylate and dicarboxylate metabolism". The latter refers to the glyoxylate or dicarboxylates involving reactions which function in the biosynthesis of carbohydrates from lipids (Li et al., 2013). Interestingly, "glyoxylate and dicarboxylate metabolism" was the most frequently detected KEGG pathway to be enriched under drought stress in *Paulownia australis* (Dong et al., 2014), and in *Zea mays* plants under heat stress (Shi et al., 2017). Taken together, this suggests enhanced basic metabolic activity under stress (Li et al., 2016) possibly in response to low carbohydrate and low energy situations, which have been linked to increased oxidative stress (Serra et al., 2015).

"Brassinosteroids biosynthesis" represents the final pathway enriched in upregulated DEGs in cv. 'Sunstar'. Brassinosteroids are plant hormones that influence plant growth and development (Arteca, 2013), but may also enhance plant tolerance to abiotic stress (Bajguz and Hayat, 2009). Interestingly, foliar application of brassinosteroids (0.2 μM and 0.1 μM of 24-epibrassinolide (24-EpiBL)) induced transient increases in the transcript abundance of *Respiratory burst oxidase homolog 1* (*RbohD1*), and thus in NADPH oxidase activity, leading to increased apoplastic H_2O_2 accumulation (Xia et al., 2013, 2009). This was accompanied by the upregulation of cytosolic ascorbate peroxidase (cAPX) and MDAR transcripts and increases in their corresponding enzyme activity in *Cucumis sativus* (Xia et al., 2009). Furthermore,

virus-induced gene silencing of the *RbohD1* gene in tomato inhibited apoplastic H₂O₂ accumulation and reduced oxidative and heat stress tolerance (Nie et al., 2013). Thus, the enrichment of the “brassinosteroids biosynthesis” KEGG pathway seemed linked to the GO term “oxidoreductase activity” via a putative role of NADPH oxidase in stress signalling in lettuce. These findings add further credence to the hypothesis of a role of NADPH oxidase in plant stress responses occurring prior to tipburn appearance.

Arguably, the most striking finding in the KEGG pathway analysis was that downregulated DEGs were enriched in the “flavonoids biosynthesis” pathway in both cultivars. This was an unexpected finding as increasing light intensity enhances flavonoid biosynthesis and concentration in several species (Agati et al., 2011; Zhang et al., 2017). Conversely, shading of *Vitis vinifera* L. berries during berry development reduced flavonoid content, and inhibited the transcription of flavonoid pathway genes (Cortell and Kennedy, 2006; Fujita et al., 2006). Thus, plants under stress that received higher PPFD than the control (Figure 3.7) would have been expected to have exhibited upregulated transcriptomic responses in regards to “flavonoids biosynthesis”. Flavonoids can inhibit the generation of ROS and reduce their levels via direct scavenging (Chen Yuting et al., 1990; Pietta, 2000; Trembl and Šmejkal, 2016). Thus, to prevent light-induced oxidative damage they are localized close to sites of ROS production, and can be found in vacuoles and cell walls of epidermal cells, in the vacuoles of mesophyll cells, and in chloroplasts (Smirnoff, 2008; Agati and Tattini, 2010). It is well documented that high temperatures inhibit flavonoids biosynthesis and induce their degradation (Boo et al., 2006; Jaakola and Hohtola, 2010). In particular, they decrease anthocyanin concentrations by suppressing the expression of the anthocyanin biosynthetic genes, and enhance anthocyanin

degradation (Mori et al., 2007; Lin-Wang et al., 2011; Feng et al., 2013). In contrast, growing lettuce under low ambient temperature (12/7°C (day/night) compared to 20/15°C (day/night)) significantly increased flavonoid content (Becker et al., 2014). This indicates that the luxuriant growth conditions of the DFTS (Figure 3.9) may not favour flavonoid accumulation, which can partly explain the downregulated DEGs enriching the “flavonoid biosynthesis” pathway. Interestingly, red lettuce varieties contain significantly higher content of phenolic compounds, anthocyanins (Llorach et al., 2008) and flavonoids (Zivcak et al., 2017) compared to green lettuce within the same growing conditions, and generally exhibit less tipburn symptoms than green varieties (Carassay et al. 2012).

5.5 Conclusions

This RNAseq profiling produced a novel data set exploring transcriptomic changes in lettuce plants grown under luxuriant growth conditions prior to the appearance of visible tipburn symptoms. Hundreds of DEGs were identified, including some known to be involved in plant stress responses such as upregulated brassinosteroid biosynthesis (Bajguz and Hayat, 2009), enhanced carbon metabolism (Serra et al., 2015) and photosynthetic activity (Pieterse et al., 2014). These findings are in good agreement with observations of plants exhibiting photoinhibition (Chapter 3) and oxidative stress (Chapter 4) presymptomatically to lettuce tipburn. DEGs involved in flavonoid biosynthesis were downregulated, suggesting a putative link between decreased flavonoid content and increased lipid peroxidation prior to the appearance of visual tipburn symptoms. However, real-time quantitative polymerase chain reaction (RT-qPCR) studies of expression profiles of DEGs related to flavonoid

biosynthesis in lettuce and presymptomatic (to tipburn) biochemical analyses of flavonoid concentration in the same tissues are required to test this hypothesis.

CHAPTER 6

GENERAL DISCUSSION

6.1 Overview of thesis.

Vertical farming (VF) aims to increase productivity per unit area by extending crop production into the vertical dimension (Utami and Jayadi, 2011; Sanyé-Mengual et al., 2013; Despommier, 2013; Bergstrand and Hultin, 2013; Eigenbrod and Gruda, 2014; Banerjee and Adenaueer, 2014; Thomaier et al., 2015). To realise this potential, VF must produce crops of high quality, and consequently of high marketability (Sago, 2016). This thesis investigated the crop productivity and quality of a prototype VFS and the challenges and opportunities for exploiting this technology.

To date, conclusive evidence that extending plant cultivation into the vertical dimension using VFS can actually increase yield per unit area has remained elusive. Chapter 2 demonstrates unequivocally that column-type VFS can produce more crop per unit area compared to horizontal hydroponic growing approaches (Table 2.1; Toulaitos et al., 2016). These VFS comprise an upright cylindrical column, and have been widely utilized in research (Liu et al., 2004; Linsley-Noakes et al., 2006; Ramírez-Gómez et al., 2012; Rius-Ruiz et al., 2014; Lee et al., 2015) and commercial applications (www.towergarden.com; www.brightagrotech.com; www.vertigro.com). Yield decreased from top to base within the VFS (Figures 2.9, 2.13 and 2.21) whilst yield was consistent through the HHS (Figure 2.9). Vertical gradients in yield within column-type VFS (Liu et al., 2004; Ramírez-Gómez et al., 2012) are likely due to basipetal gradients of PPFD (Figures 2.10, 2.15 and 2.22), which were not ameliorated by natural illumination within glasshouses (Figures 2.16). Interestingly, plants grown within the top layers of the VFS were exposed to high PPFD and high temperature and consistently exhibited tipburn symptoms (Figures 2.27 and 2.28). This is an

irreversible physiological disorder (Frantz et al., 2004; Gilliam et al., 2011) commonly observed in VFS-grown lettuce (Koyama et al., 2012; Zhang et al., 2015; Sago, 2016). However, tipburn symptoms on lettuce heads can result in up to a 50% reduction in marketable crop yields (De Swaef et al., 2015) raising important questions about the potential impact of this disorder on the economic profitability of VFS.

The underlying mechanisms of tipburn are not fully understood (Saure, 1998; Kerton et al., 2009). However, localised Ca deficiencies have been implicated in causing the disorder (Collier and Tibbitts, 1982, 1984; Barta and Tibbitts, 2000; Frantz et al., 2004; Gilliam et al., 2011). Chapter 3 employed a simplified, model growth system mimicking the environmental conditions within the top and bottom layers of the VFS, to elucidate further the underlying mechanisms. Using this system, tipburn symptoms were consistently observed 16 days after plants were exposed to high PPFD and temperature (Figures 3.13 and 3.14). These findings agree with other studies that show enhanced tipburn symptoms with increasing PPFD (Gaudreau et al., 1994; Frantz et al., 2004; Sago, 2016) and temperature (Yanagi et al., 1983; Jenni, 2005; Cancellier et al., 2010; Lee et al., 2013). In addition, independent manipulation of PPFD and temperature (Figures 3.16 and 3.17) revealed that simultaneously applying both conditions is imperative to reproduce tipburn symptoms (Figure 3.20). Plants under these conditions exhibited photoinhibition, determined from photosynthetic light response curves, 15 days after the plants were exposed to high PPFD and temperature (Figures 3.12 and 3.19, Tables 3.1 and 3.2). Since photoinhibition has been related to ROS over-accumulation leading to oxidative stress (Nooden, 2003; Takahashi and Murata, 2005; Triantaphylidès and Havaux, 2009), this suggests a role for enhanced

oxidative stress in inducing lettuce tipburn symptoms.

The hypothesis that tipburn symptoms in lettuce are due, at least in part, to the accumulation of ROS was investigated in Chapter 4 by examining presymptomatic changes in lipid peroxidation, and in the activities of major ROS-scavenging enzymes (SOD, CAT, APX and GR). These studies revealed that plants grown under high PPF and high temperature, which ultimately resulted in tipburn (Figure 4.1), exhibited oxidative stress and activation of antioxidant machinery prior to the appearance of visual symptoms (Figures 4.2 – 4.8 and Table 4.1). Foliar Ca concentration did not significantly differ between the stress and control treatments (Figures 4.2.A and B) suggesting, in contrast to the vast majority of studies (Collier and Tibbitts, 1982, 1984; Barta and Tibbitts, 2000; Frantz et al., 2004), that there were no presymptomatic links between Ca concentration and tipburn symptoms. Only one previous study examined the link between tipburn and oxidative stress in lettuce, showing that increasing ROS and MDA concentrations significantly enhanced tipburn symptoms, whilst foliar applications of ROS scavengers significantly ameliorated the symptoms (Carassay et al., 2012). However, this study induced tipburn using salinity stress and pharmacological approaches, whereas the results reported in this thesis provide the first in-depth examination of an alternative to the Ca hypothesis, using a non-invasive approach and within a (commercially) realistic growing environment.

To assess the wider significance of changes in the presymptomatic markers of oxidative stress in the development of tipburn, Chapter 5 utilised RNA sequencing analysis to investigate changes in the lettuce transcriptome prior to the onset of tipburn symptoms. Samples were collected one day prior to the appearance of the first

visual symptoms (Chapter 3), when significant stress-related events of lipid peroxidation (Chapter 4) and photoinhibition (Chapter 3) coincided. The RNAseq analysis confirmed the above mentioned stress-related events via the functional enrichment of stress-related pathways (Figures 5.4 and 5.5), such as brassinosteroid biosynthesis (Bajguz and Hayat, 2009), enhanced carbon metabolism (Serra et al., 2015) and photosynthetic activity (Pieterse et al., 2014) further supporting the hypothesis that presymptomatic oxidative stress induce tipburn in lettuce. Importantly, the findings suggested that flavonoid biosynthesis was downregulated in both cultivars under stress compared to the control, suggesting a putative presymptomatic to lettuce tipburn link between decreased flavonoid content and increased lipid peroxidation.

6.2. Ameliorating tipburn by reducing oxidative stress.

While VFS can produce more crop per unit area compared to conventional horizontal lettuce production, this achievement was significantly limited by the appearance of tipburn symptoms affecting plants grown within the VFS. Since lettuce tipburn appeared to be prompted by membrane lipid peroxidation rather than Ca deficiency, further research is required in order to establish a causal relationship between ROS and the appearance of tipburn symptoms. This raises the intriguing possibility that reducing oxidative stress could ameliorate symptoms of tipburn in lettuce. There are several potential options for the amelioration of lettuce tipburn via interventions in plant antioxidant defences, including foliar applications of brassinosteroids (BRs) (Arteca, 2013; Ramakrishna and Rao, 2014) and L-ascorbic acid (AsA) (Smirnoff and Wheeler, 2000), and biofortification of lettuce plants via applying Iodine (Blasco et al., 2008; 2011; 2013) in the hydroponic nutrient solution. These not only provide an opportunity to test causality within a fundamental plant science framework, but may

also offer meaningful solutions to the effects of tipburn to the commercial sector in the form of novel practices for mitigating the disorder, and reducing yield losses.

Foliar Ca applications have been utilized to ameliorate tipburn symptoms by increasing foliar Ca concentration and thus reducing tipburn incidence (Kruger, 1966; Thiobodeau and Minotti, 1969; Saleh, 2009) with often contradictory results (Dayod et al, 2010; Jenni and Hayes, 2010; Corriveau et al., 2012). In contrast, the results presented in this thesis suggest that foliar applications of compounds that would increase the antioxidant capacity of the plants or scavenge ROS might ameliorate tipburn symptoms by mitigating oxidative stress. Foliar applications of BRs have the potential to act in this manner (Ramakrishna and Rao, 2014) since they interact with ROS, inhibit membrane lipid peroxidation, and thus increase plant tolerance to various abiotic stresses (Bajguz and Hayat, 2009). Furthermore, BRs can increase plant tolerance to stress by enhancing the expression of antioxidant genes and thus stimulating the activity of antioxidant enzymes (Liu et al., 2009; Xia et al., 2009).

Currently, approximately 60 naturally occurring BRs or related compounds have been identified (Bishop and Koncz, 2002; Xia et al., 2009). Three bioactive BRs are mostly used in physiological and experimental studies, brassinolide (BL), 28-homobrassinolide (28-HomoBL) and 24-epibrassinolide (24-EpiBL) (Vardhini and Anjum, 2015). Foliar applications of 28-HomoBL and 24-EpiBL (0.5, 1.0, or 2.0 μM) reduced the levels of H_2O_2 , lipid peroxidation and electrolyte leakage and enhanced the activities of CAT, APX, SOD and GR of *Raphanus sativus* plants grown under Zn^{2+} stress (Ramakrishna and Rao, 2014). Similarly, pre-soaking *Brassica juncea* seeds in 24-EpiBL (10^{-10} , 10^{-8} and 10^{-6} M) enhanced the activities in leaves of

antioxidant enzymes (SOD, CAT, POD, GR, APX, MDHAR and DHAR) and decreased the level of MDA content under Zn^{2+} stress (Arora et al., 2010). In addition, foliar applications of 0.01 μM of 28-HomoBL significantly increased CAT, SOD and POD activities under cadmium stress (50, 100 or 150 μM) in the same species (Hayat et al., 2007). Foliar applications of 0.01, 0.1, and 1.0 $mg\ l^{-1}$ 24-EpiBL decreased H_2O_2 and MDA content and increased the activities of SOD, APX, CAT and POD alleviating heat-induced photoinhibition on tomato under heat stress (40/30°C) (Ogweno et al., 2008).

In lettuce plants, 3 μM foliar 24-EpiBL treatment alleviated the negative effects of salinity (50 and 100 mM NaCl) by reducing leaf electrolyte leakage (Ekinici et al., 2012). Therefore, foliar BRs applications could potentially ameliorate tipburn of lettuce symptoms by reducing oxidative stress under luxuriant growth conditions. Importantly, BRs have been reported to favour xylem development and consequently Ca^{2+} translocation, as Ca^{2+} is mostly transported through the xylem by mass flow (White and Broadley, 2003; de Freitas and Mitcham, 2012). Therefore, putative effects of BRs application on tipburn development should be further dissected in regards to the individual contributions of foliar Ca concentration versus oxidative stress.

The six carbon sugar AsA (Hancock and Viola, 2005) is a highly abundant metabolite in all plant cells, often found in concentrations of over 20 mM in chloroplasts (Smirnoff and Wheeler, 2000), and is a major contributor to the redox state of the cell (Valpuesta and Botella, 2004). As such, it is another compound that could be sprayed on lettuce plants within VFS to potentially ameliorate oxidative stress induced tipburn.

AsA protects plant tissues against oxidative damage caused by ROS either through direct scavenging or through enzyme catalysis (Noctor and Foyer, 1998) by being oxidised by ROS to the MDHA radical, which disproportionates to form AsA and DHA (Smirnoff, 2000). Interestingly, exogenous AsA application (0.5 mM) reduced lipid peroxidation levels of tomato seedlings under salinity stress (300 mM NaCl) (Shalata and Neumann, 2001). Furthermore, foliar AsA applications (0, 50, 100 and 150 ppm) decreased antioxidant enzymes activities (CAT, SOD, polyphenol oxidase (PPO) and peroxidase (POX)) as well as MDA levels in drought-stressed *Zea mays* L. (soil water potential: -1.3 MPa), indicating that AsA acted as a ROS scavenger thereby reducing the need for enzymatic protection (Dolatabadian et al., 2009). Similar results were obtained via foliar AsA application (25 mM) of canola (*Brassica napus* L.) grown under salt stress (200 mM NaCl) (Dolatabadian et al., 2008). In contrast, foliar AsA applications (0.5 mM) increased SOD, CAT and POD activities in potato plants under salinity stress (120 mM NaCl) and significantly increased fresh/dry weight of tubers compared to the non-salinised control (Sajid and Aftab, 2012). Upregulation of the antioxidant machinery occurred following foliar AsA applications to mungbean (*Phaseolus aureus* Roxb.) under heat stress (Kumar et al., 2011).

Taken together, these studies show that the effects of exogenous AsA applications are both species and stress specific. Nevertheless, foliar AsA applications consistently mitigated oxidative stress in a broad range of stresses and species either via direct ROS scavenging or by enhancing antioxidant enzyme activities highlighting the potential of this approach as a tool for ameliorating tipburn symptoms.

Supplying the rhizosphere with additional Ca, e.g. via fertigation, has proved

ineffective in ameliorating the symptoms of tipburn (Hartz et al., 2007; Dayod et al., 2010), since Ca deficiency occurs as a result of reduced transpiration and not of low rhizospheric Ca availability (White and Broadley, 2003; Gilliam et al., 2011). However, based on the findings of the present study, biofortification to increase the antioxidant capacity of plants may also ameliorate tipburn in lettuce. Biofortification is the application of mineral fertilizers to increase mineral concentrations of edible crops (White and Broadley, 2009). Hydroponically grown lettuce responded positively to iodine biofortification (0, 13, 39, 65, and 90 or 129 $\mu\text{g l}^{-1}$ as IO_3^- or I^-) as demonstrated by increases in foliar iodine content ($\sim 700 \mu\text{g iodine kg}^{-1}$ total leaf fresh weight) with no changes in crop biomass or quality (Voogt et al., 2010). Interestingly, iodine biofortification (20, 40, 80 μM as IO_3^-) increased the activities of SOD, APX and CAT, and AsA and GHS concentrations in lettuce plants (Blasco et al., 2011) but did not change MDA concentration, indicating the absence of any phytotoxic effects of iodine biofortification (Blasco et al., 2008). Furthermore, IO_3^- biofortification (20, 40 and 80 μM) of lettuce plants under salinity stress (100 mM NaCl) significantly increased the activity of antioxidant enzymes (SOD, APX, DHAR and GR) (Leyva et al., 2011). Similarly, IO_3^- biofortification (20 and 40 μM) significantly increased lettuce biomass and total phenols protecting the plants against the affects of salinity stress (100 mM NaCl) (Blasco et al., 2013). These studies highlight the potential of iodine biofortification, via the addition of IO_3^- in the form of KIO_3 to the nutrient solution, for ameliorating the symptoms of tipburn in VFS-grown lettuce.

6.3 Conclusions

This thesis combines fundamental and applied plant science investigations to contribute to the successful establishment of VFS as commercially feasible means to

increase crop productivity per area. Identification of tipburn of lettuce as a key limitation to marketability in the VFS, precipitated fundamental plant physiology and biochemistry investigations and transcriptomics studies of the mechanistic basis of this disorder. The new mechanistic insights into the development of tipburn of lettuce, and importantly the role of oxidative stress in the induction of the disorder, allow recommendations for developing novel and commercially applicable methods to remediate tipburn in VFS and hydroponics. The key findings of this PhD thesis are:

1. VFS can produce more crop per unit area compared to horizontal hydroponics.
2. Crop growth is limited by PPFD and not nutrient solution concentration gradients within the VFS.
3. Tipburn of lettuce is a key limitation to the commercial exploitation of the VFS.
4. Both high PPFD and temperature are a prerequisite for tipburn development within VFS.
5. Plants grown under luxuriant growth conditions (stress) exhibited photoinhibition and oxidative stress prior to the appearance of visual tipburn symptoms.
6. Leaf Ca concentration was not related to tipburn induction.
7. Transcriptome changes related to flavonoid biosynthesis are potentially linked to tipburn.

Taken together, this thesis provides both important information from a commercial perspective, contributing to the emerging field of vertical farming and urban agriculture, and also improves our fundamental understanding of lettuce tipburn, providing a solid foundation to investigate novel aetiologies in the induction of the disorder.

REFERENCES

- Adams, P., & Ho, L. C. (1993). Effects of environment on the uptake and distribution of calcium in tomato and on the incidence of blossom-end rot. In M. A. C. Fragoso, M. L. V. Beusichem, & A. Houwers (Eds.), *Optimization of Plant Nutrition* (pp. 583–588). Springer Netherlands. https://doi.org/10.1007/978-94-017-2496-8_90
- Aebi, H. (1984). [13] Catalase in vitro. *Methods in Enzymology*, *105*, 121–126.
- Agati, G., Cerovic, Z. G., Pinelli, P., & Tattini, M. (2011). Light-induced accumulation of ortho-dihydroxylated flavonoids as non-destructively monitored by chlorophyll fluorescence excitation techniques. *Environmental and Experimental Botany*, *73*, 3–9. <https://doi.org/10.1016/j.envexpbot.2010.10.002>
- Agati, G., & Tattini, M. (2010). Multiple functional roles of flavonoids in photoprotection. *New Phytologist*, *186*(4), 786–793. <https://doi.org/10.1111/j.1469-8137.2010.03269.x>
- Ahamed, G. J., Wang, M.-M., Zhou, Y.-H., Xia, X.-J., Mao, W.-H., Shi, K., & Yu, J.-Q. (2012). The growth, photosynthesis and antioxidant defense responses of five vegetable crops to phenanthrene stress. *Ecotoxicology and Environmental Safety*, *80*, 132–139. <https://doi.org/10.1016/j.ecoenv.2012.02.015>
- Ahmad, P. (2014). *Oxidative Damage to Plants: Antioxidant Networks and Signaling*. Academic Press.
- Aktas, H., Karni, L., Aloni, B., & Bar-Tal, A. (2003). Physiological and biochemical mechanisms leading to blossom-end rot in greenhouse-grown peppers, irrigated with saline solution. In *International Symposium on Managing Greenhouse Crops in Saline Environment 609* (pp. 81–88). Retrieved from http://www.actahort.org/books/609/609_9.htm
- Aktas, H., Karni, L., Chang, D.-C., Turhan, E., Bar-Tal, A., & Aloni, B. (2005). The suppression of salinity-associated oxygen radicals production, in pepper (*Capsicum annuum*) fruit, by manganese, zinc and calcium in relation to its sensitivity to blossom-end rot. *Physiologia Plantarum*, *123*(1), 67–74. <https://doi.org/10.1111/j.1399-3054.2004.00435.x>
- Alboresi, A., Ballottari, M., Hienerwadel, R., Giacometti, G. M., & Morosinotto, T. (2009). Antenna complexes protect Photosystem I from Photoinhibition. *BMC Plant Biology*, *9*, 71. <https://doi.org/10.1186/1471-2229-9-71>
- Al-Chalabi, M. (2015). Vertical farming: Skyscraper sustainability? *Sustainable Cities and Society*, *18*, 74–77. <https://doi.org/10.1016/j.scs.2015.06.003>
- Ali, M. B., Hahn, E.-J., & Paek, K.-Y. (2005). Effects of temperature on oxidative stress defense systems, lipid peroxidation and lipoxygenase activity in *Phalaenopsis*. *Plant Physiology and Biochemistry*, *43*(3), 213–223.
- Allakhverdiev, S. I., Kreslavski, V. D., Klimov, V. V., Los, D. A., Carpentier, R., & Mohanty, P. (2008). Heat stress: an overview of molecular responses in photosynthesis. *Photosynthesis Research*, *98*(1–3), 541–550.

- Allakhverdiev, S. I., & Murata, N. (2004). Environmental stress inhibits the synthesis de novo of proteins involved in the photodamage–repair cycle of Photosystem II in *Synechocystis* sp. PCC 6803. *Biochimica et Biophysica Acta (BBA) - Bioenergetics*, 1657(1), 23–32. <https://doi.org/10.1016/j.bbabi.2004.03.003>
- Almeselmani, M., Deshmukh, P. S., Sairam, R. K., Kushwaha, S. R., & Singh, T. P. (2006). Protective role of antioxidant enzymes under high temperature stress. *Plant Science*, 171(3), 382–388. <https://doi.org/10.1016/j.plantsci.2006.04.009>
- Amarante, C. V. T., Dias, J., Bessegato, A. A., & Ernani, P. R. (2001). Preharvest Calcium Sprays Improve Fruit Quality of 'Gala' Apples in Southern Brazil. In *International Symposium on Foliar Nutrition of Perennial Fruit Plants 594* (pp. 481–486). Retrieved from http://www.actahort.org/books/594/594_62.htm
- Andriolo, J. L., Luz, G. L. da, Witter, M. H., Godoi, R. dos S., Barros, G. T., & Bortolotto, O. C. (2005). Growth and yield of lettuce plants under salinity. *Horticultura Brasileira*, 23(4), 931–934.
- Apel, K., & Hirt, H. (2004). Reactive oxygen species: metabolism, oxidative stress, and signal transduction. *Annu. Rev. Plant Biol.*, 55, 373–399.
- Arbona, V., Manzi, M., Ollas, C. de, & Gómez-Cadenas, A. (2013). Metabolomics as a tool to investigate abiotic stress tolerance in plants. *International Journal of Molecular Sciences*, 14(3), 4885–4911.
- Aro, E.-M., Virgin, I., & Andersson, B. (1993). Photoinhibition of Photosystem II. Inactivation, protein damage and turnover. *Biochimica et Biophysica Acta (BBA) - Bioenergetics*, 1143(2), 113–134. [https://doi.org/10.1016/0005-2728\(93\)90134-2](https://doi.org/10.1016/0005-2728(93)90134-2)
- Aroca, R. (2012). *Plant Responses to Drought Stress: From Morphological to Molecular Features*. Springer.
- Arora, P., Bhardwaj, R., & Kumar Kanwar, M. (2010). 24-epibrassinolide induced antioxidative defense system of *Brassica juncea* L. under Zn metal stress. *Physiology and Molecular Biology of Plants: An International Journal of Functional Plant Biology*, 16(3), 285–293. <https://doi.org/10.1007/s12298-010-0031-9>
- Arteca, R. N. (2013). *Plant Growth Substances: Principles and Applications*. Springer Science & Business Media.
- Asada, K. (2006). Production and Scavenging of Reactive Oxygen Species in Chloroplasts and Their Functions. *Plant Physiology*, 141(2), 391–396. <https://doi.org/10.1104/pp.106.082040>
- Ashkar, S. A., & Ries, S. K. (1971). Lettuce tipburn as related to nutrient imbalance and nitrogen composition. *Amer Soc Hort Sci J*. Retrieved from <http://agris.fao.org/agris-search/search.do?recordID=US201302398443>
- Assimakopoulou, A., Kotsiras, A., & Nifakos, K. (2013). Incidence of lettuce tipburn as related to hydroponic system and cultivar. *Journal of Plant Nutrition*, 36(9), 1383–1400.
- Ayala, A., Muñoz, M. F., & Argüelles, S. (2014). Lipid Peroxidation: Production, Metabolism, and Signaling Mechanisms of Malondialdehyde and 4-Hydroxy-

- 2-Nonenal. *Oxidative Medicine and Cellular Longevity*, 2014, e360438. <https://doi.org/10.1155/2014/360438>
- Badami, M. G., & Ramankutty, N. (2015). Urban agriculture and food security: A critique based on an assessment of urban land constraints. *Global Food Security*, 4, 8–15. <https://doi.org/10.1016/j.gfs.2014.10.003>
- Bajguz, A., & Hayat, S. (2009). Effects of brassinosteroids on the plant responses to environmental stresses. *Plant Physiology and Biochemistry*, 47(1), 1–8.
- Barbosa, G. L., Gadelha, F. D. A., Kublik, N., Proctor, A., Reichelm, L., Weissinger, E., Halden, R. U. (2015). Comparison of Land, Water, and Energy Requirements of Lettuce Grown Using Hydroponic vs. Conventional Agricultural Methods. *International Journal of Environmental Research and Public Health*, 12(6), 6879–6891.
- Barradas, V. L., Jones, H. G., & Clark, J. A. (1994). Stomatal responses to changing irradiance in *Phaseolus vulgaris* L. *Journal of Experimental Botany*, 45(7), 931–936. <https://doi.org/10.1093/jxb/45.7.931>
- Barta, D. J., & Tibbitts, T. W. (1986). Effects of Artificial Enclosure of Young Lettuce Leaves on Tipburn Incidence and Leaf Calcium. *J. Amer. Soc. Hort. Sci.*, 150(3), 413–416.
- Barta, D. J., & Tibbitts, T. W. (1991). Calcium localization in lettuce leaves with and without tipburn: Comparison of controlled-environment and field-grown plants. *Journal of the American Society for Horticultural Science*, 116(5), 870–875.
- Barta, D. J., & Tibbitts, T. W. (2000). Calcium localization and tipburn development in lettuce leaves during early enlargement. *Journal of the American Society for Horticultural Science*, 125(3), 294–298.
- Baslam, M., Pascual, I., Sánchez-Díaz, M., Erro, J., García-Mina, J. M., & Goicoechea, N. (2011). Improvement of nutritional quality of greenhouse-grown lettuce by arbuscular mycorrhizal fungi is conditioned by the source of phosphorus nutrition. *Journal of Agricultural and Food Chemistry*, 59(20), 11129–11140.
- Bayley, J. E., Yu, M., & Frediani, K. (2010). Sustainable food production using high density vertical growing (VertiCrop). In *XXVIII International Horticultural Congress on Science and Horticulture for People (IHC2010): International Symposium on 921* (pp. 95–104). Retrieved from http://www.actahort.org/books/921/921_11.htm
- Beatley, T. (2007). Envisioning Solar Cities: Urban Futures Powered By Sustainable Energy. *Journal of Urban Technology*, 14(2), 31–46. <https://doi.org/10.1080/10630730701531682>
- Becker, C., Klaering, H.-P., Kroh, L. W., & Krumbein, A. (2014). Cool-cultivated red leaf lettuce accumulates cyanidin-3-O-(6 "-O-malonyl)-glucoside and caffeoylmalic acid. *Food Chemistry*, 146, 404–411.
- Benjamini, Y., & Speed, T. P. (2012). Summarizing and correcting the GC content bias in high-throughput sequencing. *Nucleic Acids Research*, gks001.

- Berkel, N. van. (1988). Preventing tipburn in Chinese cabbage by high relative humidity during the night. *Netherlands Journal of Agricultural Science*, 36. Retrieved from <http://agris.fao.org/agris-search/search/display.do?f=1989/NL/NL89018.xml;NL8804709>
- Bestwick, C. S., Adam, A. L., Puri, N., & Mansfield, J. W. (2001). Characterisation of and changes to pro and anti-oxidant enzyme activities during the hypersensitive reaction in lettuce (*Lactuca sativa* L.). *Plant Science*, 161(3), 497–506.
- Bevilacqua, M., Ciarapica, F. E., & Giacchetta, G. (2009). Business process reengineering of a supply chain and a traceability system: A case study. *Journal of Food Engineering*, 93(1), 13–22.
- Bishop, G. J., & Koncz, C. (2002). Brassinosteroids and Plant Steroid Hormone Signaling. *The Plant Cell*, 14(suppl 1), S97–S110. <https://doi.org/10.1105/tpc.001461>
- Blake, J. A. (2013). Ten Quick Tips for Using the Gene Ontology. *PLOS Computational Biology*, 9(11), e1003343. <https://doi.org/10.1371/journal.pcbi.1003343>
- Blasco, B., Leyva, R., Romero, L., & Ruiz, J. M. (2013). Iodine Effects on Phenolic Metabolism in Lettuce Plants under Salt Stress. *Journal of Agricultural and Food Chemistry*, 61(11), 2591–2596. <https://doi.org/10.1021/jf303917n>
- Blasco, B., Rios, J. j., Cervilla, L. m., Sánchez-Rodríguez, E., Ruiz, J. m., & Romero, L. (2008). Iodine biofortification and antioxidant capacity of lettuce: potential benefits for cultivation and human health. *Annals of Applied Biology*, 152(3), 289–299. <https://doi.org/10.1111/j.1744-7348.2008.00217.x>
- Block, D. R., Chávez, N., Allen, E., & Ramirez, D. (2011). Food sovereignty, urban food access, and food activism: contemplating the connections through examples from Chicago. *Agriculture and Human Values*, 29(2), 203–215. <https://doi.org/10.1007/s10460-011-9336-8>
- Blokhina, O., Virolainen, E., & Fagerstedt, K. V. (2003). Antioxidants, oxidative damage and oxygen deprivation stress: a review. *Annals of Botany*, 91(2), 179–194.
- Boo, H. O., Chon, S. U., & Lee, S. Y. (2006). Effects of temperature and plant growth regulators on anthocyanin synthesis and phenylalanine ammonia-lyase activity in chicory (*Cichorium intybus* L.). *The Journal of Horticultural Science and Biotechnology*, 81(3), 478–482.
- Borgeraas, J., & Hessen, D. O. (2000). UV-B induced mortality and antioxidant enzyme activities in *Daphnia magna* at different oxygen concentrations and temperatures. *Journal of Plankton Research*, 22(6), 1167–1183. <https://doi.org/10.1093/plankt/22.6.1167>
- Both, A. J., Albright, L. D., Langhans, R. W., Reiser, R. A., & Vinzant, B. G. (1994). Hydroponic lettuce production influenced by integrated supplemental light levels in a controlled environment agriculture facility: experimental results. In *III International Symposium on Artificial Lighting in Horticulture 418* (pp. 45–52). Retrieved from http://www.actahort.org/books/418/418_5.htm

- Bougherara, D., Grolleau, G., & Mzoughi, N. (2009). Buy local, pollute less: What drives households to join a community supported farm? *Ecological Economics*, 68(5), 1488–1495. <https://doi.org/10.1016/j.ecolecon.2008.10.009>
- Bowler, C., Montagu, M. van, & Inze, D. (1992). Superoxide dismutase and stress tolerance. *Annual Review of Plant Biology*, 43(1), 83–116.
- Bradford, M. M. (1976). A rapid and sensitive method for the quantitation of microgram quantities of protein utilizing the principle of protein-dye binding. *Analytical Biochemistry*, 72(1–2), 248–254.
- Brechner, M., & Both, A. J. (n.d.). Hydroponic Lettuce Handbook. *Cornell Controlled Environment Agriculture*. Retrieved from <http://www.cornellcea.com/attachments/Cornell%20CEA%20Lettuce%20Handbook%20.pdf>
- Broadley, M. R., Bowen, H. C., Cotterill, H. L., Hammond, J. P., Meacham, M. C., Mead, A., & White, P. J. (2003). Variation in the shoot calcium content of angiosperms. *Journal of Experimental Botany*, 54(386), 1431–1446. <https://doi.org/10.1093/jxb/erg143>
- Brumm, I., & Schenk, M. (1992). Influence of Nitrogen Supply on the Occurrence of Calcium Deficiency in Field Grown Lettuce. In *Workshop on Ecological Aspects of Vegetable Fertilization in Integrated Crop Production in the Field* 339 (pp. 125–136). Retrieved from http://www.actahort.org/books/339/339_11.htm
- Bugbee, B. (2003). Nutrient management in recirculating hydroponic culture. In *South Pacific Soilless Culture Conference-SPSCC 648* (pp. 99–112). Retrieved from http://www.actahort.org/books/648/648_12.htm
- Burgess, A. J., Retkute, R., Pound, M. P., Foulkes, J., Preston, S. P., Jensen, O. E., Murchie, E. H. (2015). High-resolution three-dimensional structural data quantify the impact of photoinhibition on long-term carbon gain in wheat canopies in the field. *Plant Physiology*, 169(2), 1192–1204.
- Calatayud, A., Alvarado, J. W., & Barreno, E. (2002). Similar Effects of Ozone on Four Cultivars of Lettuce in Open Top Chambers During Winter. *Photosynthetica*, 40(2), 195–200. <https://doi.org/10.1023/A:1021333305592>
- Camejo, D., Rodríguez, P., Angeles Morales, M., Miguel Dell'Amico, J., Torrecillas, A., & Alarcón, J. J. (2005). High temperature effects on photosynthetic activity of two tomato cultivars with different heat susceptibility. *Journal of Plant Physiology*, 162(3), 281–289. <https://doi.org/10.1016/j.jplph.2004.07.014>
- Cancellier, L. L., Adorian, G. C., Moreira Rodrigues, H. V., Siebeneichler, S. C., & Alves De Barros Leal, T. C. (2010). Potassium Levels in the Morphophysiological Response of Lettuce. *Revista Caatinga*, 23(4), 21–27.
- Carassay, L. R., Bustos, D. A., Golberg, A. D., & Taleisnik, E. (2012). Tipburn in salt-affected lettuce (*Lactuca sativa* L.) plants results from local oxidative stress. *Journal of Plant Physiology*, 169(3), 285–293. <https://doi.org/10.1016/j.jplph.2011.10.004>

- Casado-Vela, J., Sellés, S., & Bru Martínez, R. (2005). Proteomic approach to blossom-end rot in tomato fruits (*Lycopersicon esculentum* M.): Antioxidant enzymes and the pentose phosphate pathway. *Proteomics*, 5(10), 2488–2496.
- Casado-Vela, J., Sellés, S., & Bru, R. (2005). Purification and Kinetic Characterization of Polyphenol Oxidase from Tomato Fruits (*lycopersicon esculentum* Cv. Muchamiel). *Journal of Food Biochemistry*, 29(4), 381–401. <https://doi.org/10.1111/j.1745-4514.2005.00037.x>
- Casano, L. M., Gomez, L. D., Lascano, H. R., González, C. A., & Trippi, V. S. (1997). Inactivation and degradation of CuZn-SOD by active oxygen species in wheat chloroplasts exposed to photooxidative stress. *Plant and Cell Physiology*, 38(4), 433–440.
- Chadjaa, H., Vezina, L. P., Dorais, M., & Gosselin, A. (2001). Effects of Lighting on the Growth, Quality and Primary Nitrogen Assimilation of Greenhouse Lettuce (*lactuca Savita*. L). In J. A. Fernandez, P. F. Martinez, & N. Castilla (Eds.), *Proceedings of the Fifth International Symposium on Protected Cultivation in Mild Winter Climates: Current Trends for Sustainable Technologies, Vols I and II* (pp. 325–331). Leuven 1: International Society Horticultural Science.
- Chandra, S., Khan, S., Avula, B., Lata, H., Yang, M. H., ElSohly, M. A., Khan, I. A. (2014). Assessment of Total Phenolic and Flavonoid Content, Antioxidant Properties, and Yield of Aeroponically and Conventionally Grown Leafy Vegetables and Fruit Crops: A Comparative Study. *Evidence-Based Complementary and Alternative Medicine, Evidence-Based Complementary and Alternative Medicine*, 2014, 2014, e253875. <https://doi.org/10.1155/2014/253875>, 10.1155/2014/253875
- Chang, Y.-C., Grace-Martin, K., & Miller, W. B. (2004). Efficacy of Exogenous Calcium Applications for Reducing Upper Leaf Necrosis in *Lilium* Star Gazer'. *HortScience*, 39(2), 272–275.
- Chang, Y.-C., & Miller, W. B. (2004). The Relationship between Leaf Enclosure, Transpiration, and Upper Leaf Necrosis on *Lilium* Star Gazer'. *Journal of the American Society for Horticultural Science*, 129(1), 128–133.
- Chao, L., Weiqian, C., Yun, L., Hao, H., Liang, C., Xiaoqing, L., & Fashui, H. (2009). Cerium under calcium deficiency—influence on the antioxidative defense system in spinach plants. *Plant and Soil*, 323(1–2), 285–294. <https://doi.org/10.1007/s11104-009-9937-9>
- Chaplin-Kramer, R., Sharp, R. P., Mandle, L., Sim, S., Johnson, J., Butnar, I., Kareiva, P. M. (2015). Spatial patterns of agricultural expansion determine impacts on biodiversity and carbon storage. *Proceedings of the National Academy of Sciences*, 112(24), 7402–7407. <https://doi.org/10.1073/pnas.1406485112>
- Chen, J. (2007). Rapid urbanization in China: A real challenge to soil protection and food security. *CATENA*, 69(1), 1–15. <https://doi.org/10.1016/j.catena.2006.04.019>

- Chen Yuting, Zheng Rongliang, Jia Zhongjian, & Ju Yong. (1990). Flavonoids as superoxide scavengers and antioxidants. *Free Radical Biology and Medicine*, 9(1), 19–21. [https://doi.org/10.1016/0891-5849\(90\)90045-K](https://doi.org/10.1016/0891-5849(90)90045-K)
- Choi, K. Y., & Lee, Y. B. (2008). Effects of Relative Humidity on the Apparent Variability in the Incidence of Tipburn Symptom and Distribution of Mineral Nutrients between Morphologically Different Lettuce (*Lactuca sativa* L.) Cultivars. *Horticulture, Environment, and Biotechnology*. Retrieved from <http://agris.fao.org/agris-search/search.do?f=2009/KR/KR0902.xml;KR2009000807>
- Choi, K. Y., Paek, K. Y., & Lee, Y. B. (2000). Effect of air temperature on tipburn incidence of butterhead and leaf lettuce in a plant factory. *Transplant Production in the 21st Century*, 166.
- Chon, S.-U., Jang, H.-G., Kim, D.-K., Kim, Y.-M., Boo, H.-O., & Kim, Y.-J. (2005). Allelopathic potential in lettuce (*Lactuca sativa* L.) plants. *Scientia Horticulturae*, 106(3), 309–317.
- Chow, K. K., Price, T. V., & Hanger, B. C. (1992). Nutritional requirements for growth and yield of strawberry in deep flow hydroponic systems. *Scientia Horticulturae*, 52(1–2), 95–104. [https://doi.org/10.1016/0304-4238\(92\)90012-2](https://doi.org/10.1016/0304-4238(92)90012-2)
- Christakis, N. A. (2001). *Death Foretold: Prophecy and Prognosis in Medical Care*. University of Chicago Press.
- Christie, C. B., & Nichols, M. A. (2004). Aeroponics-A production system and research tool. *Acta Horticulturae*, (648), 185–190. <https://doi.org/10.17660/ActaHortic.2004.648.22>
- Christopoulou, M., McHale, L. K., Kozik, A., Reyes-Chin Wo, S., Wroblewski, T., & Michelmore, R. W. (2015). Dissection of Two Complex Clusters of Resistance Genes in Lettuce (*Lactuca sativa*). *Molecular Plant-Microbe Interactions*, 28(7), 751–765. <https://doi.org/10.1094/MPMI-06-14-0175-R>
- Clark, K. F., & Greenwood, S. J. (2016). Next-Generation Sequencing and the Crustacean Immune System: The Need for Alternatives in Immune Gene Annotation. *Integrative and Comparative Biology*, 56(6), 1113–1130. <https://doi.org/10.1093/icb/icw023>
- Collier, G. F., & Huntington, V. C. (1983). The relationship between leaf growth, calcium accumulation and distribution, and tipburn development in field-grown butterhead lettuce. *Scientia Horticulturae*, 21(2), 123–128. [https://doi.org/10.1016/0304-4238\(83\)90157-7](https://doi.org/10.1016/0304-4238(83)90157-7)
- Collier, G. F., & Tibbitts, T. W. (1982). Tipburn of lettuce. *Horticultural Reviews*, 4(2), 49–65.
- Collier, G. F., & Tibbitts, T. W. (1984). Effects of Relative Humidity and Root Temperature on Calcium Concentration and Tipburn. *J. Amer. Soc. Hort. Sci*, 109(2), 128–131.
- Conesa, A., Götz, S., García-Gómez, J. M., Terol, J., Talón, M., & Robles, M. (2005). Blast2GO: a universal tool for annotation, visualization and analysis in

- functional genomics research. *Bioinformatics*, 21(18), 3674–3676. <https://doi.org/10.1093/bioinformatics/bti610>
- Conklin, P. L., & Barth, C. (2004). Ascorbic acid, a familiar small molecule intertwined in the response of plants to ozone, pathogens, and the onset of senescence. *Plant, Cell & Environment*, 27(8), 959–970. <https://doi.org/10.1111/j.1365-3040.2004.01203.x>
- Cooper, A. (1978). Commercial applications of NFT. *Commercial applications of NFT*.
- Corriveau, J., Gaudreau, L., Caron, J., Gosselin, A., & Jenni, S. (2010). Effect of water management, fogging and Ca foliar application on tipburn of romaine lettuce (*Lactuca sativa* L.) cultivated in greenhouse. In *XXVIII International Horticultural Congress on Science and Horticulture for People (IHC2010): International Symposium on 927* (pp. 475–480). Retrieved from http://www.actahort.org/books/927/927_60.htm
- Corriveau, J., Gaudreau, L., Caron, J., Jenni, S., & Gosselin, A. (2012). Testing irrigation, day/night foliar spraying, foliar calcium and growth inhibitor as possible cultural practices to reduce tipburn in lettuce. *Canadian Journal of Plant Science*, 92(5), 889–899. <https://doi.org/10.4141/cjps2011-242>
- Cortell, J. M., & Kennedy, J. A. (2006). Effect of shading on accumulation of flavonoid compounds in (*Vitis vinifera* L.) pinot noir fruit and extraction in a model system. *Journal of Agricultural and Food Chemistry*, 54(22), 8510–8520.
- Corvalan, C., Hales, S., & McMichael, A. J. (2005). *Ecosystems and human well-being: health synthesis*. World health organization.
- Cox, E. F., & Dearman, A. S. (1981). The effect of trickle irrigation, misting and row position on the incidence of tipburn of field lettuce. *Scientia Horticulturae*, 15(2), 101–106. [https://doi.org/10.1016/0304-4238\(81\)90097-2](https://doi.org/10.1016/0304-4238(81)90097-2)
- Cox, E., & Mckee, J. (1976). Comparison of Tipburn Susceptibility in Lettuce Under Field and Glasshouse Conditions. *Journal of Horticultural Science*, 51(1), 117–122.
- Crawford, N. M. (1995). Nitrate: nutrient and signal for plant growth. *The Plant Cell*, 7(7), 859.
- Cresswell, G. C. (1991). Effect of lowering nutrient solution concentration at night on leaf calcium levels and the incidence of tipburn in lettuce (var. Gloria). *Journal of Plant Nutrition*, 14(9), 913–924.
- Cui, L., Li, J., Fan, Y., Xu, S., & Zhang, Z. (2006). High temperature effects on photosynthesis, PSII functionality and antioxidant activity of two *Festuca arundinacea* cultivars with different heat susceptibility. *Botanical Studies*, 47(1), 61–69.
- Danon, A., Miersch, O., Felix, G., Camp, R. G., & Apel, K. (2005). Concurrent activation of cell death-regulating signaling pathways by singlet oxygen in *Arabidopsis thaliana*. *The Plant Journal*, 41(1), 68–80.
- Dat, J., Vandenabeele, S., Vranová, E., Montagu, M. V., Inzé, D., & Breusegem, F. V. (2000). Dual action of the active oxygen species during plant stress responses.

- Cellular and Molecular Life Sciences CMLS*, 57(5), 779–795.
<https://doi.org/10.1007/s000180050041>
- Dawar, S., Vani, T., & Singhal, G. S. (1998). Stimulation of Antioxidant Enzymes and Lipid Peroxidation by UV-B Irradiation in Thylakoid Membranes of Wheat. *Biologia Plantarum*, 41(1), 65–73. <https://doi.org/10.1023/A:1001760432310>
- Dayod, M., Tyerman, S. D., Leigh, R. A., & Gilliham, M. (2010). Calcium storage in plants and the implications for calcium biofortification. *Protoplasma*, 247(3–4), 215–231. <https://doi.org/10.1007/s00709-010-0182-0>
- De Cremer, K., Mathys, J., Vos, C., Froenicke, L., Michelmore, R. W., Cammue, B. P. A., & De Coninck, B. (2013). RNAseq-based transcriptome analysis of *Lactuca sativa* infected by the fungal necrotroph *Botrytis cinerea*. *Plant, Cell & Environment*, 36(11), 1992–2007. <https://doi.org/10.1111/pce.12106>
- de Freitas, S. T., & Mitcham, E. I. (2012). 3 Factors Involved in Fruit Calcium Deficiency Disorders. *Horticultural Reviews*, 40, 107.
- de Oliveira, A. B., Mendes Alencar, N. L., & Gomes-Filho, E. (2013). Comparison Between the Water and Salt Stress Effects on Plant Growth and Development. In S. Akinci (Ed.), *Responses of Organisms to Water Stress*. InTech. Retrieved from <http://www.intechopen.com/books/responses-of-organisms-to-water-stress/comparison-between-the-water-and-salt-stress-effects-on-plant-growth-and-development>
- De Swaef, T., Vermeulen, K., Vergote, N., Van Lommel, J., Van Labeke, M.-C., Bleyaert, P., & Steppe, K. (2015). Plant Sensors Help to Understand Tipburn in Lettuce. *Acta Horticulturae*, (1099), 63–70. <https://doi.org/10.17660/ActaHortic.2015.1099.3>
- Demmig-Adams, B., Moeller, D. L., Logan, B. A., & Iii, W. W. A. (1998). Positive correlation between levels of retained zeaxanthin + antheraxanthin and degree of photoinhibition in shade leaves of *Schefflera arboricola* (Hayata) Merrill. *Planta*, 205(3), 367–374. <https://doi.org/10.1007/s004250050332>
- Demmig-Adams, B. & Adams, I. (1992). Photoprotection and Other Responses of Plants to High Light Stress. *Annual Review of Plant Physiology and Plant Molecular Biology*, 43(1), 599–626. <https://doi.org/10.1146/annurev.pp.43.060192.003123>
- Demšar, J., Osvald, J., & Vodnik, D. (2004). The effect of light-dependent application of nitrate on the growth of aeroponically grown lettuce (*Lactuca sativa* L.). *Journal of the American Society for Horticultural Science*, 129(4), 570–575.
- Despommier, D. (2011). The vertical farm: controlled environment agriculture carried out in tall buildings would create greater food safety and security for large urban populations. *Journal Für Verbraucherschutz Und Lebensmittelsicherheit*, 6(2), 233–236.
- Despommier, D. (2013). Farming up the city: the rise of urban vertical farms. *Trends in Biotechnology*, 31(7), 388–389.
- Dhindsa, R. S., Plumb-Dhindsa, P., & Thorpe, T. A. (1981). Leaf Senescence: Correlated with Increased Levels of Membrane Permeability and Lipid Peroxidation, and Decreased Levels of Superoxide Dismutase and Catalase.

- Journal of Experimental Botany*, 32(1), 93–101.
<https://doi.org/10.1093/jxb/32.1.93>
- Dolatabadian, A., Modarres Sanavy, S. a. M., & Sharifi, M. (2009). Alleviation of Water Deficit Stress Effects by Foliar Application of Ascorbic Acid on Zea mays L. *Journal of Agronomy and Crop Science*, 195(5), 347–355.
<https://doi.org/10.1111/j.1439-037X.2009.00382.x>
- Dolatabadian, A., Sanavy, S., & Chashmi, N. A. (2008). The effects of foliar application of ascorbic acid (vitamin C) on antioxidant enzymes activities, lipid peroxidation and proline accumulation of canola (*Brassica napus* L.) under conditions of salt stress. *Journal of Agronomy and Crop Science*, 194(3), 206–213.
- Dong, Y., Fan, G., Zhao, Z., & Deng, M. (2014). Transcriptome expression profiling in response to drought stress in *Paulownia australis*. *International Journal of Molecular Sciences*, 15(3), 4583–4607.
- Du, Z., Zhou, X., Ling, Y., Zhang, Z., & Su, Z. (2010). agriGO: a GO analysis toolkit for the agricultural community. *Nucleic Acids Research*, 38(suppl_2), W64–W70. <https://doi.org/10.1093/nar/gkq310>
- Ehret, D. L., & Ho, L. C. (1986). Translocation of Calcium in Relation to Tomato Fruit Growth. *Annals of Botany*, 58(5), 679–688.
- Eigenbrod, C., & Gruda, N. (2014). Urban vegetable for food security in cities. A review. *Agronomy for Sustainable Development*, 35(2), 483–498.
<https://doi.org/10.1007/s13593-014-0273-y>
- Eigenbrod, C., & Gruda, N. (2014c). Urban vegetable for food security in cities. A review. *Agronomy for Sustainable Development*, 35(2), 483–498.
<https://doi.org/10.1007/s13593-014-0273-y>
- Ekinci, M., Yildirim, E., Dursun, A., & Turan, M. (2012). Mitigation of Salt Stress in Lettuce (*Lactuca sativa* L. var. Crispa) by Seed and Foliar 24-epibrassinolide Treatments. *HortScience*, 47(5), 631–636.
- Elavarthi, S., & Martin, B. (2010). Spectrophotometric Assays for Antioxidant Enzymes in Plants. In R. Sunkar (Ed.), *Plant Stress Tolerance* (pp. 273–280). Humana Press. Retrieved from http://link.springer.com/protocol/10.1007/978-1-60761-702-0_16
- El-Behairy, U. A., El-Shinawy, M. Z., Medany, M. A., & Abou-Hadid, A. F. (2000). Utilization of " A-shape" system of nutrient film technique (NFT) as a method for producing some vegetable crops intensively. In *V International Symposium on Protected Cultivation in Mild Winter Climates: Current Trends for Sustainable Technologies* 559 (pp. 581–586). Retrieved from http://www.actahort.org/books/559/559_85.htm
- Eltrop, L., & Marschner, H. (1996). Growth and mineral nutrition of non-mycorrhizal and mycorrhizal Norway spruce (*Picea abies*) seedlings grown in semi-hydroponic sand culture. *New Phytologist*, 133(3), 469–478.
<https://doi.org/10.1111/j.1469-8137.1996.tb01914.x>
- Eraslan, F., Inal, A., Savasturk, O., & Gunes, A. (2007). Changes in antioxidative system and membrane damage of lettuce in response to salinity and boron

- toxicity. *Scientia Horticulturae*, 114(1), 5–10.
<https://doi.org/10.1016/j.scienta.2007.05.002>
- Erdman, J. W., Bierer, T. L., & Gugger, E. T. (1993). Absorption and Transport of Carotenoids. *Annals of the New York Academy of Sciences*, 691(1), 76–85.
<https://doi.org/10.1111/j.1749-6632.1993.tb26159.x>
- Ewing, B., Hillier, L., Wendl, M. C., & Green, P. (1998). Base-calling of automated sequencer traces using Phred. I. Accuracy assessment. *Genome Research*, 8(3), 175–185.
- Falovo, C., Roupheal, Y., Rea, E., Battistelli, A., & Colla, G. (2009). Nutrient solution concentration and growing season affect yield and quality of *Lactuca sativa* L. var. *acephala* in floating raft culture. *Journal of the Science of Food and Agriculture*, 89(10), 1682–1689. <https://doi.org/10.1002/jsfa.3641>
- Fecondini, M., Damasio de Faria, A. C., Michelon, N., Mezzetti, M., Orsini, F., & Gianquinto, G. (2010). Learning the value of gardening: results from an experience of community based simplified hydroponics in north-east Brazil. *Acta Horticulturae*, (881), 111–116.
<https://doi.org/10.17660/ActaHortic.2010.881.10>
- Feng, F., Li, M., Ma, F., & Cheng, L. (2013). Phenylpropanoid metabolites and expression of key genes involved in anthocyanin biosynthesis in the shaded peel of apple fruit in response to sun exposure. *Plant Physiology and Biochemistry*, 69, 54–61.
- Ferentinos, K. P., Albright, L. D., & Ramani, D. V. (2000). SE—Structures and Environment: Optimal Light Integral and Carbon Dioxide Concentration Combinations for Lettuce in Ventilated Greenhouses. *Journal of Agricultural Engineering Research*, 77(3), 309–315.
- Ferriol, L., Torres, J. F., Solís, G., San Bautista, A., Pascual, B., Alagarda, J., Maroto, J. V. (2009). Mini-lettuces: influence of different cultivation techniques (amounts of irrigation and different nutrient solutions) on the incidence of “tipburn”, going to seed and the accumulation of nitrates in various cultivars and four different growth cycles. *Agricola Vergel: Fruticultura, Horticultura, Floricultura, Citricultura, Vid, Arroz*, 28(330), 305...315.
- Foley, J. A., Ramankutty, N., Brauman, K. A., Cassidy, E. S., Gerber, J. S., Johnston, M., Zaks, D. P. M. (2011). Solutions for a cultivated planet. *Nature*, 478(7369), 337–342. <https://doi.org/10.1038/nature10452>
- Foyer, C. H., & Shigeoka, S. (2011). Understanding Oxidative Stress and Antioxidant Functions to Enhance Photosynthesis. *Plant Physiology*, 155(1), 93–100.
<https://doi.org/10.1104/pp.110.166181>
- Frantz, J. M., & Bugbee, B. (2005). Acclimation of plant populations to shade: photosynthesis, respiration, and carbon use efficiency. *Journal of the American Society for Horticultural Science*, 130(6), 918–927.
- Frantz, J. M., Ritchie, G., Cometti, N. N., Robinson, J., & Bugbee, B. (2004). Exploring the limits of crop productivity: beyond the limits of tipburn in lettuce. *Journal of the American Society for Horticultural Science*, 129(3), 331–338.

- Fu, W., Li, P., & Wu, Y. (2012). Effects of different light intensities on chlorophyll fluorescence characteristics and yield in lettuce. *Scientia Horticulturae*, *135*, 45–51.
- Fu, W., Li, P., Wu, Y., Tang, J., & others. (2012). Effects of different light intensities on anti-oxidative enzyme activity, quality and biomass in lettuce. *Hort. Sci*, *39*, 129–134.
- Fujita, A., Nami, G.-Y., Aramaki, I., & Hashizume, K. (2006). Organ-specific transcription of putative flavonol synthase genes of grapevine and effects of plant hormones and shading on flavonol biosynthesis in grape berry skins. *Bioscience, Biotechnology, and Biochemistry*, *70*(3), 632–638.
- Gaudet, P., & Dessimoz, C. (2017). Gene ontology: pitfalls, biases, and remedies. *The Gene Ontology Handbook*, 189–205.
- Gaudreau, L., Charbonneau, J., Vézina, L.-P., & Gosselin, A. (1994). Photoperiod and photosynthetic photon flux influence growth and quality of greenhouse-grown lettuce. *HortScience*, *29*(11), 1285–1289.
- Gaur, R. K., & Sharma, P. (2013). *Approaches to Plant Stress and their Management*. Springer Science & Business Media.
- Geisler-Lee, J., Caldwell, C., & Gallie, D. R. (2010). Expression of the ethylene biosynthetic machinery in maize roots is regulated in response to hypoxia. *Journal of Experimental Botany*, *61*(3), 857–871. <https://doi.org/10.1093/jxb/erp362>
- Gestelen, P. V., Asard, H., & Caubergs, R. J. (1997). Solubilization and Separation of a Plant Plasma Membrane NADPH-O₂- Synthase from Other NAD(P)H Oxidoreductases. *Plant Physiology*, *115*(2), 543–550. <https://doi.org/10.1104/pp.115.2.543>
- Giannopolitis, C. N., & Ries, S. K. (1977). Superoxide dismutases: I. Occurrence in higher plants. *Plant Physiology*, *59*(2), 309–314.
- Gibeaut, D. M., Hulett, J., Cramer, G. R., & Seemann, J. R. (1997). Maximal biomass of *Arabidopsis thaliana* using a simple, low-maintenance hydroponic method and favorable environmental conditions. *Plant Physiology*, *115*(2), 317.
- Gill, S. S., & Tuteja, N. (2010). Reactive oxygen species and antioxidant machinery in abiotic stress tolerance in crop plants. *Plant Physiology and Biochemistry*, *48*(12), 909–930.
- Gilliam, M., Athman, A., Tyerman, S. D., & Conn, S. J. (2011). Cell-specific compartmentation of mineral nutrients is an essential mechanism for optimal plant productivity-- another role for TPC1? *Plant Signaling & Behavior*, *6*(11), 1656–1661. <https://doi.org/10.4161/psb.6.11.17797>
- Gilliam, M., Dayod, M., Hocking, B. J., Xu, B., Conn, S. J., Kaiser, B. N., Tyerman, S. D. (2011). Calcium delivery and storage in plant leaves: exploring the link with water flow. *Journal of Experimental Botany*, *62*(7), 2233–2250. <https://doi.org/10.1093/jxb/err111>
- Goddard, M. A., Dougill, A. J., & Benton, T. G. (2010). Scaling up from gardens: biodiversity conservation in urban environments. *Trends in Ecology & Evolution*, *25*(2), 90–98. <https://doi.org/10.1016/j.tree.2009.07.016>

- Godfray, H. C. J., Beddington, J. R., Crute, I. R., Haddad, L., Lawrence, D., Muir, J. F., Toulmin, C. (2010). Food Security: The Challenge of Feeding 9 Billion People. *Science*, 327(5967), 812–818. <https://doi.org/10.1126/science.1185383>
- Gómez, C., Morrow, R. C., Bourget, C. M., Massa, G. D., & Mitchell, C. A. (2013). Comparison of intracanopy light-emitting diode towers and overhead high-pressure sodium lamps for supplemental lighting of greenhouse-grown tomatoes. *HortTechnology*, 23(1), 93–98.
- Gómez-Baggethun, E., & Barton, D. N. (2013). Classifying and valuing ecosystem services for urban planning. *Ecological Economics*, 86, 235–245. <https://doi.org/10.1016/j.ecolecon.2012.08.019>
- Goto, E., Both, A. J., Albright, L. D., Langhans, R. W., & Leed, A. R. (1996). Effect of dissolved oxygen concentration on lettuce growth in floating hydroponics. In *International Symposium on Plant Production in Closed Ecosystems 440* (pp. 205–210).
- Goto, E., & Takakura, T. (1992). Prevention of Lettuce Tipburn by Supplying Air to Inner Leaves. *Transactions of the ASAE*, 35(2), 641–645. <https://doi.org/10.13031/2013.28644>
- Grewal, S. S., & Grewal, P. S. (2012). Can cities become self-reliant in food? *Cities*, 29(1), 1–11. <https://doi.org/10.1016/j.cities.2011.06.003>
- Grimm, N. B., Faeth, S. H., Golubiewski, N. E., Redman, C. L., Wu, J., Bai, X., & Briggs, J. M. (2008). Global Change and the Ecology of Cities. *Science*, 319(5864), 756–760. <https://doi.org/10.1126/science.1150195>
- Gruda, N. (2005). Impact of environmental factors on product quality of greenhouse vegetables for fresh consumption. *Critical Reviews in Plant Sciences*, 24(3), 227–247.
- Guidi, L., Loreface, G., Pardossi, A., Malorgio, F., Tognoni, F., & Soldatini, G. F. (1997). Growth and photosynthesis of *Lycopersicon esculentum* (L.) plants as affected by nitrogen deficiency. *Biologia Plantarum*, 40(2), 235–244. <https://doi.org/10.1023/A:1001068603778>
- Gupta, S. D., & Jatothu, B. (2013). Fundamentals and applications of light-emitting diodes (LEDs) in in vitro plant growth and morphogenesis. *Plant Biotechnology Reports*, 7(3), 211–220. <https://doi.org/10.1007/s11816-013-0277-0>
- Gusman, G. S., Oliveira, J. A., Farnese, F. S., & Cambraia, J. (2013). Mineral nutrition and enzymatic adaptation induced by arsenate and arsenite exposure in lettuce plants. *Plant Physiology and Biochemistry*, 71, 307–314.
- Gutierrez, J., Bourke, P., Lonchamp, J., & Barry-Ryan, C. (2009). Impact of plant essential oils on microbiological, organoleptic and quality markers of minimally processed vegetables. *Innovative Food Science & Emerging Technologies*, 10(2), 195–202. <https://doi.org/10.1016/j.ifset.2008.10.005>
- Guttridge, C. G., Bradfield, E. G., & Holder, R. (1981). Dependence of Calcium Transport into Strawberry Leaves on Positive Pressure in the Xylem. *Annals of Botany*, 48(4), 473–480.

- Hahn, E. J., Lee, Y. B., & Ahn, C. H. (1996). A new method on mass-production of micropropagated chrysanthemum plants using microponic system in plant factory. In *International Symposium on Plant Production in Closed Ecosystems* 440 (pp. 527–532). Retrieved from http://www.actahort.org/books/440/440_92.htm
- Han, Y., Chen, Z., Lv, S., Ning, K., Ji, X., Liu, X., Zhang, X. (2016). MADS-Box Genes and Gibberellins Regulate Bolting in Lettuce (*Lactuca sativa* L.). *Frontiers in Plant Science*, 7. <https://doi.org/10.3389/fpls.2016.01889>
- Hancock, R. D., & Viola, R. (2005). Biosynthesis and catabolism of L-ascorbic acid in plants. *Critical Reviews in Plant Sciences*, 24(3), 167–188.
- Hartz, T. K., Johnstone, P. R., Smith, R. F., & Cahn, M. D. (2007). Soil Calcium Status Unrelated to Tipburn of Romaine Lettuce. *HortScience*, 42(7), 1681–1684.
- Hasanuzzaman, M., Gill, S. S., & Fujita, M. (2013). Physiological role of nitric oxide in plants grown under adverse environmental conditions. In *Plant acclimation to environmental stress* (pp. 269–322). Springer. Retrieved from http://link.springer.com/chapter/10.1007/978-1-4614-5001-6_11
- Hasanuzzaman, M., Nahar, K., Alam, M. M., Roychowdhury, R., & Fujita, M. (2013). Physiological, Biochemical, and Molecular Mechanisms of Heat Stress Tolerance in Plants. *International Journal of Molecular Sciences*, 14(5), 9643–9684.
- Havaux, M., Eymery, F., Porfirova, S., Rey, P., & Dörmann, P. (2005). Vitamin E Protects against Photoinhibition and Photooxidative Stress in *Arabidopsis thaliana*. *The Plant Cell*, 17(12), 3451–3469. <https://doi.org/10.1105/tpc.105.037036>
- Hayat, S., Ali, B., Aiman Hasan, S., & Ahmad, A. (2007). Brassinosteroid enhanced the level of antioxidants under cadmium stress in *Brassica juncea*. *Environmental and Experimental Botany*, 60(1), 33–41. <https://doi.org/10.1016/j.envexpbot.2006.06.002>
- Hayden, A. L. (2006). Aeroponic and Hydroponic Systems for Medicinal Herb, Rhizome, and Root Crops. *HortScience*, 41(3), 536–538.
- He, J., Qin, L., Liu, Y., Choong, T. W., & others. (2015). Photosynthetic Capacities and Productivity of Indoor Hydroponically Grown *Brassica alboglabra* Bailey under Different Light Sources. *American Journal of Plant Sciences*, 6(04), 554.
- He, J., Austin, P. T., & Lee, S. K. (2010). Effects of elevated root zone CO₂ and air temperature on photosynthetic gas exchange, nitrate uptake, and total reduced nitrogen content in aeroponically grown lettuce plants. *Journal of Experimental Botany*, 61(14), 3959–3969. <https://doi.org/10.1093/jxb/erq207>
- He, J., & Lee, S. K. (2004). Photosynthetic Utilization of Radiant Energy by Temperate Lettuce Grown Under Natural Tropical Condition with Manipulation of Root-Zone Temperature. *Photosynthetica*, 42(3), 457–463. <https://doi.org/10.1023/B:PHOT.0000046166.29815.94>

- He, J., Lee, S. K., & Dodd, I. C. (2001). Limitations to photosynthesis of lettuce grown under tropical conditions: alleviation by root-zone cooling. *Journal of Experimental Botany*, 52(359), 1323–1330.
- He, J., & Lee, S. K. (2001). Relationship among photosynthesis, ribulose-1, 5-bisphosphate carboxylase (Rubisco) and water relations of the subtropical vegetable Chinese broccoli grown in the tropics by manipulation of root-zone temperature. *Environmental and Experimental Botany*, 46(2), 119–128.
- Healy, R. G., & Rosenberg, J. S. (2013). *Land use and the states* (Vol. 3). Routledge.
- Heath, R. L., & Packer, L. (1968). Photoperoxidation in isolated chloroplasts: I. Kinetics and stoichiometry of fatty acid peroxidation. *Archives of Biochemistry and Biophysics*, 125(1), 189–198.
- Heller, H., Bar-Tal, A., Assouline, S., Narkis, K., Suryano, S., Forge, A. de la, ... Tsohar, D. (2014). The effects of container geometry on water and heat regimes in soilless culture: lettuce as a case study. *Irrigation Science*, 33(1), 53–65. <https://doi.org/10.1007/s00271-014-0448-y>
- Henriques, A. R. D. P., & Marcelis, L. F. M. (2000). Regulation of Growth at Steady-state Nitrogen Nutrition in Lettuce (*Lactuca sativa* L.): Interactive Effects of Nitrogen and Irradiance. *Annals of Botany*, 86(6), 1073–1080. <https://doi.org/10.1006/anbo.2000.1268>
- Heschel, M. S., Stinchcombe, J. R., Holsinger, K. E., & Schmitt, J. (2004). Natural selection on light response curve parameters in the herbaceous annual, *Impatiens capensis*. *Oecologia*, 139(4), 487–494. <https://doi.org/10.1007/s00442-004-1553-z>
- Heuvelink, E., Bakker, M. J., Hogendonk, L., Janse, J., Kaarsemaker, R., & Maaswinkel, R. (2006). Horticultural lighting in the Netherlands: new developments. *Acta Horticulturae*, (711), 25–34.
- Higashi, T., Aoki, K., Nagano, A. J., Honjo, M. N., & Fukuda, H. (2016). Circadian Oscillation of the Lettuce Transcriptome under Constant Light and Light–Dark Conditions. *Frontiers in Plant Science*, 7. <https://doi.org/10.3389/fpls.2016.01114>
- Ho, L. C., & White, P. J. (2005). A cellular hypothesis for the induction of blossom-end rot in tomato fruit. *Annals of Botany*, 95(4), 571–581.
- Hoagland, D. R., & Arnon, D. I. (1950). The water-culture method for growing plants without soil. *Circular. California Agricultural Experiment Station*, 347(2nd edit). Retrieved from <http://www.cabdirect.org/abstracts/19500302257.html>
- Hochmuth, R., & Hochmuth, G. J. (2001). A decade of change in Florida's greenhouse vegetable industry: 1991–2001. In *Proc. Fla. State Hort. Soc* (Vol. 114, pp. 280–283). Retrieved from [http://fshs.org/proceedings-o/2001-vol-114/280-283%20\(TYSON\).pdf](http://fshs.org/proceedings-o/2001-vol-114/280-283%20(TYSON).pdf)
- Hodges, D. M., DeLong, J. M., Forney, C. F., & Prange, R. K. (1999). Improving the thiobarbituric acid-reactive-substances assay for estimating lipid peroxidation in plant tissues containing anthocyanin and other interfering compounds. *Planta*, 207(4), 604–611. <https://doi.org/10.1007/s004250050524>

- Hovi, T., Näkkilä, J., & Tahvonen, R. (2004). Interlighting improves production of year-round cucumber. *Scientia Horticulturae*, *102*(3), 283–294. <https://doi.org/10.1016/j.scienta.2004.04.003>
- Huang, D., & Drescher, M. (2015). Urban crops and livestock: The experiences, challenges, and opportunities of planning for urban agriculture in two Canadian provinces. *Land Use Policy*, *43*, 1–14. <https://doi.org/10.1016/j.landusepol.2014.10.011>
- Huett, D. (1994). Growth, nutrient uptake and tipburn severity of hydroponic lettuce in response to electrical conductivity and K:Ca ratio in solution. *Australian Journal of Agricultural Research*, *45*(1), 251–267.
- Hughes, N. M., Neufeld, H. S., & Burkey, K. O. (2005). Functional role of anthocyanins in high-light winter leaves of the evergreen herb *Galax urceolata*. *New Phytologist*, *168*(3), 575–587. <https://doi.org/10.1111/j.1469-8137.2005.01546.x>
- Huntley, R. P., Sawford, T., Martin, M. J., & O'Donovan, C. (2014). Understanding how and why the Gene Ontology and its annotations evolve: the GO within UniProt. *GigaScience*, *3*, 4. <https://doi.org/10.1186/2047-217X-3-4>
- Imai, H. (1990). Alleviation of occurrence of tipburn and internal rot in tropical Chinese cabbage. *Tropical Agriculture Research Series*, (23), 203–217.
- Inthichack, P., Nishimura, Y., & Fukumoto, Y. (2012). Effect of potassium sources and rates on plant growth, mineral absorption, and the incidence of tip burn in cabbage, celery, and lettuce. *Horticulture Environment and Biotechnology*, *53*(2), 135–142. <https://doi.org/10.1007/s13580-012-0126-z>
- Inze, D., & Montagu, M. V. (2003). *Oxidative Stress in Plants*. CRC Press.
- Jaakola, L., & Hohtola, A. (2010). Effect of latitude on flavonoid biosynthesis in plants. *Plant, Cell & Environment*, *33*(8), 1239–1247.
- Jacquot, J.-P. (2009). *Oxidative stress and redox regulation in plants* (Vol. 52). Academic Press.
- Jbir-Koubaa, R., Charfeddine, S., Ellouz, W., Saidi, M. N., Drira, N., Gargouri-Bouzid, R., & Nouri-Ellouz, O. (2015). Investigation of the response to salinity and to oxidative stress of interspecific potato somatic hybrids grown in a greenhouse. *Plant Cell, Tissue and Organ Culture (PCTOC)*, *120*(3), 933–947. <https://doi.org/10.1007/s11240-014-0648-4>
- Jenni, S. (2005). Rib Discoloration: A Physiological Disorder Induced by Heat Stress in Crisphead Lettuce. *HortScience*, *40*(7), 2031–2035.
- Jenni, S., & Hayes, R. J. (2010). Genetic variation, genotype × environment interaction, and selection for tipburn resistance in lettuce in multi-environments. *Euphytica*, *171*(3), 427–439. <https://doi.org/10.1007/s10681-009-0075-5>
- Jenni, S., Truco, M. J., & Michelmore, R. W. (2013). Quantitative trait loci associated with tipburn, heat stress-induced physiological disorders, and maturity traits in crisphead lettuce. *Theoretical and Applied Genetics*, *126*(12), 3065–3079. <https://doi.org/10.1007/s00122-013-2193-7>

- Jenni, S., & Yan, W. (2009). Genotype by environment interactions of heat stress disorder resistance in crisphead lettuce. *Plant Breeding*, 128(4), 374–380. <https://doi.org/10.1111/j.1439-0523.2009.01657.x>
- Jensen, M. H. (1997). Hydroponics worldwide. In *International Symposium on Growing Media and Hydroponics 481* (pp. 719–730). Retrieved from http://www.actahort.org/books/481/481_87.htm
- Jensen, M. H. (2002). Deep flow hydroponics—Past, present and future. In *Proc. Nat. Agr. Plastics Congress* (Vol. 30, pp. 40–46).
- Jiang, L., Deng, X., & Seto, K. C. (2013). The impact of urban expansion on agricultural land use intensity in China. *Land Use Policy*, 35, 33–39.
- Jiang, P., Zhang, X., Zhu, Y., Zhu, W., Xie, H., & Wang, X. (2007). Metabolism of reactive oxygen species in cotton cytoplasmic male sterility and its restoration. *Plant Cell Reports*, 26(9), 1627–1634. <https://doi.org/10.1007/s00299-007-0351-6>
- Jim, C. Y. (2012). Sustainable urban greening strategies for compact cities in developing and developed economies. *Urban Ecosystems*, 16(4), 741–761. <https://doi.org/10.1007/s11252-012-0268-x>
- Johkan, M., Shoji, K., Goto, F., Hahida, S., & Yoshihara, T. (2012). Effect of green light wavelength and intensity on photomorphogenesis and photosynthesis in *Lactuca sativa*. *Environmental and Experimental Botany*, 75, 128–133. <https://doi.org/10.1016/j.envexpbot.2011.08.010>
- Jokinen, K., Särkkä, L. E., & Näkkilä, J. (2012). Improving sweet pepper productivity by LED interlighting. *Acta Horticulturae*, (956), 59–66. <https://doi.org/10.17660/ActaHortic.2012.956.4>
- Jones. (2014). *Complete Guide for Growing Plants Hydroponically*. CRC Press.
- Jones, J. B. (1982). Hydroponics: Its history and use in plant nutrition studies. *Journal of Plant Nutrition*, 5(8), 1003–1030. <https://doi.org/10.1080/01904168209363035>
- Jones, J. J. (2004). *Hydroponics: A Practical Guide for the Soilless Grower*. CRC Press.
- Kamal-Eldin, A., & Appelqvist, L.-Å. (1996). The chemistry and antioxidant properties of tocopherols and tocotrienols. *Lipids*, 31(7), 671–701.
- Kang, J. H., KrishnaKumar, S., Atulba, S. L. S., Jeong, B. R., & Hwang, S. J. (2014). Light intensity and photoperiod influence the growth and development of hydroponically grown leaf lettuce in a closed-type plant factory system. *Horticulture, Environment, and Biotechnology*, 54(6), 501–509. <https://doi.org/10.1007/s13580-013-0109-8>
- Karuppanapandian, T., Moon, J.-C., Kim, C., Manoharan, K., & Kim, W. (2011). Reactive oxygen species in plants: their generation, signal transduction, and scavenging mechanisms. *Australian Journal of Crop Science*, 5(6), 709.
- Kato, K., Yoshida, R., Kikuzaki, A., Hirai, T., Kuroda, H., Hiwasa-Tanase, K., ... Mizoguchi, T. (2010). Molecular breeding of tomato lines for mass production of miraculin in a plant factory. *Journal of Agricultural and Food Chemistry*, 58(17), 9505–9510.

- Kerton, M., Newbury, H. J., Hand, D., & Pritchard, J. (2009). Accumulation of calcium in the centre of leaves of coriander (*Coriandrum sativum* L.) is due to an uncoupling of water and ion transport. *Journal of Experimental Botany*, *60*(1), 227–235. <https://doi.org/10.1093/jxb/ern279>
- Kim, H.-H., Goins, G. D., Wheeler, R. M., & Sager, J. C. (2004). Stomatal Conductance of Lettuce Grown Under or Exposed to Different Light Qualities. *Annals of Botany*, *94*(5), 691–697. <https://doi.org/10.1093/aob/mch192>
- Kim, K., & Portis, A. R. (2004). Oxygen-dependent H₂O₂ production by Rubisco. *FEBS Letters*, *571*(1–3), 124–128. <https://doi.org/10.1016/j.febslet.2004.06.064>
- Kimura, M., & Rodriguez-Amaya, D. B. (2003). Carotenoid Composition of Hydroponic Leafy Vegetables. *Journal of Agricultural and Food Chemistry*, *51*(9), 2603–2607. <https://doi.org/10.1021/jf020539b>
- Kirkby, E. A. (1979). Maximizing calcium uptake by plants. *Communications in Soil Science and Plant Analysis*, *10*(1–2), 89–113. <https://doi.org/10.1080/00103627909366881>
- Kirkby, E. A., & Pilbeam, D. J. (1984). Calcium as a plant nutrient. *Plant, Cell & Environment*, *7*(6), 397–405. <https://doi.org/10.1111/j.1365-3040.1984.tb01429.x>
- Knight, S. L., & Mitchell, C. A. (1988). Effects of CO₂ and Photosynthetic Photon Flux on Yield, Gas Exchange and Growth Rate of *Lactuca Sativa* L. ‘Waldmann’s Green’. *Journal of Experimental Botany*, *39*(3), 317–328. <https://doi.org/10.1093/jxb/39.3.317>
- Kong, W., Liu, F., Zhang, C., Zhang, J., & Feng, H. (2016). Non-destructive determination of Malondialdehyde (MDA) distribution in oilseed rape leaves by laboratory scale NIR hyperspectral imaging. *Scientific Reports*, *6*. <https://doi.org/10.1038/srep35393>
- Kossowski, J. M., Wilcox, D. A., & Langhans, R. (1994). 544 Pp 084 Air Supply for Lettuce Tipburn Prevention and Its Effects on Transpiration and Photosynthesis. *HortScience*, *29*(5), 509–509.
- Koyama, R., Itoh, H., Kimura, S., Morioka, A., & Uno, Y. (2012). Augmentation of Antioxidant Constituents by Drought Stress to Roots in Leafy Vegetables. *HortTechnology*, *22*(1), 121–125.
- Koyama, R., Sanada, M., Itoh, H., Kanechi, M., Inagaki, N., & Uno, Y. (2012). In vitro evaluation of tipburn resistance in lettuce (*Lactuca sativa* L.). *Plant Cell, Tissue and Organ Culture (PCTOC)*, *108*(2), 221–227. <https://doi.org/10.1007/s11240-011-0033-5>
- Kozai, T., Niu, G., & Takagaki, M. (2015a). *Plant Factory: An Indoor Vertical Farming System for Efficient Quality Food Production*. Academic Press.
- Kozai, T., Niu, G., & Takagaki, M. (2015b). *Plant Factory: An Indoor Vertical Farming System for Efficient Quality Food Production*. Academic Press.
- Kratky, B. A. (2005). Growing Lettuce in Non-Aerated, Non-Circulated Hydroponic Systems. *Journal of Vegetable Science*, *11*(2), 35–42. https://doi.org/10.1300/J484v11n02_04

- Krieger-Liszkay, A. (2005). Singlet oxygen production in photosynthesis. *Journal of Experimental Botany*, 56(411), 337–346. <https://doi.org/10.1093/jxb/erh237>
- Krieger-Liszkay, A., Fufezan, C., & Trebst, A. (2008). Singlet oxygen production in photosystem II and related protection mechanism. *Photosynthesis Research*, 98(1–3), 551–564.
- Kruger, N. J. (1994). The Bradford method for protein quantitation. *Basic Protein and Peptide Protocols*, 9–15.
- Kruger, N. S. (1966). Tipburn of lettuce in relation to calcium nutrition. *Queensland J. Agric. Sci*, 23, 379–385.
- Ksas, B., Becuwe, N., Chevalier, A., & Havaux, M. (2015). Plant tolerance to excess light energy and photooxidative damage relies on plastoquinone biosynthesis. *Scientific Reports*, 5, 10919. <https://doi.org/10.1038/srep10919>
- Kubatsch, A., Grüneberg, H., & Ulrichs, C. (2007). The Effect of Low Light Intensity and Temperature on Growth of Schefflera arboricola in Interior Landscapes. *HortScience*, 42(1), 65–67.
- Kudoh, H., & Sonoike, K. (2002). Irreversible damage to photosystem I by chilling in the light: cause of the degradation of chlorophyll after returning to normal growth temperature. *Planta*, 215(4), 541–548.
- Kumar, S., Kaur, R., Kaur, N., Bhandhari, K., Kaushal, N., Gupta, K., Nayyar, H. (2011). Heat-stress induced inhibition in growth and chlorosis in mungbean (*Phaseolus aureus* Roxb.) is partly mitigated by ascorbic acid application and is related to reduction in oxidative stress. *Acta Physiologiae Plantarum*, 33(6), 2091. <https://doi.org/10.1007/s11738-011-0748-2>
- Kumar, S., & Pandey, A. K. (2013). Chemistry and Biological Activities of Flavonoids: An Overview. *The Scientific World Journal*, 2013, e162750. <https://doi.org/10.1155/2013/162750>
- La Rosa, D., Barbarossa, L., Privitera, R., & Martinico, F. (2014). Agriculture and the city: A method for sustainable planning of new forms of agriculture in urban contexts. *Land Use Policy*, 41, 290–303. <https://doi.org/10.1016/j.landusepol.2014.06.014>
- Lachapelle, P.-P., & Shipley, B. (2012). Interspecific prediction of photosynthetic light response curves using specific leaf mass and leaf nitrogen content: effects of differences in soil fertility and growth irradiance. *Annals of Botany*, mcs032. <https://doi.org/10.1093/aob/mcs032>
- Lages Barbosa, G., Almeida Gadelha, F. D., Kublik, N., Proctor, A., Reichelm, L., Weissinger, E., Halden, R. U. (2015). Comparison of Land, Water, and Energy Requirements of Lettuce Grown Using Hydroponic vs. Conventional Agricultural Methods. *International Journal of Environmental Research and Public Health*, 12(6), 6879–6891. <https://doi.org/10.3390/ijerph120606879>
- Lambers, H., III, F. S. C., & Pons, T. L. (2013). *Plant Physiological Ecology*. Springer Science & Business Media.
- Lambin, E. F., Gibbs, H. K., Ferreira, L., Grau, R., Mayaux, P., Meyfroidt, P., Munger, J. (2013). Estimating the world's potentially available cropland using

- a bottom-up approach. *Global Environmental Change*, 23(5), 892–901. <https://doi.org/10.1016/j.gloenvcha.2013.05.005>
- Lambin, E. F., & Meyfroidt, P. (2011). Global land use change, economic globalization, and the looming land scarcity. *Proceedings of the National Academy of Sciences*, 108(9), 3465–3472. <https://doi.org/10.1073/pnas.1100480108>
- Lanauskas, J., & Kvikliene, N. (2006). Effect of calcium foliar application on some fruit quality characteristics of ‘Sinap Orlovskij’ apple. *Agronomy Research*, 4(1), 31–36.
- Larcher, W. (2003). *Physiological Plant Ecology: Ecophysiology and Stress Physiology of Functional Groups*. Springer Science & Business Media.
- Larkindale, J., & Huang, B. (2004). Thermotolerance and antioxidant systems in *Agrostis stolonifera*: involvement of salicylic acid, abscisic acid, calcium, hydrogen peroxide, and ethylene. *Journal of Plant Physiology*, 161(4), 405–413.
- Larkindale, J., & Knight, M. R. (2002). Protection against Heat Stress-Induced Oxidative Damage in *Arabidopsis* Involves Calcium, Abscisic Acid, Ethylene, and Salicylic Acid. *Plant Physiology*, 128(2), 682–695. <https://doi.org/10.1104/pp.010320>
- Leclerc, J., Miller, M., Joliet, E., Thicoipe, J., & Despujols, J. (1992). Necrosis Prevention and Mineral and Vitamin Contents of Webb Lettuce. *Agrochimica*, 36(1–2), 108–115.
- Lee, J. G., Choi, C. S., Jang, Y. A., Jang, S. W., Lee, S. G., & Um, Y. C. (2013). Effects of air temperature and air flow rate control on the tipburn occurrence of leaf lettuce in a closed-type plant factory system. *Horticulture, Environment, and Biotechnology*, 54(4), 303–310.
- Lee, J. G., Lee, B. Y., & Lee, H. J. (2006). Accumulation of phytotoxic organic acids in reused nutrient solution during hydroponic cultivation of lettuce (*Lactuca sativa* L.). *Scientia Horticulturae*, 110(2), 119–128. <https://doi.org/10.1016/j.scienta.2006.06.013>
- Lee, J., Kim, J., Choi, J.-P., Lee, M., Kim, M. K., Lee, Y. H., Kim, H. (2016). Intracellular Ca²⁺ and K⁺ concentration in *Brassica oleracea* leaf induces differential expression of transporter and stress-related genes. *BMC Genomics*, 17, 211. <https://doi.org/10.1186/s12864-016-2512-x>
- Lee, J., Park, I., Lee, Z.-W., Kim, S. W., Baek, N., Park, H.-S., Kim, H. (2013). Regulation of the major vacuolar Ca²⁺ transporter genes, by intercellular Ca²⁺ concentration and abiotic stresses, in tip-burn resistant *Brassica oleracea*. *Molecular Biology Reports*, 40(1), 177–188. <https://doi.org/10.1007/s11033-012-2047-4>
- Lee, J. S., Lim, T. G., & Kim, Y. H. (2014). Growth and Phytochemicals in Lettuce as Affected by Different Ratios of Blue to Red LED Radiation. *Acta Hort*, 1037, 843–848.
- Lee, S., Ge, C., Bohrerova, Z., Grewal, P. S., & Lee, J. (2015a). Enhancing plant productivity while suppressing biofilm growth in a windowfarm system using

- beneficial bacteria and ultraviolet irradiation. *Canadian Journal of Microbiology*, *61*(7), 457–466. <https://doi.org/10.1139/cjm-2015-0024>
- Lee, S., Ge, C., Bohrerova, Z., Grewal, P. S., & Lee, J. (2015b). Enhancing plant productivity while suppressing biofilm growth in a windowfarm system using beneficial bacteria and ultraviolet irradiation. *Canadian Journal of Microbiology*, *61*(7), 457–466. <https://doi.org/10.1139/cjm-2015-0024>
- Léran, S., Edel, K. H., Pervent, M., Hashimoto, K., Corratgé-Faillie, C., Offenborn, J. N., Lacombe, B. (2015). Nitrate sensing and uptake in *Arabidopsis* are enhanced by ABI2, a phosphatase inactivated by the stress hormone abscisic acid. *Science Signaling*, *8*(375), ra43-ra43. <https://doi.org/10.1126/scisignal.aaa4829>
- Leverenz, J. W., Falk, S., Pilström, C.-M., & Samuelsson, G. (1990). The effects of photoinhibition on the photosynthetic light-response curve of green plant cells (*Chlamydomonas reinhardtii*). *Planta*, *182*(2), 161–168.
- Li, C., Nong, Q., Solanki, M. K., Liang, Q., Xie, J., Liu, X., Li, Y. (2016). Differential expression profiles and pathways of genes in sugarcane leaf at elongation stage in response to drought stress. *Scientific Reports*, *6*. Retrieved from <https://www.ncbi.nlm.nih.gov.ezproxy.lanacs.ac.uk/pmc/articles/PMC4864372/>
- Li, H., Chen, X.-P., Zhu, F., Liu, H.-Y., Hong, Y.-B., & Liang, X.-Q. (2013). Transcriptome profiling of peanut (*Arachis hypogaea*) gynophores in gravitropic response. *Functional Plant Biology*, *40*(12), 1249–1260.
- Lieten, P. (2004). *Effect of K:Ca:Mg ratio on performance of 'Elsanta' strawberries grown on peat*. In *V International Strawberry Symposium 708* (pp. 397–400). Retrieved from http://www.actahort.org/books/708/708_69.htm
- Lin, B. B., Philpott, S. M., & Jha, S. (2015). The future of urban agriculture and biodiversity-ecosystem services: Challenges and next steps. *Basic and Applied Ecology*, *16*(3), 189–201.
- Lin, K.-H., Huang, M.-Y., Huang, W.-D., Hsu, M.-H., Yang, Z.-W., & Yang, C.-M. (2013). The effects of red, blue, and white light-emitting diodes on the growth, development, and edible quality of hydroponically grown lettuce (*Lactuca sativa* L. var. capitata). *Scientia Horticulturae*, *150*, 86–91. <https://doi.org/10.1016/j.scienta.2012.10.002>
- Linsley-Noakes, G., Wilken, L., & de Villiers, S. (2006). High density, vertical hydroponics growing system for strawberries. *Acta Horticulturae*, *708*, 365.
- Lin-Wang, K., Micheletti, D., Palmer, J., Volz, R., Lozano, L., Espley, R., Allan, A. C. (2011). High temperature reduces apple fruit colour via modulation of the anthocyanin regulatory complex. *Plant, Cell & Environment*, *34*(7), 1176–1190. <https://doi.org/10.1111/j.1365-3040.2011.02316.x>
- Liu, W., Chen, D. K., & Liu, Z. X. (2004). High efficiency column culture system in China. *Acta Horticulturae*, *691*, 495–500.
- Llorach, R., Martínez-Sánchez, A., Tomás-Barberán, F. A., Gil, M. I., & Ferreres, F. (2008). Characterisation of polyphenols and antioxidant properties of five lettuce varieties and escarole. *Food Chemistry*, *108*(3), 1028–1038.

- Long, S. P., Humphries, S., & Falkowski, P. G. (1994). Photoinhibition of photosynthesis in nature. *Annual Review of Plant Biology*, *45*(1), 633–662.
- Lötze, E., Joubert, J., & Theron, K. I. (2008). Evaluating pre-harvest foliar calcium applications to increase fruit calcium and reduce bitter pit in ‘Golden Delicious’ apples. *Scientia Horticulturae*, *116*(3), 299–304.
- Lovell, S. T. (2010). Multifunctional Urban Agriculture for Sustainable Land Use Planning in the United States. *Sustainability*, *2*(8), 2499–2522. <https://doi.org/10.3390/su2082499>
- Mahdavi, S., Kafi, M., Naderi, R., & Sadat, T. (2012). Vertical mobile planting system consistent with the pattern of solar radiation and effects of system on light exposure and growth of Gerbera cut flowers (Gerbera jamesonii cv. Antibes), in greenhouse culture. *Journal of Agricultural Technology*, *8*(4), 1461–1468.
- Makino, A., Miyake, C., & Yokota, A. (2002). Physiological functions of the water–water cycle (Mehler reaction) and the cyclic electron flow around PSI in rice leaves. *Plant and Cell Physiology*, *43*(9), 1017–1026.
- Manzocco, L., Foschia, M., Tomasi, N., Maifreni, M., Dalla Costa, L., Marino, M., Cesco, S. (2011). Influence of hydroponic and soil cultivation on quality and shelf life of ready-to-eat lamb’s lettuce (Valerianella locusta L. Laterr). *Journal of the Science of Food and Agriculture*, *91*(8), 1373–1380. <https://doi.org/10.1002/jsfa.4313>
- Marino, G., Aqil, M., & Shipley, B. (2010). The leaf economics spectrum and the prediction of photosynthetic light–response curves. *Functional Ecology*, *24*(2), 263–272.
- Martin, J. A., Johnson, N. V., Gross, S. M., Schnable, J., Meng, X., Wang, M., ... Wang, Z. (2014). A near complete snapshot of the Zea mays seedling transcriptome revealed from ultra-deep sequencing. *Scientific Reports*, *4*, 4519. <https://doi.org/10.1038/srep04519>
- Martín-Diana, A. B., Rico, D., Barry-Ryan, C., Frías, J. M., Henehan, G. T. M., & Barat, J. M. (2007). Efficacy of steamer jet-injection as alternative to chlorine in fresh-cut lettuce. *Postharvest Biology and Technology*, *45*(1), 97–107. <https://doi.org/10.1016/j.postharvbio.2007.01.013>
- Masson, J., Tremblay, N., & Gosselin, A. (1991). Nitrogen Fertilization and HPS Supplementary Lighting Influence Vegetable Transplant Production. I. Transplant Growth. *Journal of the American Society for Horticultural Science*, *116*(4), 594–598.
- Massot, C., Bancel, D., Lauri, F. L., Truffault, V., Baldet, P., Stevens, R., & Gautier, H. (2013). High temperature inhibits ascorbate recycling and light stimulation of the ascorbate pool in tomato despite increased expression of biosynthesis genes. *PloS One*, *8*(12), e84474.
- Mateus-Rodriguez, J. R., Haan, S. de, Andrade-Piedra, J. L., Maldonado, L., Hareau, G., Barker, I., Benítez, J. (2013). Technical and Economic Analysis of Aeroponics and other Systems for Potato Mini-Tuber Production in Latin

- America. *American Journal of Potato Research*, 90(4), 357–368. <https://doi.org/10.1007/s12230-013-9312-5>
- Mavrogianopoulos, G., Aglogalos, P., & Lycoskoufis, I. (2011, June). A continuous recirculating drip growing system. In *International Symposium on Advanced Technologies and Management Towards Sustainable Greenhouse Ecosystems: Greensys2011* 952 (pp. 659-666).
- McDonald, M. S. (2003). *Photobiology of Higher Plants*. John Wiley & Sons.
- Meriño-Gergichevich, C., Alberdi, M., Ivanov, A. G., & Reyes-Díaz, M. (2010). Al³⁺-Ca²⁺ Interaction in plants growing in acid soils: al-phytotoxicity response to calcareous amendments. *Journal of Soil Science and Plant Nutrition*, 10(3), 217–243.
- Mestre, T. C., Garcia-Sanchez, F., Rubio, F., Martinez, V., & Rivero, R. M. (2012). Glutathione homeostasis as an important and novel factor controlling blossom-end rot development in calcium-deficient tomato fruits. *Journal of Plant Physiology*, 169(17), 1719–1727.
- Miller, G., Suzuki, N., Ciftci-Yilmaz, S., & Mittler, R. (2010). Reactive oxygen species homeostasis and signalling during drought and salinity stresses. *Plant, Cell & Environment*, 33(4), 453–467. <https://doi.org/10.1111/j.1365-3040.2009.02041.x>
- Misaghi, I. J., & Grogan, R. G. (1978). Physiological-basis for tipburn development in head lettuce. *Phytopathology*, 68(12), 1744–1753.
- Misaghi, I., Matyac, C., & Grogan, R. (1981). Soil and Foliar Applications of Calcium-Chloride and Calcium Nitrate to Control Tipburn of Head Lettuce. *Plant Disease*, 65(10), 821–822.
- Mittler, R. (2002). Oxidative stress, antioxidants and stress tolerance. *Trends in Plant Science*, 7(9), 405–410.
- Mittler, R., Vanderauwera, S., Gollery, M., & Van Breusegem, F. (2004). Reactive oxygen gene network of plants. *Trends in Plant Science*, 9(10), 490–498. <https://doi.org/10.1016/j.tplants.2004.08.009>
- Mogk, J. E., Wiatkowski, S., & Weindorf, M. J. (2010). Promoting urban agriculture as an alternative land use for vacant properties in the city of Detroit: Benefits, problems and proposals for a regulatory framework for successful land use integration. *Wayne L. Rev.*, 56, 1521.
- Møller, I. M., Jensen, P. E., & Hansson, A. (2007). Oxidative Modifications to Cellular Components in Plants. *Annual Review of Plant Biology*, 58(1), 459–481. <https://doi.org/10.1146/annurev.arplant.58.032806.103946>
- Mori, K., Goto-Yamamoto, N., Kitayama, M., & Hashizume, K. (2007). Loss of anthocyanins in red-wine grape under high temperature. *Journal of Experimental Botany*, 58(8), 1935–1945.
- Morimoto, T., Torii, T., & Hashimoto, Y. (1995). Optimal control of physiological processes of plants in a green plant factory. *Control Engineering Practice*, 3(4), 505–511.
- (Mubarakshina) Borisova, M. M., Kozuleva, M. A., Rudenko, N. N., Naydov, I. A., Klenina, I. B., & Ivanov, B. N. (2012). Photosynthetic electron flow to oxygen

- and diffusion of hydrogen peroxide through the chloroplast envelope via aquaporins. *Biochimica et Biophysica Acta (BBA) - Bioenergetics*, 1817(8), 1314–1321. <https://doi.org/10.1016/j.bbabi.2012.02.036>
- Mulabagal, V., Ngouajio, M., Nair, A., Zhang, Y., Gottumukkala, A. L., & Nair, M. G. (2010). In vitro evaluation of red and green lettuce (*Lactuca sativa*) for functional food properties. *Food Chemistry*, 118(2), 300–306. <https://doi.org/10.1016/j.foodchem.2009.04.119>
- Mullineaux, P. M., Karpinski, S., & Baker, N. R. (2006). Spatial dependence for hydrogen peroxide-directed signaling in light-stressed plants. *Plant Physiology*, 141(2), 346–350.
- Murata, N., Takahashi, S., Nishiyama, Y., & Allakhverdiev, S. I. (2007). Photoinhibition of photosystem II under environmental stress. *Biochimica et Biophysica Acta (BBA) - Bioenergetics*, 1767(6), 414–421. <https://doi.org/10.1016/j.bbabi.2006.11.019>
- Murchie, E. H., & Niyogi, K. K. (2011). Manipulation of photoprotection to improve plant photosynthesis. *Plant Physiology*, 155(1), 86–92.
- Nagata, R. T., & Stratton, M. L. (1994). Development of an objective test for tipburn evaluation. In *PROCEEDINGS-FLORIDA STATE HORTICULTURAL SOCIETY* (Vol. 107, pp. 99–99). Retrieved from [http://fshs8813.wpengine.com/proceedings-o/1994-vol-107/99-101%20\(NAGATA\).pdf](http://fshs8813.wpengine.com/proceedings-o/1994-vol-107/99-101%20(NAGATA).pdf)
- Napier, D. R., & Combrink, N. J. J. (2006). Aspects of calcium nutrition to limit plant physiological disorders. In P. H. Joubert (Ed.), *Proceedings of the Vth International Pineapple Symposium* (pp. 107–116). Leuven 1: International Society Horticultural Science.
- Neumann, P. M., Weissman, R., Stefano, G., & Mancuso, S. (2010). Accumulation of xylem transported protein at pit membranes and associated reductions in hydraulic conductance. *Journal of Experimental Botany*, 61(6), 1711–1717. <https://doi.org/10.1093/jxb/erq037>
- Nie, W., Wang, M., Xia, X., Zhou, Y.-H., Shi, K., Chen, Z., & Yu, J. Q. (2013). Silencing of tomato RBOH1 and MPK2 abolishes brassinosteroid-induced H₂O₂ generation and stress tolerance. *Plant, Cell & Environment*, 36(4), 789–803.
- Nishiyama, Y., Allakhverdiev, S. I., & Murata, N. (2006). A new paradigm for the action of reactive oxygen species in the photoinhibition of photosystem II. *Biochimica et Biophysica Acta (BBA) - Bioenergetics*, 1757(7), 742–749. <https://doi.org/10.1016/j.bbabi.2006.05.013>
- Noctor, G., & Foyer, C. H. (1998). Ascorbate and glutathione: keeping active oxygen under control. *Annual Review of Plant Biology*, 49(1), 249–279.
- Nooden, L. D. (2003). *Plant Cell Death Processes*. Academic Press.
- Nor'aini, M. F., Finch, R. P., & Burdon, R. H. (1997). Salinity, oxidative stress and antioxidant responses in shoot cultures of rice. *Journal of Experimental Botany*, 48(2), 325–331.

- Norén, H., Svensson, P., & Andersson, B. (2004). A convenient and versatile hydroponic cultivation system for *Arabidopsis thaliana*. *Physiologia Plantarum*, *121*(3), 343–348. <https://doi.org/10.1111/j.0031-9317.2004.00350.x>
- Ogweno, J. O., Song, X. S., Shi, K., Hu, W. H., Mao, W. H., Zhou, Y. H., Nogués, S. (2008). Brassinosteroids alleviate heat-induced inhibition of photosynthesis by increasing carboxylation efficiency and enhancing antioxidant systems in *Lycopersicon esculentum*. *Journal of Plant Growth Regulation*, *27*(1), 49–57.
- Oliveira, D. C. R. de, Leal, P. A. M., Honório, S. L., & Soares, E. K. B. (2013). Sensory quality attributes of lettuce obtained using different harvesting performance systems. *Food Science and Technology*, *33*(2), 239–244. <https://doi.org/10.1590/S0101-20612013005000031>
- Olle, M. (2012). Increase of leaf tipburn in chervil and lettuce by restricting volume of growing medium. *Acta Agriculturae Scandinavica, B*, *62*(2), 188–192. <https://doi.org/10.1080/09064710.2011.577444>
- Olle, M., & Bender, I. (2009). Causes and control of calcium deficiency disorders in vegetables: a review. *The Journal of Horticultural Science and Biotechnology*, *84*(6), 577–584. <https://doi.org/10.1080/14620316.2009.11512568>
- Olle, M., & Viršile, A. (2013). The effects of light-emitting diode lighting on greenhouse plant growth and quality. *Agricultural and Food Science*, *22*(2), 223–234.
- Orsini, F., Kahane, R., Nono-Womdim, R., & Gianquinto, G. (2013). Urban agriculture in the developing world: a review. *Agronomy for Sustainable Development*, *33*(4), 695–720.
- Ouzounis, T., Razi Parjikelaei, B., Fretté, X., Rosenqvist, E., & Ottosen, C.-O. (2015). Predawn and high intensity application of supplemental blue light decreases the quantum yield of PSII and enhances the amount of phenolic acids, flavonoids, and pigments in *Lactuca sativa*. *Frontiers in Plant Science*, *6*. <https://doi.org/10.3389/fpls.2015.00019>
- Pacione, M. (1999). *Applied Geography: Principles and Practice : an Introduction to Useful Research in Physical, Environmental and Human Geography*. Psychology Press.
- Palzkill, D. A., Tibbitts, T. W., & Williams, P. H. (1976). Enhancement of calcium transport to inner leaves of cabbage for prevention of tipburn. *J. Am. Soc. Hortic. Sci*, *101*, 645–648.
- Panda, S. K., & Khan, M. H. (2004). Changes in growth and superoxide dismutase activity in *Hydrilla verticillata* L. under abiotic stress. *Brazilian Journal of Plant Physiology*, *16*(2), 115–118.
- Pandey, B., & Seto, K. C. (2015). Urbanization and agricultural land loss in India: Comparing satellite estimates with census data. *Journal of Environmental Management*, *148*, 53–66. <https://doi.org/10.1016/j.jenvman.2014.05.014>
- Papa, R., Gargiulo, C., & Zucaro, F. (2016). Towards the Definition of the Urban Saving Energy Model (UrbanSEM). In R. Papa & R. Fistola (Eds.), *Smart*

- Energy in the Smart City* (pp. 151–175). Springer International Publishing.
https://doi.org/10.1007/978-3-319-31157-9_9
- Park, J.-S., & Kurata, K. (2009). Application of Microbubbles to Hydroponics Solution Promotes Lettuce Growth. *HortTechnology*, *19*(1), 212–215.
- Peek, M. S., Russek-Cohen, E., Wait, A. D., & Forseth, I. N. (2002). Physiological response curve analysis using nonlinear mixed models. *Oecologia*, *132*(2), 175–180.
- Périard, Y., Caron, J., Lafond, J. A., & Jutras, S. (2015). Root water uptake by Romaine lettuce in a muck soil: Linking tip burn to hydric deficit. *Vadose Zone Journal*, *14*(6). Retrieved from <https://dl.sciencesocieties.org/publications/vzj/abstracts/14/6/vzj2014.10.0139>
- Pettersen, R. I., Torre, S., & Gislerød, H. R. (2010). Effects of intracanopy lighting on photosynthetic characteristics in cucumber. *Scientia Horticulturae*, *125*(2), 77–81. <https://doi.org/10.1016/j.scienta.2010.02.006>
- Pickrell, J. K., Marioni, J. C., Pai, A. A., Degner, J. F., Engelhardt, B. E., Nkadori, E., Pritchard, J. K. (2010). Understanding mechanisms underlying human gene expression variation with RNA sequencing. *Nature*, *464*(7289), 768–772. <https://doi.org/10.1038/nature08872>
- Pieterse, C. M. J., Dicke, M., Wees, S. C. M. V., & Poelman, E. H. (2014). *Induced plant responses to microbes and insects*. Frontiers E-books.
- Pietta, P.-G. (2000). Flavonoids as antioxidants. *Journal of Natural Products*, *63*(7), 1035–1042.
- Poorter, H., Bühler, J., van Dusschoten, D., Climent, J., & Postma, J. A. (2012). Pot size matters: a meta-analysis of the effects of rooting volume on plant growth. *Functional Plant Biology*, *39*(11), 839–850.
- Poorter, H., Fiorani, F., Stitt, M., Schurr, U., Finck, A., Gibon, Y., ... others. (2012). The art of growing plants for experimental purposes: a practical guide for the plant biologist. *Functional Plant Biology*, *39*(11), 821–838.
- Potvin, C., Lechowicz, M. J., & Tardif, S. (1990). The Statistical Analysis of Ecophysiological Response Curves Obtained from Experiments Involving Repeated Measures. *Ecology*, *71*(4), 1389–1400. <https://doi.org/10.2307/1938276>
- Puerta, A. R., Sato, S., Shinohara, Y., & Maruo, T. (2007). A Modified Nutrient Film Technique System Offers a More Uniform Nutrient Supply to Plants. *HortTechnology*, *17*(2), 227–233.
- Qin, L., Guo, S., Ai, W., & Tang, Y. (2008). Selection of candidate salad vegetables for controlled ecological life support system. *Advances in Space Research*, *41*(5), 768–772. <https://doi.org/10.1016/j.asr.2007.09.037>
- Qin, L., Guo, S., Ai, W., Tang, Y., Cheng, Q., & Chen, G. (2013). Effect of salt stress on growth and physiology in amaranth and lettuce: Implications for bioregenerative life support system. *Advances in Space Research*, *51*(3), 476–482. <https://doi.org/10.1016/j.asr.2012.09.025>
- Ramakrishna, B., & Rao, S. S. R. (2014). Foliar application of brassinosteroids alleviates adverse effects of zinc toxicity in radish (*Raphanus sativus* L.)

- plants. *Protoplasma*, 252(2), 665–677. <https://doi.org/10.1007/s00709-014-0714-0>
- Ramel, F., Birtic, S., Ginies, C., Soubigou-Taconnat, L., Triantaphylidès, C., & Havaux, M. (2012). Carotenoid oxidation products are stress signals that mediate gene responses to singlet oxygen in plants. *Proceedings of the National Academy of Sciences*, 109(14), 5535–5540.
- Ramírez-Gómez, H., Sandoval-Villa, M., Carrillo-Salazar, A., & Muratalla-Lúa, A. (2012). Comparison of hydroponic systems in the strawberry production. *Acta Horticulturae*, 947, 165–172.
- Read, M., & Tibbits, T. W. (1970). Lettuce Growth and Tipburn Incidence as Influenced by Co/Sub 2/ Concentration and Light Intensity. *HortScience; (United States)*, 5:4. Retrieved from http://www.osti.gov/energycitations/product.biblio.jsp?osti_id=6438968
- Resh, H. M. (2012). *Hydroponic Food Production: A Definitive Guidebook for the Advanced Home Gardener and the Commercial Hydroponic Grower*. CRC Press.
- Reyes-Chin-Wo, S., Wang, Z., Yang, X., Kozik, A., Arikkit, S., Song, C., ... Micheltore, R. W. (2017). Genome assembly with in vitro proximity ligation data and whole-genome triplication in lettuce. *Nature Communications*, 8, 14953. <https://doi.org/10.1038/ncomms14953>
- Richards, J. T., Edney, S. L., Yorio, N. C., Stutte, G. W., Cranston, N., Wheeler, R. M., & Goins, G. D. (2004). *Effects of Lighting Intensity and Supplemental CO2 on Yield of Potential Salad Crops for ISS* (SAE Technical Paper No. 2004-01-2296). Warrendale, PA: SAE International. Retrieved from <http://papers.sae.org/2004-01-2296/>
- Richterich, P. (1998). Estimation of Errors in “Raw” DNA Sequences: A Validation Study. *Genome Research*, 8(3), 251–259. <https://doi.org/10.1101/gr.8.3.251>
- Risso, D., Schwartz, K., Sherlock, G., & Dudoit, S. (2011). GC-Content Normalization for RNA-Seq Data. *BMC Bioinformatics*, 12, 480. <https://doi.org/10.1186/1471-2105-12-480>
- Ritter, E., Angulo, B., Riga, P., Herrán, C., Relloso, J., & Jose, M. S. (2001). Comparison of hydroponic and aeroponic cultivation systems for the production of potato minitubers. *Potato Research*, 44(2), 127–135. <https://doi.org/10.1007/BF02410099>
- Rius-Ruiz, F. X., Andrade, F. J., Riu, J., & Rius, F. X. (2014). Computer-operated analytical platform for the determination of nutrients in hydroponic systems. *Food Chemistry*, 147, 92–97.
- Rotter, R. P., Carter, T. R., Olesen, J. E., & others. (2011). Crop–climate models need an overhaul. *Nature Climate Change*, 1, 175–177.
- Ryan, P. R., & Kochian, L. V. (1993). Interaction between aluminum toxicity and calcium uptake at the root apex in near-isogenic lines of wheat (*Triticum aestivum* L.) differing in aluminum tolerance. *Plant Physiology*, 102(3), 975–982.

- Ryder, E. J., & Waycott, W. (1998). Crisphead Lettuce Resistant to Tipburn: Cultivar Tiber and Eight Breeding Lines. *HortScience*, *33*(5), 903–904.
- Sago, Y. (2016). Effects of Light Intensity and Growth Rate on Tipburn Development and Leaf Calcium Concentration in Butterhead Lettuce. *HortScience*, *51*(9), 1087–1091.
- Sairam, R. K., Rao, K. V., & Srivastava, G. C. (2002). Differential response of wheat genotypes to long term salinity stress in relation to oxidative stress, antioxidant activity and osmolyte concentration. *Plant Science*, *163*(5), 1037–1046. [https://doi.org/10.1016/S0168-9452\(02\)00278-9](https://doi.org/10.1016/S0168-9452(02)00278-9)
- Sajid, Z. A., & Aftab, F. (2012). Foliar spray of ascorbic acid improves salinity tolerance in *Solanum tuberosum* L. *Acta Horticulturae*, (1145), 69–74. <https://doi.org/10.17660/ActaHortic.2012.1145.10>
- Sakihama, Y., Cohen, M. F., Grace, S. C., & Yamasaki, H. (2002). Plant phenolic antioxidant and prooxidant activities: phenolics-induced oxidative damage mediated by metals in plants. *Toxicology*, *177*(1), 67–80. [https://doi.org/10.1016/S0300-483X\(02\)00196-8](https://doi.org/10.1016/S0300-483X(02)00196-8)
- Saleh, S. A. (2009). Precision Stressing by Supplemental Ca and *Bacillus subtilis* FZB24 to Improve Quality of Lettuce under Protected Cultivation. In L. G. Albrigo & R. Ehsani (Eds.), *International Symposium on Application of Precision Agriculture for Fruits and Vegetables* (Vol. 824, pp. 297–302). Leuven 1: Int Soc Horticultural Science.
- Sanyé-Mengual, E., Orsini, F., Oliver-Solà, J., Rieradevall, J., Montero, J. I., & Gianquinto, G. (2015). Techniques and crops for efficient rooftop gardens in Bologna, Italy. *Agronomy for Sustainable Development*, *35*(4), 1477–1488. <https://doi.org/10.1007/s13593-015-0331-0>
- Saure, M. C. (1998). Causes of the tipburn disorder in leaves of vegetables. *Scientia Horticulturae*, *76*(3–4), 131–147. [https://doi.org/10.1016/S0304-4238\(98\)00153-8](https://doi.org/10.1016/S0304-4238(98)00153-8)
- Saure, M. C. (1998). Causes of the tipburn disorder in leaves of vegetables. *Scientia Horticulturae*, *76*(3), 131–147. [https://doi.org/10.1016/S0304-4238\(98\)00153-8](https://doi.org/10.1016/S0304-4238(98)00153-8)
- Saure, M. C. (2005). Calcium translocation to fleshy fruit: its mechanism and endogenous control. *Scientia Horticulturae*, *105*(1), 65–89.
- Saure, M. C. (2014). Why calcium deficiency is not the cause of blossom-end rot in tomato and pepper fruit – a reappraisal. *Scientia Horticulturae*, *174*, 151–154. <https://doi.org/10.1016/j.scienta.2014.05.020>
- Savvas, D. (2003). Hydroponics: A modern technology supporting the application of integrated crop management in greenhouse. *Journal of Food, Agriculture & Environment*, *1*, 80–86.
- Savvas, D., Stamati, E., Tsirogiannis, I. L., Mantzos, N., Barouchas, P. E., Katsoulas, N., & Kittas, C. (2007). Interactions between salinity and irrigation frequency in greenhouse pepper grown in closed-cycle hydroponic systems. *Agricultural Water Management*, *91*(1–3), 102–111. <https://doi.org/10.1016/j.agwat.2007.05.001>

- Scandalios, J. G. (1993). Oxygen stress and superoxide dismutases. *Plant Physiology*, *101*(1), 7.
- Scheller, H. V., & Haldrup, A. (2005). Photoinhibition of photosystem I. *Planta*, *221*(1), 5–8. <https://doi.org/10.1007/s00425-005-1507-7>
- Schmitz-Eiberger, M., Haefs, R., & Noga, G. (2002). Calcium deficiency - Influence on the antioxidative defense system in tomato plants. *Journal of Plant Physiology*, *159*(7), 733–742. <https://doi.org/10.1078/0176-1617-0621>
- Schnitzler, W. H. (2012). Urban hydroponics for green and clean cities and for food security. In *International Symposium on Soilless Cultivation 1004* (pp. 13–26). Retrieved from http://www.actahort.org/books/1004/1004_1.htm
- Seddon, S., & Cheshire, A. (2001). Photosynthetic response of *Amphibolis antarctica* and *Posidonia australis* to temperature and desiccation using chlorophyll fluorescence. *Marine Ecology Progress Series*, *220*, 119–130. <https://doi.org/10.3354/meps220119>
- Seginer, I., Albright, L. D., & Ioslovich, I. (2006). Improved strategy for a constant daily light integral in greenhouses. *Biosystems Engineering*, *93*(1), 69–80.
- Serra, A.-A., Couée, I., Heijnen, D., Michon-Coudouel, S., Sulmon, C., & Gouesbet, G. (2015). Genome-Wide Transcriptional Profiling and Metabolic Analysis Uncover Multiple Molecular Responses of the Grass Species *Lolium perenne* Under Low-Intensity Xenobiotic Stress. *Frontiers in Plant Science*, *6*. <https://doi.org/10.3389/fpls.2015.01124>
- Sewelam, N., Kazan, K., & Schenk, P. M. (2016). Global Plant Stress Signaling: Reactive Oxygen Species at the Cross-Road. *Frontiers in Plant Science*, *7*. <https://doi.org/10.3389/fpls.2016.00187>
- Shalata, A., & Neumann, P. M. (2001). Exogenous ascorbic acid (vitamin C) increases resistance to salt stress and reduces lipid peroxidation. *Journal of Experimental Botany*, *52*(364), 2207–2211. <https://doi.org/10.1093/jexbot/52.364.2207>
- Shannon, J. (2014). Food deserts Governing obesity in the neoliberal city. *Progress in Human Geography*, *38*(2), 248–266. <https://doi.org/10.1177/0309132513484378>
- Sharkey, T. D. (2005). Effects of moderate heat stress on photosynthesis: importance of thylakoid reactions, rubisco deactivation, reactive oxygen species, and thermotolerance provided by isoprene. *Plant, Cell & Environment*, *28*(3), 269–277.
- Sharma, P., Jha, A. B., Dubey, R. S., & Pessarakli, M. (2012a). Reactive Oxygen Species, Oxidative Damage, and Antioxidative Defense Mechanism in Plants under Stressful Conditions. *Journal of Botany*, *2012*, e217037. <https://doi.org/10.1155/2012/217037>
- Sharma, P., Jha, A. B., Dubey, R. S., & Pessarakli, M. (2012b). Reactive Oxygen Species, Oxidative Damage, and Antioxidative Defense Mechanism in Plants under Stressful Conditions. *Journal of Botany*, *2012*, e217037. <https://doi.org/10.1155/2012/217037>

- Sharma, P., Jha, A. B., Dubey, R. S., & Pessarakli, M. (2012c). Reactive Oxygen Species, Oxidative Damage, and Antioxidative Defense Mechanism in Plants under Stressful Conditions. *Journal of Botany*, 2012, e217037. <https://doi.org/10.1155/2012/217037>
- Shi, J., Yan, B., Lou, X., Ma, H., & Ruan, S. (2017). Comparative transcriptome analysis reveals the transcriptional alterations in heat-resistant and heat-sensitive sweet maize (*Zea mays* L.) varieties under heat stress. *BMC Plant Biology*, 17(1), 26.
- Shi, K., Hu, W.-H., Dong, D.-K., Zhou, Y.-H., & Yu, J.-Q. (2007). Low O₂ supply is involved in the poor growth in root-restricted plants of tomato (*Lycopersicon esculentum* Mill.). *Environmental and Experimental Botany*, 61(2), 181–189. <https://doi.org/10.1016/j.envexpbot.2007.05.010>
- Shibata, T., Iwao, K., & Takano, T. (1994). Effect of vertical air flowing on lettuce growing in a plant factory. *Greenhouse Environment Control and Automation* 399, 175–182.
- Shikanai, T., Takeda, T., Yamauchi, H., Sano, S., Tomizawa, K.-I., Yokota, A., & Shigeoka, S. (1998). Inhibition of ascorbate peroxidase under oxidative stress in tobacco having bacterial catalase in chloroplasts. *FEBS Letters*, 428(1–2), 47–51. [https://doi.org/10.1016/S0014-5793\(98\)00483-9](https://doi.org/10.1016/S0014-5793(98)00483-9)
- Short, A., Guthman, J., & Raskin, S. (2007). Food Deserts, Oases, or Mirages? Small Markets and Community Food Security in the San Francisco Bay Area. *Journal of Planning Education and Research*, 26(3), 352–364. <https://doi.org/10.1177/0739456X06297795>
- Singhal, G. S. (1999). *Concepts in Photobiology: Photosynthesis and Photomorphogenesis*. Springer Science & Business Media.
- Smirnoff, N. (2000). Ascorbic acid: metabolism and functions of a multi-faceted molecule. *Current Opinion in Plant Biology*, 3(3), 229–235. [https://doi.org/10.1016/S1369-5266\(00\)80070-9](https://doi.org/10.1016/S1369-5266(00)80070-9)
- Smirnoff, N. (2008). *Antioxidants and Reactive Oxygen Species in Plants*. John Wiley & Sons.
- Smirnoff, N., & Wheeler, G. L. (2000). Ascorbic Acid in Plants: Biosynthesis and Function. *Critical Reviews in Biochemistry and Molecular Biology*, 35(4), 291–314. <https://doi.org/10.1080/10409230008984166>
- Sol, D., González-Lagos, C., Moreira, D., Maspons, J., & Lapiedra, O. (2014). Urbanisation tolerance and the loss of avian diversity. *Ecology Letters*, 17(8), 942–950. <https://doi.org/10.1111/ele.12297>
- Son, K.-H., & Oh, M.-M. (2013). Leaf shape, growth, and antioxidant phenolic compounds of two lettuce cultivars grown under various combinations of blue and red light-emitting diodes. *HortScience*, 48(8), 988–995.
- Sørensen, J. N., Johansen, A. S., & Poulsen, N. (1994). Influence of growth conditions on the value of crisphead lettuce. *Plant Foods for Human Nutrition*, 46(1), 1–11. <https://doi.org/10.1007/BF01088455>
- Specht, K., Siebert, R., Hartmann, I., Freisinger, U. B., Sawicka, M., Werner, A., ... Dierich, A. (2014a). Urban agriculture of the future: an overview of

- sustainability aspects of food production in and on buildings. *Agriculture and Human Values*, 31(1), 33–51.
- Specht, K., Siebert, R., Hartmann, I., Freisinger, U. B., Sawicka, M., Werner, A., ... Dierich, A. (2014b). Urban agriculture of the future: an overview of sustainability aspects of food production in and on buildings. *Agriculture and Human Values*, 31(1), 33–51.
- Specht, K., Siebert, R., Thomaier, S., Freisinger, U. B., Sawicka, M., Dierich, A., ... Busse, M. (2015). Zero-Acreage Farming in the City of Berlin: An Aggregated Stakeholder Perspective on Potential Benefits and Challenges. *Sustainability*, 7(4), 4511–4523.
- Steinberg, S. L., Ming, D. W., Henderson, K. E., Carrier, C., Gruener, J. E., Barta, D. J., & Henninger, D. L. (2000). Wheat Response to Differences in Water and Nutritional Status between Zeoponic and Hydroponic Growth Systems. *Agronomy Journal*, 92(2), 353. <https://doi.org/10.2134/agronj2000.922353x>
- Sudhakar, C., Lakshmi, A., & Giridarakumar, S. (2001). Changes in the antioxidant enzyme efficacy in two high yielding genotypes of mulberry (*Morus alba* L.) under NaCl salinity. *Plant Science*, 161(3), 613–619. [https://doi.org/10.1016/S0168-9452\(01\)00450-2](https://doi.org/10.1016/S0168-9452(01)00450-2)
- Suzuki, N., Koussevitzky, S., Mittler, R., & Miller, G. (2012). ROS and redox signalling in the response of plants to abiotic stress. *Plant, Cell & Environment*, 35(2), 259–270. <https://doi.org/10.1111/j.1365-3040.2011.02336.x>
- Suzuki, N., & Mittler, R. (2006). Reactive oxygen species and temperature stresses: a delicate balance between signaling and destruction. *Physiologia Plantarum*, 126(1), 45–51.
- Suzuki, N., Rivero, R. M., Shulaev, V., Blumwald, E., & Mittler, R. (2014). Abiotic and biotic stress combinations. *New Phytologist*, 203(1), 32–43. <https://doi.org/10.1111/nph.12797>
- Swindell, W. R. (2006). The association among gene expression responses to nine abiotic stress treatments in *Arabidopsis thaliana*. *Genetics*, 174(4), 1811–1824.
- Taiz, L., & Zeiger, E. (2010). *Plant Physiology*. Sinauer Associates, Incorporated.
- Takahashi, S., & Badger, M. R. (2011). Photoprotection in plants: a new light on photosystem II damage. *Trends in Plant Science*, 16(1), 53–60. <https://doi.org/10.1016/j.tplants.2010.10.001>
- Takahashi, S., & Murata, N. (2005). Interruption of the Calvin cycle inhibits the repair of Photosystem II from photodamage. *Biochimica et Biophysica Acta (BBA) - Bioenergetics*, 1708(3), 352–361. <https://doi.org/10.1016/j.bbabi.2005.04.003>
- Takahashi, S., & Murata, N. (2008). How do environmental stresses accelerate photoinhibition? *Trends in Plant Science*, 13(4), 178–182. <https://doi.org/10.1016/j.tplants.2008.01.005>
- Tan, M., Li, X., Xie, H., & Lu, C. (2005). Urban land expansion and arable land loss in China—a case study of Beijing–Tianjin–Hebei region. *Land Use Policy*, 22(3), 187–196.

- Taylor, M. D., & Locascio, S. J. (2004). Blossom-end rot: A calcium deficiency. *Journal of Plant Nutrition*, 27(1), 123–139. <https://doi.org/10.1081/PLN-120027551>
- Thiobodeau, P. O., & Minotti, P. L. (1969). influence of calcium on the development of lettuce tipburn. In *Proc Amer Soc Hort Sci*. Retrieved from <http://agris.fao.org/agris-search/search.do?recordID=US201301237256>
- Thomaier, S., Specht, K., Henckel, D., Dierich, A., Siebert, R., Freisinger, U. B., & Sawicka, M. (2015). Farming in and on urban buildings: Present practice and specific novelties of Zero-Acreage Farming (ZFarming). *Renewable Agriculture and Food Systems*, 30(Special Issue 01), 43–54. <https://doi.org/10.1017/S1742170514000143>
- Thomas, B. (2010). Food deserts and the sociology of space: Distance to food retailers and food insecurity in an urban American neighborhood. *International Journal of Human and Social Sciences*, 5(6), 400–409.
- Thompson, H. C., Langhans, R. W., Both, A.-J., & Albright, L. D. (1998). Shoot and Root Temperature Effects on Lettuce Growth in a Floating Hydroponic System. *Journal of the American Society for Horticultural Science*, 123(3), 361–364.
- Thompson, J. E., Legge, R. L., & Barber, R. F. (1987). The role of free radicals in senescence and wounding. *New Phytologist*, 105(3), 317–344.
- Tornaghi, C. (2014). Critical geography of urban agriculture. *Progress in Human Geography*, 0309132513512542. <https://doi.org/10.1177/0309132513512542>
- Torres, J. F., Ferriol, L. I., Solís, G., Bautista, A. S., Bono, M. S., Laza, P., ... Maroto, J. V. (2009). Experiments on the control of tipburn by foliar applications of calcium to various cultivars of mini-lettuces and their proclivity for early flowering and the accumulation of nitrates. *Agricola Vergel: Fruticultura, Horticultura, Floricultura, Citricultura, Vid, Arroz*, 28(332), 417–425.
- Torres, J. F., Ferriol, L., Solís, G., San Bautista, A., Bono, M. S., Laza, P., ... Maroto, J. V. (2009). Nitrogen fertilization of diverse cultivars and production cycles of mini lettuces: preliminary studies. *Agricola Vergel: Fruticultura, Horticultura, Floricultura, Citricultura, Vid, Arroz*, 28(333), 500–508.
- Trapnell, C., Williams, B. A., Pertea, G., Mortazavi, A., Kwan, G., Van Baren, M. J., ... Pachter, L. (2010). Transcript assembly and quantification by RNA-Seq reveals unannotated transcripts and isoform switching during cell differentiation. *Nature Biotechnology*, 28(5), 511–515.
- Treml, J., & Šmejkal, K. (2016). Flavonoids as Potent Scavengers of Hydroxyl Radicals. *Comprehensive Reviews in Food Science and Food Safety*, 15(4), 720–738. <https://doi.org/10.1111/1541-4337.12204>
- Triantaphylidès, C., & Havaux, M. (2009). Singlet oxygen in plants: production, detoxification and signaling. *Trends in Plant Science*, 14(4), 219–228. <https://doi.org/10.1016/j.tplants.2009.01.008>
- Triantaphylidès, C., Krischke, M., Hoeberichts, F. A., Ksas, B., Gresser, G., Havaux, M., ... Mueller, M. J. (2008). Singlet Oxygen Is the Major Reactive Oxygen

- Species Involved in Photooxidative Damage to Plants. *Plant Physiology*, 148(2), 960–968. <https://doi.org/10.1104/pp.108.125690>
- Truco, M. J., Ashrafi, H., Kozik, A., Van Leeuwen, H., Bowers, J., Wo, S. R. C., ... others. (2013). An ultra-high-density, transcript-based, genetic map of lettuce. *G3: Genes/ Genomes/ Genetics*, 3(4), 617–631.
- Turhan, E., Karni, L., Aktas, H., Deventurero, G., Chang, D. C., Bar-Tal, A., & Aloni, B. (2006). Apoplastic anti-oxidants in pepper (*Capsicum annuum* L.) fruit and their relationship to blossom-end rot. *Journal of Horticultural Science & Biotechnology*, 81(4), 661–667.
- Twine, N. A., Janitz, K., Wilkins, M. R., & Janitz, M. (2011). Whole Transcriptome Sequencing Reveals Gene Expression and Splicing Differences in Brain Regions Affected by Alzheimer's Disease. *PLOS ONE*, 6(1), e16266. <https://doi.org/10.1371/journal.pone.0016266>
- Ünlükara, A., Cemek, B., Karaman, S., & Erşahin, S. (2008). Response of lettuce (*Lactuca sativa* var. *crispa*) to salinity of irrigation water. *New Zealand Journal of Crop and Horticultural Science*, 36(4), 265–273.
- Upadhyaya, H., Panda, S. K., & Dutta, B. K. (2011). CaCl₂ improves post-drought recovery potential in *Camellia sinensis* (L) O. Kuntze. *Plant Cell Reports*, 30(4), 495–503. <https://doi.org/10.1007/s00299-010-0958-x>
- Utami, S. N. H., Darmanto, & Jayadi, R. (2012). Utami, S. N. H., and R. Jayadi. Vertical Gardening for Vegetables. *Acta Horticulturae*, (958), 195–202. <https://doi.org/10.17660/ActaHortic.2012.958.23>
- Valpuesta, V., & Botella, M. A. (2004). Biosynthesis of L-ascorbic acid in plants: new pathways for an old antioxidant. *Trends in Plant Science*, 9(12), 573–577. <https://doi.org/10.1016/j.tplants.2004.10.002>
- Vavrina, C. S., Obreza, T. A., & Cornell, J. (1993). Response of chinese cabbage to nitrogen rate and source in sequential plantings. *HortScience*, 28(12), 1164–1165.
- Vimolmangkang, S., Sitthithaworn, W., Vannavanich, D., Keattikunpairroj, S., & Chittasupho, C. (2010). Productivity and quality of volatile oil extracted from *Mentha spicata* and *M. arvensis* var. *piperascens* grown by a hydroponic system using the deep flow technique. *Journal of Natural Medicines*, 64(1), 31–35. <https://doi.org/10.1007/s11418-009-0361-5>
- Von Caemmerer, S. von, & Farquhar, G. D. (1981). Some relationships between the biochemistry of photosynthesis and the gas exchange of leaves. *Planta*, 153(4), 376–387.
- Voogt, W., Holwerda, H. T., & Khodabaks, R. (2010). Biofortification of lettuce (*Lactuca sativa* L.) with iodine: the effect of iodine form and concentration in the nutrient solution on growth, development and iodine uptake of lettuce grown in water culture. *Journal of the Science of Food and Agriculture*, 90(5), 906–913. <https://doi.org/10.1002/jsfa.3902>
- Wahid, A., Gelani, S., Ashraf, M., & Foolad, M. R. (2007). Heat tolerance in plants: an overview. *Environmental and Experimental Botany*, 61(3), 199–223.

- Wang, H., Qiu, F., & Swallow, B. (2014). Can community gardens and farmers' markets relieve food desert problems? A study of Edmonton, Canada. *Applied Geography*, *55*, 127–137. <https://doi.org/10.1016/j.apgeog.2014.09.010>
- Wang, Z., Gerstein, M., & Snyder, M. (2009). RNA-Seq: a revolutionary tool for transcriptomics. *Nature Reviews Genetics*, *10*(1), 57–63. <https://doi.org/10.1038/nrg2484>
- Warber, S. L., DeHudy, A. A., Bialko, M. F., Marselle, M. R., & Irvine, K. N. (2015). Addressing 'Nature-Deficit Disorder': A Mixed Methods Pilot Study of Young Adults Attending a Wilderness Camp. *Evidence-Based Complementary and Alternative Medicine*, *2015*, e651827. <https://doi.org/10.1155/2015/651827>
- Weerakoon, A. t., Meyers, I. a., Symons, A. l., & Walsh, L. j. (2002). Pulpal Heat Changes With Newly Developed Resin Photopolymerisation Systems. *Australian Endodontic Journal*, *28*(3), 108–111. <https://doi.org/10.1111/j.1747-4477.2002.tb00402.x>
- Weydert, C. J., & Cullen, J. J. (2010). Measurement of superoxide dismutase, catalase, and glutathione peroxidase in cultured cells and tissue. *Nature Protocols*, *5*(1), 51–66. <https://doi.org/10.1038/nprot.2009.197>
- White. (2012). *Long-distance transport in the xylem and phloem, in Marschner's Mineral Nutrition of Higher Plants, 3rd Edn, ed. Marschner P., editor. (London: Academic Press;), 49–70.* Academic Press.
- White, P. J., & Broadley, M. R. (2003). Calcium in plants. *Annals of Botany*, *92*(4), 487–511.
- Wien, H. C., & Villiers, D. S. de. (2005). (196) Inducing Lettuce Tipburn with Relative Humidity Modification. *HortScience*, *40*(4), 1053–1053.
- Winsor. (1978). Some aspects of the nutrition of tomatoes grown in recirculating solutions. Retrieved July 21, 2015, from http://www.actahort.org/books/82/82_15.htm
- Wissemeyer, A. H., & Zühlke, G. (2002b). Relation between climatic variables, growth and the incidence of tipburn in field-grown lettuce as evaluated by simple, partial and multiple regression analysis. *Scientia Horticulturae*, *93*(3–4), 193–204. [https://doi.org/10.1016/S0304-4238\(01\)00339-9](https://doi.org/10.1016/S0304-4238(01)00339-9)
- Wolch, J. R., Byrne, J., & Newell, J. P. (2014). Urban green space, public health, and environmental justice: The challenge of making cities 'just green enough.' *Landscape and Urban Planning*, *125*, 234–244.
- Wolff, X. Y., & Coltman, R. R. (1990). Productivity Under Shade in Hawaii of Five Crops Grown as Vegetables in the Tropics. *Journal of the American Society for Horticultural Science*, *115*(1), 175–181.
- Xia, X.-J., Wang, Y.-J., Zhou, Y.-H., Tao, Y., Mao, W.-H., Shi, K., ... Yu, J.-Q. (2009). Reactive oxygen species are involved in brassinosteroid-induced stress tolerance in cucumber. *Plant Physiology*, *150*(2), 801–814.
- Yamori, W., & Shikanai, T. (2016). Physiological Functions of Cyclic Electron Transport Around Photosystem I in Sustaining Photosynthesis and Plant Growth. *Annual Review of Plant Biology*, *67*(1). Retrieved from

<http://www.annualreviews.org/doi/abs/10.1146/annurev-arplant-043015-112002>

- Yanagi, A. A., Bullock, R. M., & Cho, J. J. (1983). Factors involved in the development of tipburn in crisphead lettuce in Hawaii [Physiological disorder]. *Journal American Society for Horticultural Science*, 108. Retrieved from <http://agris.fao.org/agris-search/search/display.do?f=2012/OV/OV201203123003123.xml;US19840032984>
- Yang, W., Zhu, C., Ma, X., Li, G., Gan, L., Ng, D., & Xia, K. (2013). Hydrogen Peroxide Is a Second Messenger in the Salicylic Acid-Triggered Adventitious Rooting Process in Mung Bean Seedlings. *PLOS ONE*, 8(12), e84580. <https://doi.org/10.1371/journal.pone.0084580>
- Yu, Y. J., Zhao, X. Y., & Xu, J. B. (2002). Screening Method for Resistance to Tipburn in Chinese Cabbage. In *XXVI International Horticultural Congress: Advances in Vegetable Breeding 637* (pp. 189–193). Retrieved from http://www.actahort.org/books/637/637_22.htm
- Zhang, F.-Q., Wang, Y.-S., Lou, Z.-P., & Dong, J.-D. (2007). Effect of heavy metal stress on antioxidative enzymes and lipid peroxidation in leaves and roots of two mangrove plant seedlings (*Kandelia candel* and *Bruguiera gymnorhiza*). *Chemosphere*, 67(1), 44–50. <https://doi.org/10.1016/j.chemosphere.2006.10.007>
- Zhang, J., Wang, J., Jiang, W., Liu, J., Yang, S., Gai, J., & Li, Y. (2016). Identification and Analysis of NaHCO₃ Stress Responsive Genes in Wild Soybean (*Glycine soja*) Roots by RNA-seq. *Frontiers in Plant Science*, 7. <https://doi.org/10.3389/fpls.2016.01842>
- Zhang, Q., Liu, M., & Ruan, J. (2017). Metabolomics analysis reveals the metabolic and functional roles of flavonoids in light-sensitive tea leaves. *BMC Plant Biology*, 17, 64. <https://doi.org/10.1186/s12870-017-1012-8>
- Zhou, Y.-H., Zhang, Y.-Y., Zhao, X., Yu, H.-J., Shi, K., & Yu, J.-Q. (2009). Impact of Light Variation on Development of Photoprotection, Antioxidants, and Nutritional Value in *Lactuca sativa* L. *Journal of Agricultural and Food Chemistry*, 57(12), 5494–5500. <https://doi.org/10.1021/jf8040325>
- Zivcak, M., Brückova, K., Sytar, O., Brestic, M., Olsovska, K., & Allakhverdiev, S. I. (2017). Lettuce flavonoids screening and phenotyping by chlorophyll fluorescence excitation ratio. *Planta*, 1–15.